Coping with Through Life Fast Jet Upgrades: Towards a Decentralised Electrical System

Chung Man (Kenny) Fong

November 2015

A thesis submitted for the degree of Doctor of Engineering to

Department of Electronic and Electrical Engineering

University of Strathclyde

This thesis is the result of the author's original research. It has been composed by the author and has not been previously submitted for examination which has led to the award of a degree.

Abstract

Fast jet aircraft go through continuous upgrades throughout their operational lifecycle to keep them operationally relevant until the next replacement fast jet is available. Such lifecycles can stretch over timescales of a few decades for the same fast jet aircraft (e.g. the Panavia Tornado iterations). Overall, these upgrades for typical legacy fast jet aircraft are likely to be "electronic" in nature where specific upgrades examples include additional or replacement (more powerful) sensors, mission computing, electronic warfare, communication and pilot interface equipment to increase mission effectiveness.

Apart from some self-powering pod based equipment, the end result of through life upgrades is a continuously increasing power demand against an unchanged main electrical system within a spatially unchanging compact and limited weight allowance environment (the airframe).

Under normal conditions, the generic fast jet system is powered by a centralised source of power generation: being engine mechanical off-take driven generator/s (one for each channel). The generator and off-take are installed at the manufacturing stage of the aircraft and at the start of the fast jet service life, the capacity of the generator is greater than the initial loading. However with the through life upgrades, past trend have shown that such built in growth is not enough. Hence to cope with such power increases one can change the main generators during the operational life of the fast jet. However, this requires cumbersome and expensive rework of the associated mechanical off take and the more powerful replacement generator will still need to fit into the same space as the original generator (with the same space constraints). Hence the replacement generator needs to be more power dense. Load shedding can also be considered but due to the lack of hotel or non critical loads on a fast jet aircraft when compared to civil aircraft (i.e. in-flight entertainment) minimises the scope to load shed.

Alternatively or in a supplementary nature, the thesis proposes an examination of moving towards a decentralised electrical system whereby supplementary generation sources can be inserted around the aircraft (smaller capacity but larger number of generation sources distributed around the aircraft to conform to remaining space for the compact airframe i.e. "filling the gaps"). The proposal of this thesis is that such distributed generation will work in parallel to the existing main generation leaving it intact with limited rework/replacement. The upgrades themselves will also be added in conjunction with the equipment upgrades to minimise the downtime of the aircraft.

However, such approach has not been widely seen on contemporary fast jet to date. Such distributed integration of supplementary generation also requires loose coupling for retrofit/modification purposes. Hence this thesis looks into techniques for paralleling of sources in other domains with similar paralleling needs such as Electric Vehicles (EVs), microgrids, distributed generation and renewables research to draw read across.

This thesis firstly reviews different types of sources that are potentially suitable for such application and provide "weight" to the argument of having distributed generation. From the literature review of the paralleling techniques from other domains, the thesis has down selected and explores the adaption of three possible integration methods to integrate such power generation into the fast jet network in a distributed manner. These include

- Using passive links of existing rectifiers around the fast jet electrical system as DC integration points.
- Use of Shunt Active Filtering to inject power into the fast jet system in parallel to the main generation (additional to harmonic reduction functionality). This is achieved by placing additional sources onto the DC link of the filter.
- Converting passive rectifiers around the fast jet electrical system into active rectifiers/inverters to feed power back into the system (using the distributed location of the load, reusing the same wiring of the load as well as powering of local loading). This is to replace diodes one by one with an active switch within the passive rectifiers.

Underpinning these techniques is the proposed use of a common voltage master current slave scheme at the separate DC links which is used to control power flow.

Illustration of the operation and benefits of these are presented against generic fast jet electrical system simulations within the thesis.

The novelty of the work comes from firstly, the proposal to move towards a more decentralised system in the unique upgrade problem on fast jet where there is little space left to accommodate bulk generation upgrades. Addition to these, the novelty of the work also comes from the exploration of the three integration methods stated above which represents a "first pass" attempt to increase the penetration of such distributed generation.

Acknowledgements

I'd like to thank my supervisors, Dr Stuart Galloway, Ian Harrington in no particular order. I would also like to thank Graeme Burt, Anne Morris, Stewart Willocks, Campbell Booth, Eddie Gould, Roger Dixon, Roger Goodall, University of Strathclyde's AES group, BAE Systems MAI R and T group and our other colleagues at the University of Strathclyde, BAE Systems and University of Loughborough. I would like to thank them for providing invaluable support and patience throughout my doctorate and write up.

I'd especially like to thank my parents, Cheung and Suet especially for their patience. This thesis is dedicated to them. I would also like to thank my extended family and friends for their invaluable support over the years.

Contents

List of Figures

List of Tables

Abbreviations

AC	Alternating Current
ACM	Air Combat Manoeuvres
Active TRU	Active Transformer Rectifier Unit
AES Group	Advanced Electrical Systems Group
AESA	Active Electronically Scanned Array
APU	Auxiliary Power Unit
ATRU	Auto Transformer Rectifier Unit
BTC	Bus Tie Contactor
CNI	Communication Navigation Identification
COTS	Commercial Off The Shelf
DASS	Defensive Aid SubSystems
DEW	Directed Energy Weapons
Dq0	Direct Quadrature Zero
ECS	Environmental Control System
EO	Electro Optics
EV	Electric Vehicle
EW	Electronic Warfare
FFT	Fast Fourier Transform
FLIR	Forward Looking InfraRed
GC	Generator Contactor
GCU	Generator Control Unit
HALE	High Altitude Lone Endurance
HMD	Head Mounted Display
HUD	Head Up display
IR	InfraRed
ISR	Intelligence Surveillance Reconnaissance
ITHD	current Total Harmonic Distortion
JSF	Joint Strike Fighter (F35)
M/DG/R	Microgrid/Distributed Generation/Renewables
MAI	Military Air and Information

MALE	Medium Altitude Long Endurance
MEA	More Electric Aircraft
NLL	Non Linear Load
OEM	Original Equipment Manufacturer
PCC	Point of Common Coupling
PEM	Poly Electrolyte Membrane
PMG	Permanent Magnet Generator
PQS	real reactive and apparent power
RAT	Ram Air Turbine
RATG	Ram Air Turbine Generator
RCS	Radar Cross Section
RTCA	Radio Technical Commission for Aeronautics association
SAF	Shunt Active Filter
SEAD	Suppression of Enemy Air Defences
SIGINT	SIGnal INTelligence
TEG	Thermo Electric Generator
THD	Total Harmonic Distortion
TRU	Transformer Rectifier Unit
UAV	Unmanned Aerial Vehicle
UPQC	Unified Power Quality Conditioner
VTHD	Voltage Total Harmonic Distortion

1 Introduction

1.1 The fast jet through life power demand increase problem

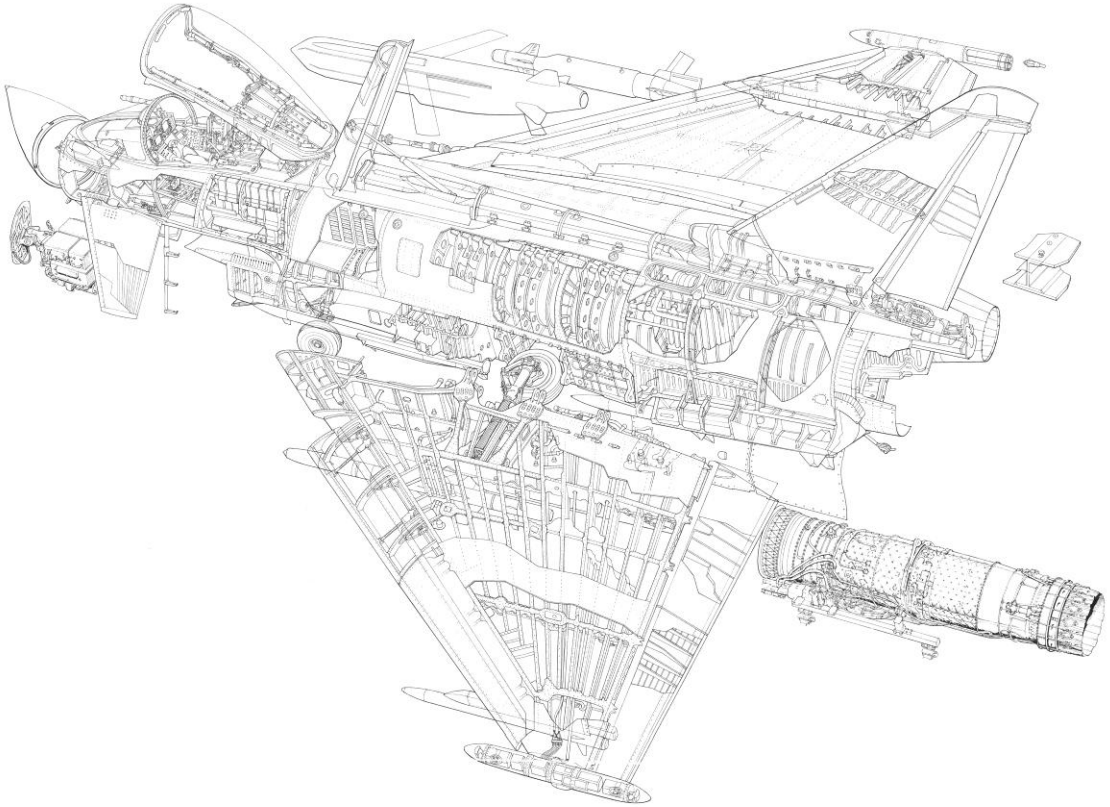

Figure 1- Eurofighter cutaway [1]

Due to the substantial development and individual cost [27],[33]-[42] of fast jet aircraft, they tend to have extensive in service lives (in the range of 3-5 decades [13]-[15],[33]-[42]) to maximise the investment made. Typical fast jet aircraft continuously require upgrades during their operational life to keep them relevant before the next design replaces them completely. A range of real life fast jet aircraft examples are summarised in Table 1 including their operational lifespan to illustrate their long lifecycles.

During these long life cycles; “mission creep” can necessitate additional roles beyond that of the initial design of the fast jet. This can drive the need for additional on-board equipment to satisfy the new roles and in turn can increase the electrical power demand of the aircraft (one example being the Litening pod [16] for pop up targeting).

Even within the original designed roles, to maintain operational effectiveness coupled with general technology advancement; more through life on board upgrades are added as they become available and standardised (such as Forward Looking InFared (FLIR) [31] for air to air combat).

Overall, these upgrades for typical legacy fast jet aircraft are likely to be “electronic” [2]-[12]. Specific upgrades examples include additional or replacement sensors such as more advanced and power demanding Active Electronically Scanned Array (AESA) radars (including intrinsic communications and jamming capabilities), L band radars [18], FLIR [31], smarter weapons [19] targeting pods [16],[20],[21], Directed Energy Weapon (DEW) and Communication Navigation Identification (CNI) upgrades such as satellite communications, GPS, Identification Friend or Foe (IFF) etc, SIGnal INTelligence (SIGINT) sensors, Electronic Warfare (EW) loads [22],[23], cockpit interface such as “glass cockpit”/Head Mounted Display(HMD) and other avionics in general. These are added to the fast jet airframe which mostly remains the same shape and size even within different production iterations of the same design (a typical example being the different iterations of the Lockheed Martin F16 [17])

Apart from some self-powering pod based equipment such as the ALQ 99 jamming pods [24], the end result of through life upgrades is a continuously increasing power demand against an unchanged main electrical system within a spatially unchanging compact and limited weight allowance environment. Also in Table 1, a summary of approximate dimensions and weight constraints of example fast jet aircraft are included to put into perspective the spatial constraint of such environment.

In the context of this thesis, the nature of the electrical system of interest under examination (which is elaborated in chapter 2) is a conventional 400Hz, 3 phase, 115Vrms system in a two islanded channel setup with associated engine driven generators. These make up the majority of legacy in service fast jet to date [33],[34],[35]-[42]). The AC busbars of these usually includes loads that contain passive rectifiers that convert the three phase 115Vrms to 270VDC, and Transformer Rectifier Units (TRUs) that transform and rectify the 115Vrms to 28VDC for the 28VDC busbars. Overall, the fast jet aircraft requires 10s of kVA of power generation [25][26] to supply the on-board loading.

Table 1- Summary of different fast jet aircraft cost, lifecycle, dimensions and weight [33]-[42]

Airframe	Introduction – end of service life	Length, Wingspan, Height (m, m, m)	Empty Weight (kg)	Power Generation
BAE Systems / EADS Eurofighter Typhoon	2003 to present (projected 20-30 years)	15.96m, 10.95m, 5.28m	11000	2x30kVA [26]
Panavia Tornado ADV	1985 to 2011	18.68m, 8.6m-13.91m, 5.95m	14500	2x45kVA [26]
Mc Donnell Douglas F4	1960 to present	17.75.2m, 11.7m, 5m	13757	
Dassault Rafale	2000 to present	15.27m, 10.8, 5.34m	9500-10196 (carrier version)	2x 30kVA [26]
Dassault Mirage 2000	1982 to present	14.36m, 9.13m, 5.2m	7500	2x 25kVA [26]
Saab Gripen c	1997 to present	14.1m, 8.4m, 4.5m	6800	
Mc Donnell Douglas/Boeing F15 eagle	1976 to present	19.43m, 13.05m, 5.63m	12700	2x60kVA [26]
Mc Donnell Douglas / Boeing F15e strike eagle	1988 to present	19.43m, 13.05m, 5.63m	14300	
Lockheed Martin F16	1978 to present	15.06m, 9.96m, 4.88m	8570	1x 40kVA [26]
Mc Donnell Douglas / Boeing F18 hornet	1983 to present	17.1m, 12.3m. 4.7m	10400	
Boeing F18 Super Hornet	1999 to present	18.31m, 13.62m, 4.88m	14552	2x 65kVA [26]

1.1.1 Distinction between fast jet and other aerospace platforms

There are key design drivers which differentiate fast jet aircraft from other types of aerospace platforms and other domains, making through life upgrades more difficult to manage. These are summarised below.

1. Fast jet aircraft exhibit intrinsic high aerodynamic performance such as but not limited to:
    a. Supersonic speeds that can include top speeds of up to Mach 1.8 to Mach 2.5 [33]-[42].
    b. High g forces additional to top speed. For example, the BAE Systems Eurofighter can pull up to nine times the force of gravity [43] which is typical of modern day fast jet.

    To enable these design requirements, both the shape and size of the fast jet are constrained into a very tightly packed airframe for thrust to weight ratio and aerodynamics. This becomes a large constraint when comparing to upgrading electrical generation capacity on terrestrial, marine or even civil aerospace transport systems which has relatively more space and weight allowances.

2. Mirroring the fast jets own employment of sensory such as radar, InFrared (IR) and SIGNIT; the effectiveness and survivability of the fast jet aircraft itself are also highly correlated to its own ability to minimises the oppositions sensory effectiveness. Apart from proactive measures such as jamming [24],[28], the airframe's Radar Cross Section (RCS), thermal emission and electromagnetic emissions are also increasingly optimized as part of the design (such as the Lockheed Martin F22 raptor). As a result, these further constrain the shape of the airframe reducing the space that can be used for upgrades and as well as the types of additional electrical generation upgrades that can be added. For example: Ram Air Turbine Generator (RATG) can increase overall RCS or engine independent gas turbine generators can produce additional exhaust heat, which both would need to be carefully managed.

As such, flexibility in the electrical connection of any additional power generation sources into the existing fast jet electrical system would be severely constrained.

1.1.2 Demand increase levels

Electrical demand trends of multiple past fast jet aircraft designs has shown a tendency to increase and eventually exceed the originally designed generation capacity by 100%. Such trends affects the in service designs but will also likely manifest itself in any future designs if built in growth strategies are not rethought.

Rolling forward with legacy systems designs without the context of new more electrically dependent applications is a risk and one of the areas where the research of this thesis provides value. This is by considering the strategy of using alternative power generation and utilising existing onboard auxiliary or emergency generation to supplement the existing main generation within the fast jet aircraft.

1.2 Base built in growth, but not enough

At the introduction of a fast jet aircraft design into service; there is built in growth factored in, which essentially equates to the initial generator capacity being greater than the initial on-board loading. However, examining the past trends; through life demands eventually exceeds this prebuilt growth for multiple platforms which can be 100% greater than the base capacity. One could argue adding much greater capacity at the start of the fast jet aircraft lifecycle to meet the eventual 100% increase trend. However, the main constraints of adding this larger base capacity are

1) Overly large bulk generation capacity at the beginning of the lifecycle will only become underutilised. This could then mean an overly large generator may be operating at lower efficiencies under-loaded.
2) Size of the built in growth may be already at a maximum in terms of power density available at the original design stage and incapable of meeting the future upgrades regardless.

1.2.1 Conventional contingency options

Contingency approaches to meeting such through life upgrades currently include the following two options.

1.2.1.1 Up-rating of main generation through life

When the demand eventually exceeds existing generation caused by through life upgrade; one option is to replace the main generation itself with more power dense equivalent at later stages of the operational lifecycle. However this is constrained by the associated mechanical linkage to the engine driven gear box for retrofit options for in service aircraft, whereby to incorporate further capacity, the gear box itself will also need to be up-rated/replaced. This requires mechanical retrofit work and could be cumbersome and expensive from a system integrator point of view.

The one to one replacement also limits the scope of additional generation which will still face the same volume and weight constraints as before.

However there is precedence of the actual engine/s themselves being replaced in different iterations of the same aircraft 'design' such as the F16a/b to its current iteration F16e/f [17]. This could potentially allow for associated replacement of the engine off take as well as generator. However this is considered a major change to the system and may not always be possible.

1.2.1.2 Load shedding

For the load shedding option, the fast jet is largely made up of mission capability and flight critical loads with little hotel loads such in-flight entertainment that one might see in civil aerospace applications. Loads on a fast jet are less acceptable for shedding such as Defensive Aid SubSystems (DASS), radar or FLIR where survivability is at risk, further constraining the load shedding options.

However there is still scope to curtail some of the more inert loads such as electrical booster pumps that run continuously during flight. Work pertaining to this has been performed in the past but with little success due to cavitation problems in the fuel flow.

There are also load shedding scenarios whereby whole busbars are shed when one of the two main engine driven generation becomes offline or for ground operations. However the former is essentially a reduced mission capability/"enough to get home" state, whereby not considered as part of normal operations and not ideal for completing missions.

1.2.2 Alternative and unconventional option of supplementary generation

Alternatively, one unexplored strategy that this thesis proposes is: to insert engine mechanical off take independent power generation to supplement the main generation, in conjunction to the demand increases. This is not common practice for fast jets with a contemporary fast jet electrical system solely utilising centralised engine driven generation during normal operations. Such strategy of adding supplementary generation could also take advantage of power generation technology advancements as they become available during the life span of the fast jet. Such a strategy if adopted would be a phased modification approach that coincides with the demand upgrades themselves and the benefit of such approach is to reduce the offline time of the fast jet aircraft from service. This approach would obviously increase on-board generation but requires space within an already packed aircraft mentioned in section 1.1.1. Hence it is desirable that the application of additional power is distributed around the airframe to better conform to the remaining space available (giving argument for a "decentralised" electrical system reflected by the thesis title).

1.2.2.1 Dynamic employment of redundancy

In addition to the approach of adding new distributed generation sources into the fast jet electrical system; there may be the opportunity to better utilise redundant electrical sources already on the aircraft. By design, the fast jet aircraft has built in auxiliary or emergency power generation power that 'sits' idle or offline during normal operations in flight. One-possible option to increase the power generation is to combine the output of these with the main generation during peak demand times which have not been practiced traditionally within fast jet. These emergency or auxiliary

power sources supply flight critical and system critical loads upon main generation failure as well as general loads during ground operations when the engine driven generation has yet to come online.

There are however some constraints to this, such as

- Back up generation may not be rated for the increased utilisation duration e.g. the cycle life of a nickel cadmium battery.
- Some of the emergency power generation will also have limited generation capacity or energy compared to the main engine driven generator. For example, the 28VDC emergency power can only provide less than a $1/6^{th}$ of what a single generator outputs. Hence this approach would not be sufficient to meet the 100% increase of power demand, and therefore additional power would be required regardless.
- Some auxiliary generation sources are also not rated for in flight operations at all such as ground based Auxiliary Power Units (APUs) albeit having relatively high output (greater than ½ of a single generator output for example in the Eurofighter). To overcome this, one to one replacement with a flight cleared equivalent can be considered. One main consideration however is: the replacement APU also needs to provide bleed air for Environmental Control System (ECS) which puts additional constraints to the alternative options such as use of a Poly Electrolyte Membrane (PEM) fuel cell.

The dynamic utilisation of redundant generation already in the system, whether auxiliary or emergency has some constraints. However, by exploring the means of achieving increased utilisation provides a flexible option to supplement the overall power generation while making use of sources that otherwise acts as in flight deadweight.

Furthermore, the paralleling mechanisms are similar for both the addition of supplementary generation and dynamic operation of existing auxiliary/emergency generation in which both require similar interface and control to parallel them with the main generation. Hence these two options can essentially be thought of the same solution and as such the research in this thesis considers the solution for both to be the same.

1.3 Chapter summary

In summary of the fast jet through life upgrade problem presented in this thesis, apart from one to one up rating of the inadequate main generation or constrained load shedding, there is no standardised approach to meet the generic through life upgrade problem on fast jet [2]-[12].

One more proactive option with little pursuit to date on fast jet is the paralleling of distributed generation sources around the aircraft and in particular having additional generation sources to work in conjunction to the existing main generation during normal operations. Utilisation of existing auxiliary or emergency generation in the same way can also provide additional power to raise the combined peak generation output to meet the increase in demands. Both have the potential to allow an increase in peak power generation while being space conforming within a compact fast jet environment.

However to enable the addition of more power for already in service fast jet aircraft; there is a need for a flexible integration scheme to work in conjunction with the electrical system and main generation which are already operating as part of the fast jets normal operations. Hence attributes of these power integration solutions should include limited disruption/modification to limit rework and preserve integrity of the base electrical system. Thus the research presented in the rest of the thesis aimed to develop and assess possible solutions aligning with this context.

With little precedence of through life application of such paralleling within in service fast jet, the work of the thesis explores integration methods from other domains for read across. These mainly being Electric Vehicles (EV) and Microgrid/Distributed Generation/Renewable (which will be referred to as M/DG/R in the rest of the thesis), which have similar attributes for paralleling of power. In particular the connection of back into the main terrestrial grid is analogous to adding additional power into the fast jet electrical system which both needs to adhere to voltage, phase and frequency of an already operating main electrical system. With these in mind, the explored integration methods for fast jet application were down selected from the literature review. The subsequent down selected techniques examined are summarised as the following three integration methods with their exploration and simulated operations presented in the rest of this thesis:

1.3.1 Use of rectifiers already in the fast jet electrical system as integration points

Akin to the EV and M/DG/R, the proposed use of existing DC link capacitors around typical fast jet electrical systems as the physical connection points for adding supplementary generation is considered. These DC links exist around the fast jet aircraft in the form of AC busbar non-linear loads

which have rectifier stages as well as the TRUs (the generic fast jet electrical architecture is elaborated in chapter 2). These are distributed around the aircraft and hence lend themselves as potential distributed integration points. Using such DC links, the thesis proposes the connection of additional power generation through DC DC converters. To parallel these to the DC link and between multiple additional generation sources: the thesis proposes the use of a voltage master current slave scheme for control (similar setups have been researched for EV applications [44]). In effect, the additional DC sources will offset the power drawn from the main generation whereby the loading aft of the rectifier will be shared between the main generation and the newly added generation (ultimately allowing load sharing/paralleling). The voltage of the DC link is proposed, to still be held by the main generation through the normal rectification generation (acting as the voltage master) and any additional sources connected to the DC link will be operated in current slave mode. The current slave control will dictate the amount of current injected into the system through the DC link.

1.3.2 Use of SAF to integrate power back into the main fast jet electrical system

Additional to this, the thesis also proposes the use of a Shunt Active Filter (SAF) on a fast jet electrical system to satisfy the dual functionality of harmonic current reduction as well as injecting additional power generation into the system directly onto the AC busbars. With this, additional power generation can then be connected at the DC link of the SAF itself for feed through back to the AC system (again through DC DC converters). It is also intended that the DC link of the SAF will operate in a similar voltage master and current slave scheme whereby the voltage master will be maintained with the SAF voltage control providing commonality.

1.3.3 Conversion of unidirectional/legacy rectifiers already in the fast jet electrical system into active equivalent to allow power flow back additional for local loading

Finally, the third integration solution the thesis proposes is in the changing of passive rectifier stages of non-linear loads as well as TRUs within the fast jet electrical system to active bi directional equivalents/inverters. This is a proposed follow up to the method of solely integrating power to the DC side of passive rectifiers or TRUs to offset the power draw from the main generation. The main constraint of solely integrating power to these passive rectifier DC links is; the amount of DC side generation can become saturated if the added capacity exceeds the DC side loading/local loading. By converting the passive rectifier to an active equivalent, such saturation can be dealt with by allowing the excess power generation to be fed back into the AC busbar (while reusing the same wiring back to the AC busbar). This is also intended to be operated within the voltage master current slave scheme where the DC link voltage will be controlled by the active equivalent of the rectifier.

1.3.4 Novelty of contributions

The novelty of the work in this thesis is the proposed strategy of supplementary generation (which have not been examined to date) for conveniently adding distributed power around the compact fast jet electrical system to meet the unique fast jet upgrade problem.

In line with this, the novelty of the work also comes from the proposed application of researched or established parallel techniques from other domains such as EVs and M/DG/R but within the fast jet electrical system context. As such the value of the work covered in this thesis is also in the exploration of such application (including adaption, tailoring) against the unique aggressive electrical power/load demand increase problem, that are not common in the civil aerospace domains.

1.4 Thesis content overview

In terms of the content of this thesis, this section provides a descriptive summary of each chapter:

Chapter 1 being this chapter; covers the introduction of the fast jet through life upgrade and the proposed strategy of supplementary generation to cope. An initial summary of the three proposed integration methods aligning with this are presented.

Chapter 2 presents the characterising of the basic generic fast jet electrical system. This includes model based bench marking for quantifying the effects of the three proposed supplementary generation integration solutions in later chapters.

Chapter 3 covers the literature review and read through of topologies and paralleling control techniques from EV and M/DG/R for application for the fast jet upgrade problem. From these, the three integration methods proposed for fast jet application were down selected/adapted from.

Chapter 4 explores the first of the three proposed integration methods. This is the proposed integration of supplementary generation at the DC link of existing rectifiers around a fast jet electrical system for supplying local loading to offset the draw from the main generation. Through simulations, illustration of intended operations and functionality is provided.

Chapter 5 explores the second of the three integration methods. This is the SAF application on fast jet for integrating power back into the electrical system. Again simulations are used for illustration of operations and benefits of power integration to supplement the main generation.

Chapter 6 explores the third of the three integration methods which the proposed conversion of passive rectifiers into active equivalent for power flow back into the main fast jet electrical system additional to local loading. This is essentially the first proposed integration (chapter 4) with the power integration at the same DC link but instead of passive rectifiers, the diodes are replaced by switches to allow bi directional current flow.

Chapter 7 looks into the coherent operations of all three integration methods working within the same fast jet electrical system. Ultimately this is to illustrate the broad integration benefits from all three methods to increase overall power penetration. This chapter also illustrates loose coupled operation of these three integration methods on the intended incremental application on the fast jet and with limited changes to the main generation.

Chapter 8 is the conclusion chapter which discusses the proposed strategy of supplementary generation and the performance of the three integration methods. Suggestion of further work is also provided to further mature the proposed integration methods for eventual deployment.

1.5 Publications associated with author

Other research work undertaken by the author include [45],[46]. These are included to provide precedence of previous peer assessed publication research work by the author.

2 Fast jet electrical system characterisation

2.1 Chapter overview

Chapter 1 discussed the general fast jet through life upgrade problem and the general strategy of distributed generation to cope. This chapter further characterises a generic fast jet electrical system to aid the examination of such distributed power integration solutions.

This is followed by an overview of a generic fast jet electrical system as well as the constrained spatial positioning of its electrical system and associated equipment within the airframe. The purpose of this is to provide more detail about the nature of the generic fast jet electrical systems within the airframe which undergo increasing through life power demands and highlight the difficulty in adding more generation into the system.

An electrical model of such a generic fast jet electrical system for the purpose of profiling electrical load during operations is then presented. The aim of the profiling was to allow the power integration methods proposed in this thesis to be compared to a baseline fast jet electrical system for illustrating power alleviation of the main generation while maintaining power quality.

To reiterate, the power integration methods proposed in this thesis are to meet increases in power demand on a fast jet. These consist of three separate integration methods that allow more decentralised power integration to potentially conform to the limited remaining space. These are elaborated in chapter 3 in terms of their down select/formulation for the fast jet application from other domains such as EVs and M/DG/R research.

Also, additional to adding more generation sources into the system through these methods, some of the existing auxiliary or emergency sources can also utilise the same methods to parallel with the main generation to increase overall peak power output.

2.2 Overview of a generic fast jet electrical system and spatial representation

In this section, the electrical architecture of the generic fast jet electrical system is provided as well as a spatial illustration of this electrical system and major electrical equipment within a generic airframe.

2.2.1 Electrical system

Firstly a generic electrical system that typically provides the power within a fast jet aircraft is illustrated in Figure 2. This consists of a three phase, 115Vrms, twin channel system with power provided by associated engine driven generators, outputting 400Hz constant frequency in the power range of 10s of kVA.

In this electrical system, the Generator Control Unit (GCU) is responsible for controlling the output of the generators including voltage, frequency and magnitude based tripping, over current and differential current tripping via a Generator Contactor (GC) as well as connection of busbars for single generator scenarios. The Bus Tie Contactor (BTC) is usually in the open position to allow the two channels to operate as islands.

The main generators supply associated AC busbars which subsequently supply multiple three phase and single phase AC loads, via thermal breakers at the busbars. The different types of electrical loading include non-linear loading which are loads with built in passive rectification stages for “electronic” type loads such as avionics, mission computing, EW, cockpit displays, radar, and DASS. Others loads are the linear loads which include resistive loads such as lighting, heating as well as fixed speed induction motors such as electrical fuel pumps, boost pumps and fans.

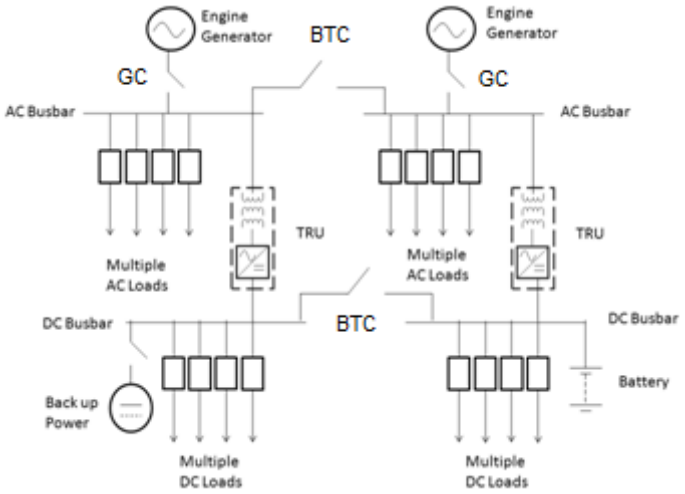

Figure 2- Generic two channel electrical system of a conventional fast jet aircraft

The AC busbar of each channel also feeds a twelve pulse TRU (Figure 3) supplying part of the generator power to 28VDC busbar/s for multiple DC loads. This bus can make up around 1/6th of the main generator capacity on each channel on a typical fast jet aircraft.

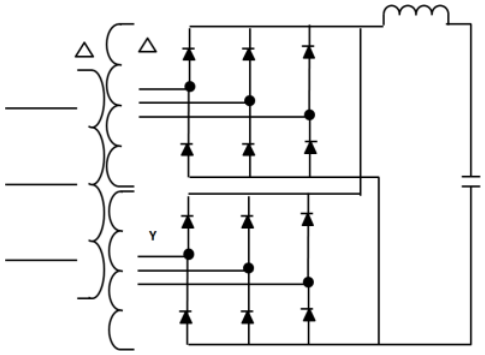

Figure 3- TRU to convert to 28VDC from 115Vac 3 phase

In terms of the quantity of individual electrical loads on a fast jet aircraft; these can amass to the region of hundreds to make up 10s of kW of loading per channel.

During start-up of an aircraft, power is provided by the APU or ground power before engine generation is available. In some cases, the APU is only cleared for ground based operations and becomes deadweight in flight but in other examples there are in flight operated equivalents [49] in which their turbine generator are also used as the emergency power supply in flight (this is elaborated in chapter 3).

A dedicated source of backup or emergency power is provided for redundancy for the 28VDC bus, either running on engine off-take or ram air turbine (also elaborated in chapter 3). Additional to this, a battery connected to the DC busbar/s also provides power to the critical loads during loss of all generator power.

A generic three phase, 115Vac, 400Hz and two channel electrical architecture with a representative power generation level of 30kVA per channel from each main generator (60kVA in total) is used as the baseline for studies in the rest of this thesis.

Although the 400Hz 3 phase 115Vrms system has been described, there are other types of electrical systems that have come into service for fast jet in the past 15 years. One example includes variable frequency based distribution used in the Dassault Rafale [47] which omits the constant speed drive and utilise 360-800Hz three phase distribution instead of solely 400Hz. Another type is a 270VDC based system which also omits the constant speed drive and utilise rectification stages at the

generator output for 270VDC distribution [48]. The Lockheed Martin F22 is an example of a 270VDC system[48].

This thesis will primarily focus on power integration on the more conventional 400Hz AC system that is primarily in service to date. However, it should also be noted, that the integration method proposed in this thesis could potentially be applied to variable frequency systems also.

2.2.1.1 Harmonics within the fast jet electrical system

A large proportion of "electronic" loads include radar, avionic racks, DASS, FLIR utilize non-linear passive rectification front ends (most basic topologies shown in Figure 4 for three phase and single phase)[29]. To reduce weight of these loads, the smoothing inductance is reduced but at the expense of allowing high amounts of harmonic currents to manifest as part of the normal loading. In terms of overall power demand, the non-linear loading can make up about 1/3 to 1/2 of the total loading on each channel. General adverse effects of such harmonics are discussed in [53].

In addition to these loads and contributing to a lesser extent of harmonic current draw is the twelve pulse TRU itself (topology shown in Figure 3).

To compound the possible harmonic problem in fast jet, the majority of through life upgrades themselves will be non-linear in nature (incorporating some form of rectification) which would also increase the harmonic current content drawn from the main engine generation. Hence not only will through life upgrades increase power demands, but they are also likely to adversely affect the power quality of the AC system further.

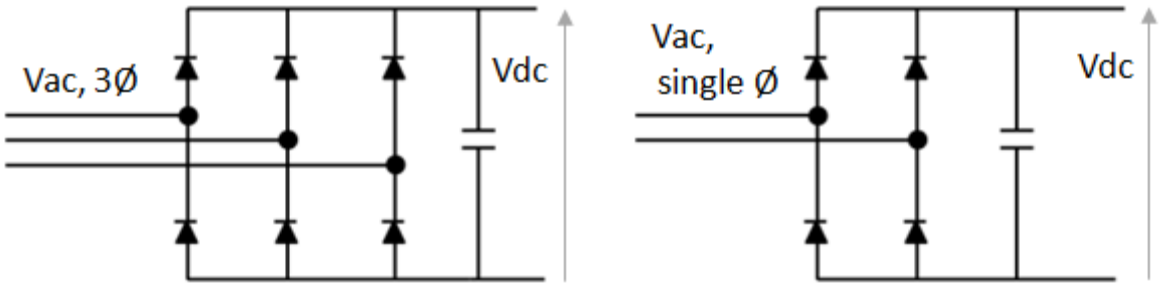

Figure 4- Basic passive 3 phase (left) and single phase rectifier topologies (right)

To mitigate harmonics at the equipment level, the current harmonics drawn from loads such as avionics equipment can be alleviated by altering the traditional six diode rectification front end with an active equivalent or with the use of higher pulse (e.g. 12, 18, 24) Auto Transformer Rectifiers (ATRUs) [52]. At the system level, harmonics can be dealt with by use of passive filters [54] or active filters such as Shunt Active Filters (SAF [54]) or Unified Power Quality Conditioner (UPQC) [55].

One widely acknowledged recommendation for harmonic limits on aircraft is, RTCA DO 160 [56]. This provides recommended levels of harmonic current limits for loads which include recommendations for 400Hz three phase 115Vrms aircraft electrical systems. These recommendations are summarised in Table 2 as a fraction of the 400Hz fundamental I_1. The voltage THD limit at the PCC is also recommended at less than 8%. As such, these were used as one of the main benchmarking parameters when assessing the power integration methods proposed within the thesis.

Table 2- DO 160F 3 phase limits for equipment current harmonics [56]

Harmonic Order	Limits
3^{rd}, 5^{th} 7^{th}	$I_3=I_5=I_7=0.02I_1$
Odd triplen Harmonics (h=9, 15, 21,…..39)	$I_h=0.1I_1/h$
11^{th}	$I_{11}=0.1I_1$
13^{th}	I_{13}-$0.08I_1$
Odd Non Triplen Harmonics 17, 19	$I_{17}=I_{19}=0.04I_1$
Odd Non Triplen Harmonics 23, 25	$I_{23}=I_{25}=0.03I_1$
Odd Non Triplen harmonics 29, 31, 35, 37	$I_h=0.3I_1/h$
Even Harmonics 2 and 4	$I_h=0.01I_1/h$
Even Harmonics> 4(h=6, 8, 10,….40)	$I_h=0.0025I_1$

2.2.2 Spatial representation

The spatial representation of a generic fast jet electrical system is presented in this section to shed light on the location of electrical equipment in relation to the airframe and to each other. This is in order to appreciate not only where the major loads are located within the compact airframe but also where supplementary generation can potentially be inserted. In this spatial representation a generic fast jet of 15m length and 10m wingspan is used.

Figure 5 illustrates the prime movers/jet engines of a typical twin engine fast jet aircraft in which the engine air inlet (depicted as see through blue and green) and the jet engines (solid grey) in the engine bay are shown. The blue and green solid blocks represent the subsequent generator location in relation to these engines. The mechanical off take from the generator has been omitted in the spatial illustration for simplicity.

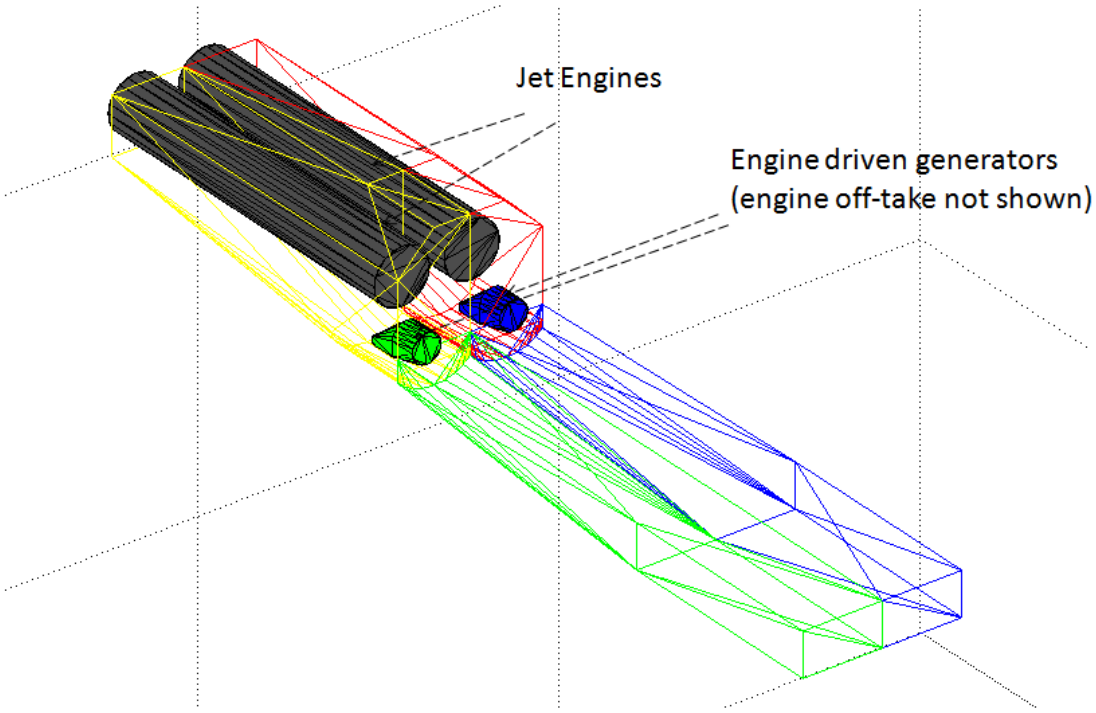

Figure 5- Generic fast jet engine and engine driven generator layout (engine bay and engine inlet)

Forward of the engine bay section, Figure 6 below depicts the location of the AC busbars, TRU, DC busbars and APU. These are housed inside the centre fuselage which is located on top of the engine air inlet and in front of the engine bays.

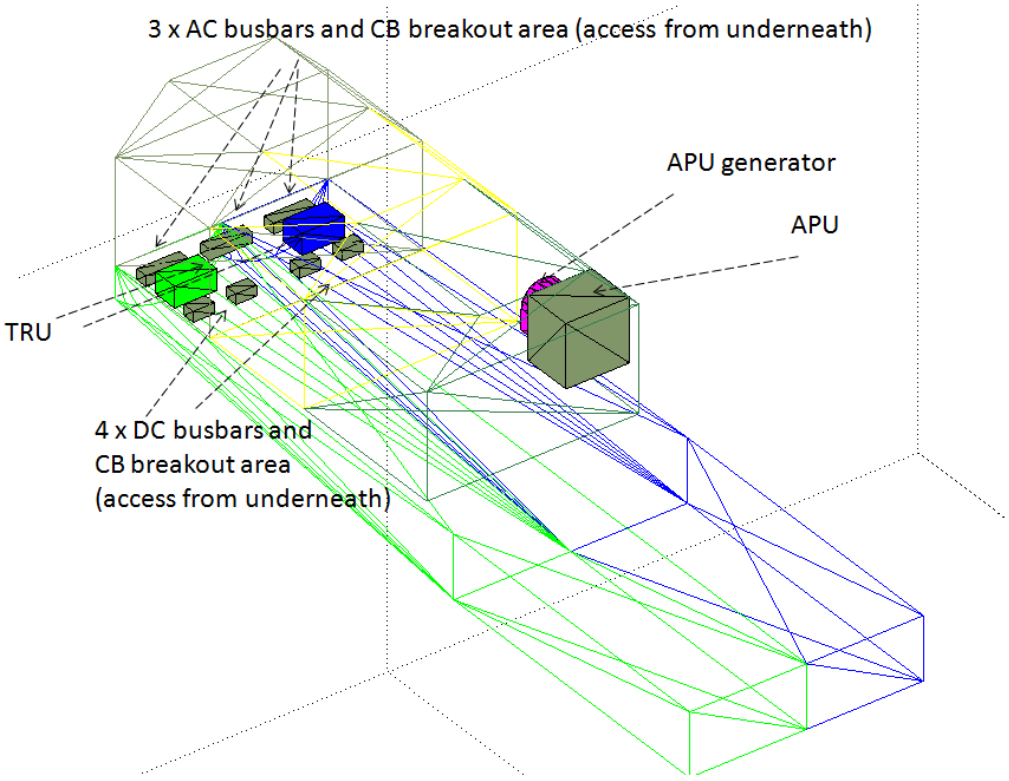

Figure 6- Generic fast jet electrical busbars, TRU and APU in centre fuselage

Figure 7 depicts some of the major loading (in solid red) which is situated around the cockpit and Radome. These loads are non-linear in nature and require DC power through passive rectification from the AC busbars as mentioned before.

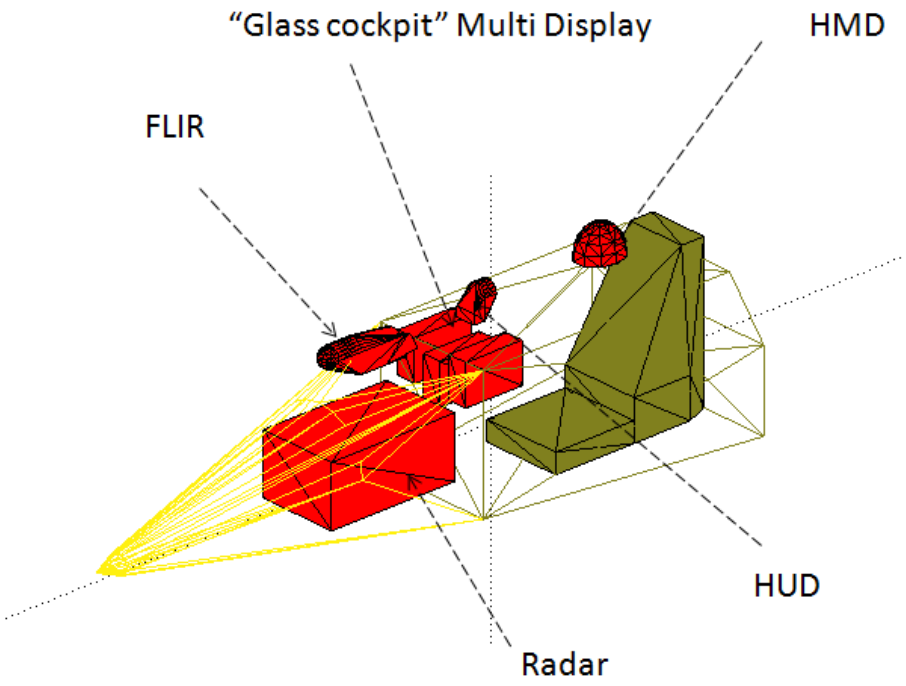

Figure 7- Generic major fast jet cockpit and radome loads

Shown as solid red blocks in Figure 8, more avionics are situated behind the cockpit in left and right avionic bays organised into racks. Similarly to the Radome and cockpit loads, these avionic racks loads also require rectification (and are non-linear in nature) to the AC power.

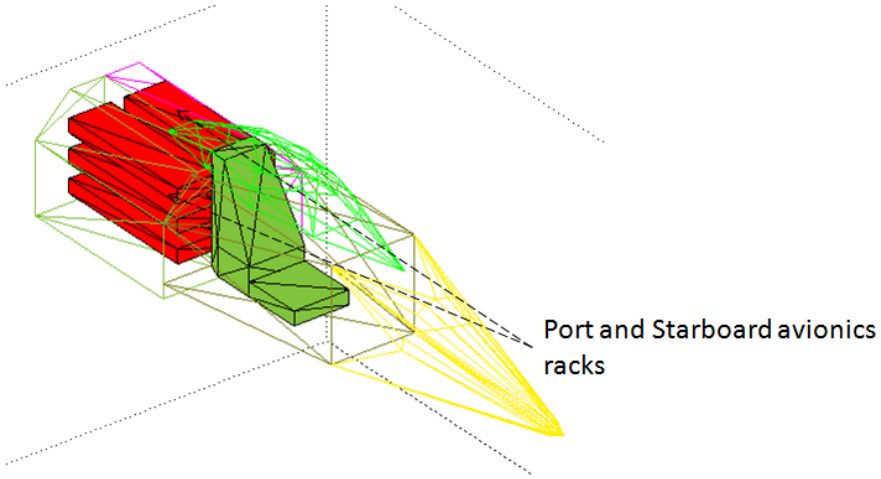

Figure 8- Generic fast jet mission computing avionics racks

Additional to internal loads, different missions require different load outs on the external connection points/hardpoints (Mil Std 1760 [50]). Two variations are the Lockheed Martin F22 Raptor or F35 JSF which primarily utilise internal weapon bays for “day one” capabilities, however even these have external hardpoints on the wings to increase load out when maximum stealth is not needed.

Hardpoint mounted loads draw power for sensors and processing communications while they are attached to the fast jet (internal battery is utilised upon release). This is usually for a short amount of time compared to the overall mission duration. As such, this could offer a potential opportunity to utilise the likes of auxiliary or emergency power in parallel to the main generation to provide for the associated peak power.

Figure 9 below shows these hard point locations around the generic aircraft model highlighted in solid red whereby thirteen hardpoints are shown (the centre hardpoint is taken up by a solid green cylinder representative of a fuel tank instead of an electrical load which maybe the set up for some cases to increase aircraft flight range). Additional to these thirteen hardpoint loads, wingtip pods are also depicted which have DASS loads drawing from the main electrical system.

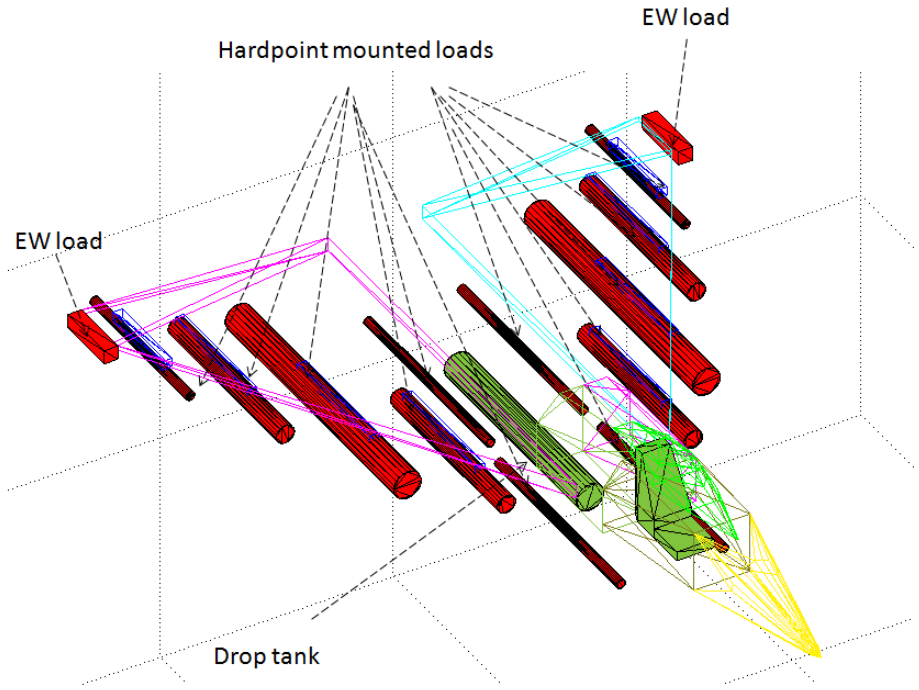

Figure 9- Generic fast jet hardpoint mounted and wingtip loads

With different sections of the fast jet presented, Figure 10 (left hand side) below illustrates these sections and electrical loads integrated as the complete fast jet aircraft (other systems such as mechanical, hydraulics omitted to focus on electrical equipment). The right hand side of Figure 10 illustrates the closed off opaque airframe equivalent, with the systems inside and out of view to

illustrate the lack of protrusion of equipment. Similarly other types of upgrades mostly likely will need to adhere to this as well, including addition of power generation.

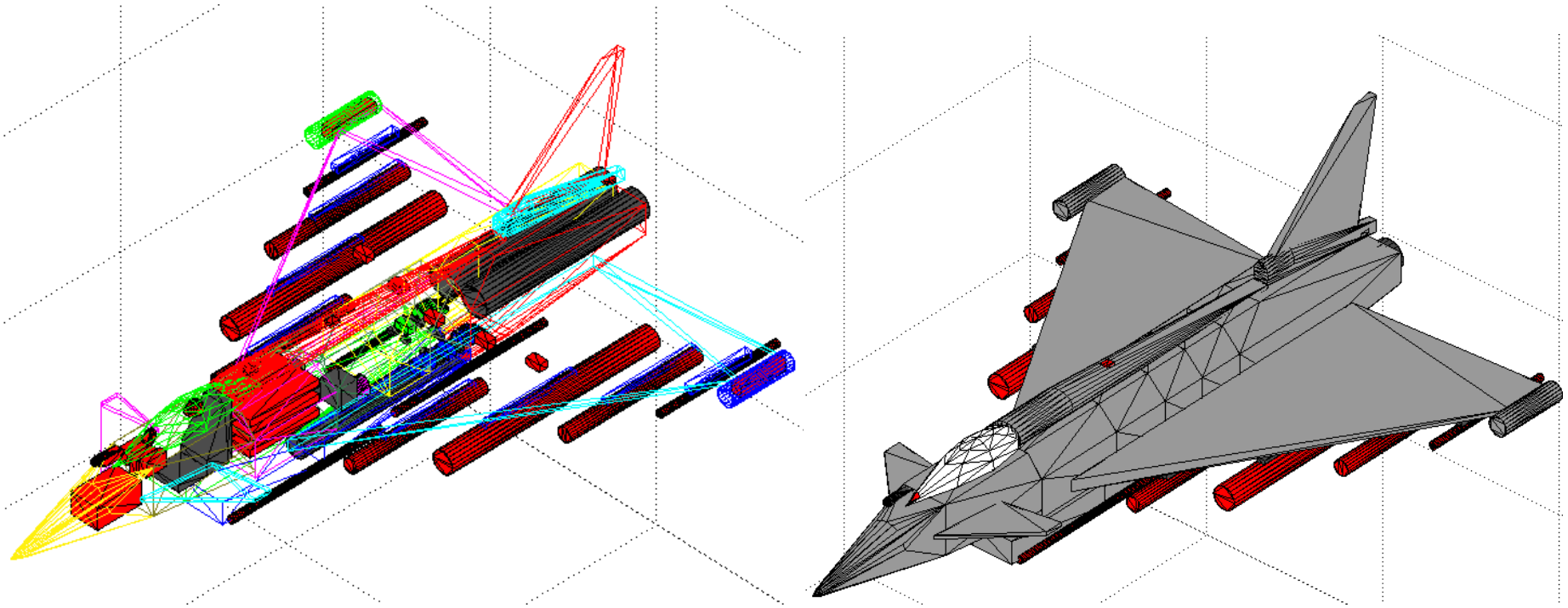

Figure 10- Complete generic fast jet illustration see through (left) and opaque (right)

2.3 Load characterising and benchmarking of power draw

This section presents the quantitative benchmarking of different loading types using individual load models within a larger representative fast jet electrical system model. The parameters of the representative generic fast jet electrical system model are given in Table 3 which includes approximate aircraft generator stator, feeder and load branch impedances. The individual load models which represent different load types were then applied to this for subsequent benchmarking. By achieving these bench marks, the comparison of the power integration solutions of this thesis could be assessed in terms of the power alleviation they provide to the main generation while maintaining power quality.

Table 3- Parameters of the fast jet generator, feeder, line impedance used for modelling

Model component	Parameter	Value
3 Phase Voltage Supply Representing Synchronous Generator	Nominal voltage	115Vrms
	Frequency	400Hz
	Nominal apparent power capacity	30kVA (50kVA short term)
	Nominal apparent power capacity current at nominal voltage	86Arms
	Stator inductance	20uH
	Stator resistance	0.02Ohms
Feeder Impedance	Length	1m to PCC
	Number of wire per phase	7 x gauge 9 in parallel
	Inductance	0.1652uH
	Resistance	370uOhms
Default Loading Line Impedance	Length	10m from PCC to Load
	Number of wire per phase	2x gauge 8 in parallel
	Inductance	7.97uH
	Resistance	10.3mOhms

2.3.1 Benchmarking simulation details

The benchmarking was performed utilising the Matlab/Simulink, SimPowerSystems package [58]. The following major, three phase balanced fast jet aircraft load types were benchmarked:

- Linear loading (e.g. heat/resistive loads)
- Induction machine loading (e.g. fuel pumps and cooling fans)
- Non-linear loading (e.g. avionic racks, radar, FLIR, DASS and some hardpoint loading)
- TRU loading (e.g. 28VDC busbar)

In the benchmarking, typical individual load power demand levels used/examined were approximately 10kW for three phase linear/induction machine/non-linear loading and 5kW for TRU.

This is to simply mimic bulk loading levels of major loads within a fast jet electrical system with a per channel rating of 30kVA (generation capacity).

Further benchmarking included a combination of these individual loading models, approximating the combined loading on a single fast jet aircraft electrical system channel. This is approximately a 25kW draw (from a 30kVA capacity channel, at the start of service life before any through life demand increases have been introduced). The current draw profile of this model was validated by comparing against real life fast jet aircraft electrical loading data and *ITHD* to confirm that such profile are typical of what an actual fast jet exhibits.

Further examination of different non-linear load power levels additional to the base 10kW level case were examined as well as an examination in varying the number of non-linear loads drawing from the same PCC from the main generation. This is due to: through life upgrades are likely to be "electronic" in nature and likely to cause further increase to the harmonic distortion as mentioned in chapter 1.

2.3.2 Benchmarking metrics

With the presence of non-linear loading from the majority of "electronic" load types on a typical fast jet aircraft electrical system, the use of instantaneous power theory calculations [57] given by equations 1-3 was deployed within the simulations in order to derive the separate power components for benchmarking real power *P,* reactive power *Q* and apparent power *S*. Equations 1 and 2 are Clarke transformation of the three phase voltages and currents.

$$\begin{bmatrix} \mathrm{V_a} \\ \mathrm{V_b} \\ \mathrm{V_c} \end{bmatrix} = \begin{bmatrix} \mathrm{V_{a1}}\cos(\omega_1 t) + \sum_{an}^{\infty} \mathrm{V_{an}}\cos(n\omega_1 t + \emptyset_{an}) \\ \mathrm{V_{b1}}\cos\left(\omega_1 t - \frac{2\pi}{3}\right) + \sum_{bn}^{\infty} \mathrm{V_{bn}}\cos\left(n\omega_1 t + \emptyset_{bn} - \frac{2\pi}{3}\right) \\ \mathrm{V_{c1}}\cos\left(\omega_1 t + \frac{2\pi}{3}\right) + \sum_{cn}^{\infty} \mathrm{V_{cn}}\cos\left(n\omega_1 t + \emptyset_{cn} + \frac{2\pi}{3}\right) \end{bmatrix}$$

……..(1)

$$\begin{bmatrix} \mathrm{I_a} \\ \mathrm{I_b} \\ \mathrm{I_c} \end{bmatrix} = \begin{bmatrix} \mathrm{I_{a1}}\cos(\omega_1 t) + \sum_{an}^{\infty} \mathrm{I_{an}}\cos(n\omega_1 t + \varphi_{an}) \\ \mathrm{I_{b1}}\cos\left(\omega_1 t - \frac{2\pi}{3}\right) + \sum_{bn}^{\infty} \mathrm{I_{bn}}\cos\left(n\omega_1 t + \varphi_{bn} - \frac{2\pi}{3}\right) \\ \mathrm{I_{c1}}\cos\left(\omega_1 t + \frac{2\pi}{3}\right) + \sum_{cn}^{\infty} \mathrm{I_{cn}}\cos\left(n\omega_1 t + \varphi_{cn} + \frac{2\pi}{3}\right) \end{bmatrix}$$

……..(2)

The instantaneous components of *P* and *Q* and subsequently apparent power *S* can then be given by eq'n 3 once the α and β axis version of voltage and current are revealed from vector control transformation.

$$S = (V_\alpha + jV_\beta)(I_\alpha - jI_\beta) = P + Q = (V_\alpha I_\alpha + V_\beta I_\beta) + j(V_\beta I_\alpha - V_\alpha I_\beta)$$

……..(3)

By doing so, establishment of the real, reactive and apparent (*P*, *Q* and *S*) power from the main generator at the PCC under different loading was possible (whether for linear or non-linear loading) and revealing the real power utilised at the loads. Breaking down the components of *P* and *Q* profiles through time, the 400 Hz components of voltage and current becomes the averaged components of $\bar{P}$ and $\bar{Q}$ and the harmonic components are the superimposed oscillating components $\hat{P}$ and $\hat{Q}$ which do represent a net transfer of energy [57].

Subsequently: *P*, *Q*, *S* values along with *FFT*, *THD* (eq'n 4), magnitude of major harmonic orders (5^{th} and 11^{th}), fundamental V_{rms} and I_{rms} and additional voltage zero crossings of the voltage waveforms were used as the main performance metrics in the benchmarking of the different types of loading. Another indicator of performance used in the bench marking is the rectified voltage quality of non-linear loads (six diode rectifiers and TRUs) which is more important than the PCC AC voltage quality itself as this becomes the input of the actual loading aft of the rectifier stage.

$$THD = \frac{\sqrt{\sum_n^{\infty} \mathrm{h_n}^2}}{\mathrm{h_1}}$$

……..(4)

2.4 Benchmarking results

In this section, the results of the bench marking are summarised for the individual loading types as well as the combined loading simulation as summarised in section 2.3.1.

2.4.1 Basic benchmarking of individual loads

The following Table 4 summarises the results of the bench marking of individual loads drawing from the fast jet electrical system model (utilising the values of Table 3). The results in the 1st row is for a 10kW purely resistive load type and represents ideal linear loading conditions where there is no reactive power (unity power factor), and negligible *VTHD* and *ITHD*.

The 2nd row is the results of a 10kW induction motor load and similarly to the resistive loading, there is negligible *VTHD* and *ITHD* at steady state.

The 3rd row of table summarises a three phase non-linear load (with a six diode rectifier) such as those used by “electronic” type loads in fast jet. Here it can be seen that there is adverse effects on the power quality as expected with a *VTHD* at 4.38% and *ITHD* at 54.36% compared to the negligible results of the linear loading case. In this scenario, resistive backend loading is used to consume the power.

The 4th row summarises the results for a 5kW TRU (with resistive backend) in which although there is harmonic content in the system, the twelve pulse nature of the TRU causes them to be relatively small compared to the six diode rectifier non-linear case. This provides a *VTHD* at 1.41% and *ITHD* at 12.44%. Also because of the twelve pulse nature of the TRU; the 5th current harmonic is smaller than the TRU 11th harmonic.

Within these results, there were some minor discrepancies in the real power drawn compared to the specified 10kW and 5kW. However this has little impact on the actual power quality examined and also all comparisons of power integration methods examined in subsequent chapters were compared back to these bench marked power draw values rather the ideal 10kW and 5kW values.

Table 4- Basic electrical benchmarking of typical fast jet load types

Case	Averaged PCC S (kVA)	Averaged PCC P (kW)	Averaged PCC Q (kVAR)	VTHD (%)	ITHD (%)	Fundamental Voltage RMS Phase A (V)	Fundamental Current RMS Phase A (A)	Current 5^{th} Harmonic (A)	Current 11^{th} Harmonic (A)	Load Draw (kW)
Resistive/Linear	9.95	9.95	0.05	0.07	0.07	114.8	28.87	0.13	0.07	9.92
Induction machine steady state	11.02	11	0.66	0.1	0.14	114.7	31.57	0.14	0.08	10.97
Non-linear(resistive back end)	10.18	9.69	2.16	4.38	54.36	114.6	29.16	14.03	2.39	9.65
TRU (resistive back end)	5.20	5.15	0.23	1.41	12.44	115.1	12.44	0.07	1.27	5.08

2.4.1.1 Linear loading benchmark results

Looking at these results in more detail, Figure 11 illustrates the *P*, *Q* and *S* profile of the resistive load benchmarking. This linear loading, provides flat profiles for the *P, Q* and *S* components whereby there are also virtually non-existent ripples. Figure 12 illustrates the *V* and *I* profiles and because the loading is linear, the waveforms of these are sinusoidal. Only phase A is displayed in this graph, as the loading examined here is balanced and the other two phases will exhibit the same magnitude and profiles (hence omitted in the illustration). This bench marking represents ideal loading conditions from a main generator as well as power quality at the PCC.

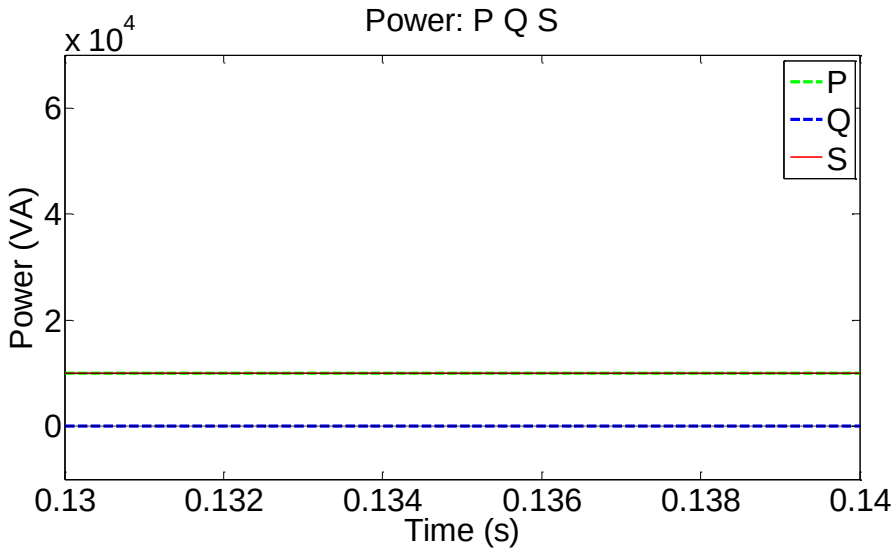

Figure 11- P, Q and S profile of 10kW linear loading

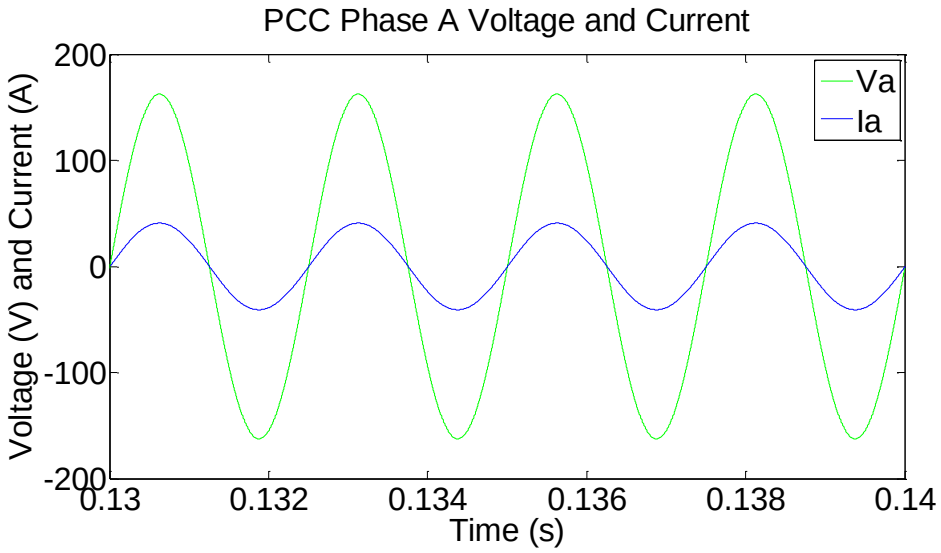

Figure 12- Voltage and current profile of 10kW linear loading

2.4.1.2 Induction machine loading benchmarking

Figure 13 and Figure 14 shows the *P*, *Q* and *S* profiles as well as the *V* and *I* profiles respectively for the induction motor load type bench marking. Although there is an initial surge of power at the start of power up (the time axis has been extended to display this), this only occurs once during each flight cycle in which for the rest of the time, the loading is in the smaller amplitude steady state levels similar to the resistive loading.

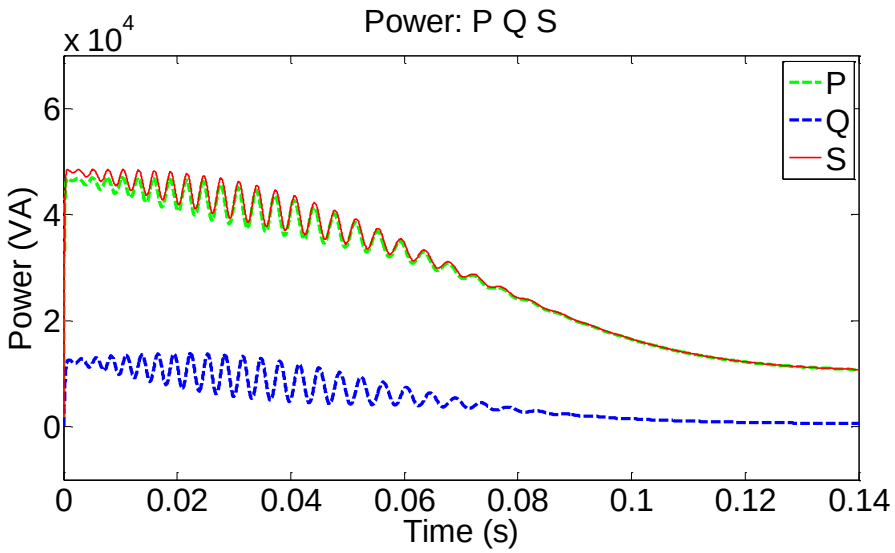

Figure 13- P, Q, and S profile of 10kW induction motor loading

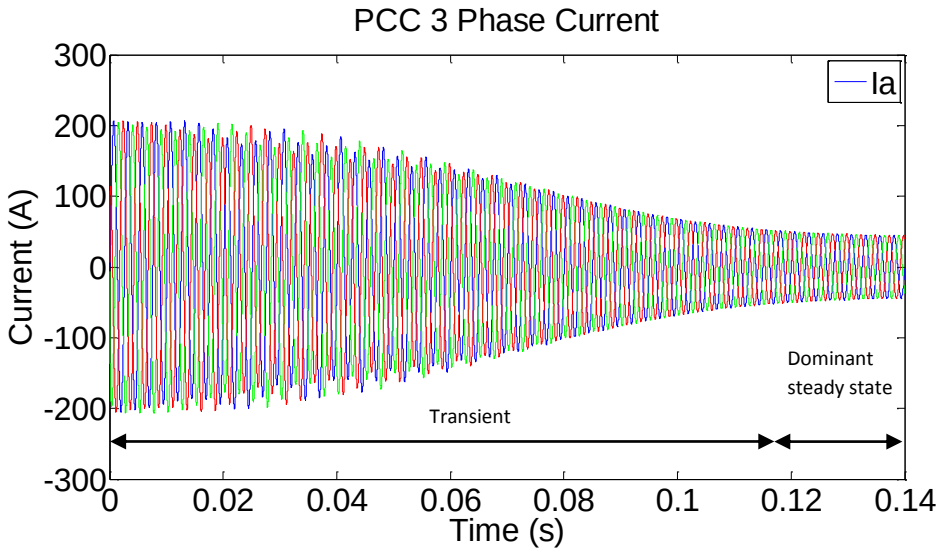

Figure 14- Voltage and current profile of 10kW induction motor loading

2.4.1.3 Non-linear loading benchmark

Contrary to the previous two load type benchmarking, the non-linear loading is more harmonic rich in terms of voltage and even more so for in terms of the current drawn at the PCC. It can be seen from Figure 15 for the power plot, that there are ripple components in the *P* and *Q* traces which do not represent actual transfer of energy. Also on the same figure, the upper dashed trace represents the theoretical 10kW line which approximates the overall real power the load is utilising (the DC loading/local loading aft of the rectifier).

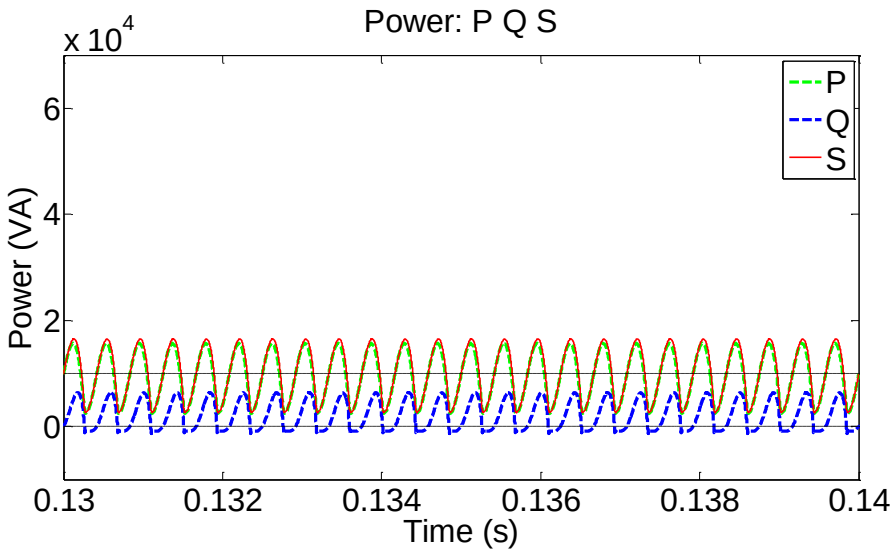

Figure 15- P, Q and S profile of 10kW non-linear loading

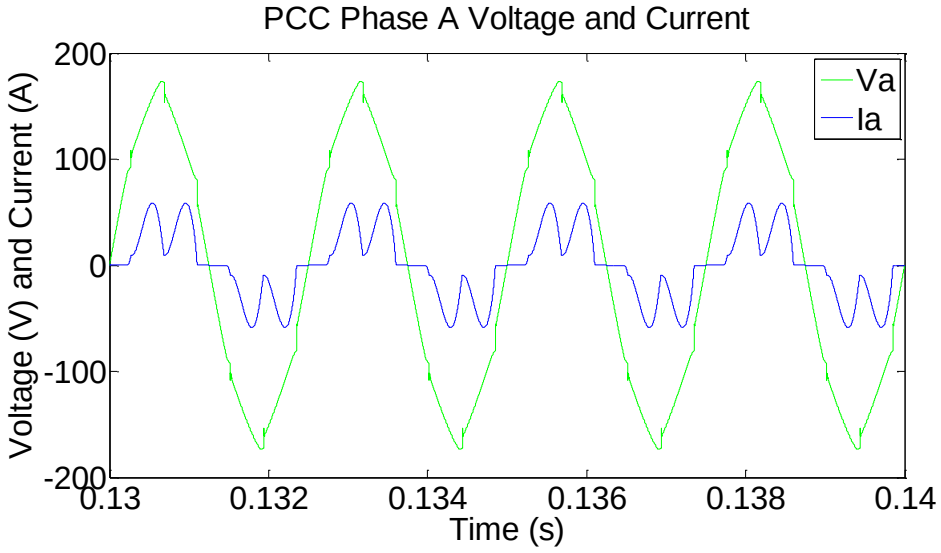

Figure 16- Voltage and current profile of 10kW non-linear loading

Figure 16 further illustrates this high harmonic content through typical *V* and *I* waveforms drawn; whereby the 5th and 7th harmonics are dominant. Such distortion could potentially cause some of the

problems discussed in [53] additional to distorting voltage supplies to other loads connected to the same PCC.

Figure 17 illustrates the *FFT* comparison of this non-linear loading against the DO 160 limits [56] specified before, in logarithmic scale. It can be seen that the 5th and 7th harmonic (the 2nd and 3rd blue points on the figure from the left axis) are dominant and has exceeded the limits of DO 160 in this particular case.

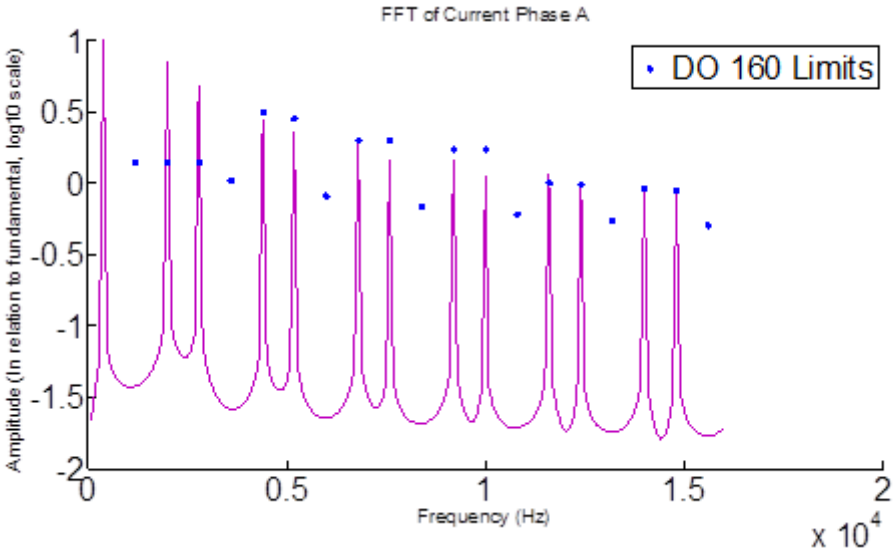

Figure 17- Current FFT plot of non-linearbench marking against DO 160 limits

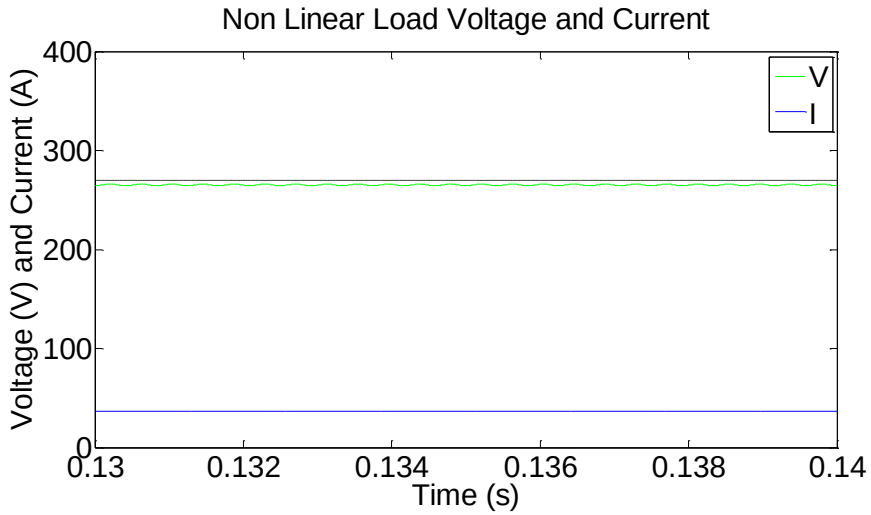

Figure 18- Voltage and current plot of DC side of non-linear load

Figure 18 illustrates the voltage quality aft of the rectifier of the non-linear load with backend resistive loading in which the dashed trace represents the 270VDC level (expected nominal levels). From this, it can be seen that the voltage is relatively ripple free and in accordance to the required

voltage levels. Hence even if the *VTHD* is high at the AC side the subsequent voltage entering the load aft of the rectifier may not be adversely affected.

2.4.1.4 TRU bench marking

Figure 19 and Figure 20 illustrates the *P*, *Q* and *S* profiles as well as the *V* and *I* profile of the 5kW TRU loading. In Figure 20, the current waveform harmonics is dominated by the 11^{th} and 13^{th} order harmonics as a result of the twelve pulse configuration of the TRU. The *ITHD* is relatively small when compared to the six diode rectifier non-linear load example presented in section 2.4.1.3. The ripple components on the *P, Q, S* profiles shown on Figure 19 are also more limited as a result. Hence it can be seen that in terms of harmonic distortion, the TRU is a relatively minor contributor within the overall electrical system.

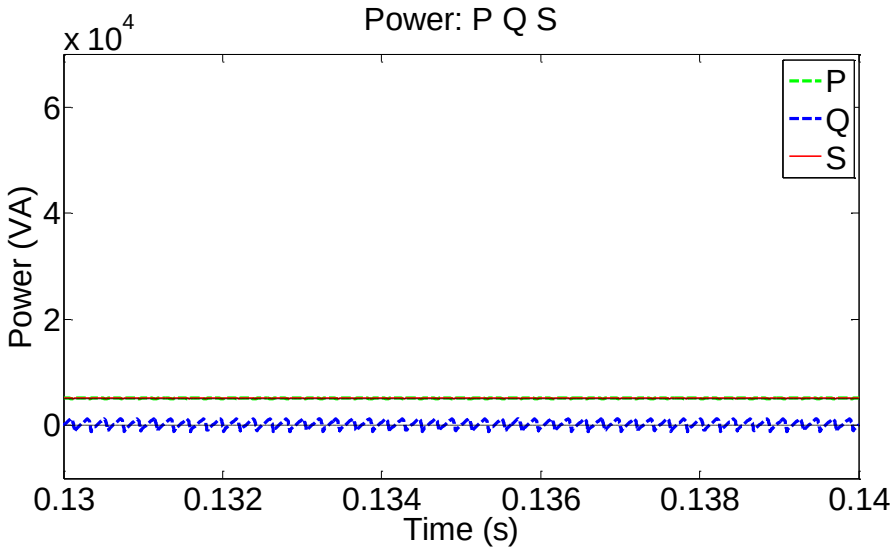

Figure 19- P, Q and S profile of 5kW TRU

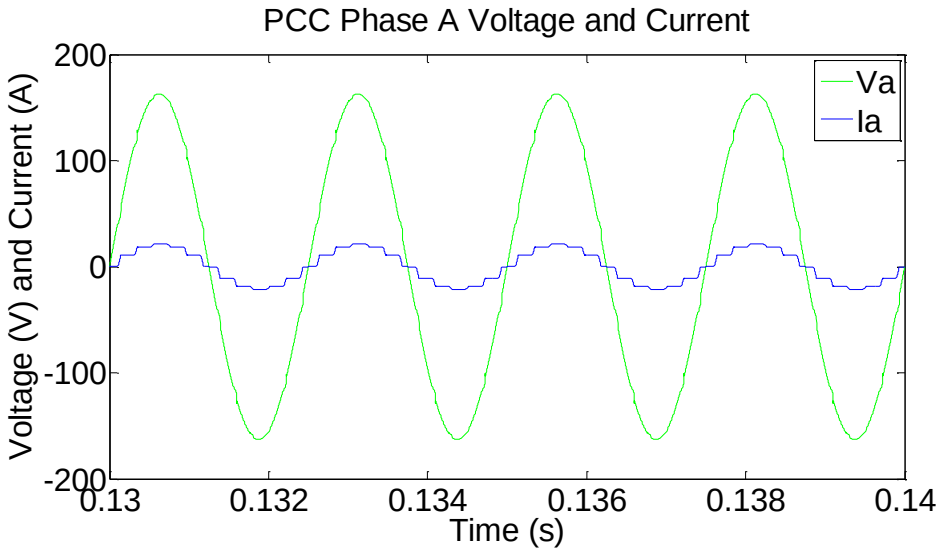

Figure 20- Voltage and current profile of 5kW TRU

In a similar manner to the results of the 10kW non-linear load benchmarking of section 2.4.1.3, Figure 21 illustrates the voltage quality aft of the TRU (the DC loading) in which the dash trace represents the expected nominal 28VDC level (in this case, it is slightly higher, at 30.5V). Again with adequate DC linkage and also smoothing inductance allows limited voltage ripple aft of the TRU.

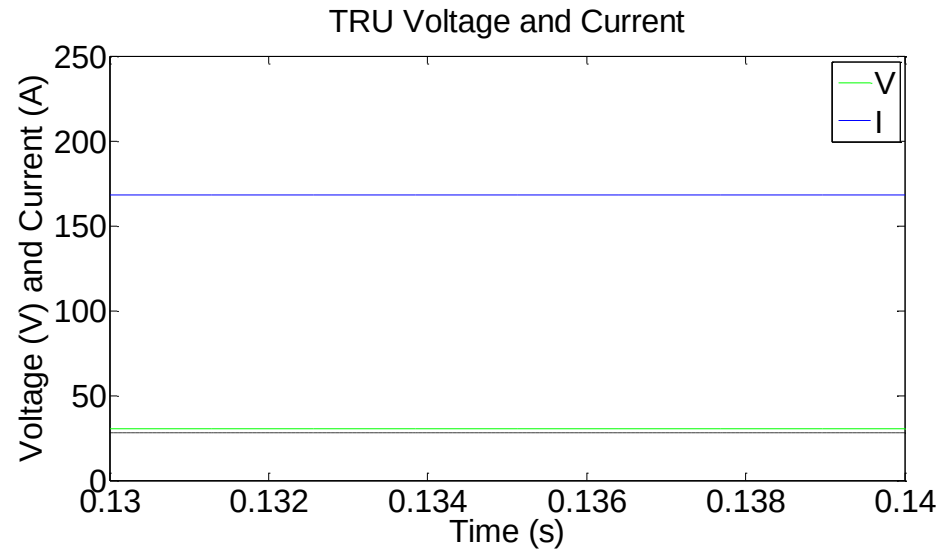

Figure 21- Voltage and current plot of DC side of TRU

2.4.2 Benchmarking of combined operation

Following from the bench marking of individual loads in the previous section, section 2.4.1, a summary of the benchmarking of an approximate single channel loading in a fast jet electrical system is presented in this section. This simulation consist of the combined operation of the 10kW linear load, the 10kW non-linear load and the 5kW TRU bench marked in the previous section; making up a combined loading of around 25kW. This combined loading was to mimic approximate baseline loading from a single channel with a 30kVA generation capacity before any demand increases have been added to the system (i.e. start of the fast jet service life). Subsequently, this allowed the simple system level effects of power integration methods examined in later chapters to be quantified.

The results of the combined loading is presented in the row 4 of

Table 5, while rows 1 to 3 are the individual load benchmarking results from the previous section 2.4.1, reiterated for comparison.

It can be seen that within the combined loading simulation, presented in row 4; the relative *ITHD* actually decreases (down to 21.3%) as the proportion of linear loading has increased when compared to the purely non-linear load case (section 2.4.1.3). The 5^{th} harmonic which is solely contributed by the non-linear load (section 2.4.1.3) is roughly the same in terms of absolute amplitude but the 11^{th} harmonic which is contributed by both the 10kW non-linear load (section 2.4.1.3) and the 5kW TRU (section 2.4.1.4) is actually smaller than their individual contributions combined or solely from the non-linear load. From this, there appears to be a certain degree of "cancellation" effect at the PCC when non-linear loading/TRU are operated in parallel which is possibly caused by the difference in harmonic phases of the non-linear load and TRU.

Table 5- Electrical benchmarking of typical fast jet load types in combined operation

Case	Averaged PCC S (kVA)	Averaged PCC P (kW)	Averaged PCC Q (kVAR)	VTHD (%)	ITHD (%)	Fundamental Voltage RMS Phase A (V)	Fundamental Current RMS Phase A (A)	Current 5^{th} Harmonic (A)	Current 11^{th} Harmonic (A)	Load Draw (kW)
Resistive	9.95	9.95	0.05	0.07	0.07	114.8	28.87	0.13	0.07	9.92
Non-linear(resistive back end)	10.18	9.69	2.16	4.38	54.36	114.6	29.16	14.03	2.39	9.65
TRU	5.20	5.15	0.23	1.41	12.44	115.1	12.44	0.07	1.27	5.08
Combined loading	24.51	24.3	2.21	4.26	21.35	113.6	71.75	13.69	1.75	24.17

Figure 22 and Figure 23 illustrates the respective *P, Q, S* profiles as well as the *V* and *I* profiles of this combined operation of loads drawing from the same PCC in a single channel. The upper dashed trace of Figure 22 represents the theoretical 25kW real power draw level (what the loads actually utilise).

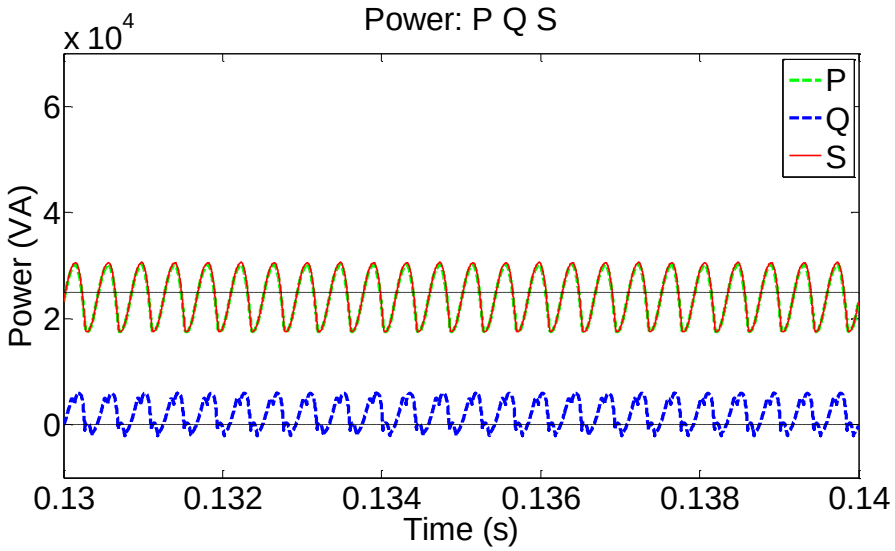

Figure 22- P, Q and S profile of combined loading

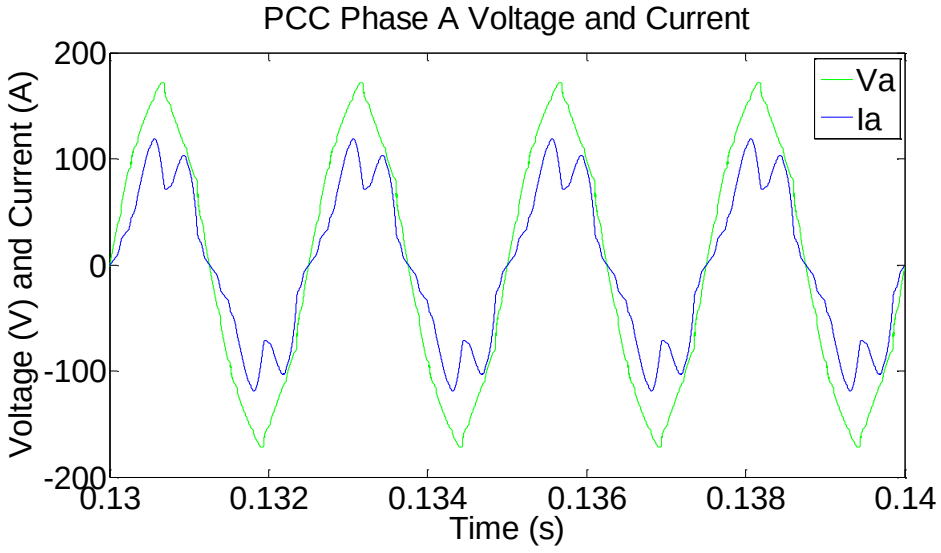

Figure 23- Voltage and current profile of combined loading

2.4.2.1 Benchmarking of varying non loading levels

As the high level of voltage and current distortion occurs with non-linear loading as well as likely future upgrades being non-linear as well; this was prioritised for further examination within the benchmarking of this chapter. As such, this section presents benchmarking comparison of varying non-linear loading levels to examine the effect trends of increasing non-linear loads. This was in terms of looking at 1) varying power draw from a single non-linear load and 2) varying the number of multiple non-linear loads drawing from the same PCC.

2.4.2.1.1 Varying draw from a single non-linear load

Firstly, Figure 24 illustrates the subsequent varying *VTHD* and *ITHD* with increasing loading from a single non-linear load. In this, the DC link at the non-linear load is kept constant. It can be seen that there is a general increase in *VTHD* and a decrease in relative *ITHD* (but increasing terms). This also causes the 8% *VTHD* (recommended by DO 160 [56]) to be exceeded at around the 35kW point shown in Figure 24 (represented by the green trace).

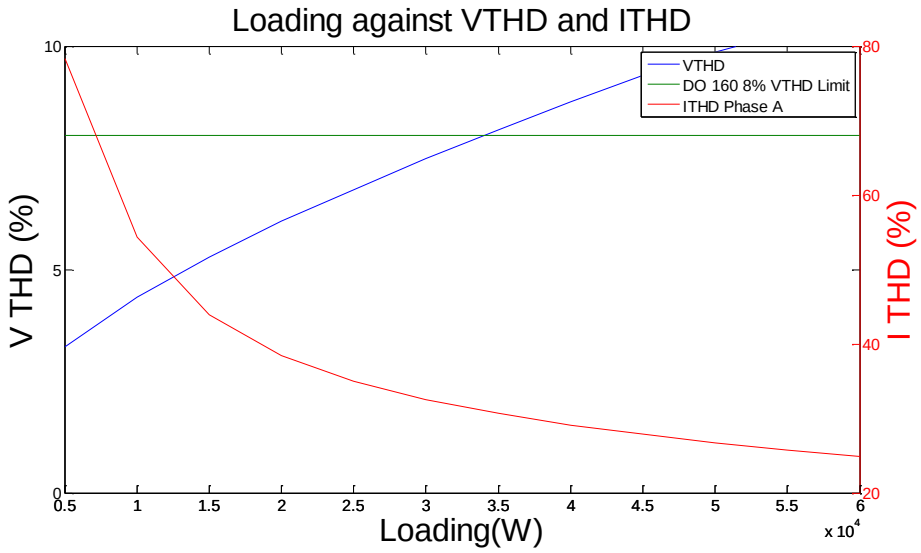

Figure 24- VTHD and ITHD against increasing loading level of a single non-linear load

2.4.2.1.2 Varying the number of non-linear loads

Table 6 below summarises the results of varying the number of identical non-linear loads drawing from the same PCC, ascending from 1x10kW to 6x10kW in 10kW increments. A similar trend in *VTHD* and *ITHD* was observed. In this, it can be seen that there is a decrease in fundamental voltage amplitude and also a decrease in power delivered to the load. This was observed for resistive back end, however, if constant power load was used, this would result in more current being drawn to maintain the power levels to the load. Again the 8% *VTHD* starts to become exceeded between the 3x10kW (30kW) to 4x10kW (40kW) region.

Table 6- Results of varying the number of non-linear loads drawing from the same PCC

Case	Averaged PCC S (kVA)	Averaged PCC P (kW)	Averaged PCC Q (kVAR)	VTHD (%)	ITHD (%)	Fundamental Voltage RMS Phase A (V)	Fundamental Current RMS Phase A (A)	Current 5th Harmonic (A)	Current 11th Harmonic (A)	Load Draw (kW)
1x10kW Non-linear load	10.18	9.69	2.16	4.38	54.36	114.6	29.16	14.03	2.39	9.65
2x10kW Non-linear load	19.79	18.78	4.22	6.19	39.05	113.7	56.67	20.47	4.083	2x 9.34
3x10kW Non-linear load	29.01	27.49	6.43	7.95	34.05	112.8	83.6	26.59	5.34	3x 9.12
4x10kW Non-linear load	37.84	35.79	8.69	9.50 (exceeded DO 160 limit)	30.94	111.9	109.8	31.81	6.20	4x 8.90
5x10kW Non-linear load	46.29	43.73	10.95	10.89 (exceeded DO 160 limit)	28.73	111	135.4	36.36	6.76	5x 8.70
6x10kW Non-linear load	54.19	51.18	13.14	11.66 (exceeded DO 160 limit)	26.75	110.3	157.9	39.48	6.65	6x 8.52

2.5 Summary

This chapter has presented the design details of a generic 400hz, three phase, 115Vrms fast jet electrical system to further set the scene of the power demand problem of this thesis and provide a point of comparison to assess the impact of the architectural changes proposed. This also included the spatial illustration of the electrical system and major loads within a generic fast jet airframe: driving home the unique space constraints of introducing more generation.

Electrical steady state models of the generic fast jet electrical system have been developed to quantitatively benchmark the typical loads of a fast jet electrical system through electrical simulation with representative system impedance (main generator stator, feeder and line impedance). This simulation based benchmarking included individual loads typical of a fast jet, combined operations of these and effects of varying power/varying number of non-linear loads drawing from the same PCC. Non-linear loads were examined further, as likely future upgrades on in service fast jet will be non-linear loads. These models provide the platform for assessing the effects of the power integration solutions proposed within later chapter of this thesis.

3 Literature review and proposed fast jet power integration solutions

3.1 Chapter overview

As mentioned in chapter 1 and making up the main work of this thesis: in the face of through life equipment upgrades increasing power demands on fast jet aircraft, one way to cope is to introduce supplementary power generation. This is to introduce power into the system to supplement the already existing main generation in a space conforming and distributed manner. This is mentioned in chapter 1 and 2 with the compact nature of fast jet design constraining bulk generation additions to the airframe. As such any additional generation needs to be distributed to fit into the remaining space and because the fast jet electrical system and main generation are already present and operating as part of the fast jets normal operations; limited rework is desired in an attempt to maintain the integrity of what is already there. As such any integration of supplementary generation onto the aircraft is desired to be loosely coupled and adhering; in that, their operations require minimal modifications to the existing generation but at the same time can also work together with it. Such integration of supplementary generation has not been widely applied on fast jet to date. Hence this chapter presents the literature review which identified potentially transferable/adaptable solutions of topologies and control for paralleling for fast jet applications. These are taken from other domains such as civil aerospace, M/DG/R and EVs.

Firstly, a literature review is provided to support the argument for supplementary generation on fast jet by identifying existing and maturing power generation sources that are flight cleared and have precedence of in-flight operation. It is desired that these generation sources are engine mechanical off take independent to aid distributed solutions around the remaining space of the fast jet aircraft.

This literature review started off with examining such sources researched in other aerospace applications (other than fast jet) to identify what could potentially be transferred for the fast jet through life upgrade problem. Although not cleared for fast jet as of yet, these do provide examples with pedigree of in flight operations.

This was then followed by the review of established auxiliary and emergency power used in actual fast jet electrical systems but have not traditionally been paralleled or operated during normal operations with the main generation. As such, identification of these sources provides example of

flight cleared generation sources that can potentially lend themselves to meet the upgrade problem for fast jet.

In summary, established fast jet auxiliary power sources such as RATG, engine mechanical off take independent turbine generators to less widely applied up and coming alternatives such as Thermo Electric Generators (TEG) and Solid Oxide fuel cells were identified as potential sources for the supplementary generation application on fast jet.

However, without widely applied paralleling of such supplementary generation within fast jet and as the main focus of this chapter; a literature review of topologies and paralleling techniques in other non-aerospace domains was conducted and is presented. The review included examining techniques that enable supplementary generation sources to be flexibly incorporated into existing electrical systems which are used across a wide range of application domains not typically including fast jet. From this review; read across of enabling techniques can be applied to integrate such power generation on fast jet and in particular to cope with the underlying problem of through life upgrade. With this, down selected paralleling techniques for adding supplementary generation to an already defined and operating electrical network in other domains were chosen for further investigation. This provides the basis and current state of the art which their application (including tailoring) for fast jets are subsequently explored in chapters 4-7.

3.2 Generation sources literature review

In order to examine adding supplementary generation onto a fast jet electrical system as a viable option to meet increasing through life power demands; this section identifies research of alternative generation (alternative to main engine driven generation) in aerospace systems. This offers an insight of alternative generation sources that could be potentially applied to the fast jet upgrade problem in parallel to the main generation (including flight clearance precedence) to meet the increase in through life demands. Included in this, are the generation in other aerospace research, as well as existing auxiliary and emergency generation examples. The latter also gives indication of power output levels of sources that have been successfully operated on fast jet to date (but not in parallel to main generation). These are more mature and readily applicable today, whereas the sources researched for other aerospace applications could be applied in the future as they become more proven and power dense.

3.2.1 Alternative aerospace generation sources

This section presents the literature review results of alternative generation sources other than engine driven generation.

3.2.1.1 PEM fuel cells

In [59] the in-flight demonstration of a paralleled PEM fuel cell and battery system for powering a light electric propeller driven aircraft is described. In this set up, two operation modes are examined: with or without power electronics to control power flow. In both set ups, the battery is not recharged during flight and only provides the power peak required for take-off. Power levels demonstrated were 40kW for around 7 minutes for the take-off phase utilising both the fuel cell and battery, and 20kW for the rest of the flight solely on the fuel cell supply. The voltage level of the electrical system was rated at 270VDC. Figure 25 below shows the approximate power profile against time on the left and the basic electrical architecture on the right.

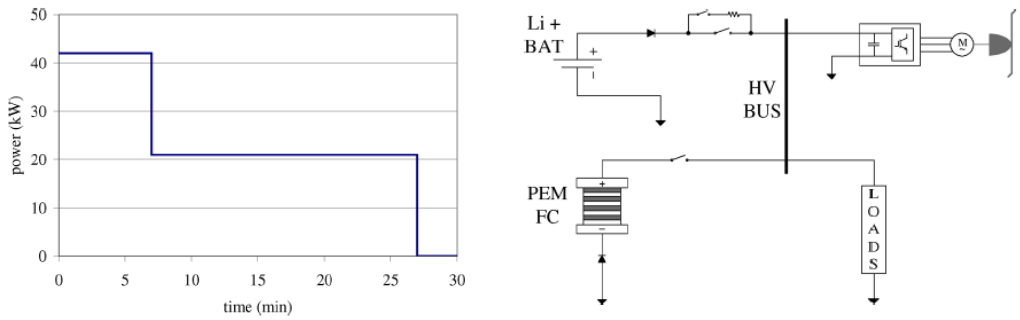

Figure 25- Power draw and electrical setup Boeing E-plane [59]

The aircraft used was a modified "*Austrian HK36 Super Dimona motor glider".* The base aircraft design itself has an empty weight of 560kg (excluding fuel) and a maximum take-off weight of 770kg [60]. The modification in [59] added a fuel cell, battery, power electronics and control, electric motor and thermal management which increased the operational weight up to 870kg including the pilot [59]. Although not specified in the paper for the pilot's weight; hypothetically, if the pilot has a weight of around 90kg as a rough estimation, then this would imply an increase of around 400kg maximum weight for the system changes (including battery but excluding equipment that may be taken out of the original aircraft, such as the heavy fuel engine). Although a direct weight increase in fuel cell system cannot be calculated from this: a magnitude scale comparison to engine driven generator power densities of conventional fast jet aircraft can be made (this being typically around 1kW/kg for conventional fast jet aircraft).

From this, it is obvious that the PEM fuel cell option is significantly less power dense. However, this much lower power density does not necessary discard the PEM fuel cell as a useful supplementary generation candidate; as the application of such fuel cell would not be a direct replacement to the main generation itself. The benefits of fuel cell would be in the potential flexible distributed locating for conforming to remaining space of the fast jet (without the need to be connected to a gearbox off take). The demonstrated continuous 20kW output is also very well aligned with the 10s of kVA levels associated with fast jet loading [25]. Further to this, the application could be split into a number of smaller fuel cells to give the 20kW total output as fuel cell power to weight ratio (scalability) is more linear when compared to gas turbine generators [103].

At small Unmanned Aerial Vehicle (UAV) level fuel cells have also been utilised. An example is the Aeropak fuel cell module provided by Horizon, shown in Figure 26 [67] below. This utilises PEM fuel cells with NaBH4 packs or compressed hydrogen bottles as the main fuel source which is aimed at the lower size scale man portable UAVs. The continuous power level is rated at 200W (short peak rating of 600W for 2 minutes) at a system weight of 470g excluding the fuel pack (plus the fuel pack would add 1570g for 1 litre of NaBH4 for 900WH). Similar to the Boeing E-Plane [59] presented; the benefits of engine off-take independence as well as ease of handling means this could be a potential supplementary source of generation for fast jet application. Figure 27 is a concept illustration of such potential application of PEM within the generic fast jet model (presented in chapter 2).

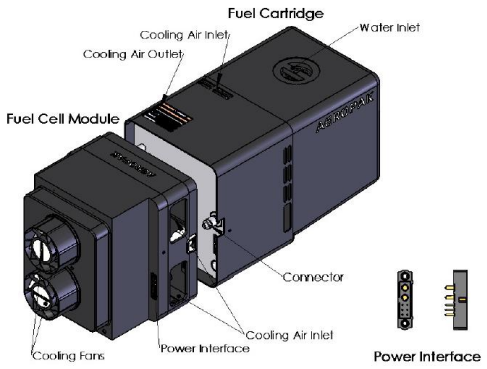

Figure 26- Example COTS PEM fuel cell for small UAV applications [67]

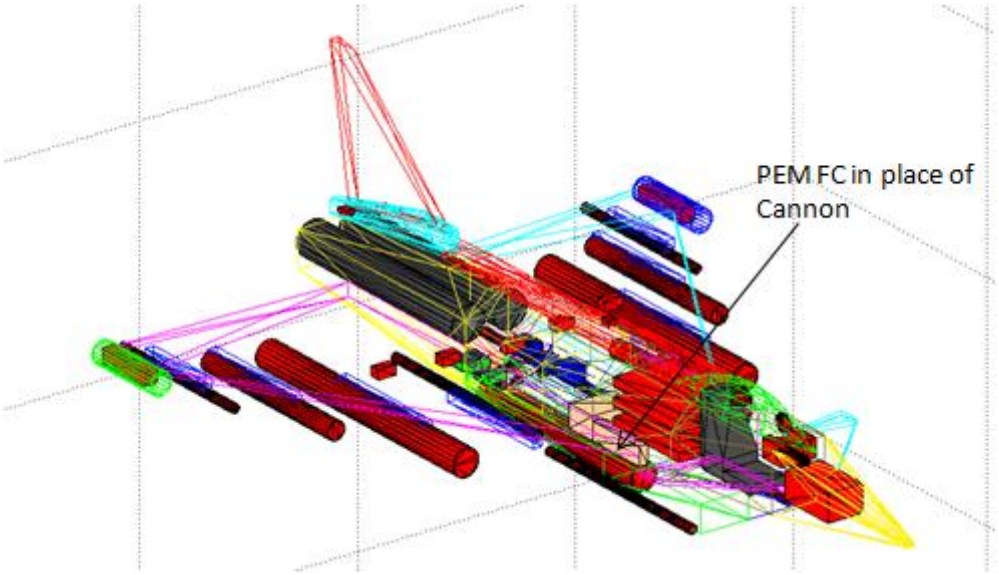

Figure 27- Concept art of PEM fuel cell application within a generic fast get

3.2.1.2 Solid Oxide fuel cell

Another example of unconventional power supply in aerospace is summarised in [60]. In this, a proposed Solid Oxide fuel cell APU is presented (as opposed to the PEM fuel cell of the previous section) for the tail-cone on civil aircraft application. This proposal incorporates a hybrid Solid Oxide fuel cell and fuel cell exhaust gas driven turbine generator: paralleling the output of the individual generation sources through rectifiers into a common DC link (shown in the right of Figure 28). The Solid Oxide fuel cell also provides the benefit of partial reforming of aircraft fuel, compared to the need for separate on-board fuel supply that is required by PEM fuel cells [61] (i.e. hydrogen fuel

tanks or NaBH4). The turbo machinery in this setup itself is driven by fuel cell exhaust which drives a single generator set (shown in the left of Figure 28). The output voltage levels stated is aimed at 540V at 440kW, with downstream power conversion for the standard 270VDC, three phase 230Vac and 115Vac levels through individual converters. The air supply to the system is provided by a ram air inlet also located in the cone as well as the exhaust outlet shown in Figure 29.

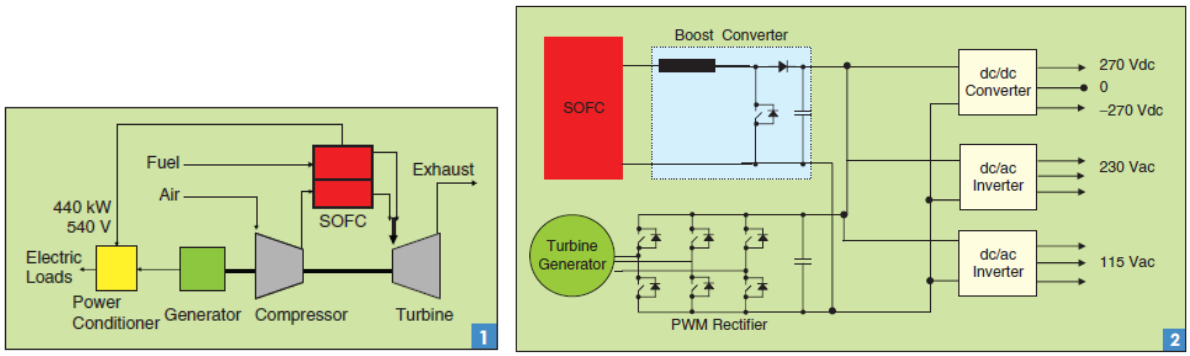

Figure 28 System and electrical architecture of described Solid Oxide fuel cell for civil aircraft [61]

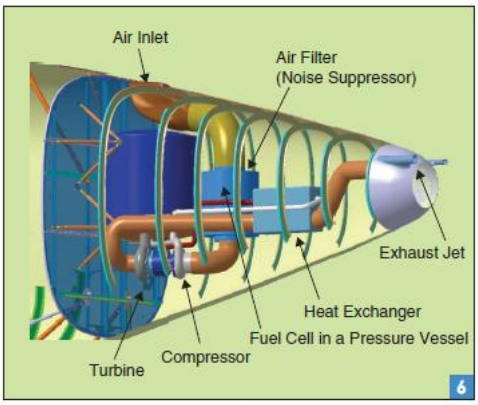

Typical packaging concept, using outside air, at the tail end of the airplane.

Figure 29- Set up of tail cone APU concept from Boeing [61]

The system weight requirement of this was specified at >500W/kg which is more comparable, but still less than the 1kW/kg standard for fast jet main generator power density. In terms of fuel supply, the same commercial jet fuel to what is utilised in the engines would be used. Again similar to the PEM fuel cell, this could also be potentially applied to the fast jet set up. Concept art of possible application on the generic fast jet is shown in

Figure 30.

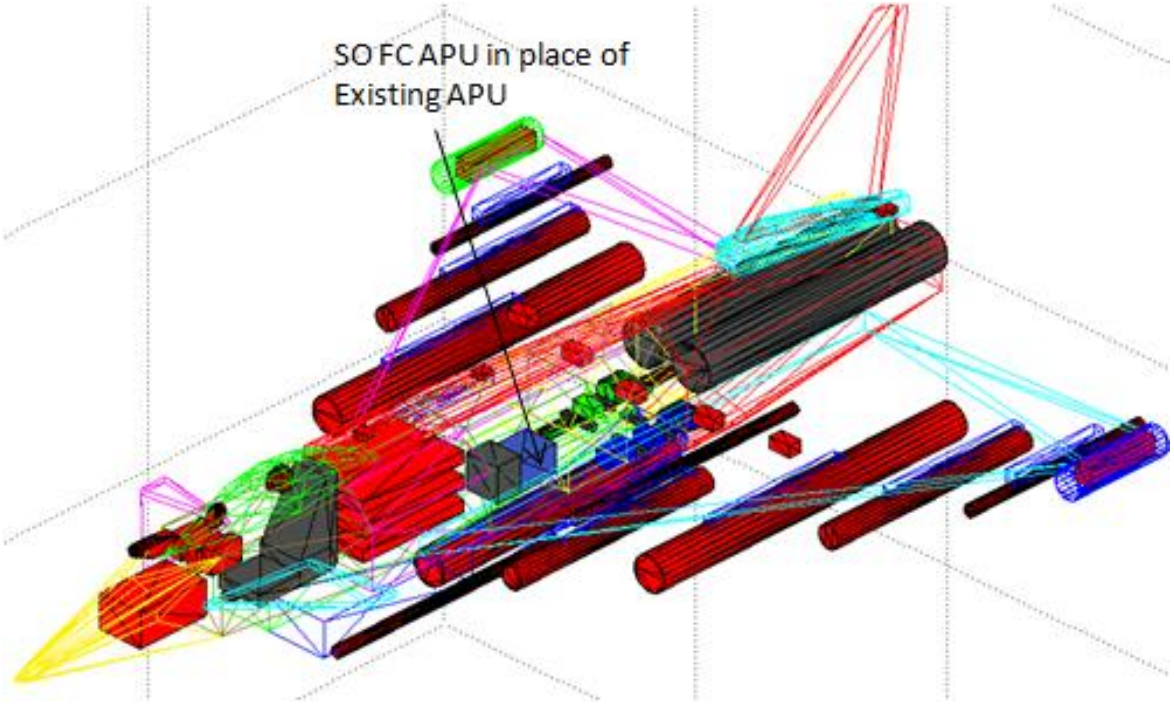

Figure 30 Concept art of solid oxide fuel cell application within a generic fast Jet in place of original APU

3.2.1.3 Solar power

Another example of alternative sources within aerospace can be found in long endurance UAV designs which use solar cells on the surface of the airframe. Such long endurance UAVs are aimed for persistent Intelligence Surveillance Reconnaissance (ISR) applications (e.g [64]) and the airframe wing design usually has a high aspect ratio. This increases the lift to weight ratio for slow efficient flight and provides large surface areas for mounting of solar cells (the primary electrical generation of this type of aircraft). As such the aircraft can become self-sustaining with the non-diminishing solar energy over the operation period which also charges energy storage for night time operation (for in flight endurance in terms of weeks rather than hours or days [64]). However these designs are not optimised for agility/flight manoeuvres or speed but more for endurance and cruise efficiency and as such, are in the opposite operational spectrum to the fast jet.

Technology development and demonstrators of such UAVs include NASA's HELIOS [62] shown in Figure 31 and aero-environment Zephyr [63]. The two HELIOS UAVs iterations were hybrid solar, lithium ion powered UAVs and with a maximum weight of 2000kg and 2300kg respectively. The latter HELIOS iteration shown in Figure 31 was also fitted with a fuel cell for night flight with solar power providing 18.5kW during the day.

Figure 31- Illustration of Helios solar UAV [63]

In a similar type of role, the use of unmanned lighter than air aircraft/airships as ISR and communication platforms has similar power requirements but with higher emphasis on electrical generation for on-board avionics over lift generation (for these applications the lift is provided by the lighter than air buoyancy). Such airships include the US "Integrated Sensor Is Structure" [65] program which proposed an airship of 140m in length with the concept art shown in Figure 32. The main sensor being an AESA radar is designed to be placed in the centre with air buoyancy sections front and aft to provide lift. Solar cells are envisioned to be placed on the upper surface of the airship in conjunction with structure mounted storage pods.

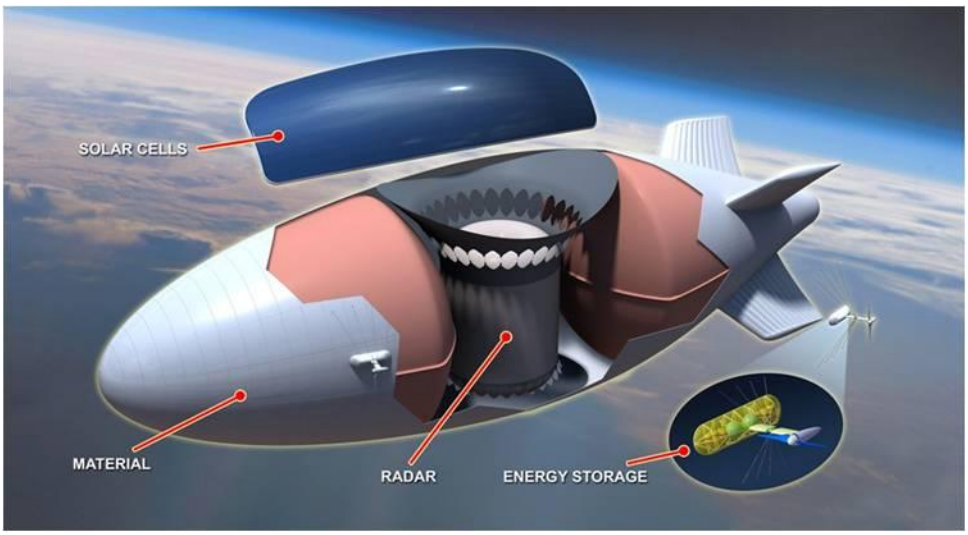

Figure 32- Illustration of solar powered ISR lighter than air platform [66]

The solar powered option itself does provide the benefit of engine off-take and fuel independence which would minimise the rework and linkage to engine off-take as well as location flexibility for fast jet application. However, the mission requirement for all weather, day and night operations with unconstrained deployment location as well as combat manoeuvres (solar cells still needs to be facing

sunlight) may preclude solar power as an effective candidate for fast jet. The application of solar generation for the high endurance UAV and unmanned lighter than air aircraft are also aided by the fact these have relatively large surface area to mount the solar cells compared to the fast jet application. To put into perspective; the HELIOS has a 75m wingspan and 5m length for a power level of 18.7kW in contrast to a Eurofighter [33] at 15m long, 10m wing span. The HELIOS wing is also more rectangular shaped compared to the Eurofighter which is a canard shape meaning the actual surface area will also be relative more in the HELIOS even after normalising aircraft length and wingspan. Another less immediate constraint with adding solar cells to fast jet aircraft is there may be a potential to conflict with the ability to have radar absorbing material as well on the surface of the aircraft.

3.2.1.4 Thermoelectric

Apart from fuel cell or solar power; the use of TEG is also a potential up and coming type of generation method offering an alternative to engine driven generation. The use of TEG includes the main benefits of no moving parts and relative simplicity, fuel independence (making use of waste heat) similar to solar cell but with less reliance on weather or time of day (however, this may be dictated by ambient temperature depending on the location of the TEG system and phase of flight).

Shifting away from aerospace slightly, [69] exemplifies on-going work for the application of thermo electric generation for typically land based vehicles which has reached around 500W power levels in the past few years for exhaust heat extraction applications. Higher power levels of 1kW applications have been pursued. Concept art and lab based demonstration illustration are shown in Figure 33 [68][69]. In such application, the TEG material has been applied between the exhaust piping surface and ambient air, acting as the respective hot and cold surfaces.

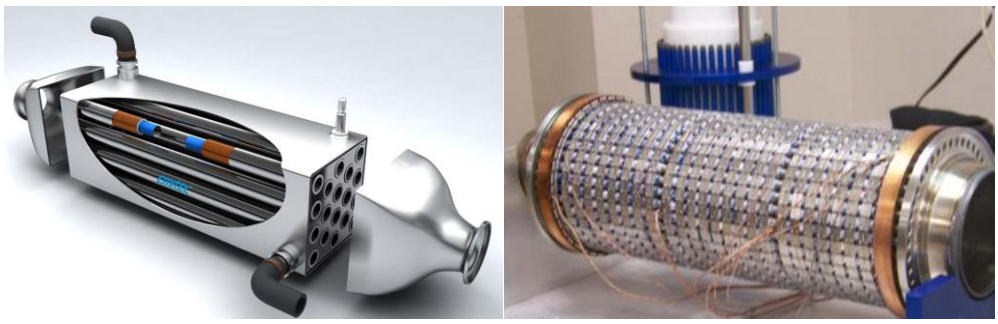

Figure 33- Example research land vehicle TEG application [68][69]

In theory, similar set ups can be applied to an aircraft system. Past studies performed by BAE Systems have included looking at the application of the fast jet pre cooler whereby TEG could be applied inside the dorsal spine of the fast jet aircraft fuselage in which bleed air, is air cooled

through a heat exchanger similar to the automobile exhaust adaption. However due to the low efficiencies of around 6% and in particular, material weakness in a fast jet environment, this application was not realised. Concept art of the application of TEG on a generic fast jet aircraft at the pre cooler is illustrated in Figure 34.

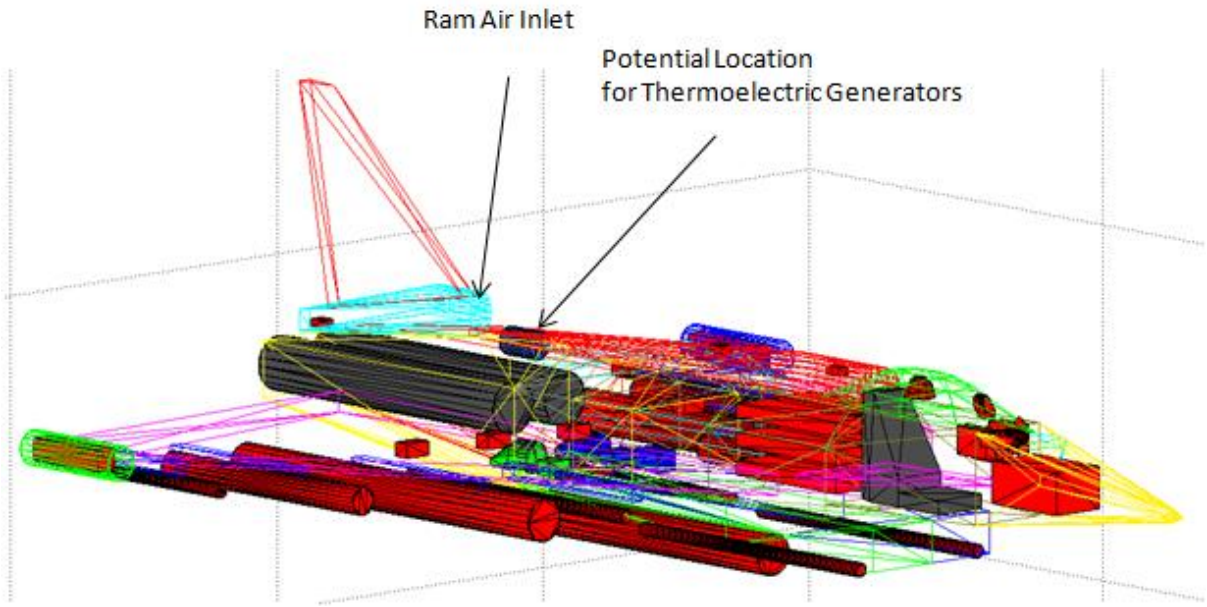

Figure 34 Concept art illustrating location of TEG at pre cooler in a generic fast jet aircraft

Boeing has also proposed the use of the thermoelectric generator technologies to make use of the heat around an aircraft engine. Relating to this, [70], a patent, describes a 30 device setup, sandwiched between metal sheets to be applied around the engine. The device concept is illustrated in Figure 35. Example proximity temperatures of a civil high by pass generic engine are illustrated by Figure 36 [71]. The TEG packages are placed in proximity to the turbine engine core cowling and turbine engine nozzle. There were no specifications of power generation capacity or system weight within the patent.

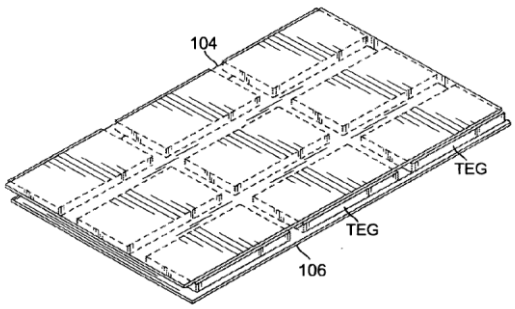

Figure 35- Boeing Patent illustration of TEG application around engine [70]

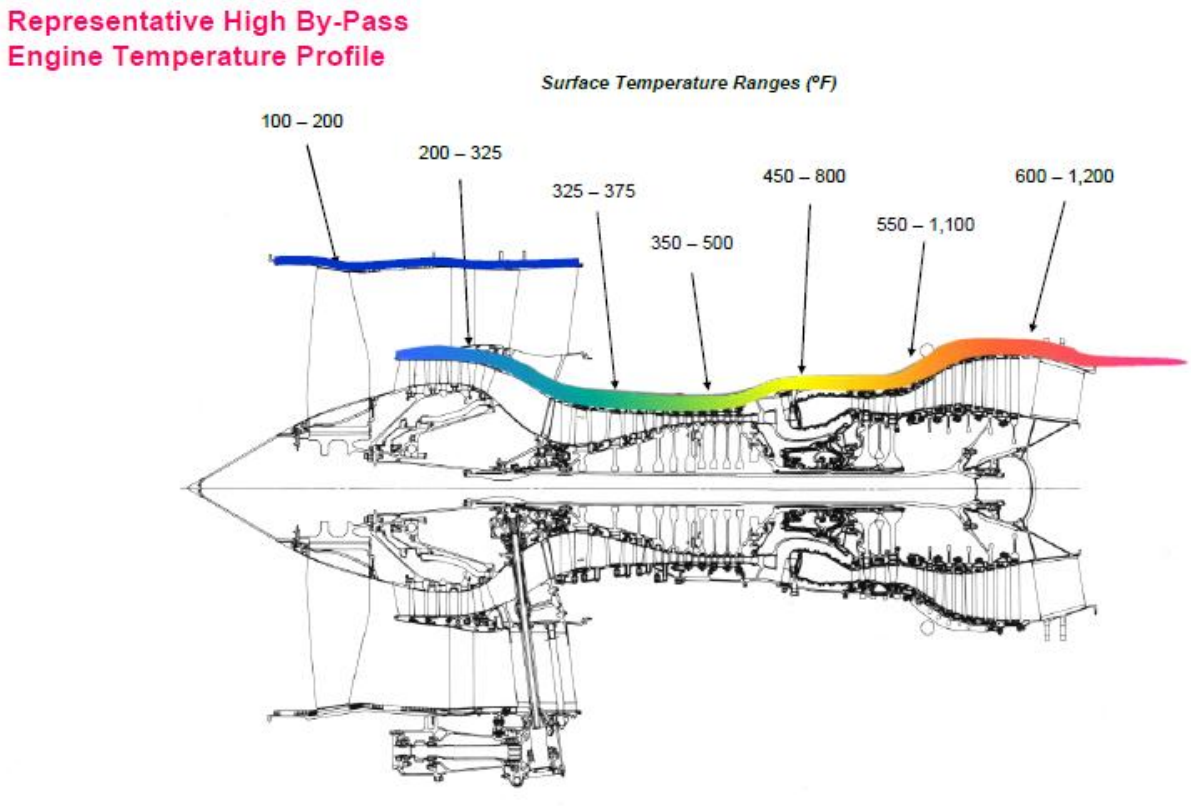

Figure 36- Illustration of typical surface temperatures around a high bypass engine [71]

Also from Boeing; patent [72] proposes the use of TEG within the skin of the aircraft fuselage itself for the temperature difference. Difference between the outside ambient air in flight and cabin air from the ECS provide the cold and hot temperatures delta. Proposed voltage output includes 12V DC, 28V DC, 110 volts AC with downstream conversion. The system also incorporates a battery for better management of energy. The patent also supports the argument of local generation for loading to potentially reduce weight of cabling. Shown in Figure 37 is the proposed location of the TEG around an aircraft highlighted in red on the left hand side as well as the electrical setup on the right hand side respectively. Again, actual power levels or weight were not mentioned in the patent.

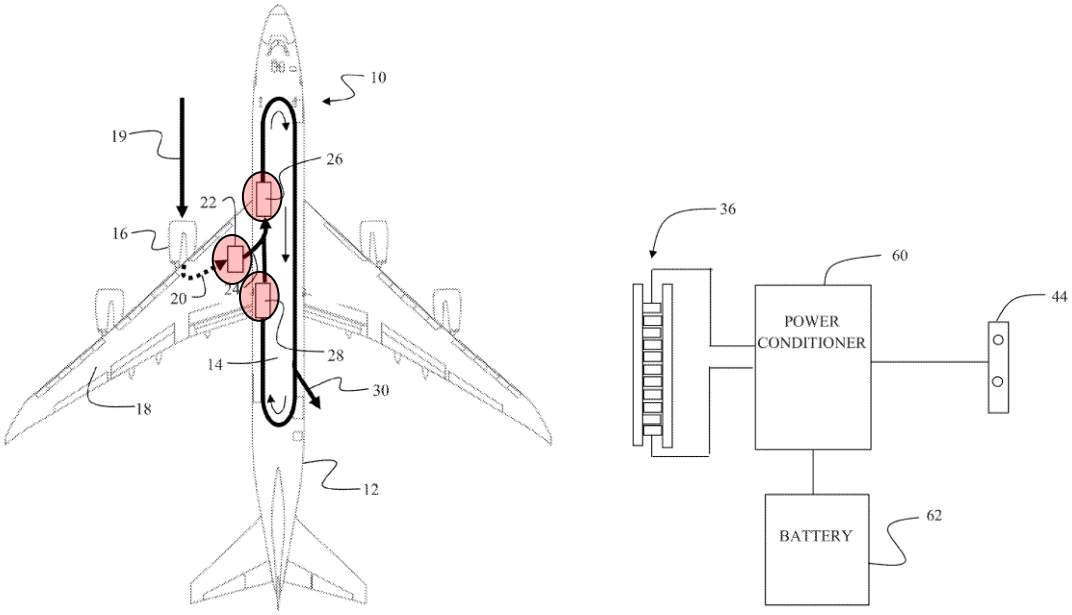

Figure 37- Fuselage and wing skin placed TEG from Boeing Patent location (left) and electrical set up (right) [72]

This concludes the literature review of Alternative aerospace generation sources which have been applied or have been proposed for non-fast jet applications. The overview of alternative generation provided in this chapter extends beyond those presented but those that have been included have potential to be considered for fast jet applications. These could be, for example, the application of Solid Oxide fuel cell within the fuselage of the airframe. This example of supplementary generation has a power output that would satisfy the 10s of kVA/kW range akin to existing fast jet designs [25] and have high potential for flight operations (although more work is needed to examine the more rigorous operation requirements within a fast jet environment compared to civil applications). The benefits of engine off take independence offers better conformance to the location which these options could potentially provide.

3.2.2 Engine mechanical off take independent turbine generators

Most electrical systems on board fast jet have auxiliary or emergency power generation. Emergency power generation is utilised when main engine driven generation and/or the engine itself is not available. Auxiliary power is utilised when engine driven generation is offline such as ground operations.

For fast jets, during most of the flight time in normal operations; the auxiliary and emergency power generation sources are not operated and do not contribute to any generation in parallel to the main generation even during peak demands. Identifying and discussing auxiliary and emergency generation that have been applied in fast jets to date provides examples of in service generation

that are power dense enough for fast jet applications and flight cleared for such as well. Hence having these paralleled with the main generation to meet the fast jet upgrade problem by increasing the peak generation available could also allow an avenue to cope with the increasing through life demand increase problem. As identified in the rest of this section, most of these are turbine generator based generation either driven by bleed air or have their own jet fuel gas turbine (independent of the engine mechanical off take).

3.2.2.1 RATG

The RATG extracts energy from the aircraft's outside ambient airflow. As long as the aircraft is in flight, power can be produced from the airflow. Utilisation of RATG includes commercial aircraft such as the Boeing 777 [74] and the BAE Systems Hawk trainer shown in Figure 38 [73] (highlighted in red) for emergency power. Both of these utilise mechanically released RAT, protruding through a hatch of the airframe from a compartment when they are required.

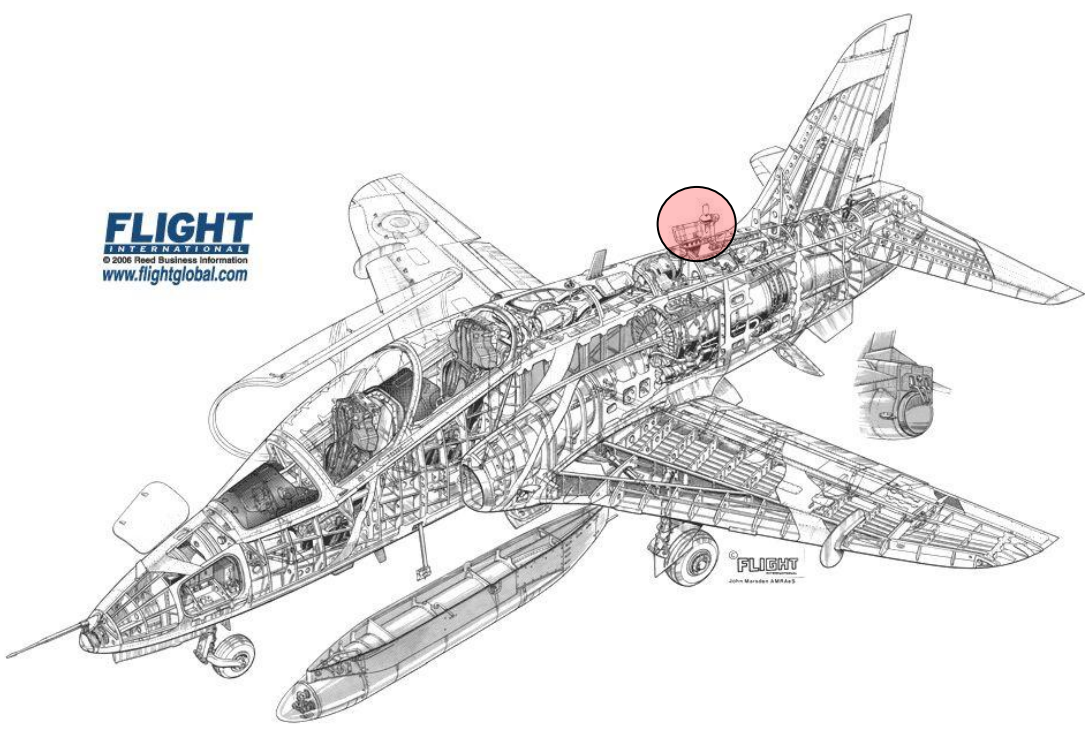

Figure 38- BAE Systems Hawk RATG [73]

Additional to the Boeing 777 or BAE Systems Hawk discussed, another example of engine off-take RATG is the ALQ 99 jamming pods mentioned in chapter 1 [24]. These are applied for the US Navy prowler and F18G electronic attack variant from Boeing shown in Figure 39 [77]. The jamming pods themselves are connected onto the weapon stations/hardpoints of the aircraft and the tip mounted RATG directly provides power to the pods (up to three pods for different bandwidths of jamming). Typical power levels the RATG can produce is about 27kVA [76] which is close to the 30kVA mark for

the generic fast jet examined in this thesis. The caveat for such utilisation is in operating in conjunction with 'jamming' where the aircraft RCS is of a lesser concern.

Figure 39- Pod mounted RATG for ALQ 99 on EA 6B [77] and F18G [78]

HI RAT diameter	[in]	2	5	10	15	20	25
HI RAT diameter	[cm]	5	12.7	25.4	38.1	50.8	63.5
Electrical Power	[kW]	<1	3→6	14→25	30→55	55→100	→140
*At 220 knot CAS, 25000 feet							

Maximum Power	[kW]	278
Maximum Altitude	[Feet]	40000
Max Speed	[Mach]	0.82
Turbine Rotational Speed	[rpm]	3000 to 40000
Turbine Maximum Efficiency	[%]	41

Figure 40- HiRAT RATG example [79]

Platform independent RATG systems are also available in the market/Commercial Off The Shelf (COTS). An example is the Hi RAT series [79] with the power levels shown in Figure 40. Typical applications include EW, ISR pods and emergency power for military and commercial aircraft, UAV, Air launch decoys, and tactical missiles. The typical maximum ceiling is around 40kft, a maximum 41% efficiency and maximum speed of up to mach 0.82.

Another example is from the previous company Ghetzler which provides designs [80] (shown in Figure 41) that can operate in supersonic speeds.

Figure 41- Gheztler RATG example [80]

Currently there is also work to enhance the operability of the traditional RATG within commercial aircraft. [81] describes the hybridisation of the RATG with supercapacitor in order to manage the demand fluctuations of electrically driven control surfaces with the minimisation of RATG sizing (such benefits could also extend to other transients or even pulse loads for the fast jet). The proposed system explored applications for a primarily 270VDC system in which the RATG operated with an electrical output between 300-800Hz at 115Vrms. This is then rectified to produce the 270VDC level. The specified output of the RATG is 15A at 270V (4.05kW max) but is also required for a peak load of greater than 25A at 1/5 of the time. Hence a supplementary supercapacitor is required for storing energy for such peak demand times as part of the studies. The specified supercapacitor is specified at 250VDC max (to be stepped up through DC DC converter) to 125VDC (50% discharge, minimal) at 58F or 1.36MJ of convertible/usable energy.

A reduced power, lower voltage network was initially utilised instead for validation of the proposed system [81] and demonstrated a possible reduction of RAT power sizing to 50% maximum transient loading. In relation to the fast jet application this could be suited to pulse type loads while minimising size of RATG needed possibly minimising radar returns associated with the RATG.

In general, the RATG offers a high power solution again akin to the 10s of kVA for fast jet design [25] to date. Such application could be connected to one of the fast jet hardpoints for local loading and for it to feed power back to the wider electrical system. However, one could argue that, this will take up one of the hardpoints and reducing the ability to use this hardpoint for other functions. In such case, dual pylons could be considered. Other more conformal solutions could also be pursued such as a more conformal option in front of the pre cooler inlet for the ECS

The RATG is also more technologically mature when compared to fuel cells or TEG examined in section 3.2.1, albeit having moving parts. RATG also need a feed of ram air inlet which would need additional flight clearance for its aerodynamic effects and could potentially increase radar returns. Concept art of their application is presented around the generic fast jet aircraft in Figure 42 and Figure 43.

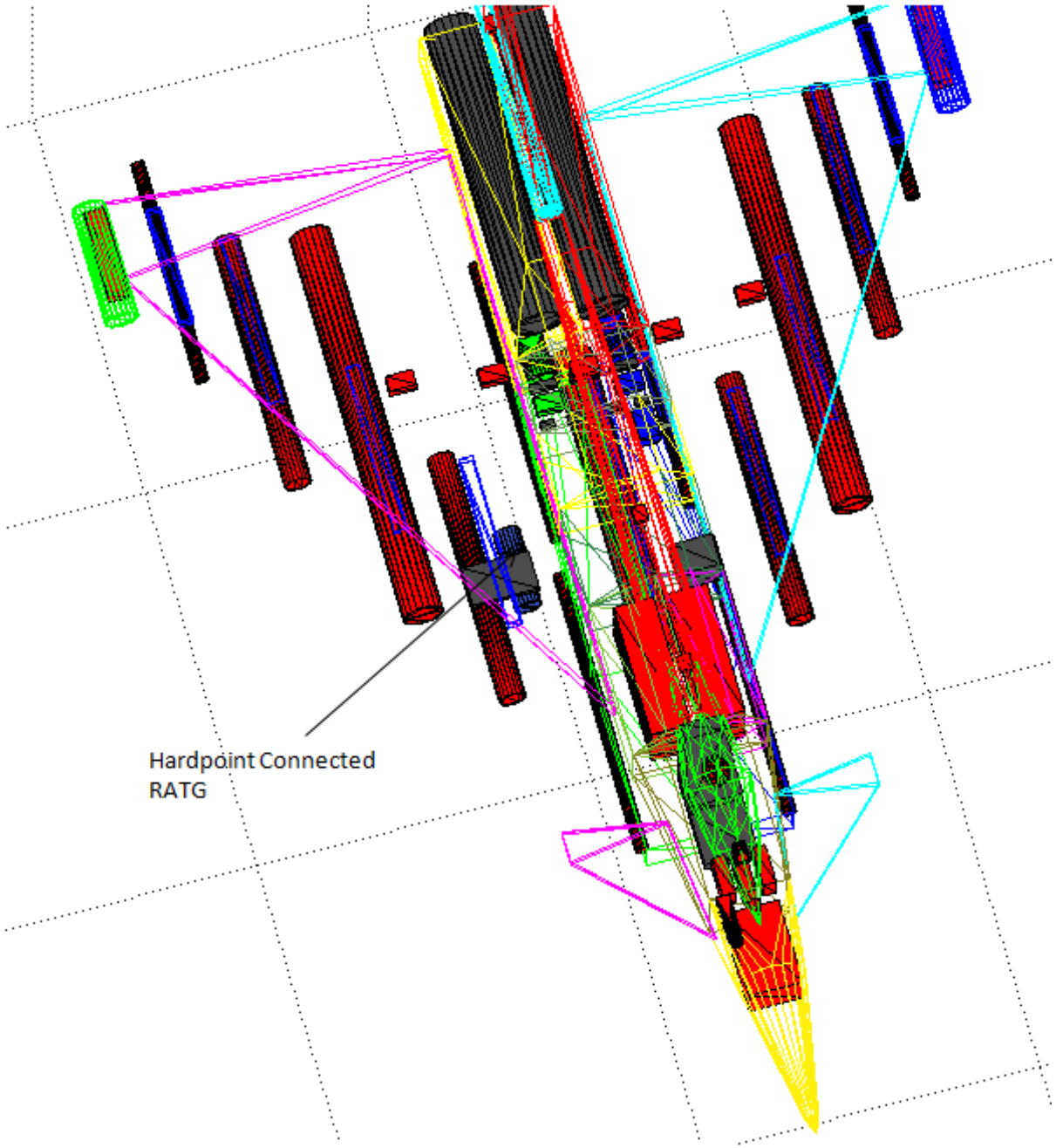

Figure 42 Concept art of RATG applied at one of generic fast jet hardpoints

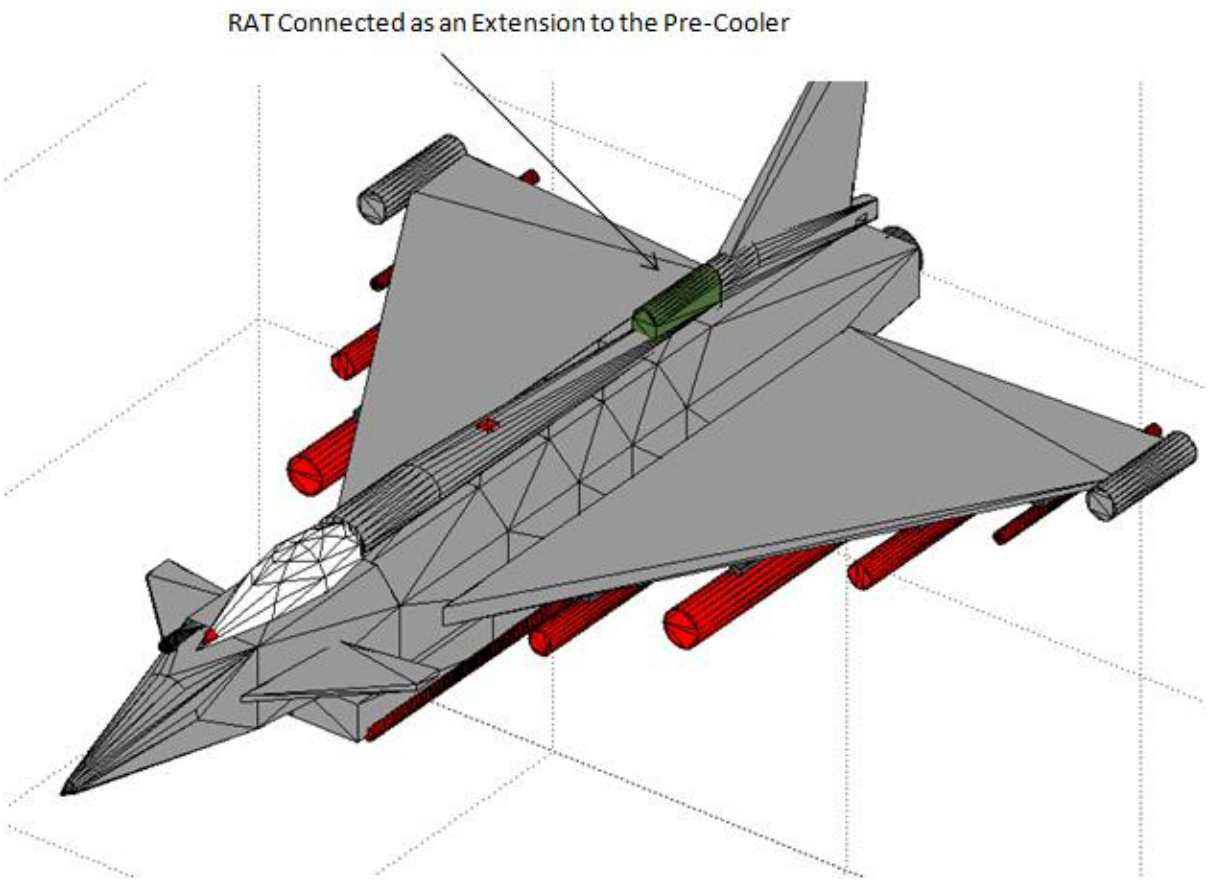

Figure 43 Concept art of RATG applied in front of a generic fast jet pre cooler inlet (opaque)

3.2.2.2 Engine independent gas turbine generators

Additional to the RATG there are also engine mechanical off take independent turbine generators (utilising on-board compressed propellant storage or bleed air from the engine for jet fuel based combustion). An example from Honeywell, is utilised in the Lockheed Martin F-16 iterations which make use of catalysed hydrazine H70 [74] to directly drive the turbine generator shown in Figure 44 whereby H70 is expelled by on-board nitrogen within Kevlar bottles. A valve system is utilised to control the flow of H70 expulsion and controls the speed of the turbine generator by varying the flow of H70 for electrical power output. The turbine generator can also operate on engine bleed air with jet fuel for internal combustion alternatively for up to five hours if the engine is still operational (i.e. providing bleed air). The mechanical turbine system can produce around 55 horsepower output (42kW mechanical power).

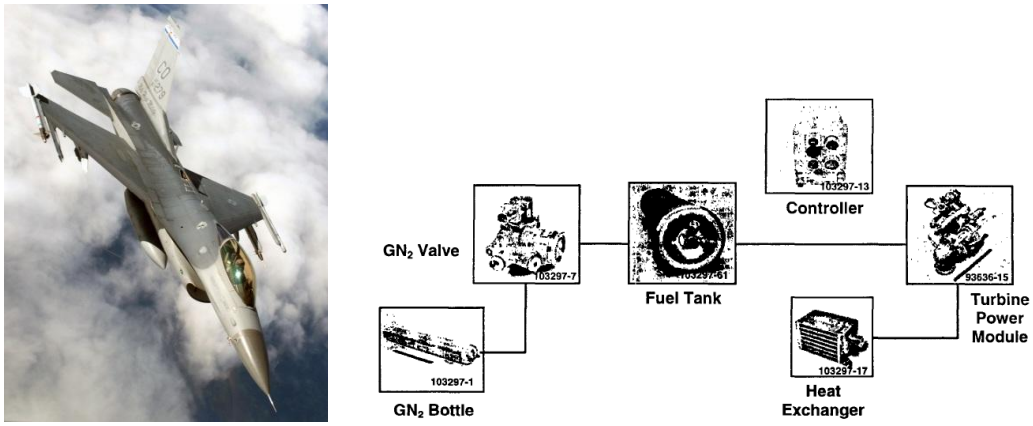

Figure 44- F16 emergency power turbine generator [74][102]

Another example which also utilises such internal emergency turbine generator is the now retired F-117 [74] which operates solely on bleed air and jet fuel combustion driven turbine generator from the main engine or APU. The system does not have on-board H70 propellant like the F16 for engine flameout situations.

Also described in [74], another variation and as a shift to move from the hazardous Hydrazine of the F-16 auxiliary power system, the Mitsubitsu F-2 system. This has two air bottles instead of the H70 hydrazine system for engine flame out situations where the air from the two bottles functions by expelling fuel from tanks for combustion (substituting the bleed air). The bottles are high pressure and made of lightweight carbon fibre. The use of air bottles reduces the need for handling and placing hazardous H70 on board the aircraft. Similarly to the F-16, the F-2 can operate on engine bleed air and jet fuel combustion which can be up to five hours and can operate throughout the entirety of the aircraft envelope (including supersonic and high altitude flight).

Two more recent aircraft designs, the F22 raptor and F35 from Lockheed Martin (which are 270VDC systems) also have incorporated turbine generator based emergency power systems provided by Honeywell. The F22 makes use of the Aux Power Generating Subsystem (APGS) [74] which integrates auxiliary power and emergency into one system as well as being responsible for performing engine starts and to provide bleed air for the ECS. The F35 EPGS [75] also integrates multi functionality to the APU and emergency power but also includes thermal management and ECS functions.

3.2.3 Generation sources summary

Table 7 below summarises the different sources reviewed in section 3.2 and ultimately list possible applications to meet the increasing power demand problem on fast jets. The exact applications of these on the fast jet will not be examined further in the rest of the thesis but the review performed so far has added 'weight' to the proposed use of supplementary generation. That is, there are existing or up and coming power generation sources that are flight cleared/potentially flight cleared for fast jets. These are engine mechanical off take independent for better distribution to remaining space on a fast and are powerful enough to meet the 10 kVA power range (apart from TEG) associated with the power demand increases.

Table 7- Summary of different sources that could potentially be paralleled to main generation

Source	Power levels and maturity	Platform/example	Pros	Cons	Verdict
PEM Fuel cell	20kW[59], [67], not widely applied for aircraft apart from small turboprop or small UAVs	Boeing E-plane, small UAVs	No moving parts	Requires high purity of hydrogen supply (on board storage tanks). Low power density	Possible option in the future but low power density for fast jet main power and requires onboard hydrogen source
Solid Oxide Fuel cell	440kW for 880 kg, not yet applied at time of reference. .0.5kW/kg proposed possible power density [60], not widely applied		Can operate on reformed jet fuel No moving parts	Reformer may be bulky. Requires high temperature	Possible option in future
Solar	18.7kW for Zepyhr [63]	Zephr, solar impulse…	No fuel supply needed, no moving parts, can be applied on any upper surface of the airframe	Too weather and time of day dependent (such as for night strikes which a large amount of the missions are) Needs to be in contact with sunlight which may not always be the case even on a sunny day with air combat manoeuvres. Can be helped by energy storage May conflict with the ability to apply radar absorbent material for some aircraft	Possible option in the future but weather dependant.

Thermo electric	600W for land based car applications. Patents from Boeing for civil aerospace applications [70], [72],	Patents from Boeing for civil aerospace applications. Automobile examples are available	No fuel supply, moving parts, makes use of waste heat	Low efficiency,	Possible option in future for pre cooler installation but due to material strength, this is currently not suitable to date unless better material strength is demonstrated
RATG	27kVA on growler, 25kW for a 25.4cm diameter version from Hi RAT. Applied and available today[76] [79][80]	Hawk, F18G, Prowler	Fuel independence (indirect), Engine off take independence. High power density	Protrudes out of aircraft (more complex flight clearance) unless a shrouded version is provided. Requires subsonic airflow. Increase RCS and subsequent studies	Highly mature [81]. Can be applied today but needs additional work to address the cons such as increase in RCS
Engine independent turbo machinery driven generation. Fuel and Compressed air or/and bleed combustion	Applied and available today [75]	F22, F2, F35	Engine off take independence but utilising bleed air. No hazardous H70. High power density utilising gas turbine. No protrusion		Highly mature. Bonus if this is already installed on aircraft but retrofit options may be difficult with need for bleed air extraction. Can be applied today.

3.3 Paralleling of sources literature review

In section 3.2, possible generation sources additional to main generation to meet the increasing power demand on fast jets were identified. This resulted in the conclusion of example sources that are powerful enough (apart from TEG) that could be used to satisfy the on board demand increase levels faced with through life upgrades and that there is precedence of their in-flight operations. However, there is a general absence of paralleling such generation sources on fast jet aircraft with the main generation to date. Hence, integration/paralleling approaches used in other domains such as EVs and M/DG/R are considered in this section in order to draw out transferrable methods. Potential transferrable solutions were identified from these and considered for suitability for use in fast jet aircraft application for tackling through life upgrades. This resulted in the main work of this thesis and is presented in chapters 4-7. In particular the down selection process emphasised the following requirements:

- Minimal changes are desired to the existing main generation
- Limited inter sources coordination between the added supplementary generation for loose coupling, aiding incremental retrofit.
- Include multiple integration points around the aircraft to maximise the choice of where sources can be placed in face of spatial constraints

3.3.1 Topologies for power integration: DC link as the common linkage point

One area of research where potential transferrable solutions can be found is within EV research [82]. Paralleling of different sources is required in such applications for synergising the power and energy densities of supercapacitors, batteries and fuel cells. The main power demand in these different EV systems is the electrical propulsion motor/traction motor which is fed through a standard six switch inverter and the sources themselves are integrated at the DC link of this.

In [82], an overview of different variations of typical power electronics topologies researched for EVs is presented. In such set ups, the common elements are the generation source(s); being DC in nature is required to be stepped up/down through basic buck/boost/buck boost converter arrangement to supply the electric propulsion/traction motor through the inverter. This is to manage different fixed voltage levels or variable voltage output from the same sources, as well as allowing for charging through regenerative braking scenarios and general load sharing if there is more than one source. A selection of topologies is shown in Figure 45 showing DC DC converters arrangements coupled with the common six switcher inverter topology at the DC link interface [82].

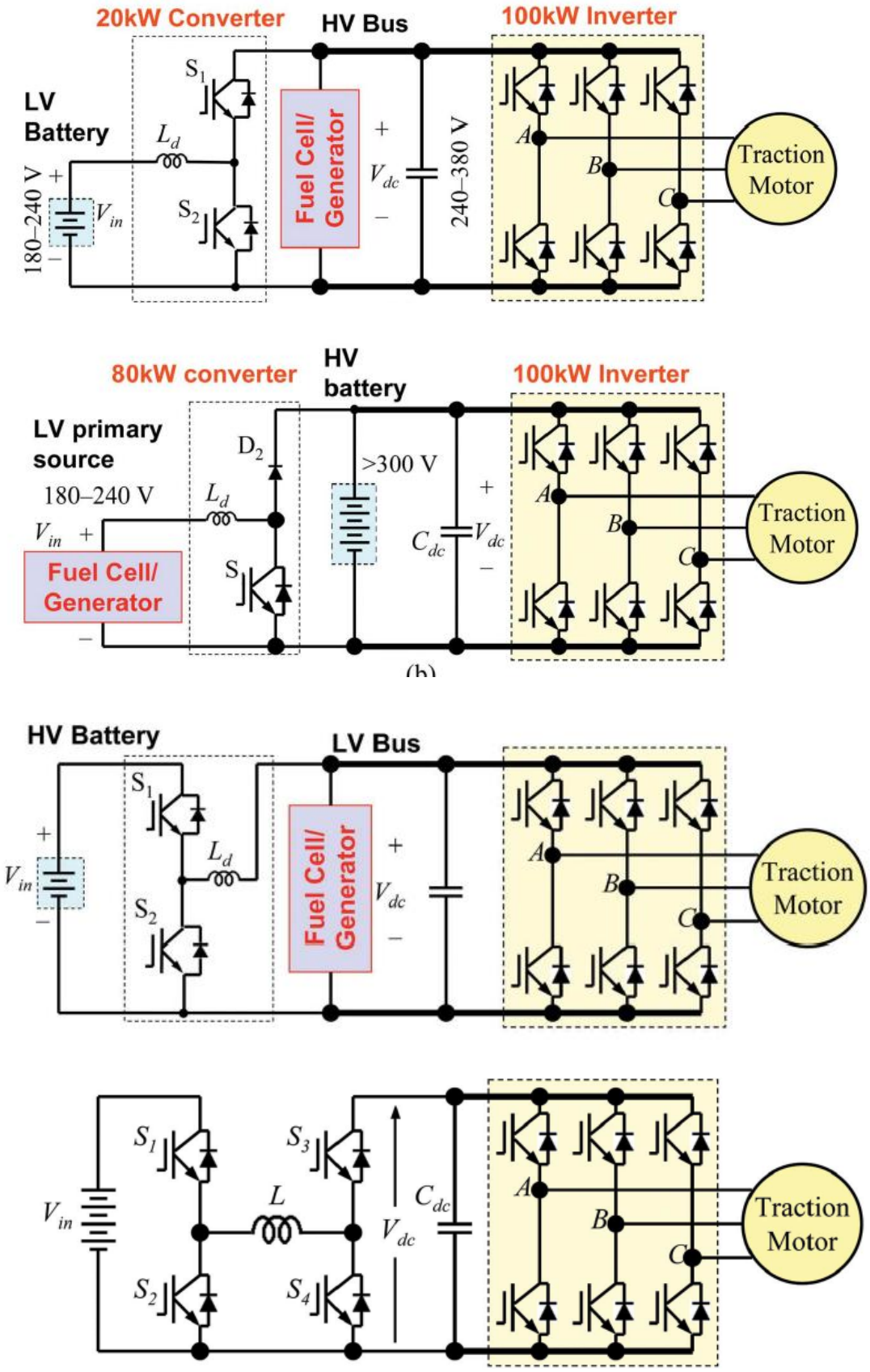

Figure 45- Different single DC DC converter to inverter combinations for EVs [82]

Similarly, this standardised arrangement of a common DC link to the inverter is seen widely in other literature. For example [83], two sources are paralleled to the same DC link whereby energy storage is operated in parallel to a PEM fuel cell through their separate DC/DC converters but both supplying the same single inverter through a common DC link (shown in Figure 46). As such load sharing between the two sources is possible. The energy storage system's DC DC converter in this case is bi directional to allow charging additional to discharging such as that for regenerative braking.

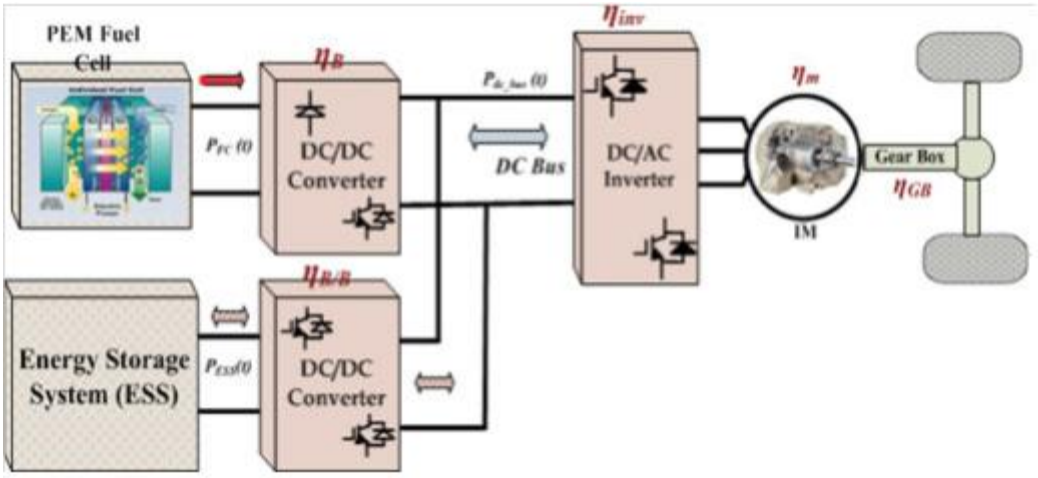

Figure 46- Dual source fed inverter via separate DC DC converters [83]

This type of topology is also standardised within M/DG/R in terrestrial network research (see [84],[85]). However, the main difference to the EV setup is in place of the common propulsion motor/traction motor: a grid connection is supported instead. With the grid connection, the inverter itself only provides part of the power of the grid which is also powered by the normal main generation on the AC side. Hence in terms of paralleling requirements, not only do the multiple DC DC sources connected to the inverter DC link need to have paralleling control but also the main inverter itself connected back to the main grid. 'Parallels' can be drawn for fast jet application, where to integrate supplementary power back to the main AC sections of the aircraft electrical: adherence to the fixed voltage level (115Vrms), frequency (400Hz) and phase is also needed.

Similarly, Figure 47 from [84] and [85] depict such topology again for M/DG/R applications; where different power sources are converge into a single three phase inverter for integration back into a larger grid (shown in Figure 47 and Figure 48).

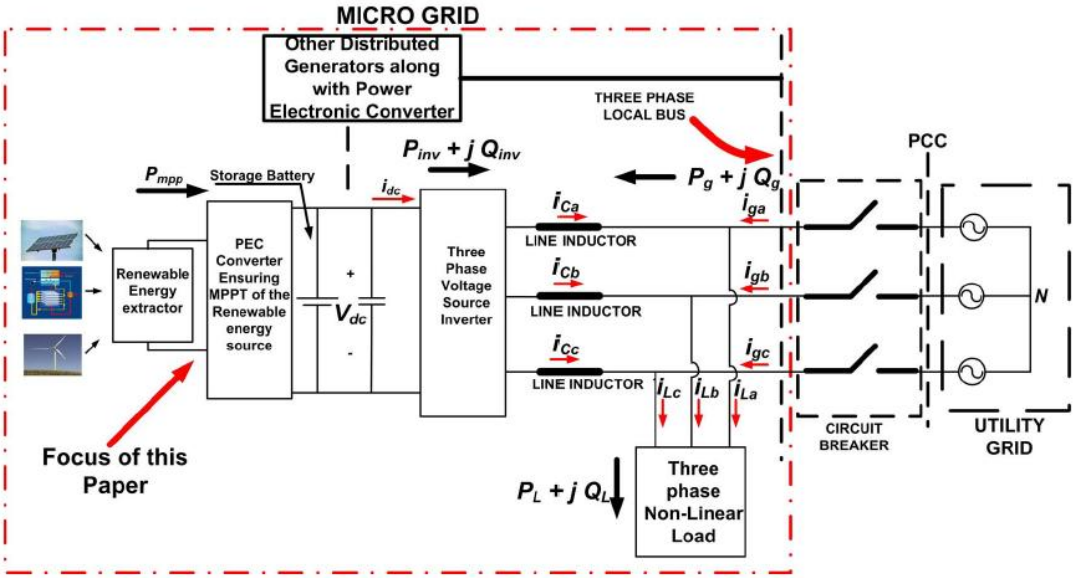

Figure 47- Renewables integration to main utility grid through common DC link [84]

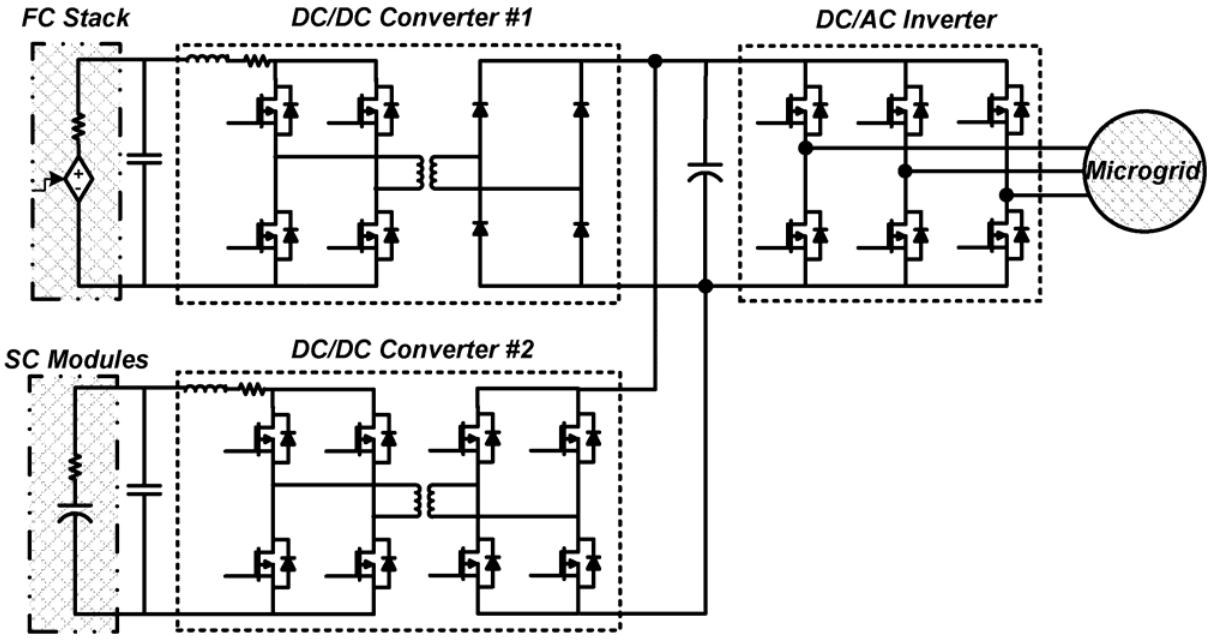

Figure 48- super caps and fuel cell stack interfaced to microgrid through DC DC converters through a common DC link [85]

In summary, the common linkage point of the configurations shown in Figure 45 to Figure 48, whether EV or M/DG/R, is the common DC linkage converging the multiple generation sources into a single inverter. The similarity of such integration becomes apparent for fast jet applications in that there is a need to integrate similar additional sources to a main AC section of a fast jet network.

In the case of when the supplementary generation source is AC such as RATG or mechanical independent turbine generator APU; 'parallels' can be drawn from terrestrial based wind generation applications [85] which are also required to be connected back to the main grid. In these scenarios, the setup of the wind turbine generators output of a permanent magnet synchronous generator is rectified (either passively or actively) to a common DC link and followed by an inverter stage to connect the power back to the main grid [86]. As such multiple wind turbine generators through this setup can be connected back to the main grid. Although not a direct replication, a similar rectification/conversion stage can also be used to interface the RATG or engine off take independent turbine generator based APU back to the AC fast jet electrical system.

Going back to the fast jet aircraft electrical system, inverters can be added into the system in the same manner to support supplementary power integration. Apart from addition of inverters; there are already DC links that exist within the fast jet electrical system. These are located in the passive rectifiers in non-linear loads (115Vrms to 270VDC) of loads such as radar, mission computing etc as well as the passive TRUs around the electrical system. Examples of these are highlighted in red on Figure 49 on a single channel of the generic fast jet electrical system.

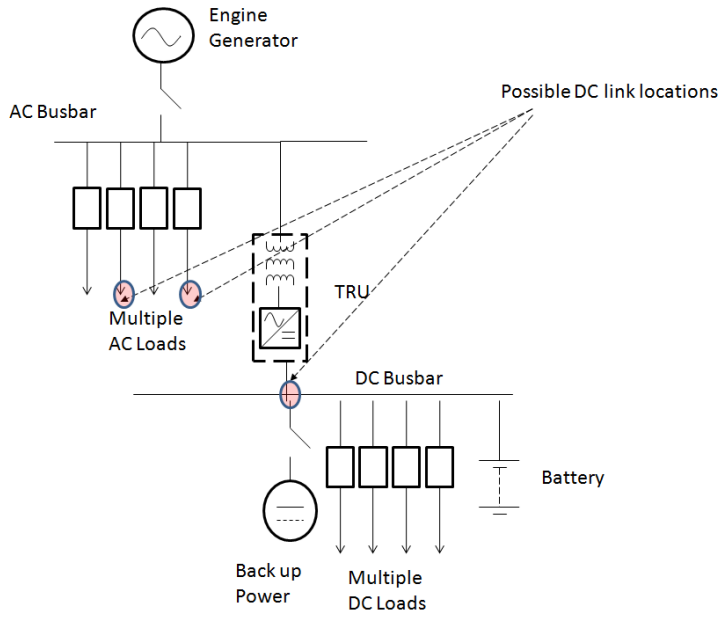

Figure 49- Example existing DC links around a single channel of the fast jet electrical system

The locations of these within the electrical system are spread out, dictated by the loads themselves and could conveniently aid the potential integration of power supplies in a more space conforming manner by providing the DC link as integration points. These however do not readily allow power integration back to the AC side when compared to the inverters examined the EV and M/DG/R literature. However, the fast jet rectifiers and TRUs do have local loading at the DC side as part of the

loads. As such, even without converting these passive rectifiers into active equivalents; the application of placing additional supplementary generation sources at these DC links could potentially provide power to the local DC loading and indirectly alleviate the draw from the main generation (essentially load share). Since the integration of power is still at the DC linkage; paralleling methods for common DC links examined in the EV and M/DG/R literature can still be utilised/read across.

This can be more readily applied for the 28VDC TRU; however there could be major constraints in accessing/connecting to the DC links of the 115Vrms to 270VDC rectifier stage in equipment. These may be within a hermitically sealed or self-contained box as part of the equipment. As such this maybe better suited for new equipment yet to be added to the aircraft and where there is scope to require access for such connection in the design from the Original Equipment Manufacturer (OEM). Otherwise discussion with the OEM of existing equipment will be needed to gain access to such DC links (if such equipment is hermitically sealed).

3.3.2 Paralleling control

With the previous section 3.3.1 examining topologies of EV and M/DG/R for read across of power integration for fast jet: this section looks into associated paralleling controls for read across to the fast jet application.

3.3.2.1 DC paralleling control

With the discussion of possible utilisation of DC linkage around the fast jet electrical system as integration points (i.e. existing passive rectifiers or any newly added inverters); literature review regarding the paralleling control of multiple DC sources at such DC links is presented here in this section. Two main types of DC based paralleling are discussed; these being droop control and voltage master current slave control respectively.

The mechanism of basic droop control operates by measuring the voltage of the individual DC DC converter terminals which is then subtracted from the predefined open circuit voltage set point. The subsequent current control is the proportional function of this voltage difference where the proportional function is the droop slope gradient determined by the user. With such droop control, multiple sources within the system can share the loading of the overall system. Literature of DC droop control in this form can be found in for M/DG/R [87], [88] to give examples of some of the applications.

[89], examines a hybrid DC AC system in which the common DC link section of the distributed sources of a terrestrial system is paralleled into a common DC bus through droop control. This is

then subsequently interfaced to the main AC grid to create a basis for power sharing. Immediately in terms of read across, a similar DC convergence of sources can be controlled using such droop control for potential application on the rectifier DC links within the fast jet electrical system (of non-linear loads and TRUs).

Alternatively, voltage master and current slave control can also be used. Within such setup, the DC link has one DC DC converter that controls/holds the voltage while other DC DC converters connected to the same DC link; control their own current injection (as current slaves). This has been utilised within EV research [44]; in this, examination of utilising voltage master current slave control to integrate super capacitor, battery and fuel cell to feed a common inverter DC link (shown in Figure 50) is presented. Again, each of the individual sources has its own DC DC converter connected to the inverter's DC link. Possible fast jet application for such control could again be at the rectifier DC link of non-linear loads or TRUs within the electrical system. The proposed difference of possible use of this for the fast jet application is: the rectifier could continue to partially draw power from the main generation and use this to act as the voltage master control to hold the DC link voltage. Whereas any added sources through DC DC converters on the DC link can be operated in current slave mode.

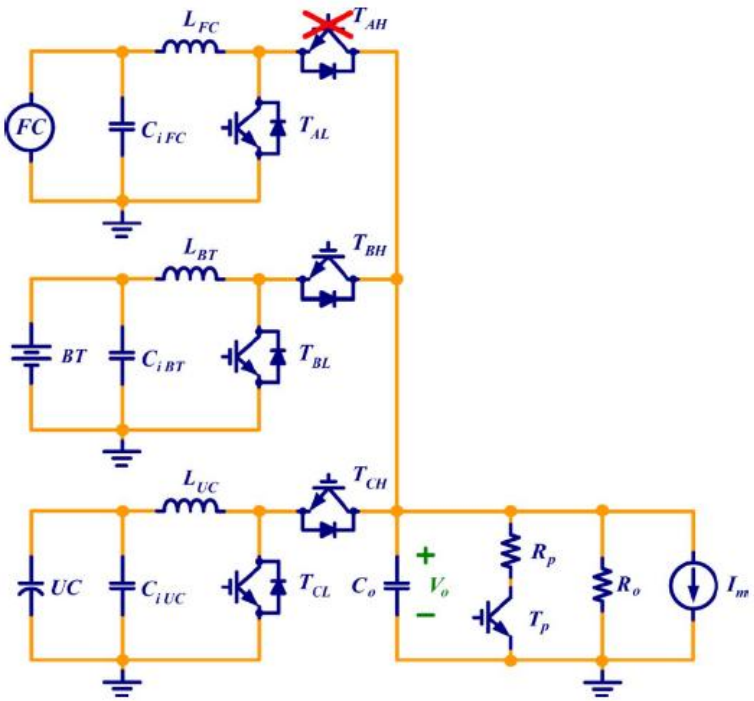

Figure 50- Voltage master current slave scheme application in EV [44]

3.3.2.2 AC Paralleling control

Additional to using passive rectifier DC links for adding power; adding inverters into the system may also be needed to increase power penetration of supplementary generation. As such, a literature review of the AC paralleling methods and in particularly for inverters to a main grid is presented in this section.

[84] Proposes the control of active and reactive power injection back into the main AC grid from smaller microgrids using *P-Q* theory to calculate current reference (current controlled). In this, the input measurements of the control are grid voltage, load current and inverter current. Here, [84] illustrates the ability to have multiple parallel inverters of associated microgrids (including with solar power and/or wind power) connected in parallel to the main grid generation. As such, this method can be potentially applied to fast jet applications for the likes of integrating multiple sources such as the RATG and fuel cell from separate locations on the aircraft.

[91] Looks into combining droop control with average power control to interface distributed generation with a main AC grid. Conventionally, AC droop is achieved by altering (drooping) frequency with real power *P* (analogous to voltage with current in DC droop control). The method examined in [91] aims to improve on this by catering for the reactive power contribution as well with modification to the conventional AC droop control.

Also relating to droop control, [92] examines a three level hierarchical control for AC and DC microgrids with underlying droop control at the paralleling level (primary operational control). The top level makes the decision on whether to import or export power (strategic tertiary control). The middle (secondary control) level manages the synchronization such as connecting and disconnecting transitions and restores overall frequency and amplitude deviations.

[93] Examines an adaptive version of droop control also for distributed generation which again controls reactive power additional to active power for finer control of reactive power sharing.

[94] also looks into the droop control which additionally caters for the reactive power similar to [91]: this is achieved with a voltage and reactive power based droop control loop additional to the frequency and real power droop control loop (shown in Figure 51).

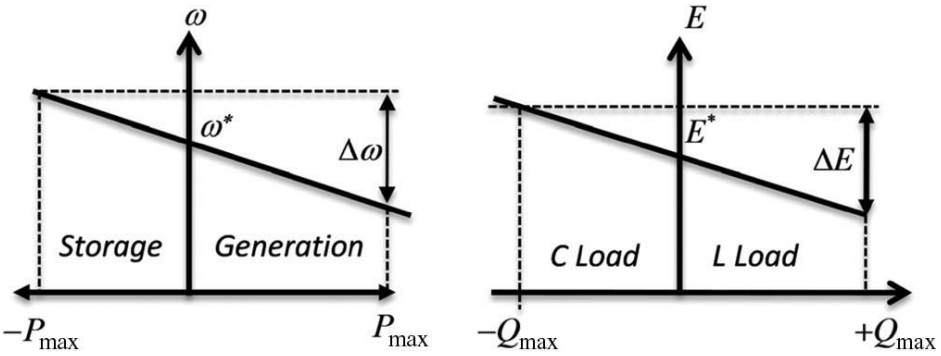

Figure 51- AC droop control [94]

3.3.2.2.1 SAF on a plane

One alternative method to AC droop control that has not been widely applied for fast jet to date is the use of SAF control. SAF/active power filter has been long established [95] and in particular for terrestrial networks. Various papers [96]-[100] have looked into the application of applying SAF on aerospace applications with example set ups. Within these, [96] also illustrates the location of multiple SAF application within a generic More Electric Aircraft (MEA) set up (shown in Figure 52). As well as showing in a lab based demonstration that the SAF can be incorporated into variable frequency systems. The main purpose of these aerospace application literatures so far, is to reduce the current harmonics drawn at the point of coupling within the aircraft electrical system. The harmonic reduction is achieved by extracting the harmonic current contents through measurements (drawn at the PCC) and injecting the anti-phase equivalent back into the system for cancellation.

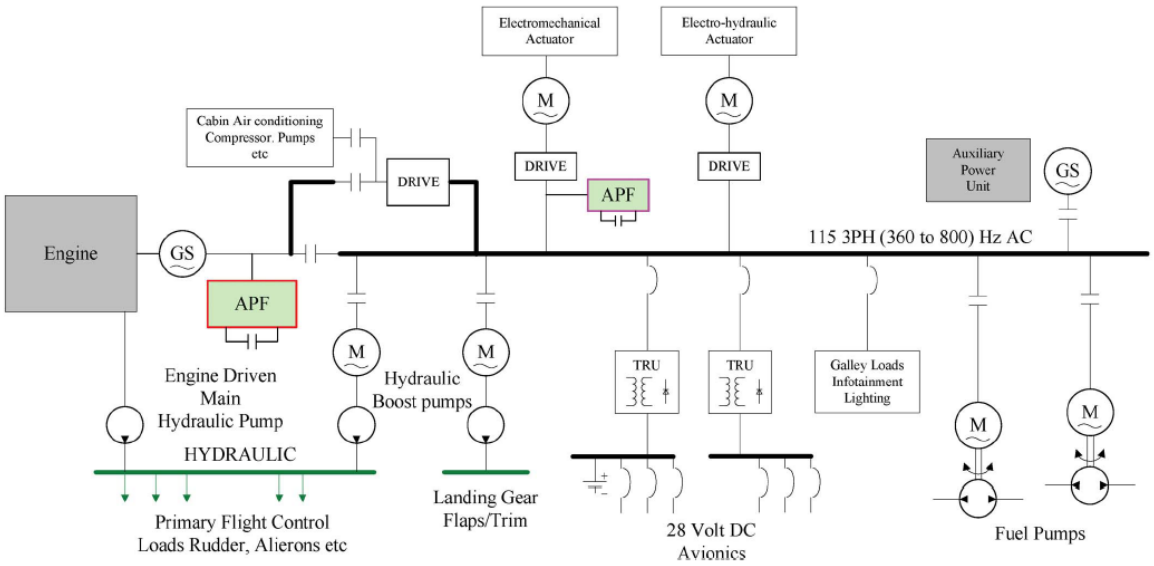

Figure 52- Illustration of SAF research for variable frequency aerospace electrical networks: more electric aircraft with SAF/Active Power Filter [96]

Due to the topology of the SAF being essentially a voltage source inverter, a secondary function that SAF can be used: is injecting power back into the main grid in parallel to existing main generation while adhering to the main generation's voltage magnitude, frequency and phase. This has been researched for application in terrestrial systems including introducing renewable generation power into the main grid [101] (illustrated in Figure 53). Other variations of such power injection have been achieved using Unified Power Quality Conditioner (UPQC, combining shunt and series filter topologies) shown in Figure 54 [55].

Using the SAF is rather convenient as it satisfies a dual functionality with harmonic current reduction within the system as well as paralleling/introduction of more power. Example of this include [101], for terrestrial applications which include using the DC link of the SAF as the connection point for the supplementary generation (similar to what was elaborated in section 3.3.1). Essentially the SAF paralleling with main grid is similar to the *P-Q* control presented in [84] in terms of being a current controller and in terms of input measurements used (SAF also takes into account the grid voltage, load current).

The SAF has not been widely applied to 400Hz, 115Vrms fast jet electrical systems to date but would provide a means of reducing current harmonics within the system. More importantly the utilisation of it to integrate more power into the system in parallel to the main generation, particularly to meet the through life upgrade problem has not been considered which could be highly beneficial.

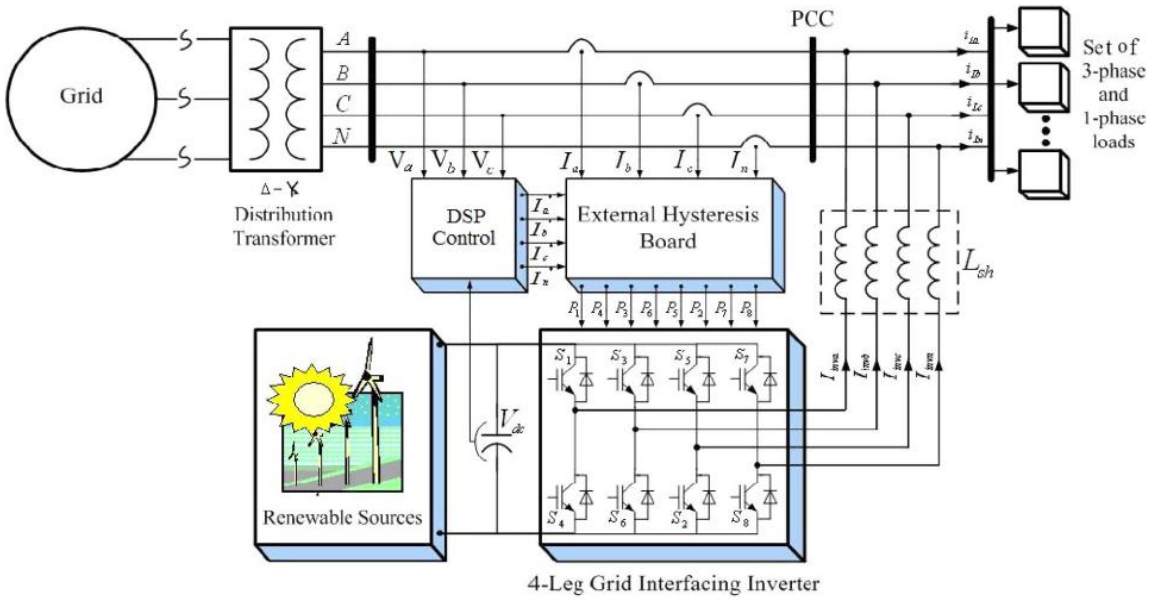

Figure 53- Example of use of SAF to integrate power back to main grid in terrestrial network [101]

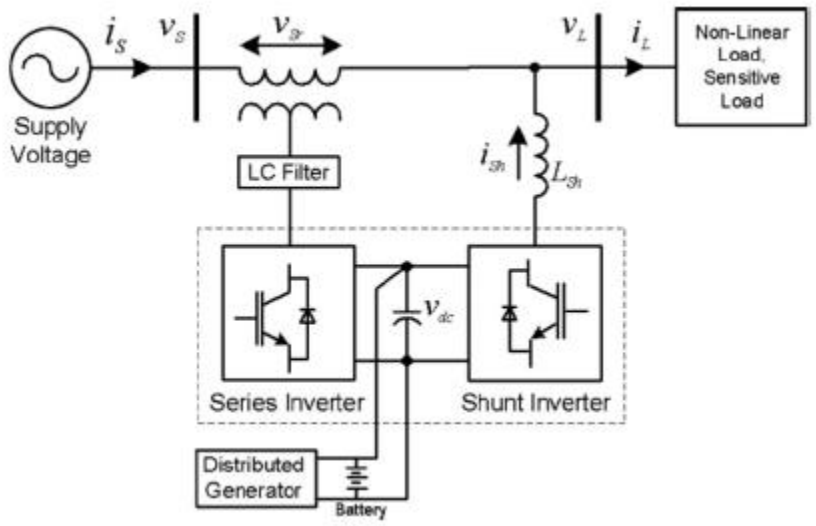

Figure 54- Illustration of UPQC to integrate distributed generator [55]

3.3.3 Topologies and paralleling literature review summary and proposed integration solutions for fast jet

To summarise the topologies and parallel techniques reviewed, a summary is provided in this section to discuss their potential application for fast jet. Within this, the resulting three integration methods chosen for fast jet applications explored in the rest of the thesis is elaborated (making up the main body of work of the thesis).

3.3.3.1 DC side integration

Making up first of the three proposed integration method, areas of interest taken from the literature review firstly included the identification of DC linkage around the aircraft as possible distributed integration points. This is akin to the common DC links to in inverter topologies of EVs and M/DG/R which multiple power sources can be connected for subsequent feed through. On fast jet, similar DC links exist within non-linear loads with rectifier stages as well as the TRUs. Different to the inverter set up of EVs and M/DG/R, the rectifiers are passive and do not allow power flow back into the AC side of the electrical system. However because; these are rectifiers, there is also DC side loading present. As such, this thesis proposes the use of these fast jet DC links in a similar manner to the EV and M/DG/R literature for integrating and parallel additional generation sources. However, rather than feeding power back into the AC side, the rectifier will continue to draw power from the mains generation. However, by adding power onto such DC links, the main generation draw will be offset

and essentially allow load sharing between the newly added generation and the existing main generation. This proposed paralleling of power can be achieved without the need to change the main generation.

In terms of paralleling of the DC link, the proposal in this thesis is to apply voltage master and current slave control similar ton [44]. Differently to an active voltage master controlled by one of the DC DC converters shown in [45]; each voltage master/DC link point can be passively "mastered" by the normal rectified main generator feed, holding the voltage at the DC link.

Figure 55 illustrates the highlighted section of the fast jet electrical system of which additional power can contribute from such integration using the TRU DC link as an example. Similarly additional to TRUs (not shown in Figure 55), this integration can also be applied to the 115VAC to 270VDC non-linear load rectifiers as well which can supply the local DC loading of the respective non-linear loads. This integration method is explored for the fast jet aircraft in chapter 4.

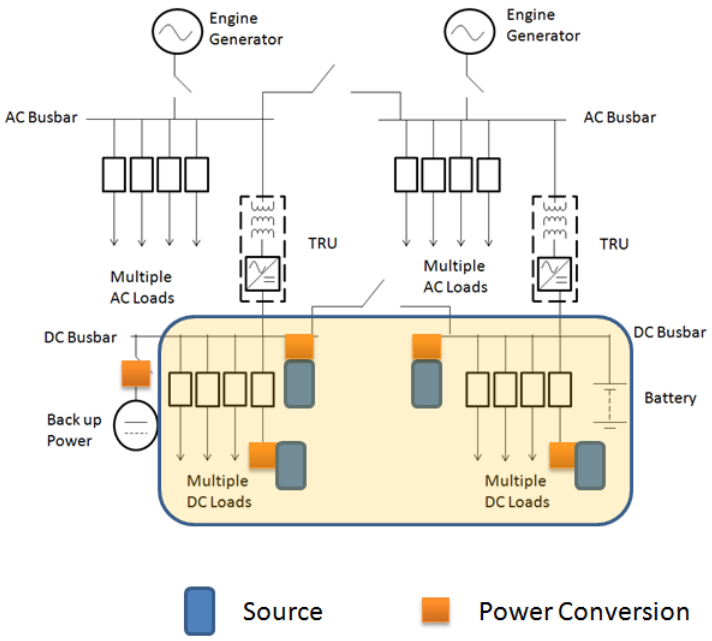

Figure 55- network section serviced by DC side integrated supplementary power

3.3.3.2 AC side integration

Making up the second of the three proposed integration method, additional to the proposed DC side only integration of supplementary generation for fast jet application on the DC link of passive rectifiers; the use of SAF can also provide a convenient method for injecting power into the electrical system in parallel to the main generation. This proposed application of SAF to utilise the secondary

power injection additional to its main functionality of reducing harmonic current draw from the PCC. One of the main benefits of such integration approach is, similar to the rectifier DC link based integration: there is no need to modify the existing main generation for paralleling. Also similar to the DC side integration proposed in section 3.3.3.1, the thesis proposes the same voltage master and current slave control setup to control paralleling on the DC link for commonality. This would be applied at the DC link of the SAF. However different to the integration of power onto a passive rectifier DC links presented in section 3.3.3.1; the voltage master for the SAF application would be "mastered"/held actively by the SAF DC voltage control itself. Figure 56 highlights the possible integration of such SAF within a fast jet electrical system and highlights the electrical sections that can make use of the subsequent added power. This is explored in chapter 5.

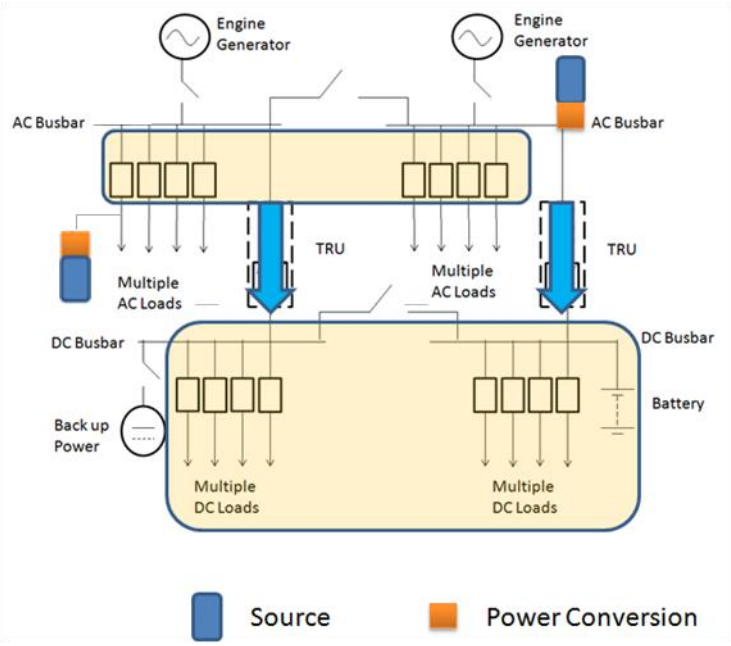

Figure 56- network section serviced by AC side integrated supplementary power

3.3.3.3 AC DC integration

Making up the last of the three proposed integration method, revisiting section 3.3.3.1 again, the amount of power integration at the DC links of the passive rectifiers or TRUs becomes saturated when the DC generation capacity exceeds DC side loading. One variation of this, which the thesis also proposes: is in the conversion of these passive stages to bi directional active equivalents. This could ultimately allow the excess power generation to be fed back into the AC sections of the fast jet electrical system (turning them essentially to inverters more akin to the EV and microgrid topologies). When comparing this to the introduction of a standalone inverter for solely power

integration, this approach offers the benefit of reduced sizing of the inverter needed as some of the power is already consumed by the local load. Another benefit is with such a setup, there is the opportunity to reuse the existing wiring of the rectifier (e.g. no need to add and route dedicated wiring into the compact airframe) as well as taking advantage of the distributed location of the load itself. Example integration points are depicted in Figure 57 against the generic fast jet electrical system as well as the zones which the additional power can contribute to. Similarly to the other proposed integration options for fast jet, this also does not require changes to the main generation. This is examined in chapter 6.

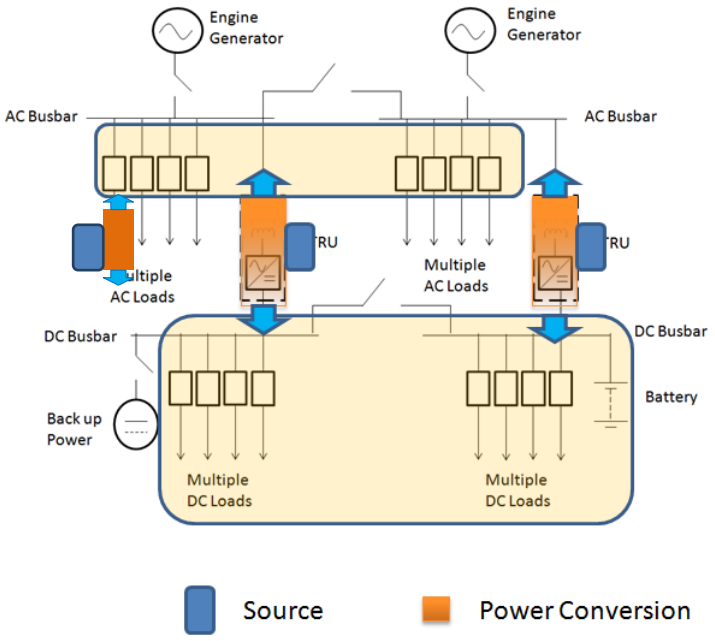

Figure 57- network section serviced by trans AC DC side integrated supplementary power

3.3.3.4 Combined operations

One of the main underlying characteristics of these three proposed integration methods is in the use of local voltage master and current slave control at the separate DC links. As such, adding power within adjacent DC links should not affect the operations of each other and allow concurrent operations aiding the idea of incremental addition and retrofit for in service fast jet. The combined operations of the three integration methods are examined in chapter 7 which simulates different configuration of concurrent power integration using all three methods.

3.4 Summary

In summary of this chapter, a literature review of possible engine off take independent generation sources that can potentially be used to supplement the main generation of a fast jet aircraft has been presented. This is to support the proposed concept of adding supplementary generation to cope with increasing through life upgrades within this thesis. The identified sources are evidential of suitable generation sources existing currently or currently maturing, that they are/can be flight cleared and are powerful enough for fast jet power demand levels arising from through life upgrades.

In the absence of paralleling such supplementary generation within a fast jet electrical system; a literature review of standardised paralleling topologies from EVs and M/DG/R was also presented to identify similarities and transferable techniques for paralleling additional generation for the fast jet application. The explored application of these for the unique fast jet upgrade problem forms the main contribution of this thesis. This resulted in proposed integration method for distributed power generation which are examined in subsequent chapters 4-7. The novel contribution of the research work comes from the application context of these methods to increase supplementary power penetration for compact fast jet in the face of the unique problem of through life upgrade demands.

4 Passive rectifier DC link based power integration for fast jet

4.1 Chapter overview

The first supplementary power integration method proposed in this thesis for fast jet application is presented. This is the DC side power integration firstly proposed in chapter 3. This is: the application of supplementary sources onto the DC link of existing passive rectifiers around the fast jet electrical system (within non-linear loads and TRU). Such integration has not been widely applied for conventional fast jet applications to date and is akin to the DC link interface of inverters that connect power of M/DG/R back to the main grid in terrestrial applications [84], [85], [89]. However, the difference for the intended fast jet application is there is no feed through of power back into the main AC grid if applied to rectifier DC links (instead of inverter DC links). However, by adding sources onto such existing DC links of passive rectifiers around the fast jet electrical system; the subsequent added power can offset the power drawn from the main generation through such rectifiers. By doing so, power can be flexibility integrated into the fast jet electrical system in parallel to the main generation: increasing the overall power generation within the system as a result to meet the increase of through life demands. The distributed DC links of the non-linear load rectifiers and TRU has the potential to allow supplementary generation to be more flexibly distributed around the remaining space of the fast jet. With this the through life upgrades that increases the demand of the fast jet can be matched without the need for single bulk main generation replacement. Solely replacing the main generation is constrained by the need to change associated mechanical linkage as well as still being constrained by the same space constraints of the original generators location. Another benefit of having such integration for non-linear load is the subsequent indirect reduction of current harmonics drawn from the reducing the overall *ITHD* [56].

This type of power integration is more readily applicable for the 28V TRU DC link of the fast jet aircraft, however applying such addition of power onto the DC link of non-linear loads with 115Vrms to 270VDC rectifiers has constraints discussed in chapter 3. This is; the DC link of the 270VDC output maybe hermitically sealed within the equipment; restricting access. Ultimately this limits the amount of access points in the system (possibly more suited for future equipment additions where there is more scope to request such access from the OEM). Overall this still offers a possible avenue of injecting power into the system and also presents a relatively easy mode of power integration

without the need for three phase AC paralleling as it indirectly offsets the power drawn from the main generation to the rectifiers.

In terms of novelty, the application of supplementary power in the fast jet context and in particular, at the existing DC links of non-linear load and TRUs have not been explored before. The novelty also comes from the use of this to specifically tackle through life fast jet demand increases within the space constrained context of the fast jet airframe.

This chapter examines such integration through simulations for both: DC link of 28VDC TRU as well as 270VDC rectifier of non-linear load to illustrate the alleviation of power from the main generation. The simulation results of these, illustrate a working instance of the proposed paralleling and: subsequent voltage and current profiles are compared against the bench marking from chapter 2 for comparison of their effects of such integration on the base fast jet electrical system.

4.2 Power integration at rectifier DC link overview

In this section, the proposed power integration mechanism at the DC links of passive rectifiers within fast jet is elaborated. This includes example of workable topology and control. The DC link integration is based on the proposed application of voltage master current slave control to allow for multiple DC sources to be connected to the same DC link while making use of the voltage held by the existing main generation through the rectifier.

Within the fast jet system, Figure 58 and Figure 59 illustrates the envisaged location and topologies of the setup for 28VDC (TRU) and 270VDC (non-linear load) options respectively within a single channel of the generic fast jet electrical system. This includes a workable buck boost converter design to interface the added generation sources to the DC link which are operated in current slave control. Successful implementation of this arrangement would see concurrent power supply to the 28VDC busbar (or 270VDC side of a non-linear load) in conjunction to the main generation without requiring changes to the GCU or additional paralleling power electronics on main generation.

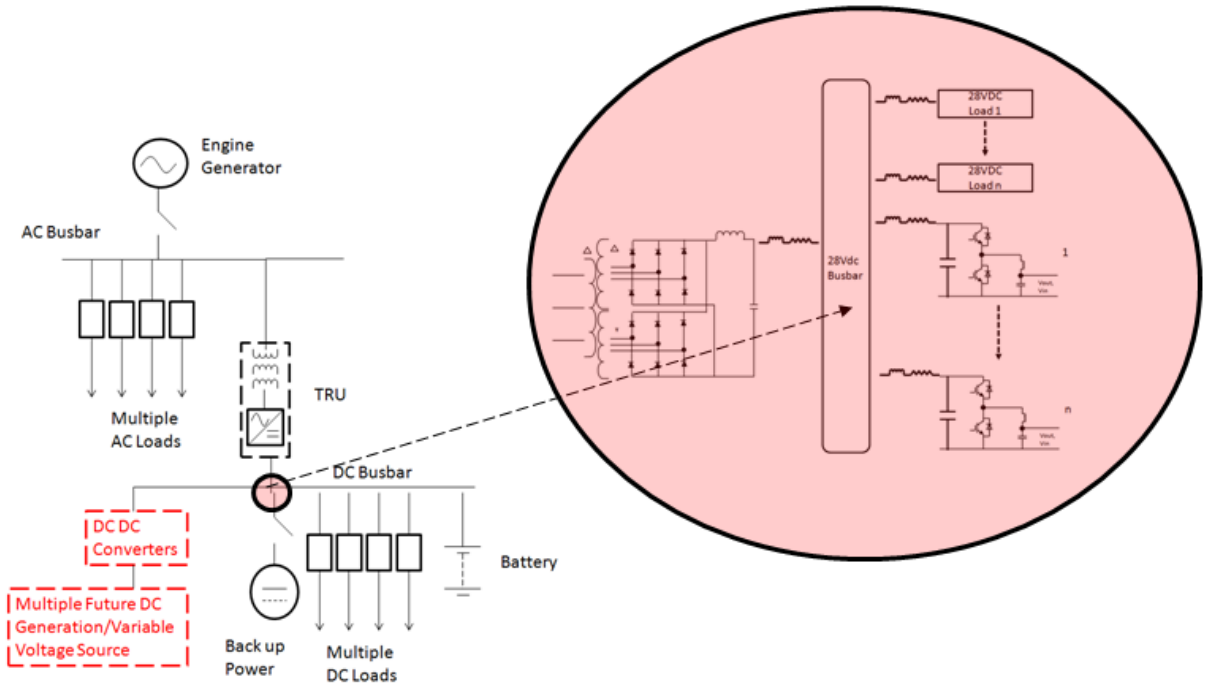

Figure 58- Illustration of proposed DC side integration with respect to generic fast jet electrical system channel for 28VDC

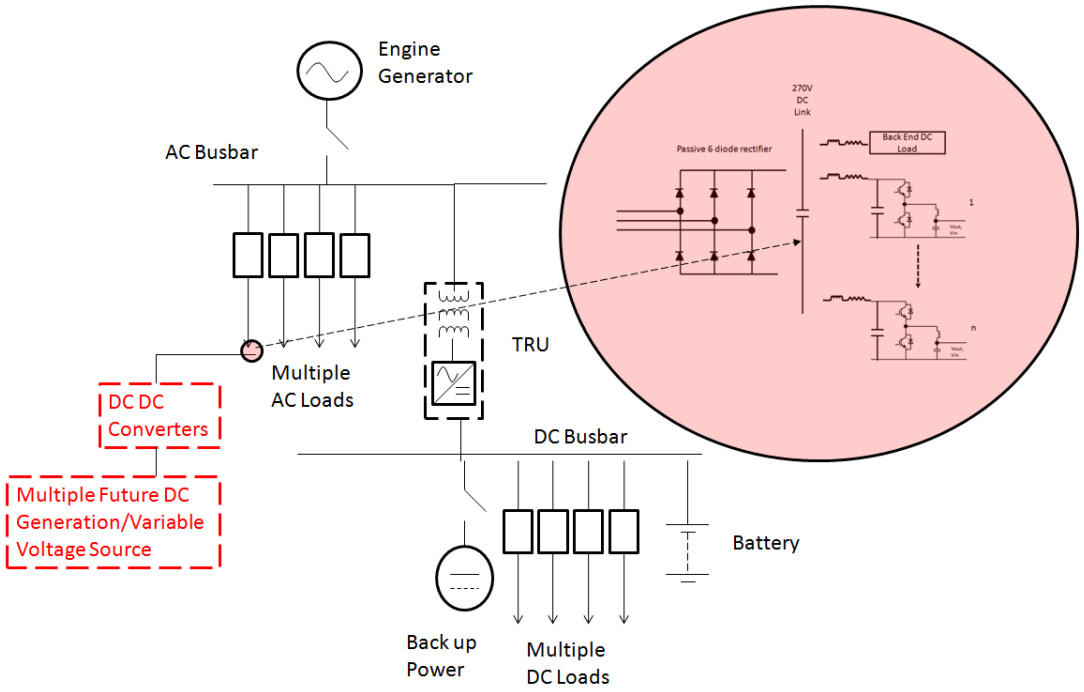

Figure 59- Illustration of proposed DC side integration with respect to generic fast jet electrical system channel for 270VDC

The basic current control proposed utilises current measurement taken at the DC generation source terminal prior the DC DC converter input stage and compares it to a current reference which is then fed into hysteresis control for switching at 40Khz. Although this control is utilised to demonstrate the DC integration in this chapter, the DC DC converter topology and control is not meant to be exclusive and could be interchanged with other control that provides similar current control functionality (i.e. different DC DC converter topologies, non-hysteresis control). The voltage master 'control' is provided passively using the existing main generation feed through to the TRU or non-linear load rectifier stage.

4.2.1 28VDC busbar emergency power as supplementary power

Additional to adding sources into the fast jet electrical system, the use of the same DC DC converters setup with current slave control for paralleling emergency power onto the 28VDC busbar is also proposed. This allows the raising of the peak generation of the overall system under normal operations with the benefits of limited weight addition.

Currently, one mechanism for connecting emergency power to the electrical system in a typical fast jet 28VDC busbar is through a "in series" diode. This is connected at all times to the 28VDC busbars whereby the voltage supply level of the emergency power generation is deliberately chosen below the normal DC busbar level of 28VDC at around less than 26VDC. Hence during normal operations when the DC bus bar is powered through the TRU, the voltage level is higher than 26V, and the

potential difference does not allow current flow in the conduction direction of the diode. However, with the loss of power through the TRU, the voltage at the DC busbar drops to below 26V and the potential difference favours current flow through the diode allowing emergency power transfer.

By replacing the diode with a buck boost converter under current slave control similar to adding additional power generation in the system; increased peak generation can be achieved. This proposed setup is illustrated in

Figure 60 (again within a single channel of the generic fast jet electrical system for illustration) where the left side represents existing practice and the right is the replacement proposal with the DC DC converter.

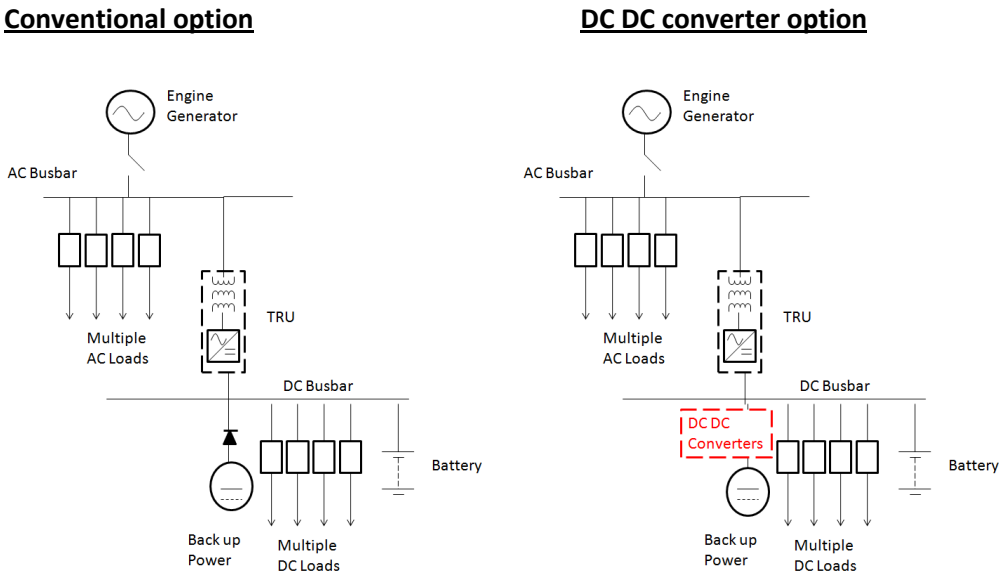

Figure 60- Replacing passive diode connection mechanism (left) for emergency power with active DC DC converter (right)

By replacing the diode with a DC DC buck boost converter as shown by

Figure 61, the current slave control can be used again and activated when required for peak demand times increasing peak power output within the overall fast jet (left hand side of

Figure 61). In other times, this can be operated in passive mode (the switches of the DC DC converter in their "off" position, shown on the right hand side of

Figure 61) whereby the passive emergency power linkage through the diode is preserved (preserving the robustness of passive operation in the case of an emergency). As mentioned in chapter 3, peak

power/active mode of such emergency power could possibly be applied during combat phases whereby sensors such as radar are operating at full power.

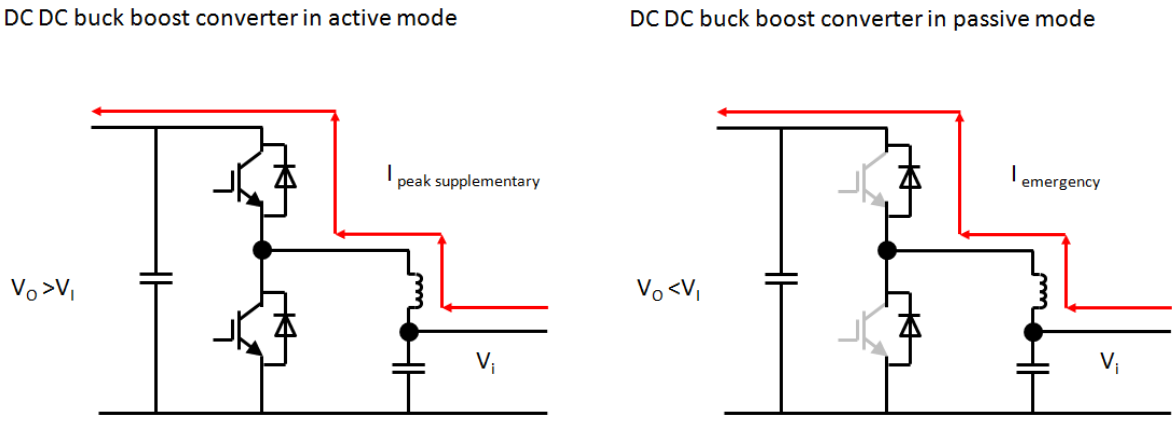

Figure 61- Active (left) and passive (right) mode of proposed DC DC converter for emergency power

4.3 Simulation results of power integration through rectifier DC links

To illustrate the operations of the proposed integration of additional power onto the DC link of passive rectifier; modelling and simulation is presented in this section. These simulation results are compared to the baseline electrical system models from chapter 2 to quantify the effects of having such integration and the subsequent alleviation of power draw from the main generation in its base configuration.

4.3.1 28VDC integration simulation results

This section presents the simulation results of the power integration at the TRU's 28VDC DC link (see Figure 58).

4.3.1.1 5kW TRU loading simulation results

The main simulation examined in this section is the simulation of the fast jet electrical system model loaded with a single 5kW TRU with the additional source/s connected to its DC link. These offset the power draw from the main generation to illustrate integration of supplementary power generation. Variations of these simulations include varying the amount of power injected by the additional power source and also varying the number of additional sources connected.

Table 8- DC DC converter model parameters used in studies for 28VDC

Component	Parameter	Value
DC DC Converter	Hysteresis Switching frequency	40Khz
	Smoothing inductance	6mH
	Input capacitance	1.5uF
	Output capacitance	15mF
	Additional output smoothing inductance	100uH
DC Source	Voltage input	24VDC
	Power supply at current set point	Power required
	Internal resistance	0.01Ohms
Passive Rectifier	Filter capacitance	2000uF

Table 8 above presents the parameters of the workable DC DC converter design and the TRU values used in the simulations. For the additional power generation source model used in the simulations, an ideal DC voltage source with an internal series resistance was utilised.

Table 9 presents the summary of these simulation results. The baseline power loaded from the main generation of the fast jet electrical system for a single TRU is around 5kW without any additional

supplementary power and is presented in first row as the baseline (benchmarked originally in chapter 2). The subsequent rows present the effects of adding different numbers and levels of DC power generation onto this same TRU DC link through individual DC DC converters under their own current slave control described in section 4.2. These simulations illustrate the indirect paralleling of the supplementary sources with the main generation using their own individual current control and indirectly reduce the power draw from the main generation drawn to the TRU. The harmonic current and voltage actually decreases as expected: as a result with adding power generation onto the DC side directly. The bottom row of Table 9 is the result of the scenario when the supplementary generation is greater than the normal loading on the DC busbar signifying saturation whereby no more power can be usefully utilised. As a result, the DC link voltage is pushed up to allow the power to be dissipated (in this instance, the loading is resistive based). In this saturation instance, the voltage was pushed up to 35VDC from 30.5VDC nominal voltage (bench marked in chapter 2) to accommodate the excess power for resistive loading.

These results demonstrate the basic concurrent operation of DC power integration onto the 28VDC busbar while still being fed by the TRU as it continues to draw power from the main generation and effectively supporting load sharing.

Table 9- Results of 28VDC integration at TRU output with supplementary power

Case	Averaged PCC S (kVA)	Averaged PCC P (kW)	Averaged PCC Q (kVAR)	VTHD (%)	ITHD (%)	Fundamental Voltage RMS Phase A (V)	Fundamental Current RMS Phase A (A)	Current 5th Harmonic (A)	Current 11th Harmonic (A)	Load Draw (kW)
TRU (from chapter 2 bench marking)	5.20	5.15	0.23	1.41	12.44	115.1	12.44	0.07	1.27	5.08
TRU with 1.25kW added to DC link	3.98	3.94	0.14	1.27	13.1	115.2	11.42	0.05	0.99	5.13
TRU with 2x 1.25kW added to DC link	2.76	2.73	0.09	1	13.49	115.3	7.91	0.04	0.69	5.17
TRU with 3x 1.25kW added to DC link	1.55	1.53	0.05	0.67	13.91	115.3	4.42	0.02	0.39	5.2
TRU with 1x 5kW added to DC link (reaching saturation point)	0.58	0.58	0.02	0.34	14.21	115.4	1.67	0.01	0.15	5.24
TRU with 1x 7.5kW added to DC link (saturated)	0.01	0.01	0.01	0	0.09	115.4	0.04	0	0	6.91 (DC link voltage increasing)

For the purpose of illustration; sample results of the 28VDC simulations are presented in Figure 62 and Figure 63 for the case in which 3 x 1.25kW of supplementary power is integrated at the DC link. This is shown on the right hand side of the figures (with bench marking of chapter 2 results on the left hand side for comparison). Within Figure 62, the *P, Q* and *S* plots at the PCC are presented where the virtual 5kW level is represented by the upper black trace which represents the power drawn from the main generation without supplementary generation. The actual real power drawn from the main generation is represented by the green trace which, on the right hand side of Figure 62 is at a reduced power level draw compared to the left side due to the supplementary power integration. This is due to the fact that the three additional 1.25kW generation sources has offset the main generation while the power to the load is still maintained at around 5kW. Figure 63 illustrates the time based *V* and *I* profiles at the PCC which reaffirms the reduced draw as well as the preservation of power quality (again with results on the right hand side and bench marking from chapter 2 shown on the left hand side for comparison).

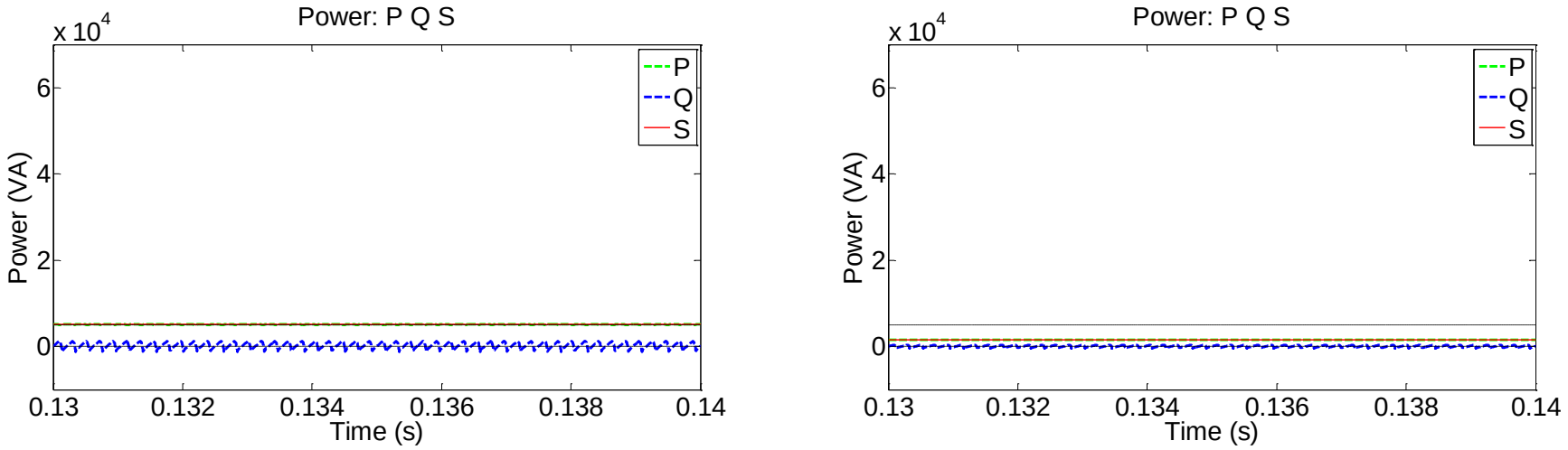

Figure 62- P, Q, S comparison between benchmarking (left) and added supplementary generation (right) using 3x DC DC converters for 3x 1.25kW sources

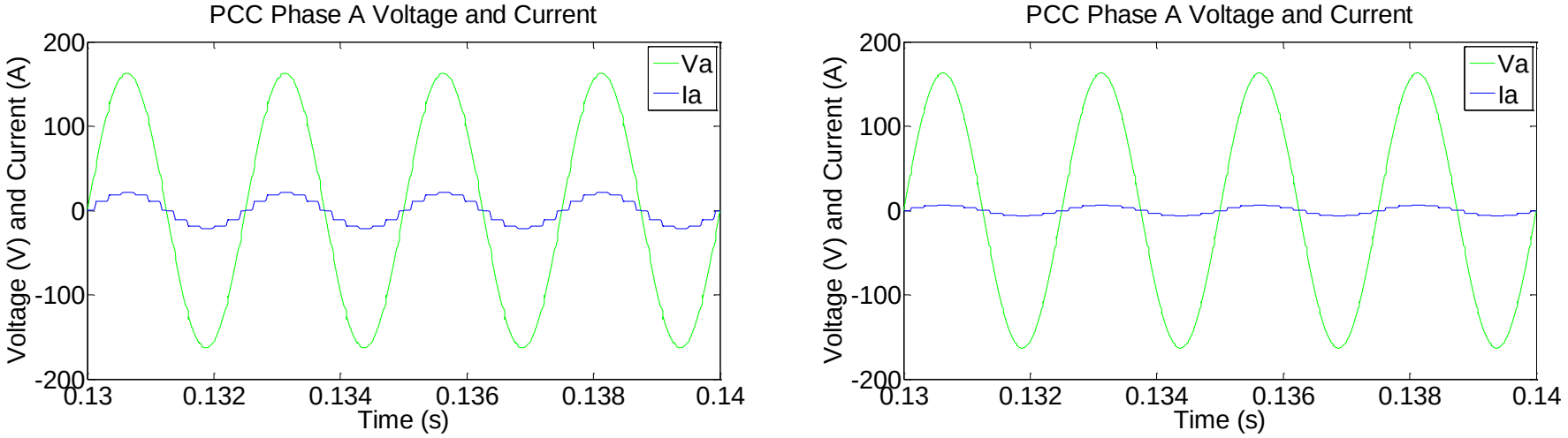

Figure 63- V, I comparison between benchmarking (left) and added supplementary generation (right) using 3x DC DC converters for 3x 1.25kW sources

Figure 64 illustrates the voltage levels at the busbar/DC link which shows the voltage quality is still maintained even with the three supplementary sources added through their respective converters.

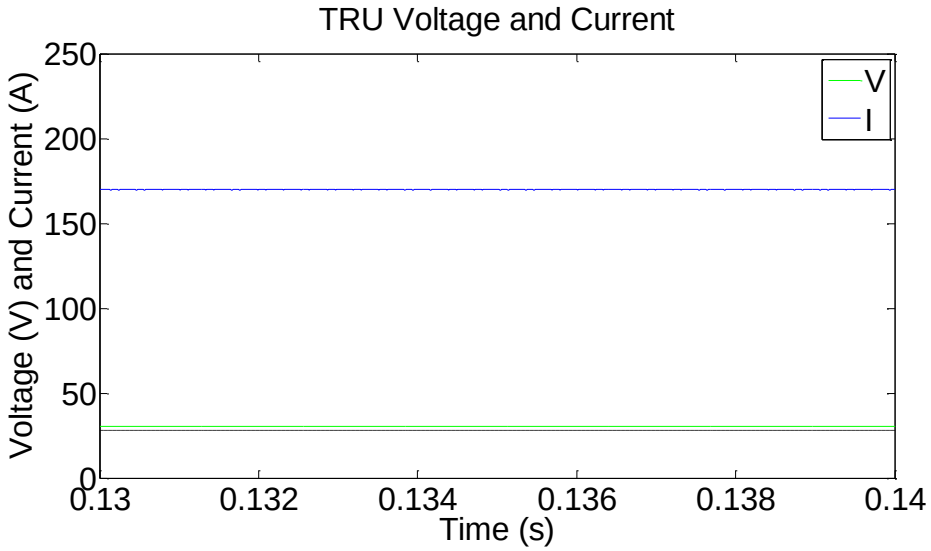

Figure 64- TRU terminal with 3x DC DC converters for 3x 1.25kW sources

4.3.1.2 25kW single channel loading simulation results

With the simulation results of the DC link integration onto standalone 5kW TRU in section 4.3.1.1, this section examines the simulated application of the same power integration at the TRU but in parallel to other loads drawing from the same PCC/AC busbar within the electrical system. This setup is the 25kW combined loading configuration (benchmarked in chapter 2) and consist of a 10kW non-linear load, a 10kW linear load and a 5kW TRU loading all drawing from the same fast jet electrical system. An additional 4kW of power is added to the TRU DC link in this scenario through a single DC DC converter.

The subsequent results taken from the PCC are presented in Figure 65 (*P, Q, S*) and Figure 66 (*V, I*) respectively. From these, the benefits of alleviation of power from the main generation can be seen more clearly. Firstly the top black trace of Figure 65 on the right hand side represents the normal 25kW real power level that the loading draws without the 4kW supplementary generation. The middle black trace of the same figure is the reduced real power draw at 21kW (which the added 4kW allows for). As such, this illustrates the proposed method of integrating additional generation which alleviates the power draw from the main generation as intended and illustrates an avenue to cope with increasing through life power demand.

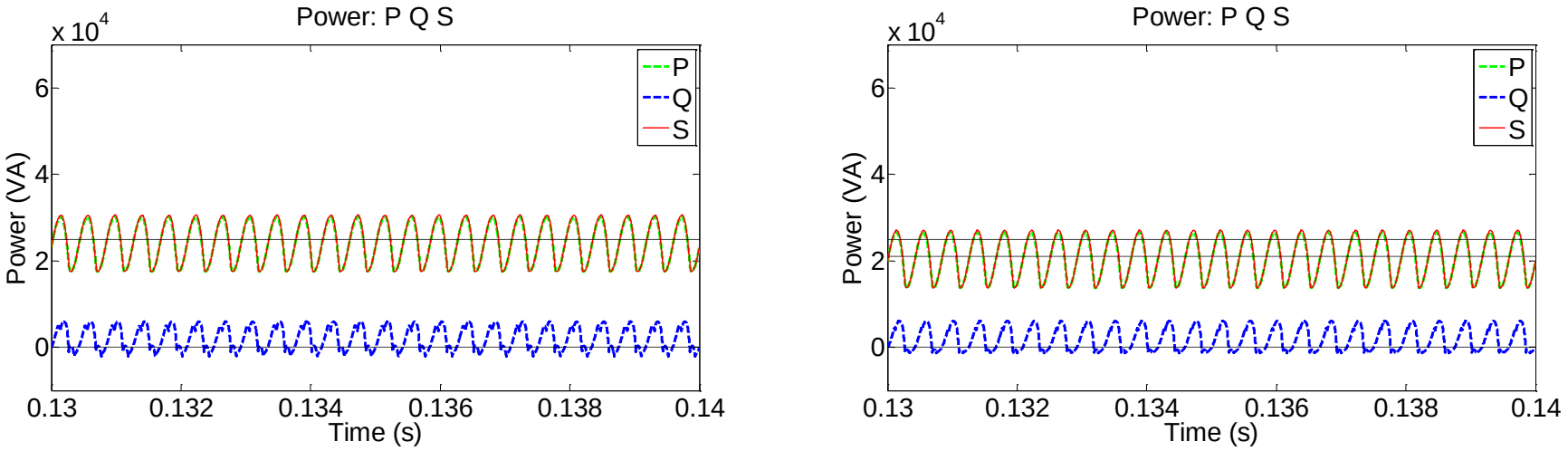

Figure 65- P, Q, S comparison between benchmarking (left) and with added SAF (right) with

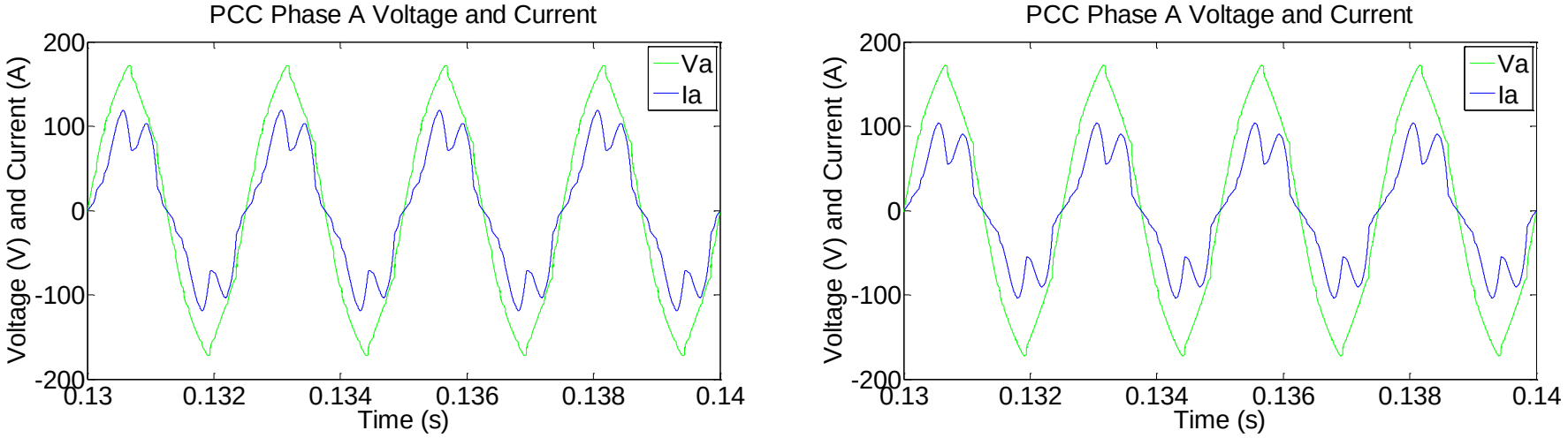

Figure 66- V, I comparison between benchmarking (left) and with added SAF (right)

4.3.2 270VDC integration simulation results

Similarly to section 4.3.1, this section presents the simulation results of power integration on the DC link of a six diode 115Vrms to 270VDC rectifier within a non-linear load (Figure 59).

4.3.2.1 10kW non-linear loading simulation results

The main simulation examined in this section is the simulation of the fast jet electrical system model loaded with a single 10kW six diode rectifier/non-linear load with the additional source/s connected to its DC link. Similarly to section 4.3.1, this power integration offsets the power draw from the main generation. Variations of amount of power injected are presented: either by varying the power injected by single additional power generation source or by varying the number of additional power generation sources integrated to the same DC link.

The PCC results of these are presented in Table 10 and for comparison again, the first row of Table 10 is the bench marking of the 10kW non-linear load without supplementary generation from chapter 2. The second row is the result for same 10kW non-linear load with a single supplementary generation of 7.5kW connected to its DC link through a DC DC converter. In this case, it is demonstrated through the simulation, that the approach decreases absolute current harmonics drawn at the PCC (although there is an increase in relative harmonics) and the voltage harmonics also decreases as a result. The third row is the result of the scenario where two separate power generation sources of 4.5kW are connected to the same DC link. This gives a total capacity of 9kW to demonstrate concurrent operation of multiple sources connected to the same DC link and this concurrent operation does not adversely affect the supply function of each other. In the final row, the result of the simulation of when power supply is greater than the 10kW local demand is presented to show saturation. As expected, similar to the TRU scenario of section 4.3.1.1, the voltage at the DC link increases to accommodate the higher power (with resistive based loading).

Table 10- Results of 270VDC integration at non-linear load output with supplementary power

Case	Averaged PCC S (kVA)	Averaged PCC P (kW)	Averaged PCC Q (kVAR)	VTHD (%)	ITHD (%)	Fundamental Voltage RMS Phase A (V)	Fundamental Current RMS Phase A (A)	Current 5th Harmonic (A)	Current 11th Harmonic (A)	Load Draw (kW)
Non-linear load (from chapter 2 bench marking)	10.18	9.69	2.16	4.38	54.36	114.6	29.16	14.03	2.39	10.18
1x 7.5kW supplementary generation	2.69	2.62	0.47	2.13	91.96	115.2	7.91	5.64	1.45	10.11
2x 4.5kW supplementary generation	1.00	0.98	0.11	1.15	109.7	115.4	3.06	2.12	1.09	10.42
1x 11kW supplementary generation (saturated)	0.09	0.08	-0.03	0.01	8.03	115.5	0.25	0.02	0	11.12

Sample illustrative results of the simulation with 2 x 4.5kW additional power generation sources integrated at the same DC link of the rectifier are illustrated in Figure 67 (*P, Q, S*) and Figure 68 (*V, I*) respectively. Again, the actual results are presented on the right hand side of the figures with the benchmarking results of chapter 2 shown on the left hand side for comparison. The upper black trace in Figure 67 is the 10kW level reference which represents the power draw if there was no supplementary power (or power consumed by the loading). On the right hand side, it can be seen that the power levels drawn from the main generation is alleviated by the added supplementary generation.

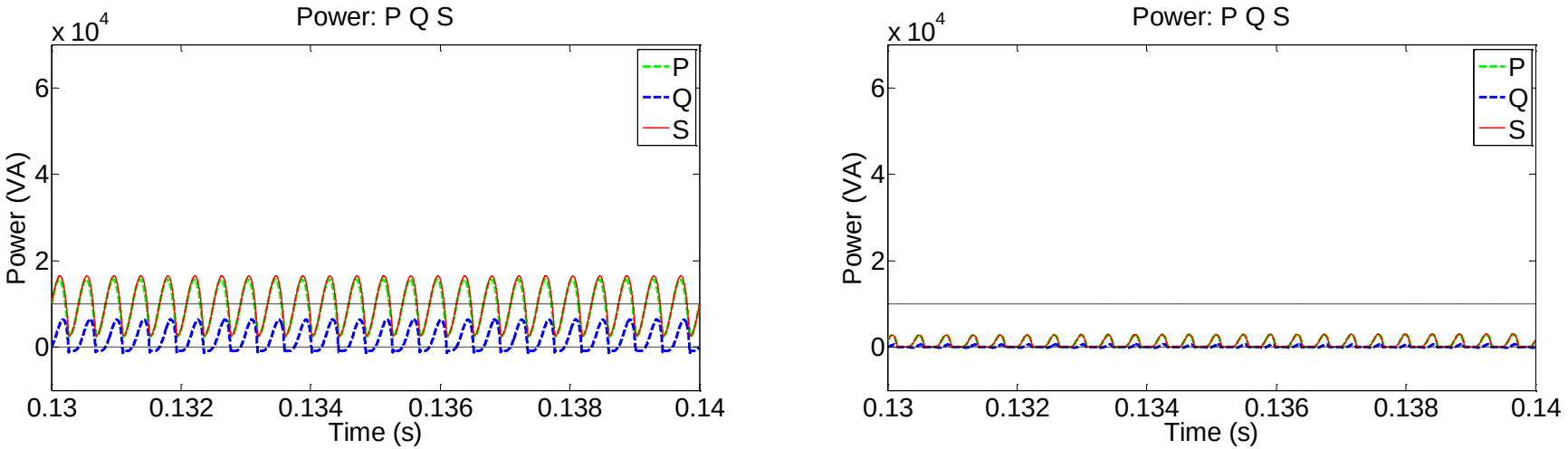

Figure 67- P, Q, and S comparison between benchmarking (left) and added supplementary generation (right) using 2x DC DC converters for 4.5kW sources

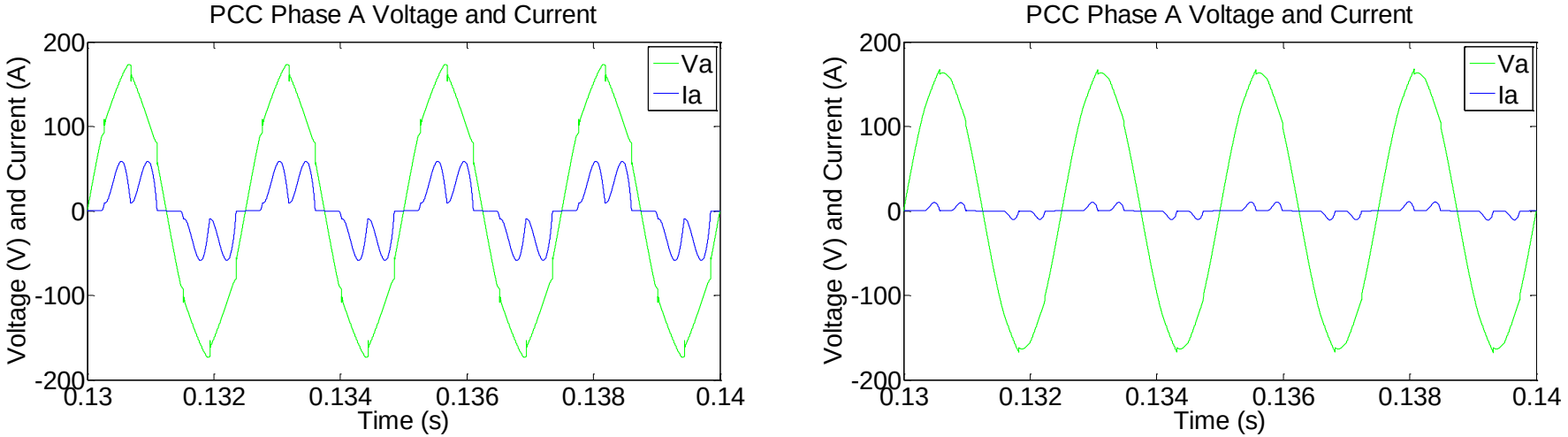

Figure 68- V, I comparison between benchmarking (left) and added supplementary generation (right) using 2x DC DC converters for 4.5kW sources

4.3.2.2 25kW single channel loading simulation results

With the simulation results showing DC link integration onto standalone 10kW non-linear load drawing from the fast jet electrical system presented in the previous section, this section presents the simulated application of this integration in parallel to other loading drawing from same electrical system. Again the same 25kW combined loading model was used (benchmarked in chapter 2) and consist of a 10kW non-linear load, a 10kW linear loading and a 5kW TRU.

In this, 9kW was added to the 10kW rectifier DC link through DC DC converter within the simulation. The illustrative results of this is presented in Figure 69 (*P, Q, S*) and Figure 70 (*V, I*) respectively. From these figures, it can be seen more clearly, the alleviation of power from the main generation when there is parallel loading within the system. Firstly the upper dashed trace of Figure 69 on both left and right hand side represents the normal 25kW real power level that the loading draws from the main generation without the 9kW supplementary generation. The middle black trace of the right hand side of the same figure is the reduced real power draw at 16kW from the main generation (which the added 9kW allows alleviates the main generation to). As such, this illustrates the proposed method of integrating additional power into system at the DC link of a non-linear load rectifier DC link and an avenue to cope with increasing through life power demand again.

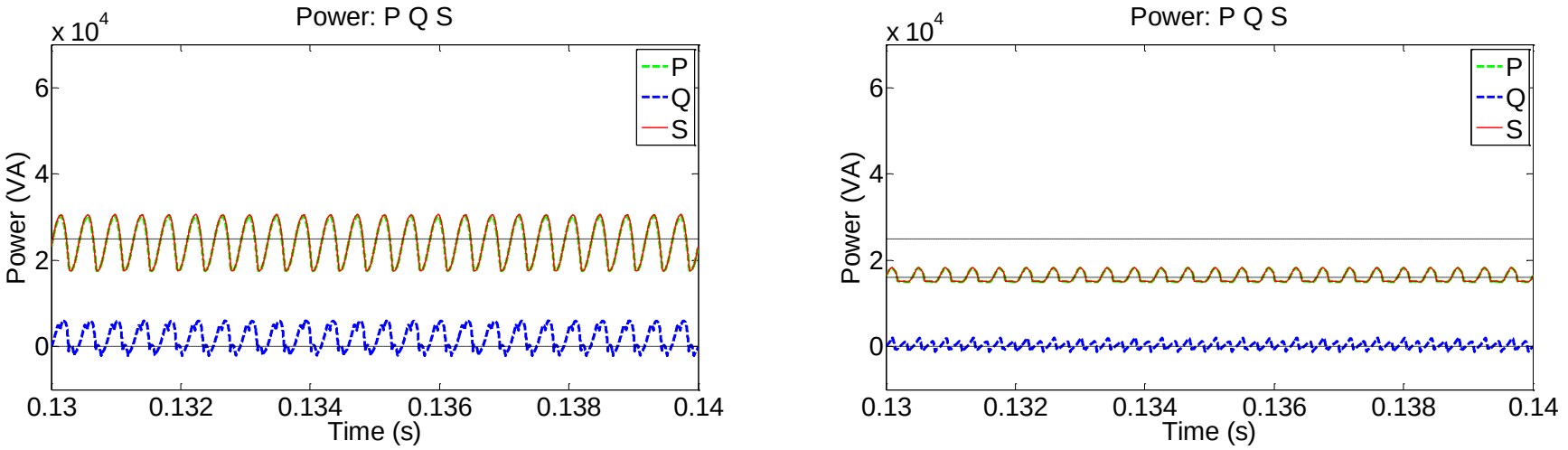

Figure 69- P, Q, S comparison between benchmarking (left) and with added SAF (right) with

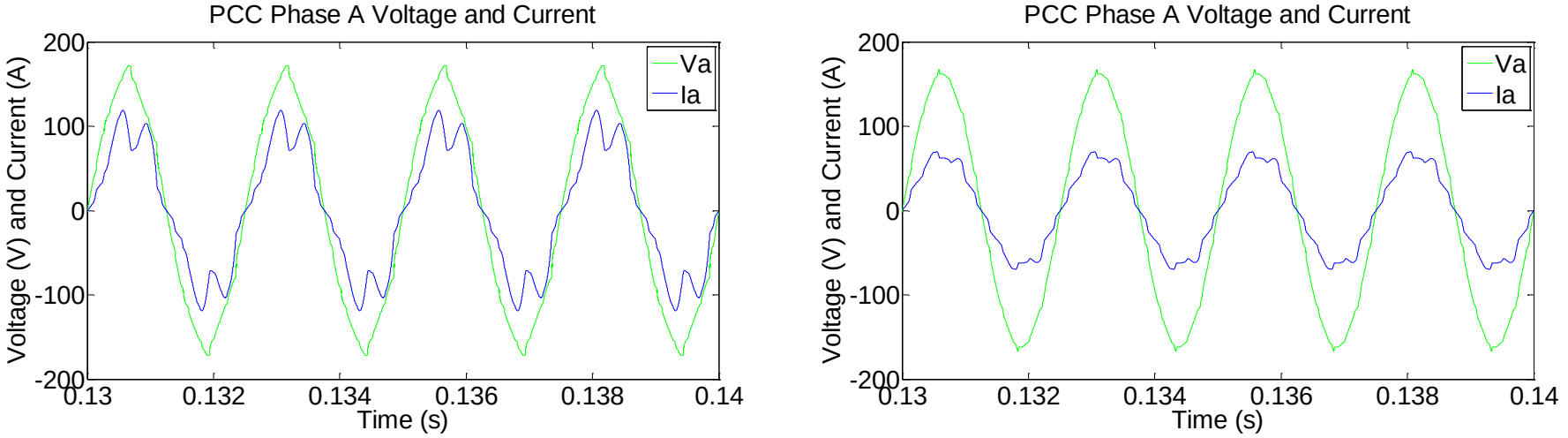

Figure 70- V, I comparison between benchmarking (left) and with added SAF (right)

4.3.3 Utilisation of emergency power simulation results

Section 4.2.1 proposed the use of existing emergency power on the 28VDC busbar in parallel to the main generation to increase the overall peak generation on the fast jet. By using similar DC DC converters to adding additional power generation into the system at the 28VDC busbar outlined in section 4.2.1 (and simulated in section 4.3.1); emergency power generation already within the system can also be utilised with a similar set up. In this, the DC DC converter can replace the conventional diode that connects the 28VDC emergency power into the system. Additional to paralleling with the main generation using the active DC DC converter interface; passive mode can potentially provide passive emergency power transfer in place of the diode. As the active paralleling functionality is already presented in simulation in section 4.3.1, this section presents the simulation of passive mode ultimately illustrating that such DC DC converter can be operated as emergency power during emergency scenarios and as supplementary power during peak demand scenarios.

Firstly, although there will always be emergency power present in the fast jet aircraft electrical system, Figure 71 is presented to illustrate the voltage and current of the TRU terminal when there is no additional emergency power provision to illustrate the profile of power loss. This is solely for subsequent comparison of the mechanism of applying emergency power application using the DC DC converters in passive mode. In this, the TRU output voltage and current gradually decreases to zero after the main power loss at 0.13s. The dashed black trace in Figure 71 represents the nominal 28VDC level of the TRU voltage during normal operations.

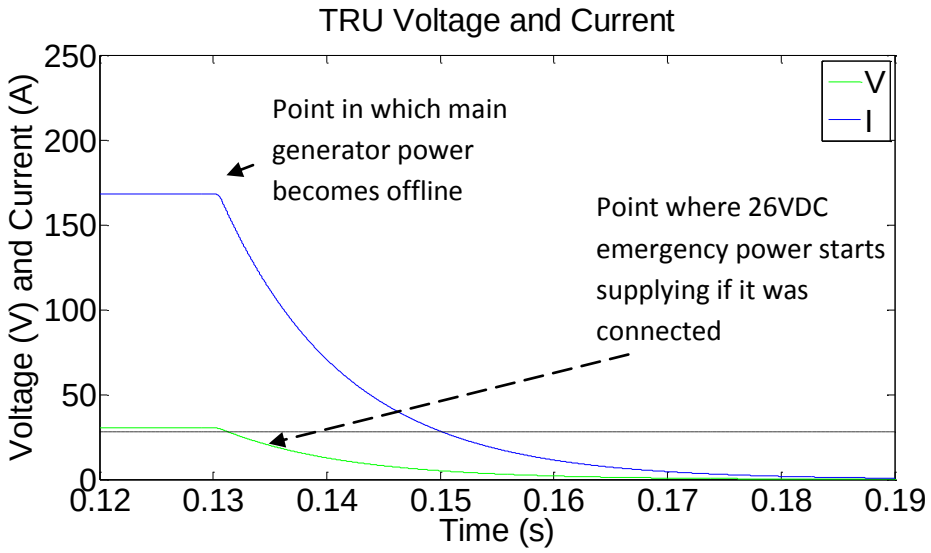

Figure 71- V and I of mains power loss with no emergency power seen at the TRU output terminal (DC output)

The results of the scenario where there is emergency power in the system but connected through a DC DC converter and "operating" in passive mode is presented in Figure 72 for the TRU terminal *V* and *I*. Again loss of main generator power is experienced at 0.13s, same as Figure 71. In this, the TRU supply, transitions from the generator to the lower voltage emergency power through the passive DC DC converter as the voltage dips. As it drops below 26V, the potential difference between the emergency source becomes favourable for current flow through the diodes of the passive DC DC converter and hence allow flow of emergency power flow. However, one main effect of utilising a DC DC converter instead of a standalone diode is the presence of smoothing inductance of the converter which adds additional limits to the speed in which the voltage can be recovered (this is shown as the dip in Figure 72). However, this could be potentially improved with further optimising of the converter parameters.

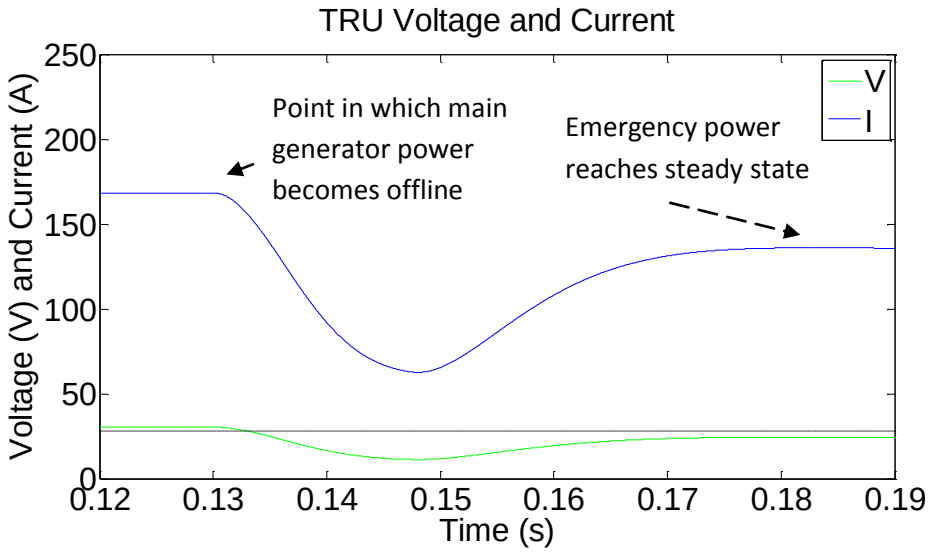

Figure 72- V and I of mains power loss with emergency power connected through DC DC converter seen at the TRU output terminal (DC output)

4.4 Summary

Additional power integration at the 28VDC TRU DC link and 270VDC non-linear load rectifier DC link of a fast jet electrical system have been presented (down selected in chapter 3). Such setup has the benefits of integrating more power into the system without the need to modify the main generation. The distributed nature of the rectifier DC links within the loads around the fast jet can potentially lend themselves for more distributed integration of additional generation sources and better use of any spare space.

With the use of simple DC DC buck boost converters controlled as current slave can allow additional power to be readily applied to the DC link of existing rectifiers within the fast jet electrical system. At the same time, the voltage can be held by the main generation indirectly through the existing rectifier itself. With this, paralleling of the additional supplementary sources with the main generation is possible with no changes needed to the main generation itself. By doing so, an indirect benefit of current harmonic draw reduction can also be realised.

Similarly, 28VDC emergency power (on the 28VDC busbar) can be paralleled with the main generation in the same way by replacing the diode interface with an equivalent DC DC converter. Hence the DC DC converter can be activated during peak demand times while operating in passive mode during other times, preserving potential emergency power flow. However one main limitation with this is the presence of smoothing inductance within the DC DC converter which can limit the response time of the emergency power supply to overtake the main generation.

The main limitation of integrating supplementary or emergency power at the existing DC links is: the power integration can only be as large as the aft loading before saturation occurs. It was also acknowledged that such integration is more applicable for the TRU option where the DC link terminal is more readily accessible. However in contrast, this may not always be the case for rectifiers in non-linear loads (115Vac to 270VDC), as the equipment maybe hermitically sealed and restricting access to the DC link. Hence this maybe better suited for future loads where there is more scope to design/request access to the link.

Overall, the novelty of this integration method is not in the converter topologies or control but in the proposed application of such within fast jet to meet increasing through life demand and to make use of the distributed nature this option brings in the face of space constraints.

5 Shunt active filtering for fast jet applications

5.1 Chapter overview

The proposed application of a SAF for fast jet aircraft down selected and proposed in chapter 3 is explored in this chapter. This is the proposed application of a SAF to integrate supplementary power directly onto the AC busbar/s to supplement the main generation in the face of through life demands in fast jet.

The first proposed method of power integration at existing DC links of non-linear loads and TRU to alleviate the draw from the main generation was examined in chapter 4. One constraint with this however is: the amount of power that can be added is limited to only the full extent of the DC side loading. Additional to this, DC links of non-linear load rectifiers (115Vac to 270VDC) may not always be accessible (i.e. hermitically sealed within the equipment). With such constraints, the amount of power penetration is still limited. Hence to supplement or as a standalone option, the application of a SAF for power integration is explored in this chapter. This makes up the second supplementary power integration method proposed for fast jet aircraft in this thesis.

The application of a SAF in an aerospace application has been researched in general [96]-[100], but limited application specific to fast jet has been seen to date. The primary function of the conventional SAF is to inject cancelling currents to cancel out the harmonic current drawn at the PCC of the electrical system caused by non-linear loading within the system [54]. To enable this functionality, the SAF operates by measuring the current drawn at the PCC and extracts the individual harmonic current magnitudes and phase. With this, the SAF injects the anti-phase equivalent into the system allowing the current drawn at the PCC to exhibit more ideal sinusoidal current profiles.

Described in chapter 3; there has been research in the concurrent utilisation of such SAFs for the convenient additional power injection back into AC electrical systems/main grids [101], [55]. These are primarily looked at for terrestrial applications; for example [101], demonstrates the use of a SAF for integrating renewables back into a terrestrial grid. The benefit is: no changes are required to the main generation that exists already in the network. In terms of operation, the SAF itself adheres to

the voltage amplitude, frequency and phase of the existing network and main generation. To use the SAF to inject power back into the network, additional power is added to the DC link of the SAF itself.

To date, this has not been applied to a fast jet. With the problem of through life upgrades, such functionality on a fast jet would provide a convenient means of integrating power without the need to alter the main generation itself and fitting with retrofit applications for in service fast jet. This is also particularly fitting for fast jet: in that, large amounts of on board loads are non-linear giving rise to high harmonic currents drawn through the PCC within the system. To add to this, future upgrades are also likely to be non-linear as well in the form of “electronics”. Hence the thesis has proposed adding additional supplementary power onto the fast jet aircraft with the use of a SAF. Exploration of operation is presented in this chapter against the generic fast jet electrical system (bench marked in chapter 2) through simulations to illustrate the alleviation of power from the main generation that such option can allow.

5.2 Power integration through a SAF on a fast jet

In this chapter, the proposed application of power integration of a SAF in a fast jet is elaborated. Example of a workable SAF topology and associated control is discussed in this section. It is proposed that the underlying paralleling control is based on voltage master current slave control, to enable flexible integration of multiple sources onto the DC link of the SAF while making use of the SAF voltage control as the voltage master. The current slave scheme also provides commonality with the proposed DC power integration for passive rectifiers and TRUs examined in chapter 4; standardising the control of the DC DC converters for retrofit across the fast jet aircraft.

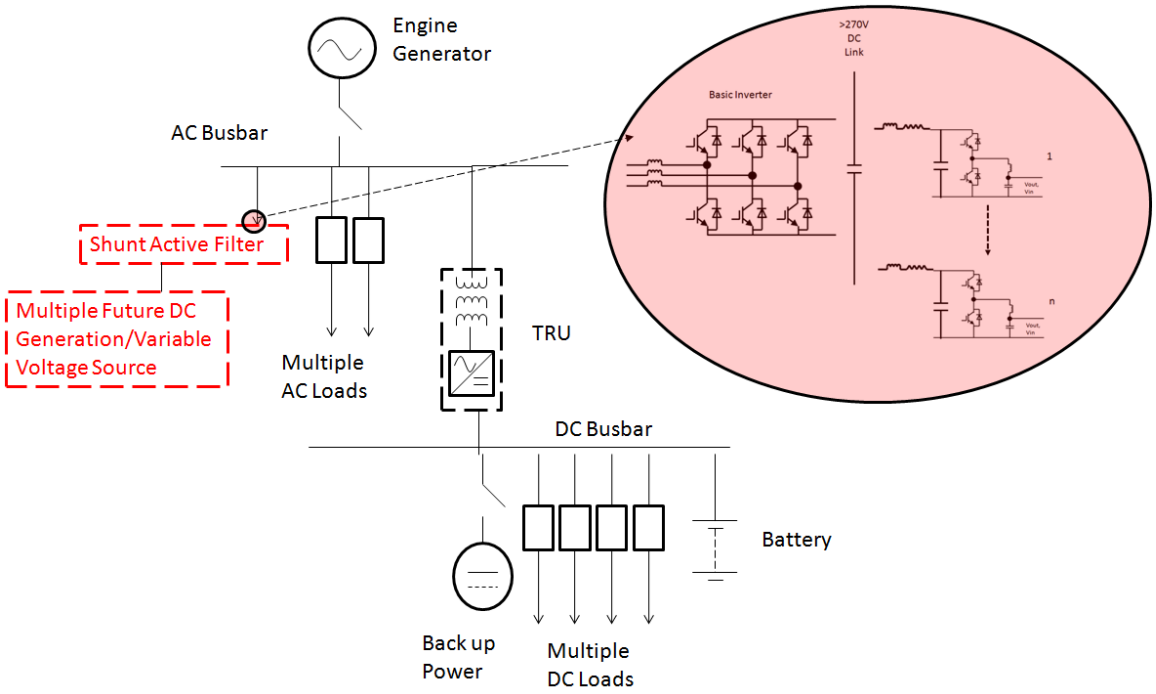

Figure 73- Illustration of proposed SAF with respect to generic fast jet electrical system channel

Within the generic fast jet system, Figure 73 illustrates the envisaged, location and topology of the SAF setup in a single channel of the generic fast jet electrical system. This includes a workable buck boost converter design (same as chapter 4) to interface the added generation sources onto the DC link which are operated in current slave control. Implementation of this arrangement would see concurrent power supply in conjunction to the main generation without requiring changes to the GCU or paralleling power electronics on the main generation itself.

The chosen topology of SAF used within this study consists of the standard six switches, three leg voltage source converter which is identical to the six switch inverter topology. Although this configuration was chosen for the studies presented, the application of SAF for power integration on

fast jet is not exclusive to this design and could potentially be interchanged with alternative topologies (such as multilevel converters [96] for better harmonic reduction performance etc).

The control of the SAF chosen within the studies of the thesis is the *dq0* based control [104] for extraction of the harmonic current content for cancellation in the electrical system. This control was chosen partly because it allows the fundamental *d* component to flow through the SAF unrestricted: equating to free flow of real power. This becomes convenient when applying additional generation sources connected onto the DC link and with the subsequent current slave control of the added supplementary generation can dictate real power *P* fed back into the AC system.

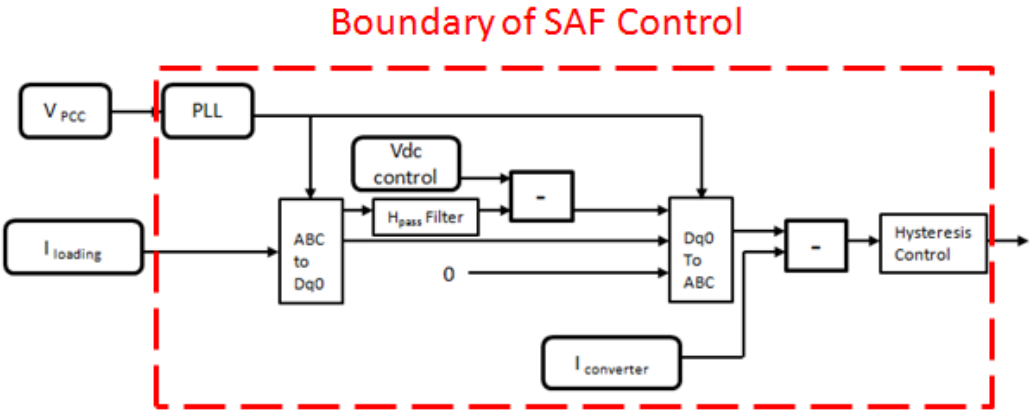

Figure 74- SAF control block diagram

The control design block diagram is illustrated in Figure 74. In this, the three phase loading current downstream ($I_{loading}$) of the SAF point is taken as the inputs in which *dq0* transform is performed against the PCC voltage reference frame. This gives the *d, q* and *0* components of the loading currents. To reduce the harmonic currents and leaving the "in phase" fundamental component unchanged, a high pass filter is utilised to extract the non-fundamental part of the *d* component. For the *q* component, a high pass filter is not utilised in an attempt to correct not only the harmonic *q* components but also the fundamental content for improvement of power factor. For this application, the *0* component is fed by a zero input which is sufficient if loading is balanced (work presented in this thesis focuses on balanced systems with unbalanced network open for exploration in further work). The *dq0* components are then subsequently converted back to the *ABC* frame for the three phases and are used as the reference current for the SAF.

To maintain the energisation of the DC link at 400VDC, a DC voltage controller is utilised and is added to the *d* component after the high pass filter stage. This also conveniently acts as the voltage master control at the DC link in anticipation of additional power integration through current slave mode (controlled by the individual DC DC converters).

5.3 Simulation results of power integration a through a SAF

To illustrate the operations of the proposed power integration through a SAF on a fast jet: modelling and simulation of this is presented in this section. These simulation results illustrate the operation of such SAF integration within the generic fast jet electrical system benchmarked in chapter 2. From this, integration effects and the subsequent alleviation of power draw from the main generation can be illustrated.

Firstly, section 5.3.1 presents the simulation of a workable standalone SAF design integrated into the generic fast jet electrical system model (bench marked in chapter 2) without any power integration. This is to establish a workable SAF design with adequate harmonic current reduction performance within a fast jet electrical network model. To reiterate: the SAF topology itself is not part of the novel contribution of this thesis but rather it is in the proposal to use a general SAF to flexibly integrate power on a fast jet electrical system in the face of increasing through life demands while keeping the original main generation intact and unchanged.

Following from this, section 5.3.2 examines the integration of additional power generation onto the DC link of this workable SAF to illustrate power feed through and in essence load sharing of the overall loading of the fast jet electrical system.

Section 5.3.3 explores the performance of the SAF against gradual increase of non-linear loading added to the baseline fast jet system. This is presented, as through life upgrades for fast jet aircraft are likely to be non-linear and further increase the current harmonics drawn from the PCC.

Section 5.3.4 examines the single engine generator failure scenario when there are SAFs present in both channels of the electrical system. With such generator failure, the bus tie contactor connects both islands into one through the bus tie contactor. This is important in the context of the study of SAF application as the co-existence of two SAF's within the same electrical island may become a problem during such generator failure scenario and hence their interaction requires exploration.

5.3.1 SAF integration on fast jet without power integration

In this section, a working instance of the SAF used in the power integration studies of this chapter is presented in simulation. Within this simulation, the application of the workable SAF is placed in the generic fast jet electrical system model while it is loaded with the 10kW non-linear load (originally benchmarked in chapter 2). This is to show the difference in harmonic current drawn/improvement of power quality at the PCC. Table 11 below summarises the component parameters utilised in this SAF. Some of these values were originally derived from [96]-[99] which provided ballpark figures for smoothing inductance, DC link capacitance for similar power level and 400Hz applications. Other

figures such as DC link voltage PI controller gains were iteratively refined as part of the development of the SAF within the modelling/simulation of this thesis.

Table 11- SAF model parameters used in studies for 115Vrms 3 phase 400Hz

Component	Parameter	Value
Line Impedance to SAF	Length	3m
	Inductance	0.495uH
	Resistance	0.011uH
DC Link Voltage controller	P	10
	I	0.5
Smoothing Inductance		100uH
Switching Frequency		240Khz
Default DC link Voltage		400VDC
DC link capacitance		10mF

5.3.1.1 Basic SAF design

Initially, the basic SAF design in simulations provided acceptable performance of current harmonic reduction but at the expense of high increases to the voltage harmonics at the PCC (exceeding the 8% set out by RTCA DO 160 [56]) when applied to the 10kW non-linear load model. In this, *ITHD* levels decreased significantly from the 54.36% to around 6.57% at steady state. This is reflected in the 5^{th} and 11^{th} harmonics which was reduced from 14.03A to 0.62A and from 2.39A to 0.31A respectively when compared to the benchmarking of chapter 2. However the *VTHD* itself increased from 4.38% to 18.23% compared to the benchmarking of chapter 2: highly exceeding the 8% RTCA DO 160 limits.

Illustrative results of the draw at the PCC are presented in Figure 75 (*P, Q*, *S*) and Figure 76 (*V*, *I*) respectively. In these figures, the left hand side is the reiteration of benchmarking results from chapter 2 and the right hand side are the results with the SAF application. Firstly from Figure 75, it can be seen that there are less ripple components within the *P, Q,* and *S* profiles (i.e. the profile is a lot flatter than the non-linear loading case without SAF). It can be also be seen in Figure 76, from the current profiles at the PCC that the shunt active filter does indeed compensate the current harmonics drawn by the non-linear load at the PCC and as a result the waveform is more sinusoidal and akin to the ideal linear resistive loading. However, as mentioned, a large increase in *VTHD* is caused as a result and additional to this is the presence of additional voltage zero crossings which could potentially cause over frequency nuisance tripping monitored by the GCU.

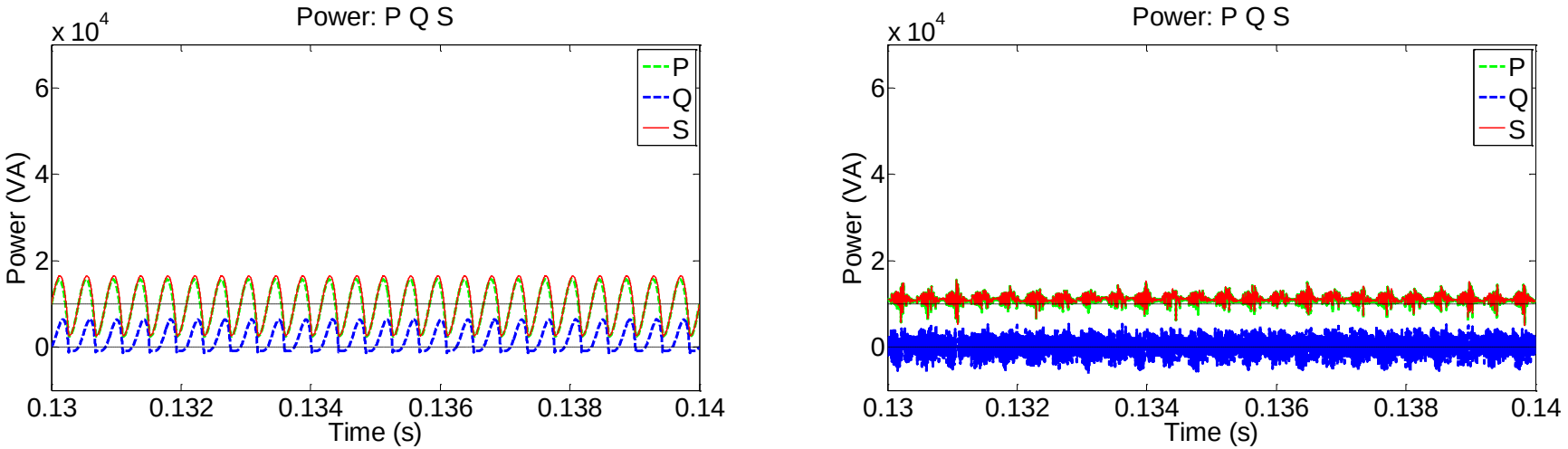

Figure 75- P, Q, S comparison between benchmarking (left) and with added SAF (right)

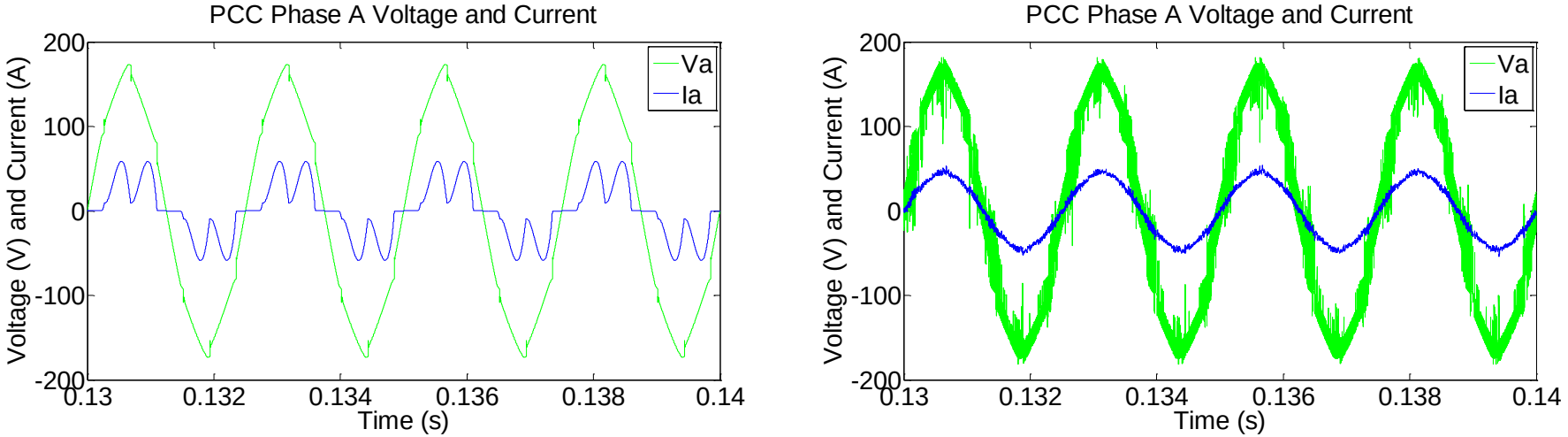

Figure 76- V, I comparison between benchmarking (left) and with added SAF (right)

5.3.1.2 Smoothing inductance at the non-linear load

With the large increase in *VTHD* caused by the SAF application to the 10kW non-linear loads as presented in section 5.3.1.1, a re-examination of literature was performed in order to produce a workable SAF design for the studies in this chapter. This included looking to literature again for aerospace based SAF application [96]-[99] which revealed one intrinsic component that exists in the non-linear loads used within these papers. This is the existence of smoothing inductance in series (as oppose to none) to the non-linear loads. In turn, this reduces the harmonic current draw even without SAF. This aspect was subsequently applied within the simulations to examine the difference in performance. In this, a small smoothing inductance of 50µH (approximately the values utilised in [96]-[98]) was added to the 10kW non-linear load model and the simulations were repeated.

With this, even without the SAF, the additional smoothing inductance already passively reduces the *ITHD* and *VTHD* at the PCC: from 54.36% to 27.73% and from 4.38% to 2.08% respectively. With SAF added, a further reduction of current harmonic from 27.73% down to 4.62% was possible, with the voltage harmonic increasing from the 2.08% to 5.17% (although still under the 8% recommended by DO 160F). Such increase in *VTHD* has been documented as being a minor side effect with the application of SAF in general within [96]-[98].

The illustrative results of these simulations with the added smoothing inductance of 50µH to the 10kW non-linear load are presented in Figure 77 and Figure 78 (with the left hand side of these being the scenario without SAF and right hand side is the scenario with SAF). These show the profile of *P, Q*, *S* and *V*, *I* at the PCC respectively.

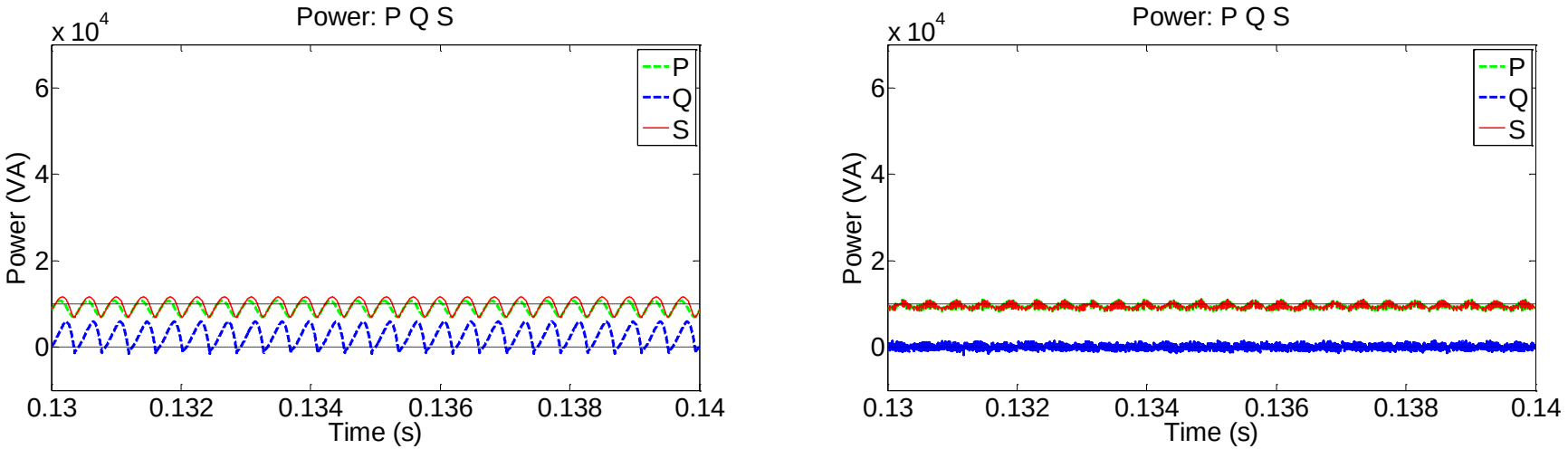

Figure 77- P, Q, S comparison between benchmarking (left) and with added SAF (right) when there is smoothing inductance at non-linear load

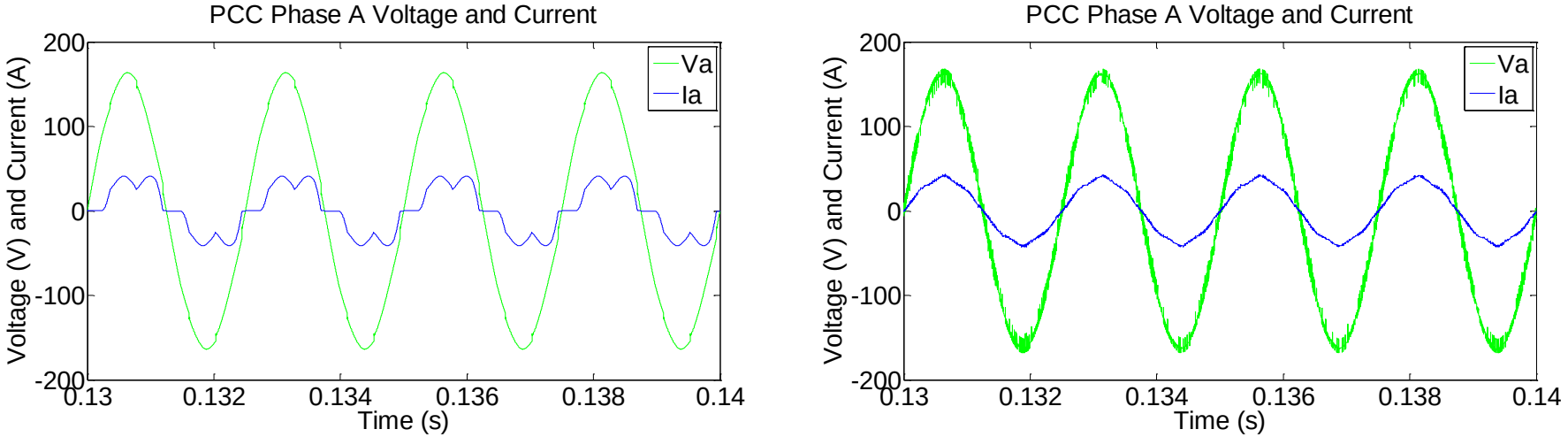

Figure 78- V, I comparison between benchmarking (left) and with added SAF (right) when there is smoothing inductance at non-linear load

5.3.1.3 Parallel capacitance at the SAF terminal

However for some fast jet applications, a number of non-linear loads have had their smoothing inductance taken out/minimised in order to save weight by the OEM. With the difficulty in assessing how much inductance is present for a broad range of loads, the author of this thesis has assumed the worst case scenario of very limited to no smoothing inductance. Hence to guarantee the maintenance of *VTHD* even with the application of a SAF in this worst case scenario, the literature review was revisited. In this, [99] was reviewed which revealed one main difference from this and the SAF setup examined in [96]-[98]. This difference within [99] was the addition of a small parallel capacitance (at the output) to the SAF topology to reduce the subsequent voltage harmonics for systems where non-linear loading have very little or no smoothing inductance.

With this, the SAF on the 10kW non-linear load simulation was subsequently repeated with the added parallel capacitance of 50µF similar to [99]. This is in contrast to the SAF application case with no parallel capacitor at the SAF and no smoothing inductance at the non-linear load presented originally in section 5.3.1.1. The immediate difference in performance was evident with the *VTHD* decrease from 18.23% to 2.18% when compared to the results of section 5.3.1.2 with no parallel capacitance at the SAF terminal. The *ITHD* rises slightly from 6.57% to around 7.88% when compared to the results of section 5.3.1.2. Although the *ITHD* is slightly higher, this is still a reasonable level when with compared to the base case of 54.36% when there is no SAF.

Figure 79 and Figure 80 illustrates the *P, Q, S*, and *V*, *I* profile of this application of capacitance at the SAF terminal (results are shown on the right hand side, with the bench marking results without SAF of chapter 2 shown in the left hand side for comparison). It can be seen from Figure 79 that the *P, Q* and *S* traces exhibit relatively flat profiles reflecting the reduction of harmonic contents. Figure 80 illustrates the voltage waveform which is more sinusoidal than the SAF case without parallel capacitance shown in Figure 76 previously.

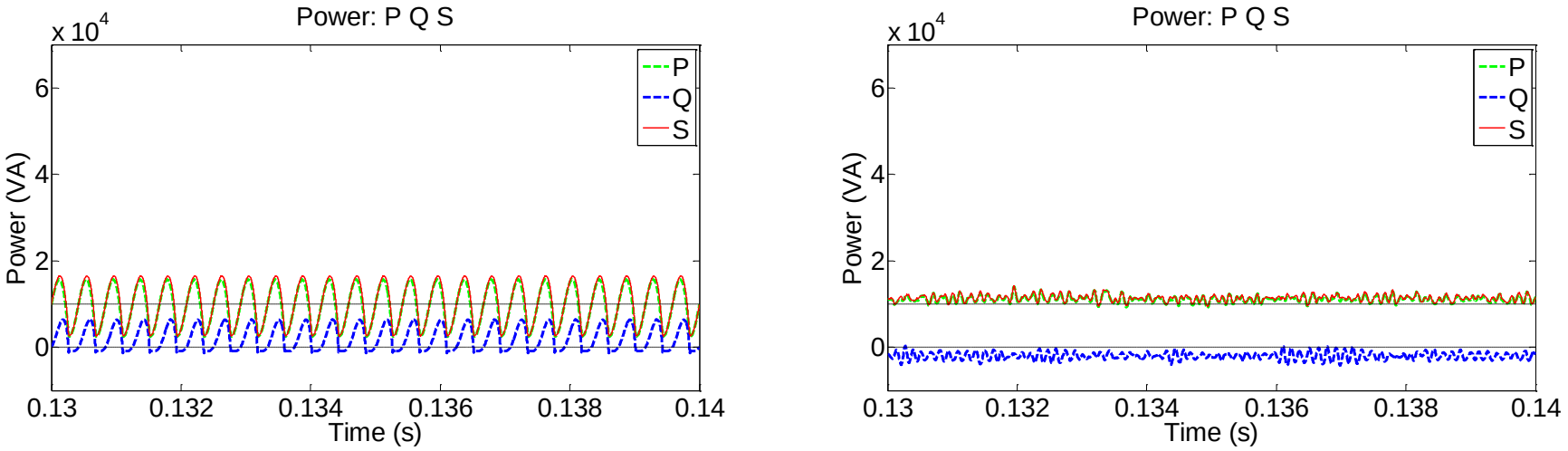

Figure 79- P, Q, S comparison between benchmarking (left) and with added SAF (right) when there is parallel capacitance at SAF

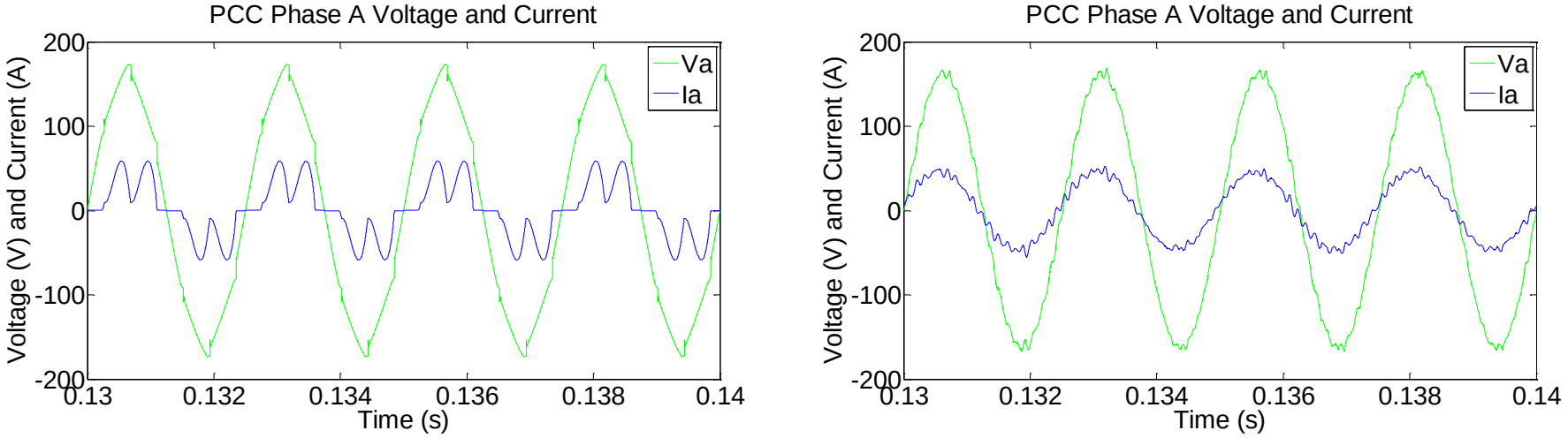

Figure 80- V, I comparison between benchmarking (left) and with added SAF (right) when there is parallel capacitance at SAF

The *FFT* of the current waveform against the DO 160 limits [56] is shown in Figure 81 (right hand side, with the bench marking without the SAF on the left from chapter 2). It can be seen that although the dominant 5^{th} or 7^{th} harmonic are under the recommended limits, some of the higher harmonics are actually exceeded as well, although overall *ITHD* is still low.

In terms of the performance of the control: Figure 82 illustrates the calculated reference of the compensation harmonics from the SAF *dq0* control (left hand side) and what has actually been generated from the output of the SAF itself (right hand side) respectively. Here it can be seen that the waveforms are closely aligned with each other and represents good adherence of the physical converters/SAF outputs to the control reference.

Following from this the configuration with parallel capacitor was chosen as the standard workable SAF design used within the rest of the thesis.

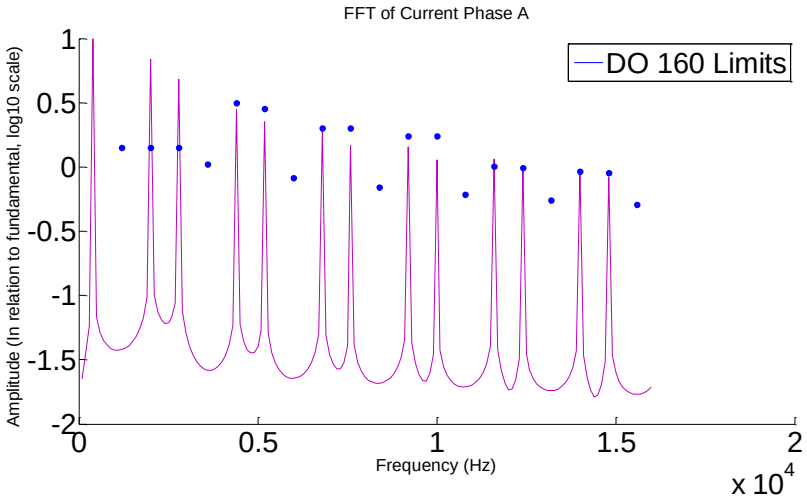

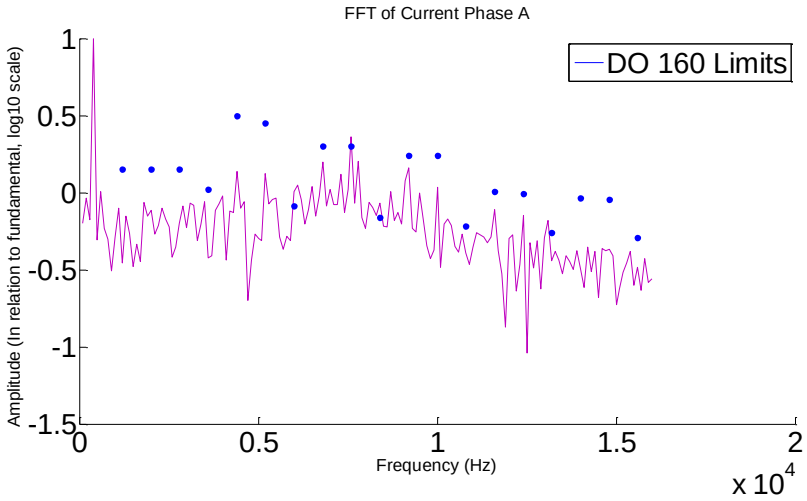

Figure 81- Comparison of current FFT of benchmark (left) and with SAF applied with parallel capacitance (right)

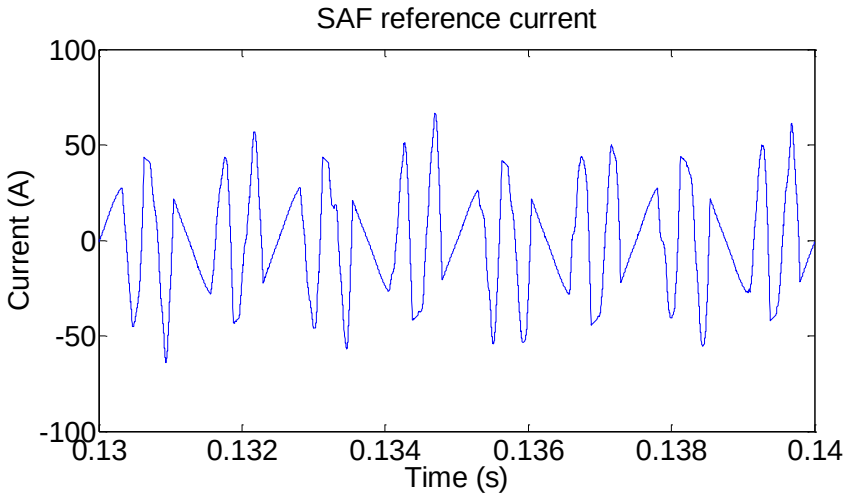

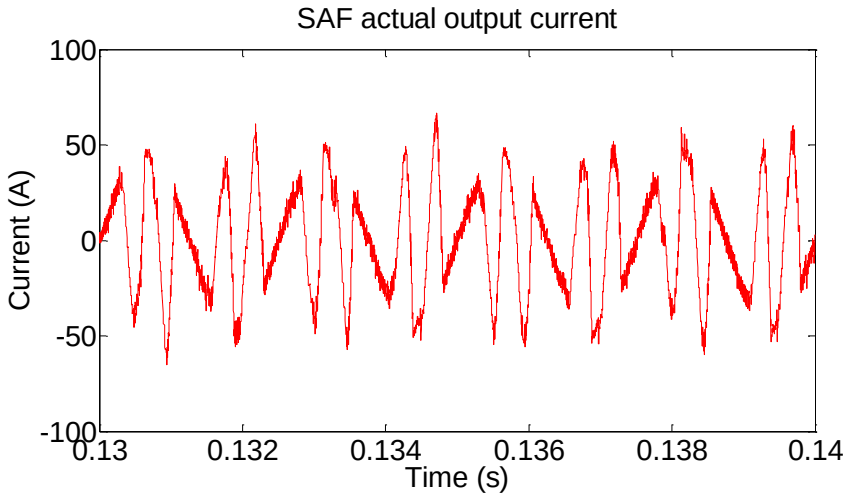

Figure 82- Comparison reference current signal (left) and actual SAF output (right)

5.3.1.4 Combined loading with SAF

With the exploration of SAF in sections 5.3.1.1 to 5.3.1.3 for a single 10kW non-linear load drawing power from the fast jet electrical system, this section expands on this with the simulated application of SAF applied to the combined 25kW mixed loading (from chapter 2). To reiterate, this 25kW model is representative of the most basic case of loading on a single channel fast jet electrical system, combining a 10kW non-linear load, a 10kW linear load and a 5kW TRU. Figure 83 and Figure 84 illustrates the respective *P, Q* and *S, V* and *I* profiles at the PCC for this scenario again (where the bench marking shown on the left hand side and the scenario with the SAF shown on the right). Similarly to before, the upper dashed trace of Figure 83 represents the virtual 25kW line for normal loading. Since there is no additional power injection, the averaged value of *P* is roughly the same in both left and right cases. However it can be seen from Figure 83, that the *P, Q* and S profiles have less ripple components, which reaffirms the reduced harmonic components with the application of SAF.

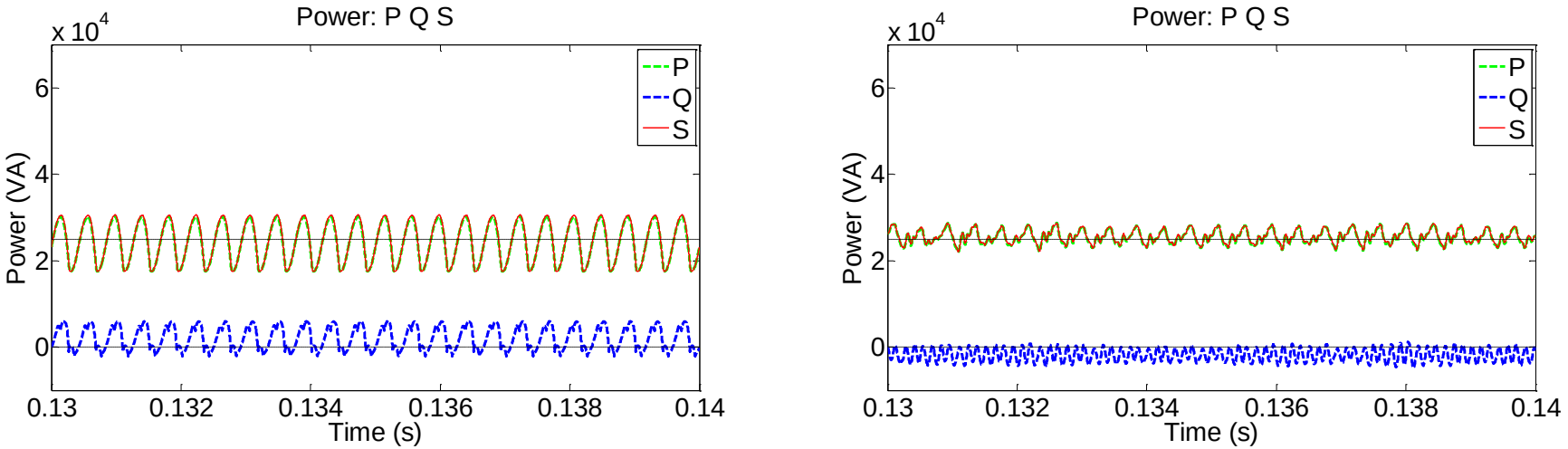

Figure 83- P, Q, S comparison between benchmarking (left) and with added SAF (right) with combined loading

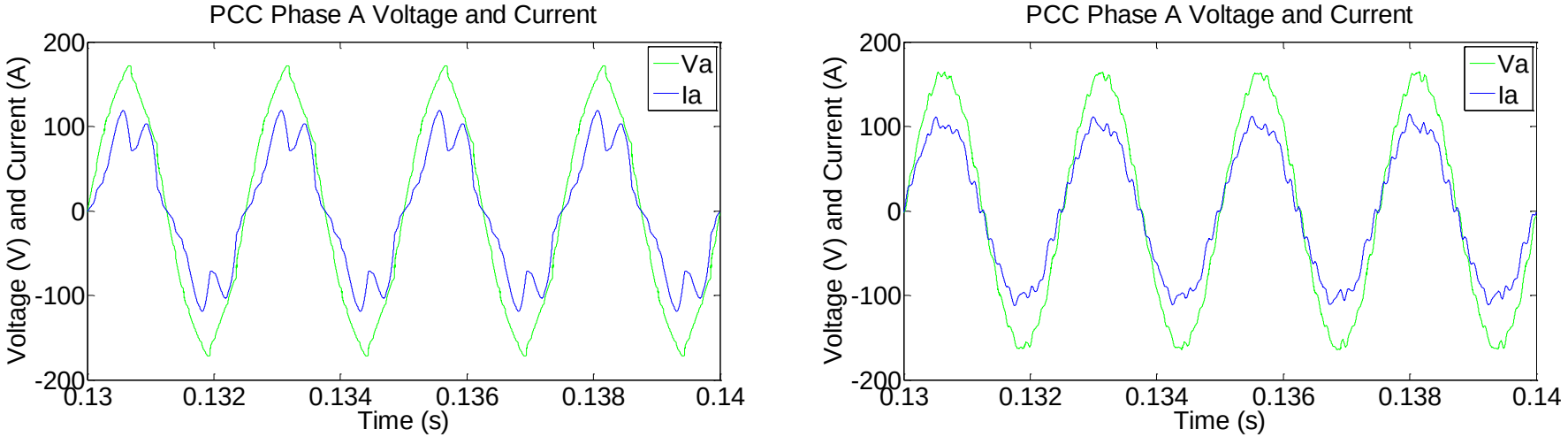

Figure 84- V, I comparison between benchmarking (left) and with added SAF (right) with combined loading

5.3.2 SAF with additional power source integration at the DC link

With simulation of basic workable SAF design operating against the generic fast jet electrical system presented in section 5.3.1: this section continues with the examination by looking into proposed integration of power onto the DC link (and its subsequent feed through into the AC system).

The 25kW mix loading scenario of the previous section 5.3.1.4 is examined again in simulation, but with power added to its DC link. The results are presented in Table 12. For comparison, row 1 summarises the baseline bench marking of chapter 2, and row 2 is the same loading with SAF but without additional power integration of section 5.3.1.4.

Different levels of power integration were examined. These were integrated to the DC link of the SAF through DC DC converters controlled as current slaves. The DC link voltage is held up by the SAF voltage control which does not require additional changes.

Row 3 of Table 12 summarises the scenario of when a 5kW supplementary power generation source is integrated to the DC link of the SAF. Firstly this causes a reduction of harmonic current drawn at the PCC compared to with no power integration (the 5^{th} harmonic decreasing from 2.91A to 0.39A and for the 11^{th} harmonic, this was from 1.76A to 0.43A). The real power *P* draw from the PCC is also reduced due to the supplementary power injection as intended, whereby a 25.5kW draw is reduced to 21.01kW (with 4.4kW successfully fed through to the AC side from the maximum 5kW supplementary source). This represents high inefficiency due to the SAF set up and could be improved upon by replacing the SAF design.

The simulation results of when a single source of 7.5kW additional power is applied to the DC link is summarised in row 4 of Table 12. In this, the further reduction of absolute harmonic currents is not as apparent in this case when comparing to the 5kW supplementary generation case against the no supplementary generation case. There is also a rise in *ITHD* but this is due to a further decrease of fundamental draw from the PCC. In this case, the power drawn from the main generation is further decreased from 25.5kW to 18.68kW with the extra supplementary power (6.82kW is successfully fed through to the AC side from the maximum 7.5kW additional supply; again at a high inefficiency).

Multiple source addition to the DC link was also examined: this is simulation of 4x 5kW supplementary power generation source added to the DC link of the SAF and these are presented in row 5. The power reduction from the main generation in this case is reduced from 25.5kW to 7.02kW (with 18.45kW successfully fed through to the AC side from the 20kW combined source:

again at a high efficiency). The *VTHD* still remains at a reasonable level (<8%) and the *ITHD* is slightly higher but this is due to a lower fundamental with current harmonics are remain the same in absolute magnitude.

Table 12- SAF with power integration

Case	Averaged PCC S (kVA)	Averaged PCC P (kW)	Averaged PCC Q (kVAR)	VTHD (%)	ITHD (%)	Fundamental Voltage RMS Phase A (V)	Fundamental Current RMS Phase A (A)	Current 5th Harmonic (A)	Current 11th Harmonic (A)
Without SAF	24.51	24.3	2.21	4.26	21.35	113.6	71.75	13.69	1.75
With SAF	25.61	25.5	-1.8	3.73	8.12	114.2	74.87	2.91	1.76
With SAF and additional 5kW power source	21.14	21.01	-2.06	2.53	4.97	114.5	61.57	0.39	0.43
With SAF and additional 7.5kW power source	18.79	18.63	-2.06	3.85	8.38	114.6	54.84	0.33	0.31
With SAF and additional 4x 5kW power source	7.45	7.02	-2.22	3.51	19.54	115.4	21.35	0.25	0.21

Example illustrative results are presented to show the alleviation of main power at the PCC with the incorporation of supplementary power through the SAF. The result of the scenario with a single 5kW supplementary power integrated onto the SAF is presented in Figure 85 (*P, Q, S*) and Figure 86 (*V, I*) respectively. The left hand side of these figures are the benchmarking of the 25kW system without any SAF from chapter 2. The upper dashed trace on the *P, Q,* and *S* waveforms on the figures again represents the virtual 25kW load (the normal power draw without any supplementary generation added) and the middle black trace (on the right hand side exclusively) represents the theoretical level the power drawn at the PCC should be when the additional generation is 100% converted for loading.

Similarly, the illustrative results of the 4x 5kW scenario is given in Figure 87(*P, Q, S*) and Figure 88(*V, I*).

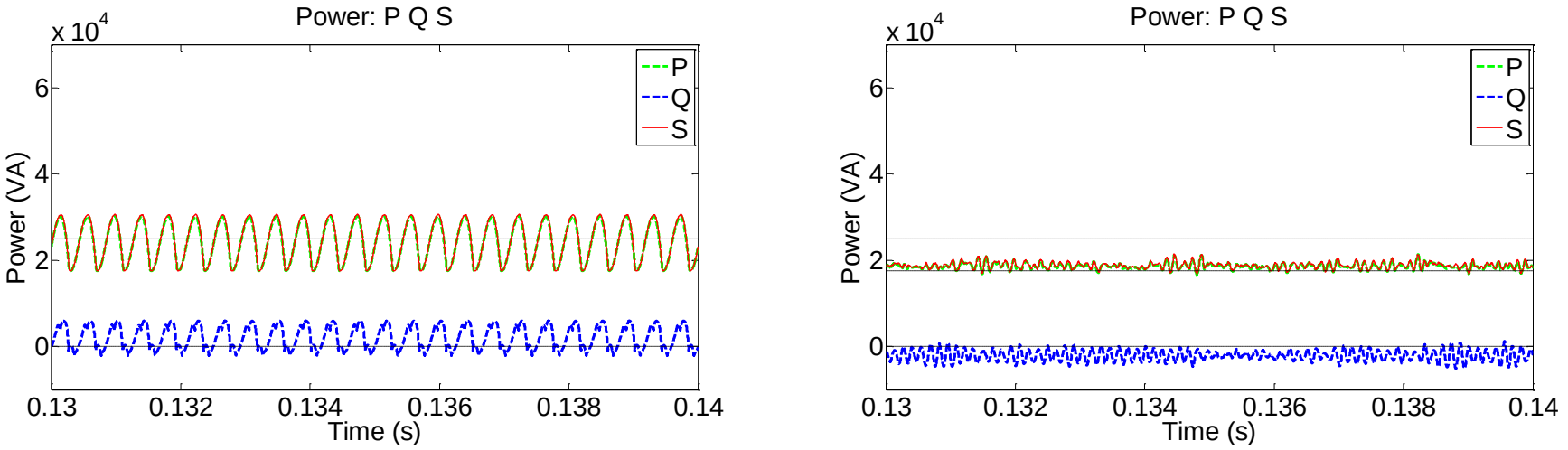

Figure 85- P, Q, S comparison between benchmarking (left) and with added SAF (right) with combined loading with 1x5kW source

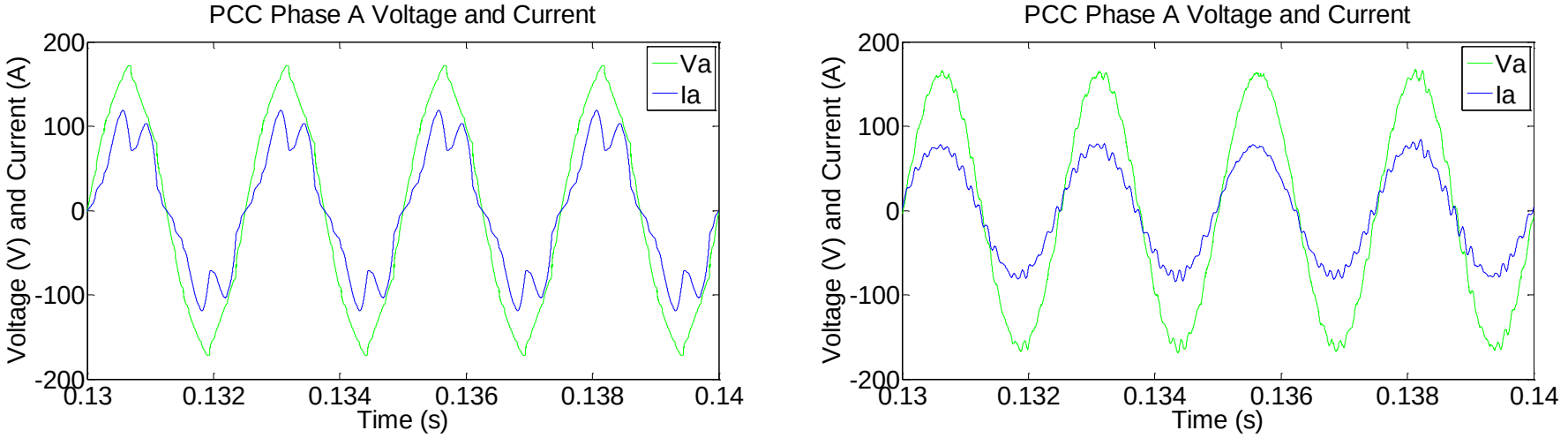

Figure 86- V, I comparison between benchmarking (left) and with added SAF (right) with combined loading with 1x5kW source

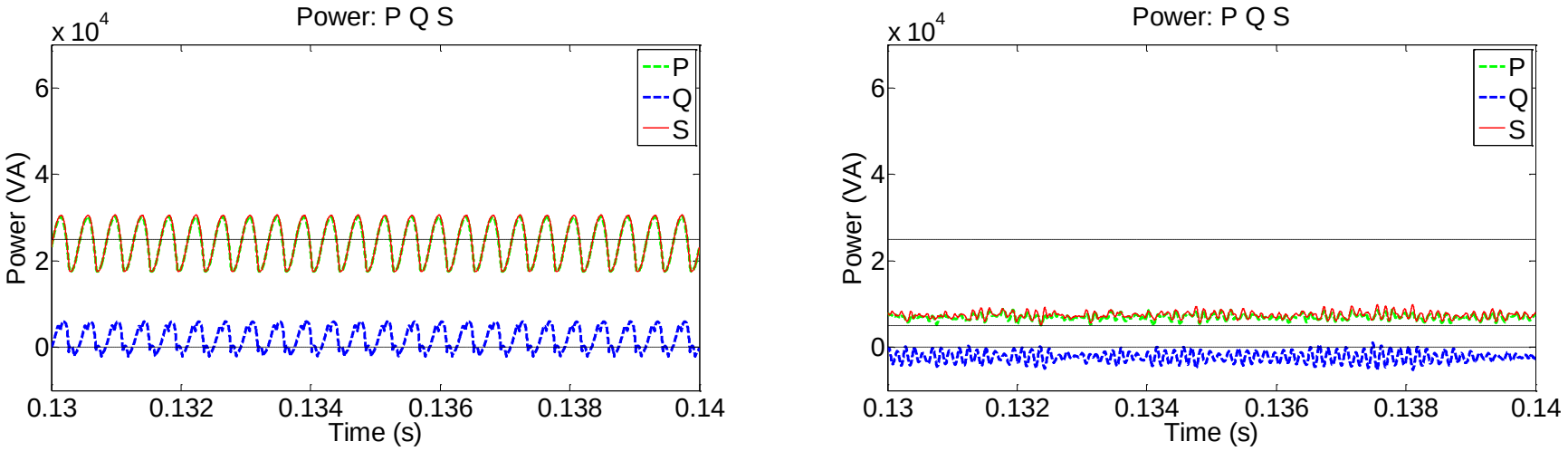

Figure 87- P, Q, S comparison between benchmarking (left) and with added SAF (right) with combined loading with 4x5kW source

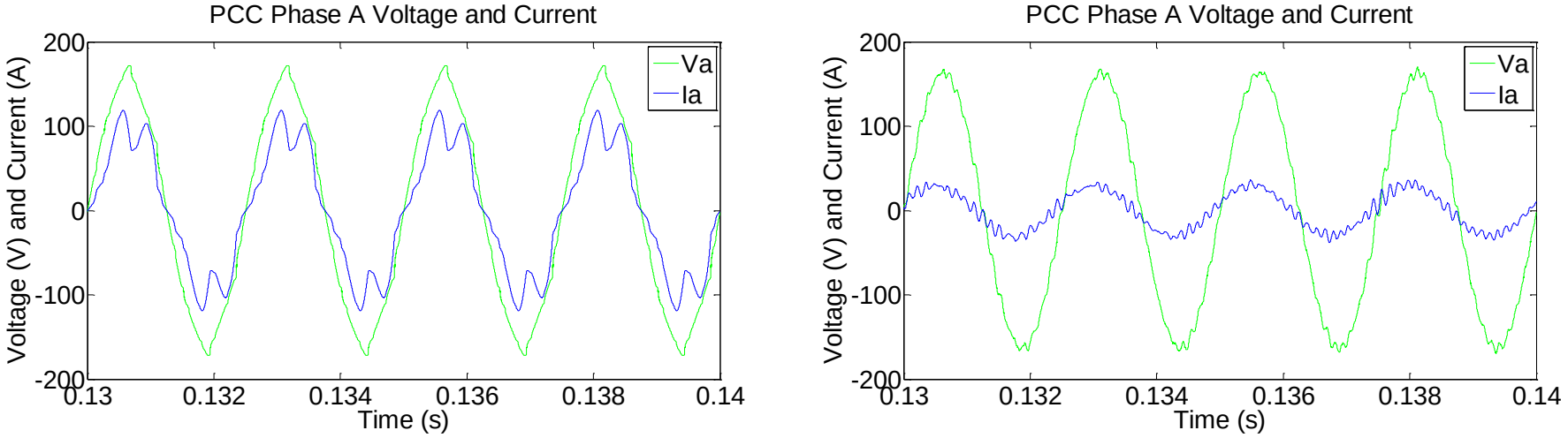

Figure 88- V, I comparison between benchmarking (left) and with added SAF (right) with combined loading with 4x5kW source

5.3.3 SAF with increased upgrade loading and no additional power source

Following examination of power integration through SAF onto the base 25kW loading (representing the start of service life of a generic fast jet aircraft): this section examines the SAF operation on the electrical system while it undergoes an increase in loading caused by through life upgrades. This is important as the power integration of this thesis including the proposed SAF application is primarily aimed at tackling the through life upgrade problem on fast jets (which is primarily made up of non-linear, electronic type loads discussed in chapter 1). Associated with this, the following simulation results examines an increase of demand of 30kW non-linear loading (3x 10kW) added onto the base electrical load of 25kW (per channel) to mimic through life upgrades taking the loading up to 55kW (per channel).

Figure 89 and Figure 90 illustrates the *P, Q, S* and *V* and *I* profiles of this added demand with the SAF applied to the PCC without any addition of power. The left hand side represents the bench mark of the increased loading without the application of SAF for comparison. In this the SAF's core functionality of harmonic current reduction is presented again (similar to section 5.3.1) at this higher power demand level (smoothing inductance was lowered to manage the higher current harmonics). The real power demand is represented by the upper dashed trace of Figure 89 representing the 55kW level. In such a scenario it is mimicked that increase in main generation capacity is possible to meet the increase in demand (in that the generator can handle full extent of through life upgrade demand increase).

Figure 91 and Figure 92 show the same application of SAF on the same loading (55kW) but with 30kW added supplementary power onto the DC link of the SAF. Again on the left hand side of the figures is the bench marking of the same loading without the SAF application. On the right hand side, is the simulation result of the application of SAF with the added 30kW power. The reduction of power drawn from the PCC (main generation) is maintained at around the 30kW mark. Hence this implies the original main generator can still be utilised to meet the increase in demand without the need to change/uprate it (the output of the main generation is represented by the middle dashed trace of Figure 91).

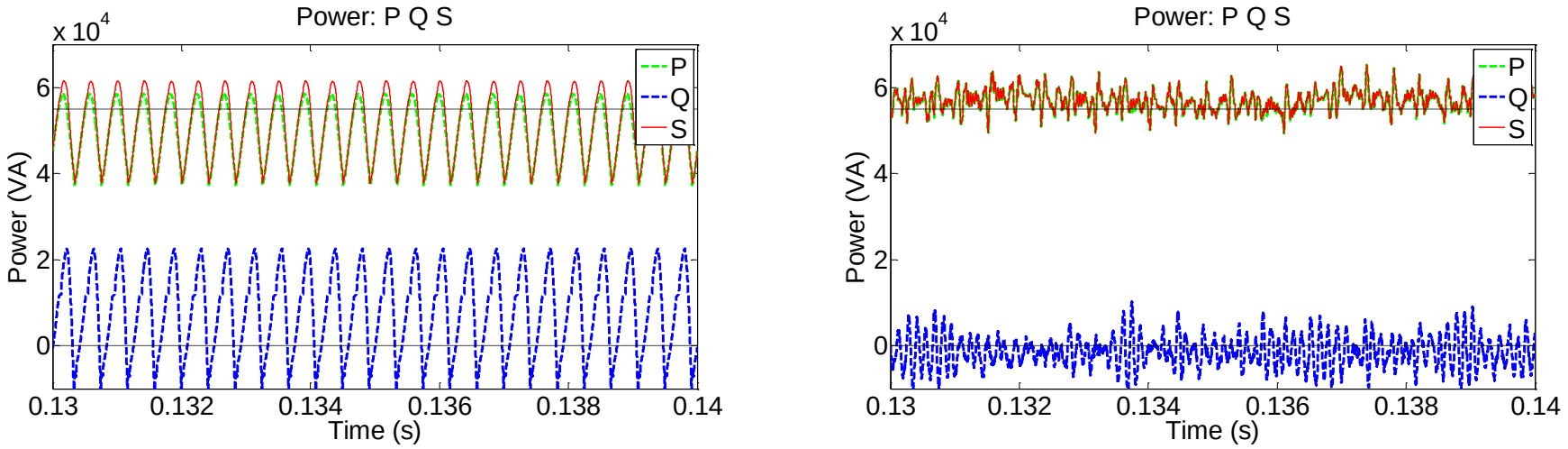

Figure 89- P, Q, S comparison between benchmarking (left) and with added SAF (right)

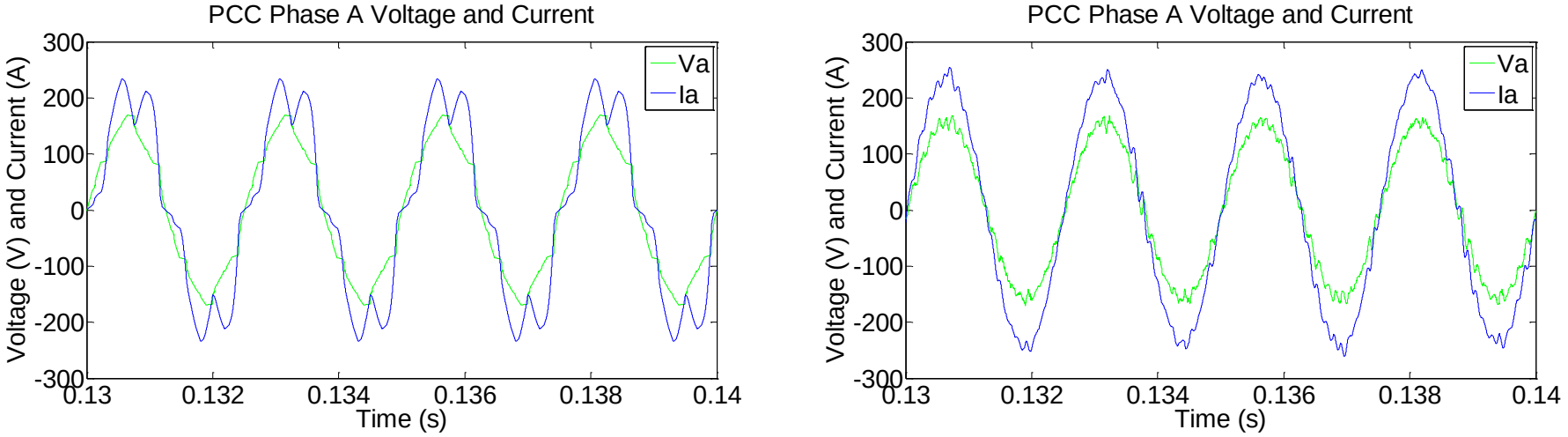

Figure 90- V, I comparison between benchmarking (left) and with added SAF (right)

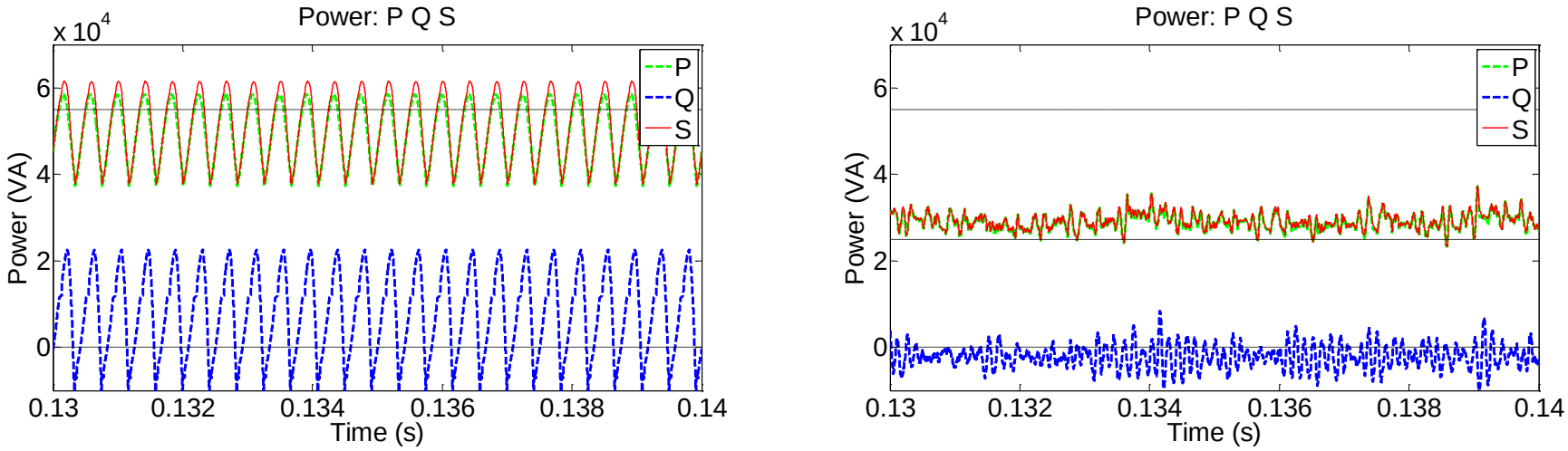

Figure 91- P, Q, S comparison between benchmarking (left) and with added SAF (right)

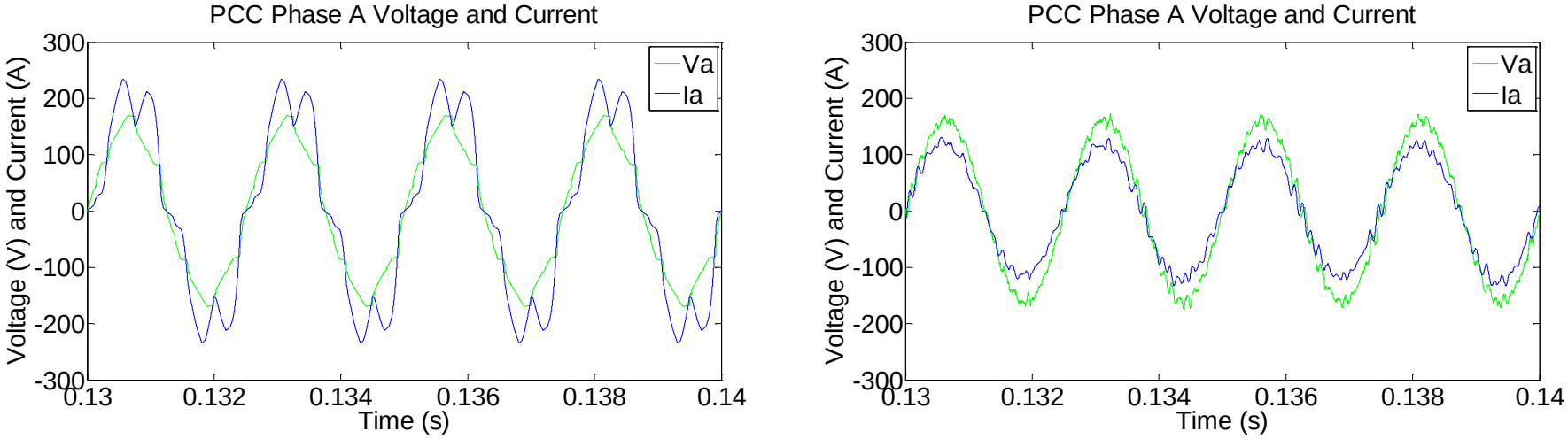

Figure 92- V, I comparison between benchmarking (left) and with added SAF (right)

5.3.4 SAF at each PCC during single engine failure

In this section, a single engine driven generator failure scenario is examined in which replication of a two channel system is presented. Each channel is drawing 25kW of mixed loading in simulation to represent the full electrical system. In this, the steady state operations of the two channels were simulated in which one engine generator is taken offline to represent single generator failure and the two channels are interconnected by a bus tie contactor. As such, the simulation shows the remaining generator burdened with the need to power loading of both channels (2x 25kW).

With the proposal for utilising a SAF for power integration, even at the simplest case, there could be a SAF on each channel of the fast jet aircraft electrical system. This does not provide a conflict when the channels are isolated, in which the two SAFs are operating in their own respective channels during normal operations. However with the single generator failure scenario, the two SAF may be operated together after interconnection. Hence this section presents the results that illustrate two SAFs operating together under such a scenario. No additional modifications were performed to the SAF design or main generator control for paralleling purposes and as such the main generators are unchanged and the SAFs are still utilising the default *dq0* based control presented in section 5.3.1.3.

The results of the interconnected channels scenario are presented in Table 13. The first result row set is when two of these channels are interconnected and drawing from the same main generator of the first channel but without the SAFs to show the baseline profiles of the interconnected scenario after a single engine generator failure. It is assumed that the generator is also operating within its design limits

The second row set is this same setup but with SAF on both channels at their respective PCC without the addition of supplementary power. The 3rd, 4th and 5th row sets summarises the results of incorporating supplementary power source through the SAFs at 7.5kW:7.5kW, 2kW:13kW and 13kW:2kW split over the two SAF.

The operations of the single engine scenario of two SAFs have allowed adequate performances in terms of voltage and current quality improvement while with the potential to maintain power feed through into the system in single engine failure operations. With this: power integration through the two SAFs is still possible. Hence these illustrate the ability to have two SAFs which originally operate in their respective isolated channels but also in conjunction with each other within a single channel when a generator failure event causes the previously islanded channels to be connected together.

Table 13- Single engine failure

Case	Averaged PCC S (kVA)	Averaged PCC P (kW)	Averaged PCC Q (kVAR)	VTHD (%)	ITHD (%)	Fundamental Voltage RMS Phase A (V)	Fundamental Current RMS Phase A (A)	Current 5th Harmonic (A)	Current 11th Harmonic (A)
Without SAF									
Channel 1	47.41	47.03	3.75	6.05	15.63	111.9	140.7	20.31	3.71
Channel 2				6.1		111.9			
With SAF but no additional power sources									
Channel 1	49.97	49.74	-3.39	4.99	7.53	112.7	147.4	6.07	4.32
channel 2				5.03		112.7			
With SAF and additional power sources (7.5kW:7.5kW)									
Channel 1	35.53	35.21	-3.89	4.33	9.50	113.8	103.4	5.00	4.15
Channel 2				4.37		113.8			
With SAF and additional power sources (2kW:13kW)									
Channel 1	35.76	35.43	-3.88	4.46	9.63	113.8	104.3	5.27	4.07
Channel 2				4.49		113.8			

With SAF and additional power sources (13kW:2kW)									
Channel 1	35.3	35.07	-3.91	1.90	4.00	113.8	103.4	1.89	1.60
Channel 2				1.92		113.8			

5.4 Summary

This chapter has summarised the adaption of standardised SAF for proposed application on the fast jet problem as part of this thesis. In that the application of SAF, can, not only reduce the harmonic currents drawn (by “electronic” type non-linear loads) at the PCC but can also allow a convenient means of integrating supplementary generation to tackle the through life fast jet upgrade problem. This approach has not been widely applied to date for the fast jet application which this chapter contributes by exploring such unique application. With such proposal of the SAF to integrate power into the fast jet electrical system: no modification is required to the main generation to parallel to the additional power.

Subsequent simulation of this SAF application provided illustrated operations of the proposal against the generic fast jet electrical system bench marked in chapter 2. In this, illustration for single 10kW non-linear load and the 25kW mix loading combination connecting to the fast jet electrical system were presented which showed improvement of *ITHD* as well as reduction of power draw from the main generation. The application of SAF against an increased level of loading to 55kW from the 25kW base loading (mimicking through life upgrades) were also presented in simulation which provided similar benefits in *ITHD* reduction and demand alleviation from the main generation. This ultimately illustrates the intended functionality of the SAF to cope with increasing through life power demands on fast jet.

The simulations of interconnected two channel operations of the generic fast jet electrical were also presented. This examined the configuration when both channels have their own respective SAF at their own PCC were presented. In this, one of the main generation is taken offline in the simulation of a two channel system to mimic single generator failure. As such the simulations illustrated the interconnected channel operation with the remaining generator providing power for both channels. Due to the SAF also being present in the system and that power is also integrated into the DC links of these; the simulations illustrated the continued power sharing with the remaining main generation and SAF integrated power. In this, concurrent operation of the two SAFs within the same system (and continued sharing of loading with the main generation in such a configuration) is shown as well as the maintaining of power quality.

6 Conversion of passive rectifiers to bi directional equivalent in fast jet applications

6.1 Chapter overview

In chapter 4, the proposed addition of power onto the DC links of existing nonlinear loads with rectifiers and TRUs in the fast jet electrical system was examined. This is the first of three proposed power integration methods for fast jet aircraft electrical systems within this thesis to tackle through life upgrades. However, one of the limits of such integration is; the maximum generation capacity that can be added is limited to the DC side loading and limit the extent of power that can be added to meet the through life demand upgrades. This is due to the basic fact that; the TRUs (shown on the left hand side of Figure 93) and non-linear load rectifier (shown on the right hand side of Figure 93) are unidirectional in terms of current direction flow.

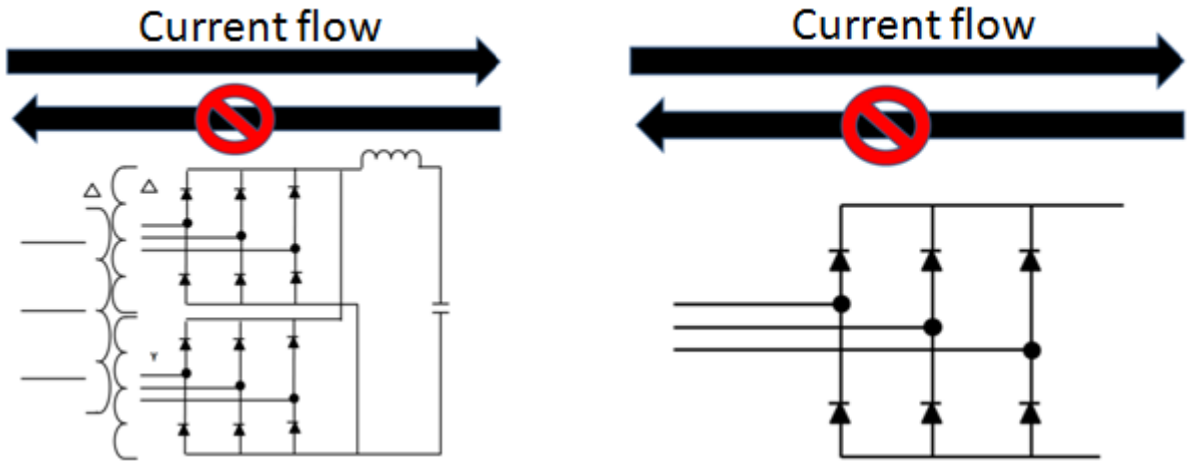

Figure 93- Limitation of unidirectional flow of passive topologies: TRU (left) and 270VDC rectifier (right)

One option to overcome this, proposed as the third of the three power integration methods in this thesis, is to convert such passive rectification stages into bi directional and active equivalents (essentially turning them into an inverter/active rectifier). One of the benefits of this option over adding a standalone inverter is: the sizing of the converter/inverter itself can be smaller as there is already local DC side loading. This implies, only the excess power is needed to be fed back to the AC

busbar. Another benefit of changing passive rectifiers to active equivalents compared to solely adding an additional inverter is; it allows the utilisation of the same wiring that already exist between the AC busbar and non-linear load or TRU (minimising rewiring downtime and reducing added mass of new wiring).

However, the disadvantage of converting the rectifiers into active equivalents is the added weight (including additional thermal management and smoothing inductance for switching) compared to the passive equivalent. However it can be argued that, if more power is needed when the power injection onto the DC side is saturated; then there would still be a need to add some form of inverter regardless (to inject power back into the AC side).

This chapter elaborates on the proposed option of converting such rectifiers into active equivalents. In particular, the chapter examines the implications of the power injected back into the AC side additional to the power being fed to the DC side loading. Ultimately this is to illustrate the alleviation of power draw from the main generation as a result and to cope with the through life power demand increases. The proposed application is intended to be operational without the need to change the existing main generation system, similar to the proposed integration options examined in chapter 4 and 5.

6.2 Converting passive rectifiers in the system to inverters overview

In this section, the proposed conversion of existing rectifiers (TRU or non-linear loading/equipment) within the fast jet system to active equivalents/inverters for feeding power back into the AC system is elaborated. The elaboration of the 28VDC TRU option is presented first in section 6.2.1 and the 270VDC rectifier option is subsequently presented in section 6.2.2 in terms of proposed control and topology for fast jet application. The essence of the proposed control is the same for setups for the 28VDC and 270VDC options.

The integration method includes the use of DC link based paralleling of the added generation sources. This is again based on the proposed application of voltage master current slave control for commonality with the integration methods of chapter 4 and chapter 5. In particular, to allow for the seamless transition from inverter mode to rectifier mode, the adapted use of *dq0* [104] control similar to the control of a SAF examined in chapter 5 is proposed. This control is elaborated in section 6.2.1 and 6.2.2 for the respective 28VDC TRU and 270VDC non-linear load rectifier options. The control can allow for the converter to switch from inverter operations to rectifier operations seamlessly depending on the generation at the DC side.

In terms of the topology options for such application, the six diode rectifier is essentially a six switch rectifier in its passive state. This is illustrated by Figure 94 which shows the six switch converter effectively becomes a six diode rectifier when all the switches are in their 'off' state. As such, by converting the diodes to switches in the TRU or non-linear load rectifier stages, the passive fall back mode can still be preserved. This passive mode could be utilised if the DC side generation of the rectifier is lower than the DC side loading. When the generation on the DC side is higher than the DC side loading, the rectifier can be switched to active mode (inverter mode), where the excess power can be fed back into the AC side. Additional to this, if the DC side generation is a lot lower than the DC side loading, the rectifier can still operate in active mode to make the draw to the rectifier from the PCC more sinusoidal (reducing current harmonics drawn by using *dq0* control).

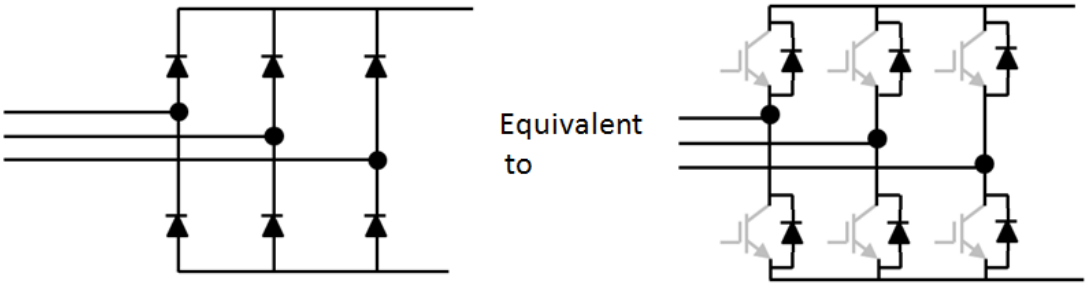

Figure 94- Comparison of passive diode topology to passive switch topology

Table 14 summarises the proposed set up along with the benefits of active conversion (row 2) against the conventional unidirectional passive equivalents (in row 1). Column 1 and 2 are the respective 28VDC (TRU) and 270VDC (AC busbar non-linear load) application options.

Again, similarly to chapter 4, the access to the 115Vac to 270VDC rectifier stage maybe restricted and possibly more suited for future non-linear loads.

Table 14- Outline of proposed conversion of passive topologies to active equivalent for the 28VDC and 270VDC options

	28V TRU	270V Rectifier of non-linear load
Conventional set up	• **Passive rectification** • **Unidirectional** • **Conventional 12 pulse TRU topology** • **~28VDC output** • **Feeding 28VDC busbar**	• **Passive rectification** • **Unidirectional** • **Conventional 6 diode rectifier** • **~270VDC output** • **Feeding the DC side loading of the non-linear load**
Proposed active rectifier	• **Passive mode: passive rectification mode fall back (business as usual)** • **Active mode: harmonic reduction capability drawn by the load even when there is little additional power at the DC end. Bidirectional where DC power source integration can exceed DC side loading and power can be supplied back to AC side in conjunction to generator. The power fed back can be up to the size of the existing transformer and cable (i.e. same components and wiring paths can be reused)** • **Conventional 12 pulse transformer, 2 x 6 diode rectifiers replaced with switches and separated with intermediate smoothing inductance** • **~28VDC out in passive or active mode (controlled by SAF voltage master control) mode** • **More parts (including switching, smoothing inductance and thermal management) and increase size and volume but with fallback to passive mode**	• **Passive mode: passive rectification mode fall back (business as usual)** • **Active mode: harmonic reduction drawn by the load, bidirectional. Power fed back can be up to the size of the existing cable (i.e. same components and wiring paths can be reused current but in opposite direction)** • **6 diode rectifiers replaced with inverter switches and separated with intermediate smoothing inductance** • **~270VDC out in passive or active (controlled by SAF voltage master control) mode** • **More parts (including switching, smoothing inductance and thermal management) and increase size and volume but with fallback to passive mode**

6.2.1 28VDC Active Transformer Rectifier Unit overview

This section elaborates specifically on the proposed 28VDC active TRU option for converting it to an active equivalent. To achieve this, the proposal is to replace the diodes with switches in a one to one basis. The proposed control for this active TRU equivalent is to utilise an adapted version from the *dq0* SAF control presented in chapter 5. However, the difference to the SAF control presented in chapter 5 is: the higher harmonic currents of the *d* components are also filtered out to force the converter to only allow fundamental current to flow in active mode (reducing eddy current losses through the transformer and allowing the DC link to remain at 28VDC). One main limitation of this fundamental current only flow is: the power flowing back into the AC side can only be fundamental and if the paralleling loading within the electrical system is harmonic rich. By injecting more fundamental current and not harmonics back into the AC system, the subsequent relative *ITHD* at the PCC will further increase (but with no increase in absolute terms). This may or may not be acceptable for the main generation draw depending on the amount of the non-linear loading left in the rest of the system.

6.2.1.1 6 pulse and 12 pulse Active TRU designs

Two topologies were examined as part of this proposal of conversion of the TRU to an active equivalent; this is split into six pulse and twelve pulse topologies. Firstly in terms of simplicity: a six switch topology is presented as a possible option. The setup of this is presented in Figure 95 whereby the six pulse option essentially represents the simplest topology to achieve bi directional flow from 28VDC back to 115Vac three phase. In this, the transformer secondary side of delta and Y in the traditional TRU are replaced by a single delta winding. The main limits of this however is during passive mode, the six pulse will draw higher harmonic current compared to the conventional twelve pulse passive TRU (potentially causing increase in eddy current losses [105]). However in active mode for rectifier operations, the current harmonics can be minimised actively by the *dq0* control.

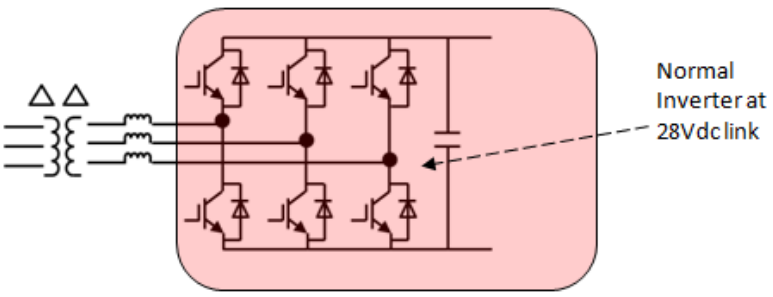

Figure 95- Proposed 6 pulse active TRU

Alternatively and in order to preserve the limited harmonic current draw characteristics of the twelve pulse TRU (as a fall back), Figure 96 below depicts the proposed twelve pulse active TRU (illustrated in active and passive mode on left and right hand side respectively). The twelve pulse option would be more complex with twice the amount of switches when compared to the six pulse option but offer options to revert back to the passive twelve pulse TRU topology in its passive state.

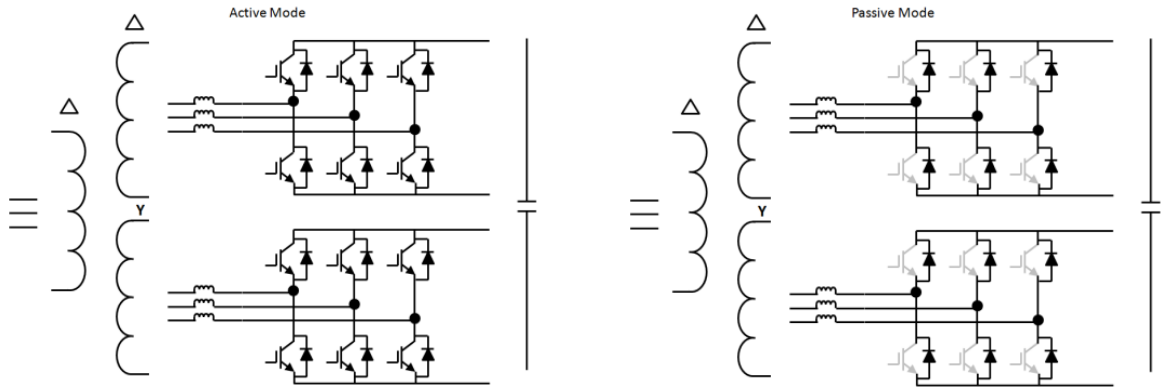

Figure 96- Proposed 12 pulse active TRU in active (left) and passive (right) mode

In Figure 96, aft of the transformer, are essentially two inverters separated from the transformer by smoothing inductance but preserving the transformer set up of both delta and Y secondary transformer arrangement. Each inverter is rated at half the power of the total DC bus bar loading. In terms of set up, the active TRU is proposed to be a one to one replacement to the conventional TRU. Figure 97 below displays the typical set up of this active twelve pulse active rectifier, within a single channel of the generic fast jet electrical system.

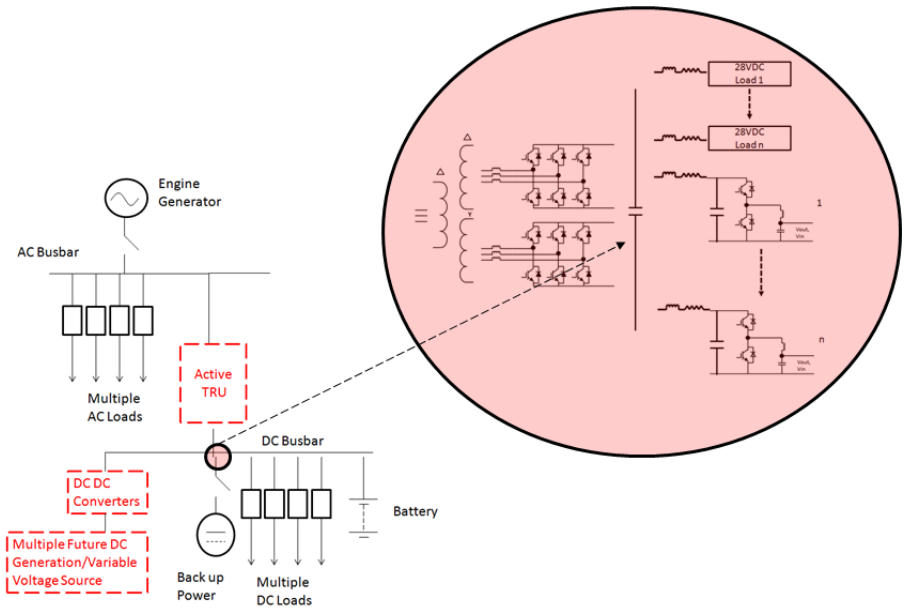

Figure 97- Illustration of proposed 12 pulse active TRU with respect to generic fast jet electrical system channel

In terms of the control for this twelve pulse active rectifier, as mentioned before, an adapted version of the *dq0* SAF control is proposed similar to the SAF in chapter 5. One of the main difference of this and the version used for SAF control in chapter 5 is; an additional high pass filter is added for the *d* component to force only fundamental power flow through the converter (as mentioned at the start of this section). The other difference is two separate current reference computation are proposed for the respective secondary converters due to the Y and delta setup. However, to enable a single master voltage reference, this is fed by a common *PI* based voltage controller to control one single DC link. This control is illustrated by Figure 98 below.

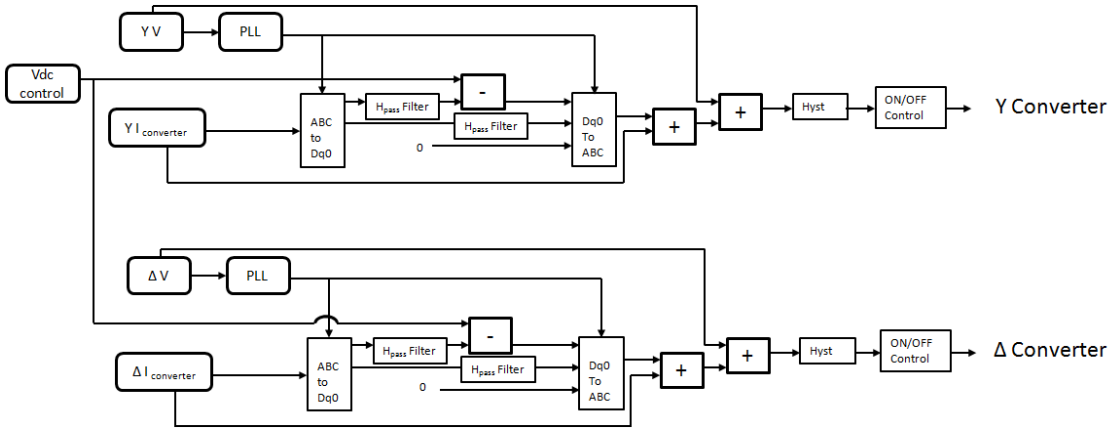

Figure 98- 12 pulse active TRU control block diagram

6.2.2 270VDC Active Rectifier overview

Turning passive components to active equivalents could be applied to the non-linear loads as well (which have six diode rectifier front ends, and presuming access to the rectifier stage is physically possible). Also compared to the active TRU option, this is simpler in terms of the reduced number of switches and the lack of transformer components/stepping down and up of voltages.

Figure 99 below displays the possible set up of this within a single channel within the generic fast jet electrical system. In this, the six switches are used to replace the six diodes within the passive rectifier.

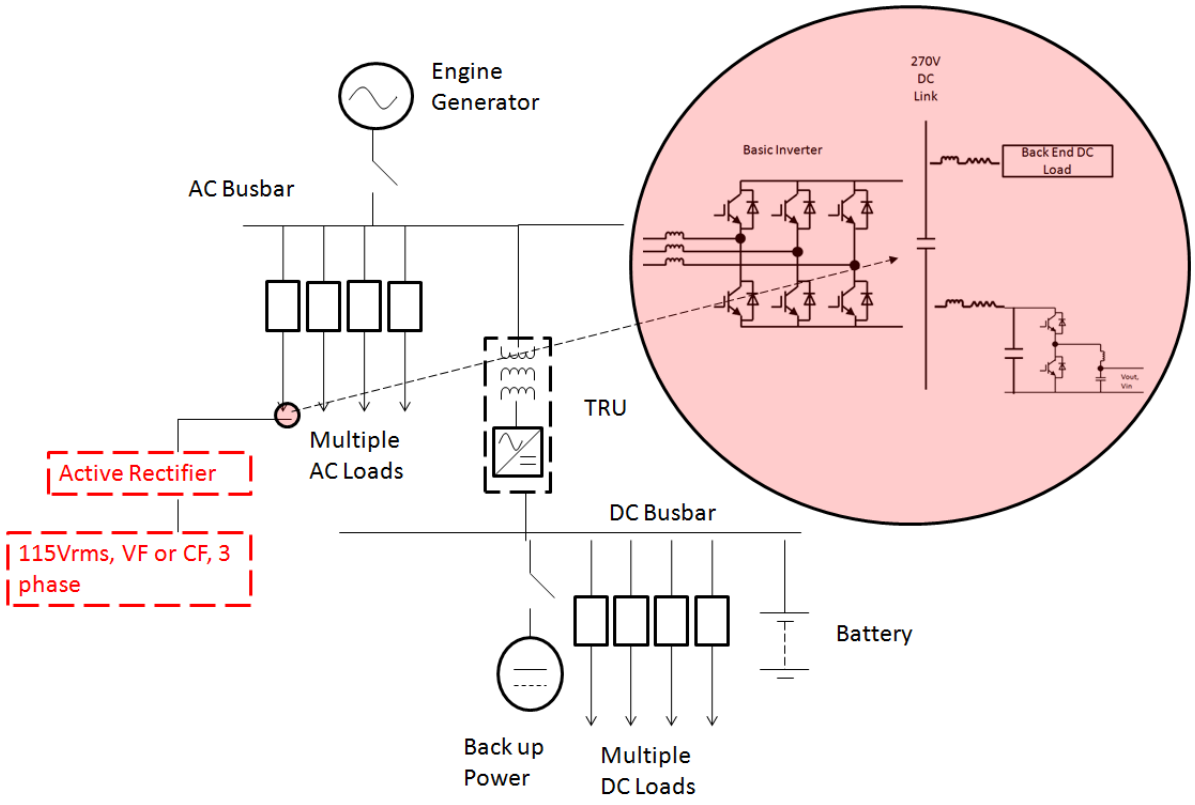

Figure 99- Illustration of proposed active rectifier with respect to generic fast jet electrical system channel

This control block is presented in Figure 100 below. Again this is an adapted version of the *dq0* control proposed for SAF in chapter 5. Similarly to the active TRU control of section 6.2.1, the *d* component is also filtered out to restrict current flow to only fundamental currents.

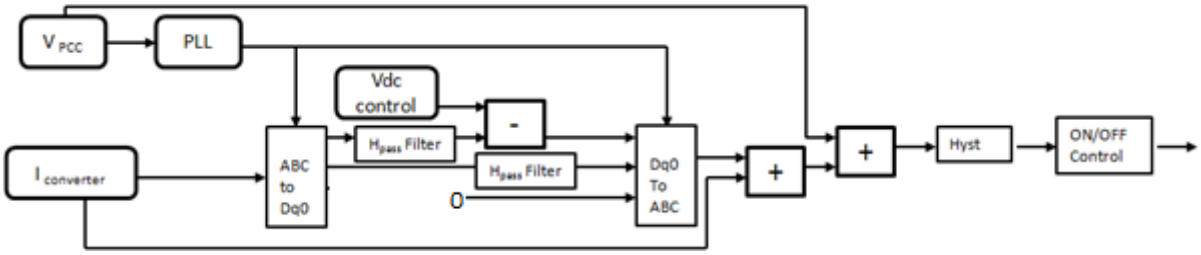

Figure 100- Active rectifier control block diagram

6.3 Simulation results of power integration with conversion of passive rectifiers into active equivalents

With the elaboration of the proposed conversion options of passive rectifiers to active equivalents in section 6.2, this section presents the simulated operation of these working against the original fast jet electrical system model (bench marked in chapter 2). The examination and simulation results of the 28VDC option are presented in section in 6.3.1 and the 270VDC option are presented in section 6.3.2 respectively.

6.3.1 28VDC Active TRU simulation results

In this section, the simulation results of the proposed twelve pulse active TRU against the fast jet electrical system is presented. This is where the 5kW TRU drawing from the fast jet electrical system is changed to an active TRU equivalent which can potentially feed power back into the AC system. The control and topologies of the twelve pulse active TRU operation (section 6.2.1.1 refers) is simulated.

6.3.1.1 Without addition of DC power sources

In the simulation in this section, the basic operations of both active and passive mode of the active TRU were simulated without additional power added to the DC link to illustrate the basic operation. The model used in the simulation consisted of one 5kW active TRU drawing from the fast jet electrical system.

For active mode, illustrative results are presented in Figure 101 and Figure 102 depicting the *P, Q* and *S* profiles and *V* and *I* draw profiles from the PCC of the fast jet electrical system model. For passive mode, the equivalent is shown in Figure 103 and Figure 104. On these figures, the left hand side are the benchmarking of the conventional passive TRU from chapter 2 for comparison (similar to the illustration setups of previous chapters), with the right hand side showing the results of the active TRU operations for comparison. From these figures, it can be seen that there is not much difference in terms of the shaping of the waveforms from passive mode or active mode and are not too dissimilar to the basic TRU or linear resistive loading. One noticeable difference for both active and passive mode is the increase in reactive power drawn due to the added smoothing inductance.

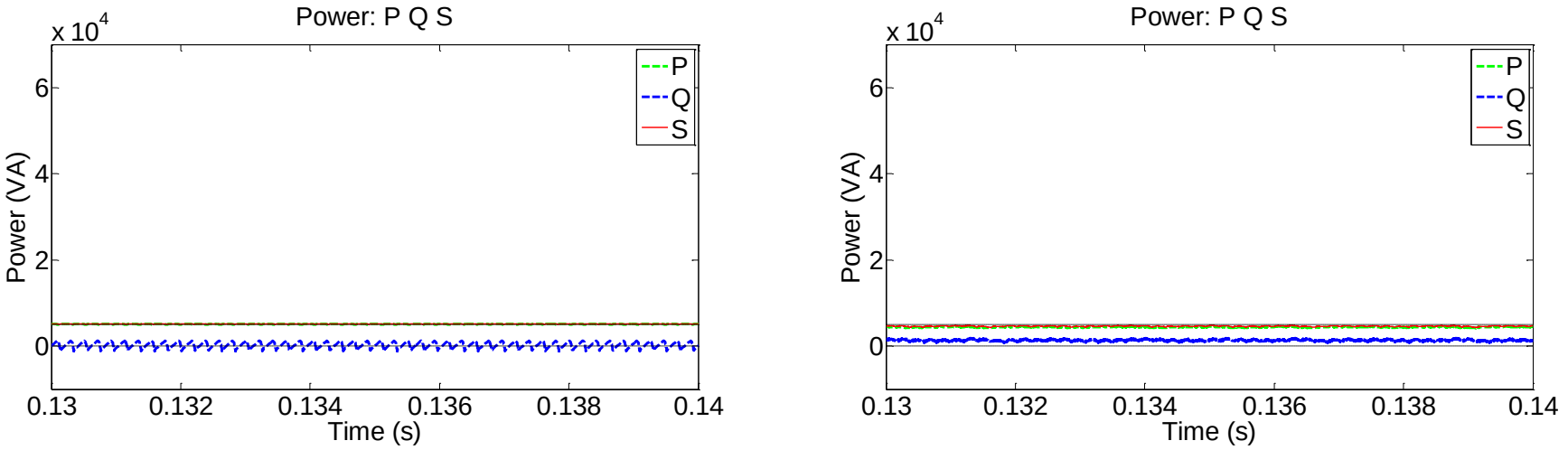

Figure 101- P, Q, S comparison between benchmarking TRU (left) and active TRU in active mode and no supplementary DC power source (right)

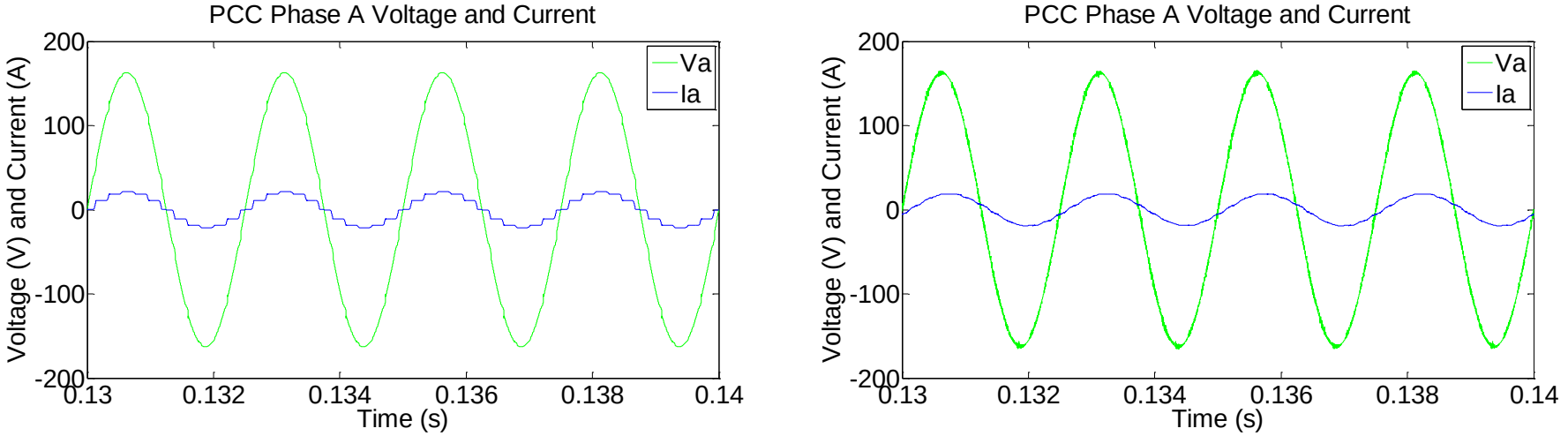

Figure 102- V, I comparison between benchmarking TRU (left) and active TRU in active mode and no supplementary DC power source (right)

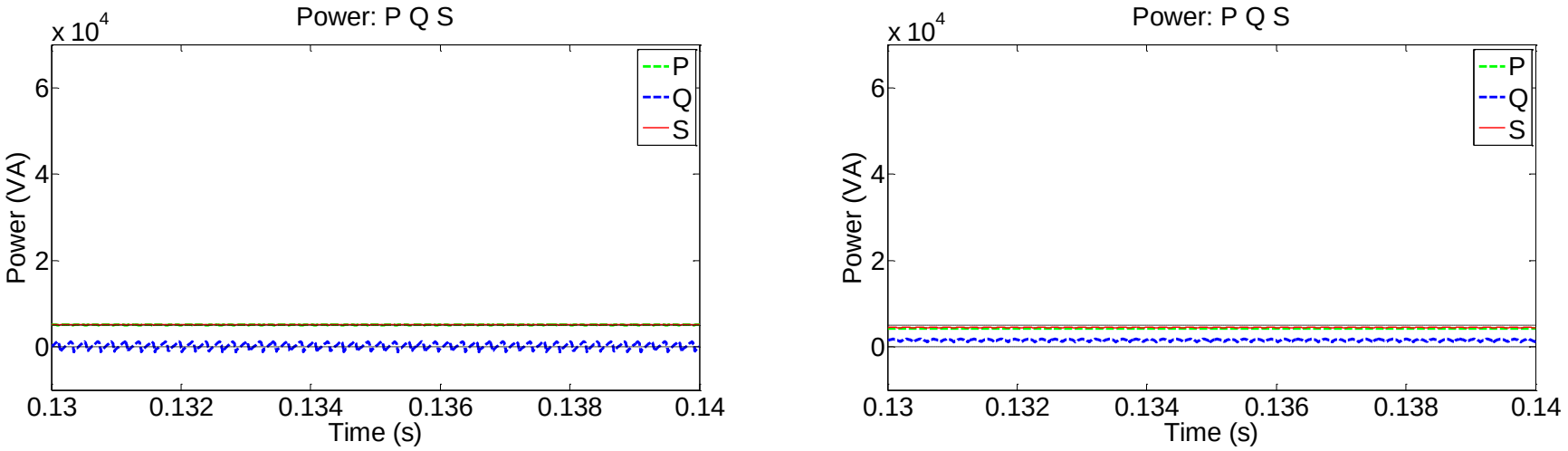

Figure 103- P, Q, S comparison between benchmarking TRU (left) and active TRU in passive mode and no supplementary DC power source (right)

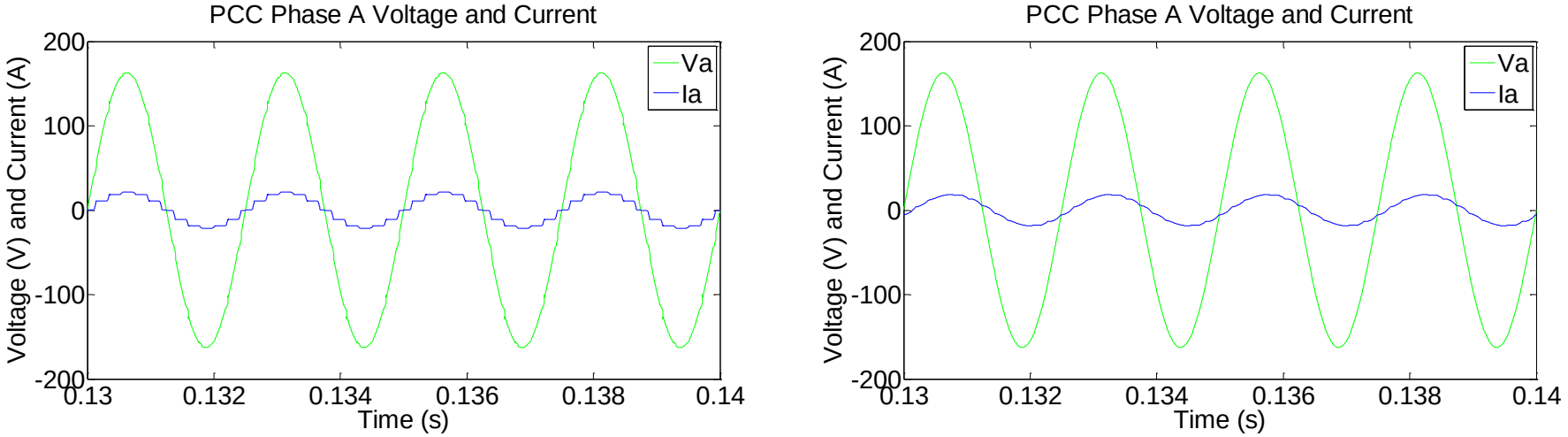

Figure 104- V, I comparison between benchmarking TRU (left) and active TRU in passive mode and no supplementary DC power source (right)

6.3.1.2 With additional DC power source

Following from the previous section 6.3.1.1, the simulation of when the supplementary power supplied has exceeded the local DC power loading requirements is presented here in this section. In this simulation, the 25kW single channel model from chapter 2 is used again. The TRU is replaced with the active TRU and a 10kW additional supplementary generation source is added to the DC link of the active TRU. Due to the fact that the 28VDC side loading is rated at 5kW approximately, there is an excess of 5kW that can be utilised elsewhere. With the active TRU, this 5kW is fed back into the AC side and can be utilised, to partly supply the 10kW rated linear load and 10kW non-linear loading (with the remainder 15kW coming from the main generation). As such only 15kW is required from the main generation ultimately illustrating load sharing.

The illustrative results of this for *P, Q,* and *S* are shown in Figure 105 and the *V* and *I* waveforms are shown in Figure 106. Again in these figures, the left hand side is the 25kW bench marking from chapter 2 with the actual results of the active TRU on the right for comparison. From the *P, Q* and *S* profiles of Figure 105, the subsequent power flow back from the DC side into the AC is confirmed with the reduction of real power from main generation down to 15kW. The middle dashed trace represents this 15kW level from the main generation with 10kW alleviated by the supplementary generation (though the flow of power is slightly less than 5kW due to inefficiencies of the inverter similarly to chapter 5).

The absolute harmonic current does not increase, but the relative *ITHD* increases because the Active TRU is now adding more fundamental current into the AC system in conjunction to the main generation draw.

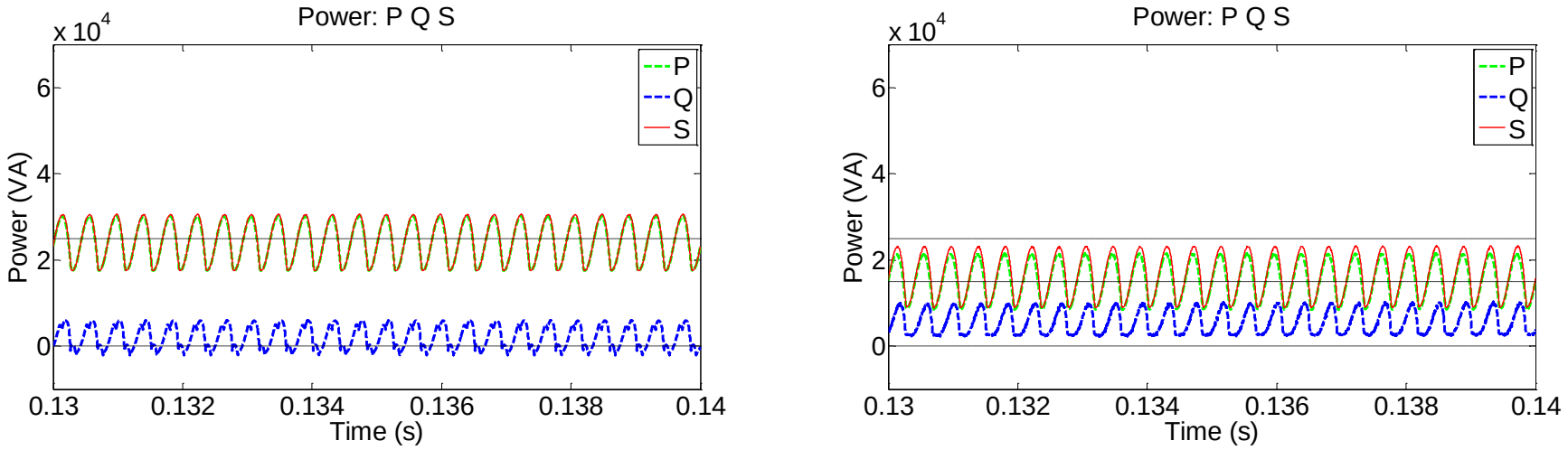

Figure 105- P, Q, S comparison between benchmarking of combined loading (left) and combined loading with active non-linear load with supplementary DC generation source (right)

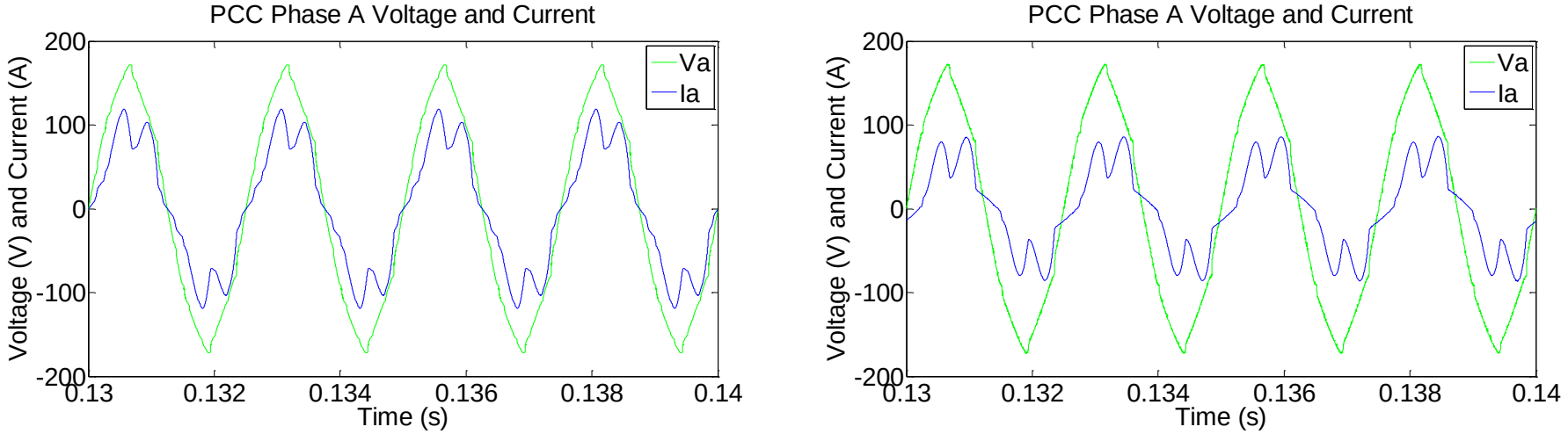

Figure 106- V, I comparison between benchmarking of combined loading (left) and combined loading with active non-linear load with supplementary DC generation source (right)

6.3.2 270VDC active rectifier simulation results

With the presentation of 28VDC active TRU operation with simulation results in section 6.3.1, this section presents the simulation results of the proposed active conversion of 270VDC passive rectifiers of non-linear loads. A 10kW non-linear load is examined where its passive rectifier is changed to an active equivalent using the control and topologies presented in section 6.2.2.

6.3.2.1 Without addition of DC power source

Initially, the standalone 10kW active rectifier drawing from the main fast jet electrical system bench marked in chapter 2 is simulated with operations in both active and passive mode with no power integration to illustrate basic operations of the proposed setup.

Example simulation results of *P, Q*, and *S* and *V* and *I* waveforms are shown in Figure 107 and Figure 108 respectively for active mode (with the bench marking of chapter 2 for a normal non-linear load shown in the left for comparison). Firstly with active mode operations, the *VTHD* remains similar when comparing to the normal passive rectifier, at around 4% compared to 4.3% (of chapter 2) respectively, while the *ITHD* has reduced significantly from 54.36% down to 6.06% and the reactive power has also decreased. The decrease in *ITHD* is partly due to the added smoothing inductance but more so due to the adapted SAF control.

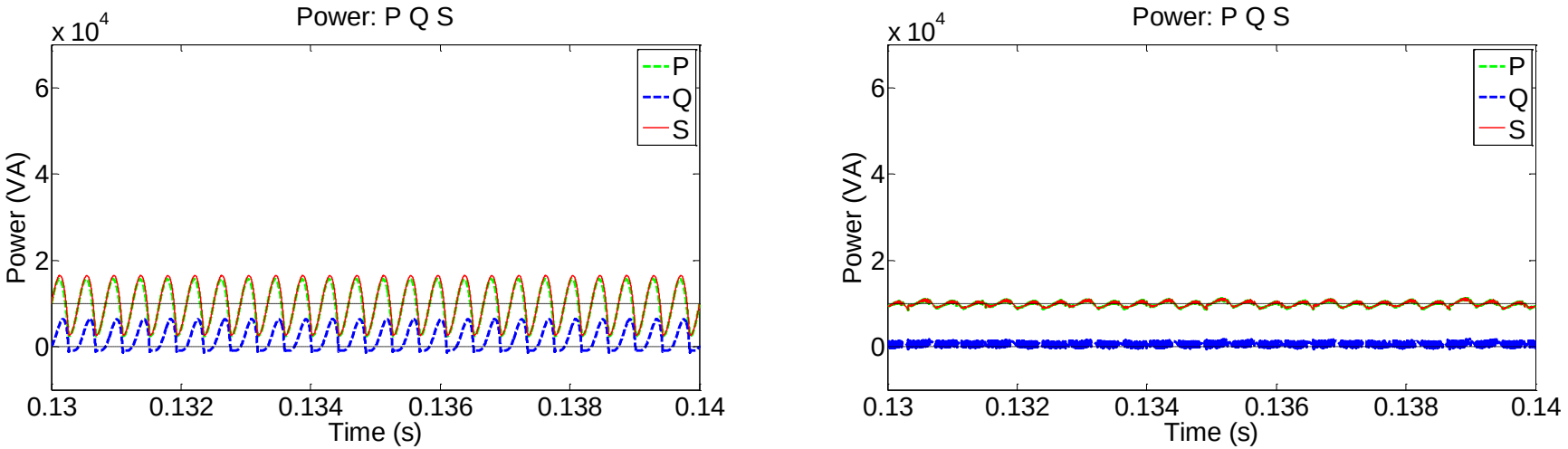

Figure 107- P, Q, S comparison between benchmarking non-linear load (left) and active non-linear load in active mode and no supplementary DC power source (right)

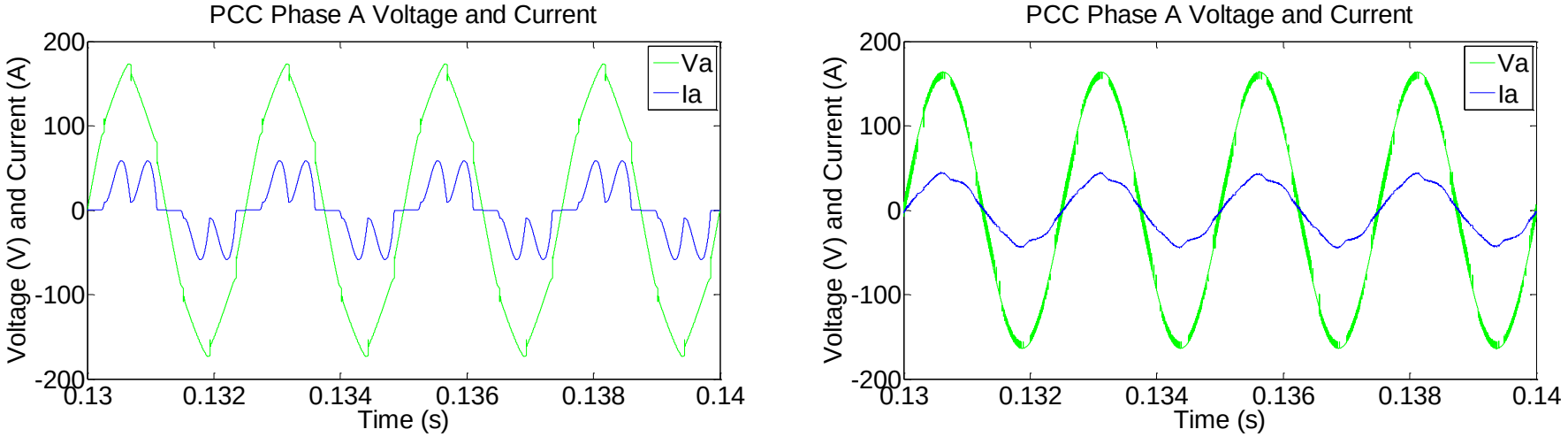

Figure 108- V, I comparison between benchmarking non-linear load (left) and active non-linear load in active mode and no supplementary DC power source (right)

6.3.2.2 With additional DC power source

With the illustration of the basic active rectifier in simulation in section 6.3.2.1, this section examines the simulation results of this, within the benchmarked 25kW loaded channel of the generic fast jet aircraft electrical system again. The passive rectifier of the non-linear load in this simulated scenario is changed to the active equivalent. To demonstrate the feed through of power back into the AC side, a 15kW supplementary generation source is connected onto the DC side of this active rectifier in which 10kW is consumed by the DC loading of the non-linear load itself. This leaves 5kW for feed through back to the AC side for the normal 5kW TRU and 10kW linear load in parallel.

Simulations results of this scenario are presented in Figure 109 to Figure 110 which shows the *P, Q* and *S* waveforms as well as the *V* and *I* waveforms. Similar to before, the results of the simulation are shown on the right hand side with the bench marking of the baseline 25kW loading from chapter 2 shown in the left hand side. The upper black trace of Figure 109 represents the power level drawn from the main generation if there is no additional/supplementary generation in the system, at 25kW. With excess power of 5kW fed back into the AC side: this 25kW is reduced with the non-linear loading completely supplied by the supplementary generation and the remaining TRU and linear loading in the rest of the network partially supplied by the same supplementary generation flowing back through the active rectifier. Hence, this illustrates the power alleviation possible with such an active rectifier setup in place of the normal passive rectifier, which not only provides for local DC loading but also the excess power can be fed back into the AC side as well. Ultimately this allows further penetration of power beyond DC side supplementary power. This allows excess DC power to be converted to AC power, hence reducing the need to increase the size of the AC electrical generator and infrastructure

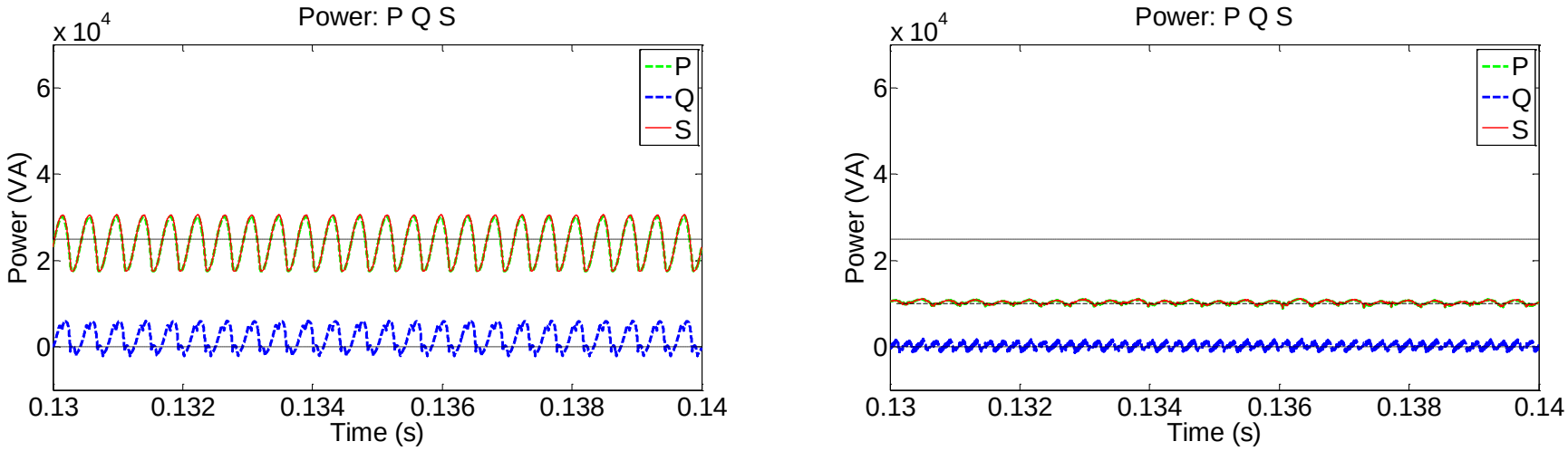

Figure 109- P, Q, S comparison between benchmarking of combined loading (left) and combined loading with active non-linear load with supplementary DC generation (right)

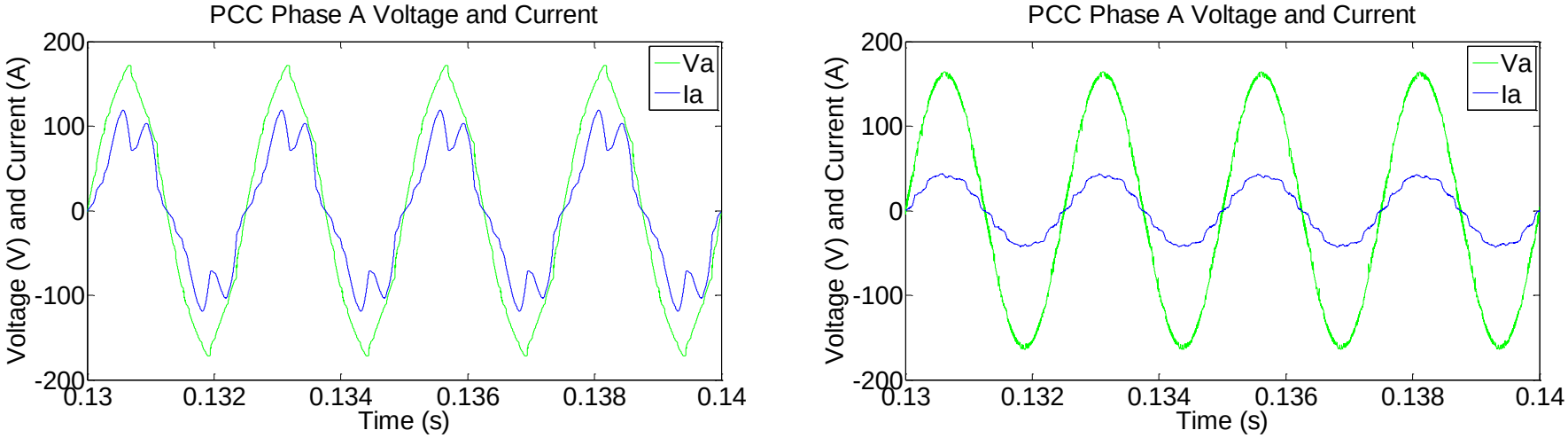

Figure 110- V, I comparison between benchmarking of combined loading (left) and combined loading with active non-linear load with supplementary DC generation

6.4 Summary

In summary, this chapter has presented the proposal of increasing power integration by converting the basic passive rectifiers (rectifiers of non-linear loads and TRU) around the electrical system to active equivalents. This is the proposed replacing of passive diodes of these rectifiers to switches on a one to one basis to convert them into active TRUs and active rectifiers. In terms of supplementary generation integration, this conversion is a follow up of the power integration presented in chapter 4 where the proposal of adding power to the DC link of passive TRU or rectifiers of non-linear loads were presented. With the conversion to the active rectifiers: excess power integrated to the DC link that is not consumed by the local DC loading can flow back into the AC side when power generation added exceeds the DC side loading.

This chapter has presented the proposed workable control and topology for such active TRUs and active rectifiers and illustrates their operation against the fast jet electrical system loading through simulations. The proposed control for this is similar to the SAF control of chapter 5 in which a version of *dq0* control is utilised. As such the real and reactive power through the active TRU or active rectifier can be controlled. Additional to feeding power back into the AC system, the preservation of the passive topology of the rectifier as a fall back mode is also possible using the same topology but replacing the passive diodes with active equivalent switches (and in series diode). With this, when the switches are in their passive 'off' state, the TRU or rectifier can be reverted back to their passive equivalents, increasing fall back redundancy. Other benefits of converting passive rectifiers to active equivalents compared to solely adding an inverter for power integration is: reduced inverter sizing, as any power integrated is partly consumed locally at the DC side and only the excess power is required to be fed back into the AC system. Another benefit of such a proposed setup is in the reusing of existing wiring from the load itself back to the AC busbar: reducing the need to add additional routing of the inverter wiring. The approach of such proposed active TRU and active rectifier requires no modification to the main generation for the parallel of power and is also fitting with the voltage master and current slave scheme common to the other two proposed integration methods proposed in chapter 4 and 5.

6.4.1 Possible use of d component and DC link voltage to switch between passive or active modes

A proposed concept mode of operation for an active rectifier is discussed here in this section to explore a possible means of switching between active and passive mode. This proposal is to use the *d* component (of the PCC draw) of the *dq0* control coupled with the DC link voltage, as indicators to switch from passive mode to active mode and vice versa. This is convenient as the *dq0* transformation

outputs and DC link voltage are already part of the control input measurement in which no additional measurements would be required.

To elaborate, Table 15 provides a summary of the modes of operation proposed with such setup. For example: when the *d* component is low while the voltage is high would indicate the supplementary power is available and in which the system can switch into active mode in anticipation of the supplementary power exceeding the DC side loading and supplementary feed through of power to the AC side. If the supplementary generation continues to increase, the *d* component will become smaller until it becomes negative meaning the power is now being fed back into the AC system. Conversely, when supplementary power is low, the resultant *d* component becomes positively high as most of the loading power is drawn from the main generation, while voltage value is also high: hence this would mean a switch to passive mode. Conversely, at start up, a low *d* component would be seen also but with the voltage rating also small. In such case the system can be made to stay in passive mode.

However, one possible prohibition of this proposal is: the connection of emergency power whether at start up or when generator is offline would mean a low *d* component but where voltage might be high enough to nudge the rectifier into active mode. This is undesirable and a finer distinction may be needed to distinguish between 28V (generator levels) and 26V (emergency power levels). Table 15 below illustrates the theoretical different modes of operation against different *d* component and DC link voltage values.

Table 15- Possible mode of operation from switching between active and passive mode of active TRU or rectifier

***d* component**	**Voltage Value**	**Condition**	**Mode of the rectifier**
Low	Low (0-26V)	Electrical system start up	**Passive**
High	High (28V)	Limited supplementary generation	**Passive**
Low (including negative)	High (28V)	High amount of supplementary power	**Active**
Low	Low (0-26V)	Emergency power (main generation offline)	**Passive**

7 Complementary operation of the three proposed power integration methods

7.1 Chapter overview

In summary: this thesis has proposed the application of three integration methods for introducing more power into in-service fast jet electrical systems. This is in the context of the through life power demand increasing and eventually exceeding the main generation installed at the start of the service life. To compound the problem, the electrical system is located within a confined and unchanging airframe which limits bulk generation upgrade discussed in chapter 1. One alternative solution with little precedence on fast jets is the application of distributed generation that conform to the confines of such airframes.

With limited precedence of such: a review of topologies and control from other domains such as EVs and M/DG/R for read through was performed and summarised in chapter 3 [82]-[94]. This resulted in the proposal of three distributed power integration applications for the unique fast jet problem making up the main work presented in this thesis. These methods were elaborated and examined separately through simulations in chapters 4-6 for the fast jet application. The integration methods novelty comes from the tailoring and proposed application for fast jet and against the through life upgrade problem. As part of the intended application, rather than standalone solutions; these three solutions are complementary in their operations to maximise penetration of power. At the same time, the application and operation of these are meant to be loose coupled to allow flexible incremental application and with limited need to modify the existing main generation.

As such, this chapter illustrates the concurrent operations of these methods through simulation. The simulations presented, mimic snapshots of the fast jet electrical system at different points in time of a generic fast jet life cycle as it faces demand increases from upgrades. Within these snapshots: the integration options examined in chapters 4-6 are applied incrementally to meet the demand increases in a complementary manner. The aim of this is to illustrate with such complementary power integration: the fast jet power demand can be met without the need to up rate the main generation sources and negate reducing the need for cumbersome rework of the mechanical off take.

7.2 Extended electrical system model and through life upgrade snapshots

To examine the complementary application of the three integration options presented in chapter 4, 5 and 6, an expanded fast jet electrical system model is used in this chapter and is presented in this section. This is used instead of the basic 25kW single channel model in previous chapters (originally presented in chapter 2) to increase representation of the multiple loads distributed around the fast jet aircraft. That is, the number of loads is increased along with their different locations represented by different line impedance more akin to the major loads of a fast jet aircraft. Also to increase representation, a two channel system is used with the provision to be connected together through bus tie contactors when single generator operation is required.

7.2.1 Extended generic fast jet electrical model

This section presents the profiling of this extended fast jet electrical model used in this chapter. The baseline of this extended electrical system model gives a *VTHD* of less than the 8% limit on both channels and the *ITHD* is around 23-24%. The absolute current harmonics drawn from the PCC in both channels are 18.48A and 14.17A for the 5^{th} harmonic (left and right channels) and 2.17A and 0.58A for the 11^{th} harmonic. These results are presented in Table 16 and represent the baseline level at the start of the generic fast jet service life.

The associated profiles of the *P, Q*, *S* profiles of the two channels within this baseline model are presented in Figure 111 to Figure 112 and the *V*, *I* profiles are shown in Figure 113 to Figure 114. The upper dashed trace of Figure 111 and Figure 112 for the left and right channel respectively, represents the virtual 30kVA/kW upper limit of the baseline main electrical generation which cannot be increased further without cumbersome modification. The real power drawn by the combined two channels is around 52kW representative of baseline loading at the start of service life of the aircraft.

Table 16 Results of the baseline extended fast jet electrical model

	Case	Averaged PCC S (kVA)	Averaged PCC P (kW)	Averaged PCC Q (kVAR)	VTHD (%)	ITHD (%)	Fundamental Voltage RMS Phase A (V)	Fundamental Current RMS Phase A (A)	Current 5th Harmonic (A)	Current 11th Harmonic (A)
Baseline										
	Channel 1	28.75	28.3	3.79	5.71	24.18	113.05	85.13	18.48	2.17
	Channel 2	24.12	23.88	2.67	4.66	23.07	113.48	71.73	14.17	0.58

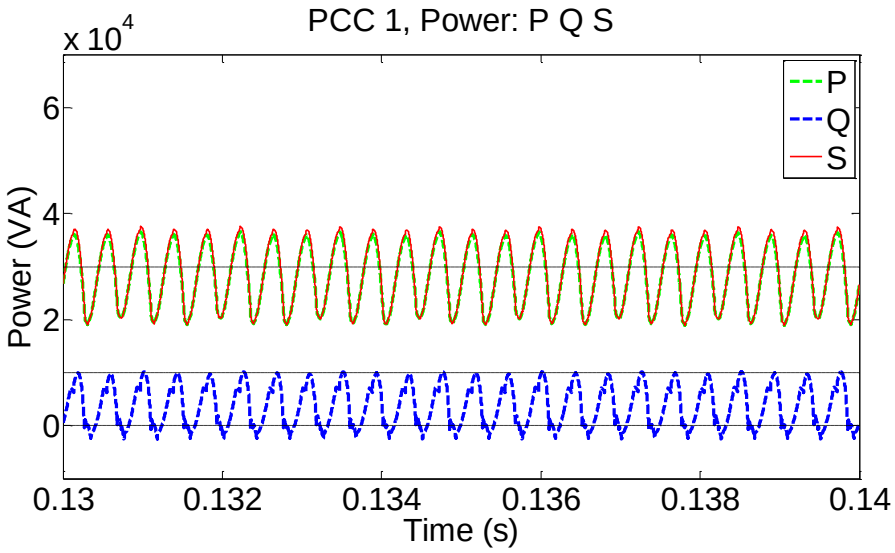

Figure 111- P, Q, S Baseline extensive electrical network channel 1

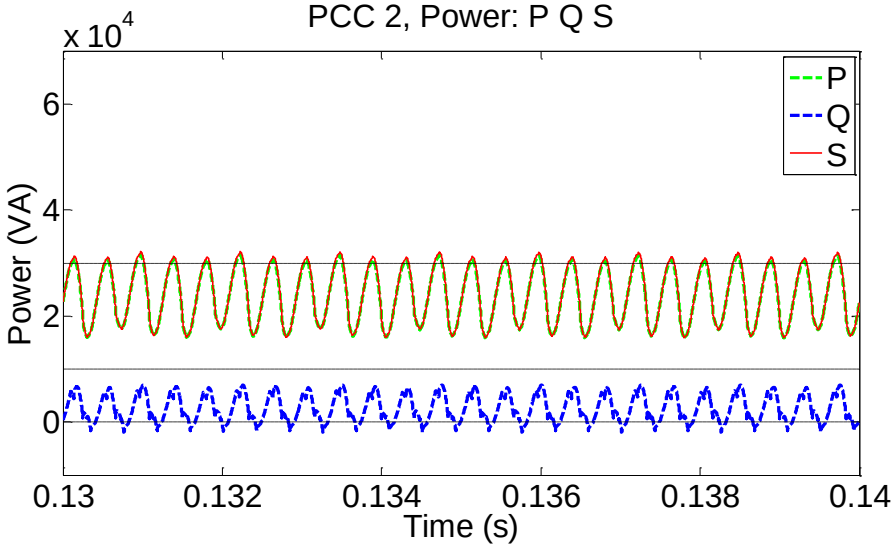

Figure 112- P, Q, S Baseline extensive electrical network channel 2

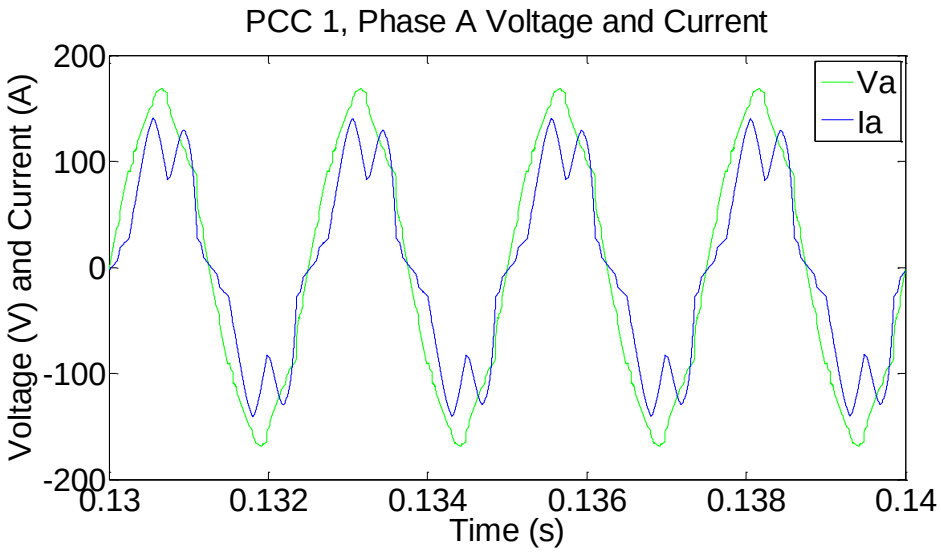

Figure 113- V, I Baseline extensive electrical network channel 1

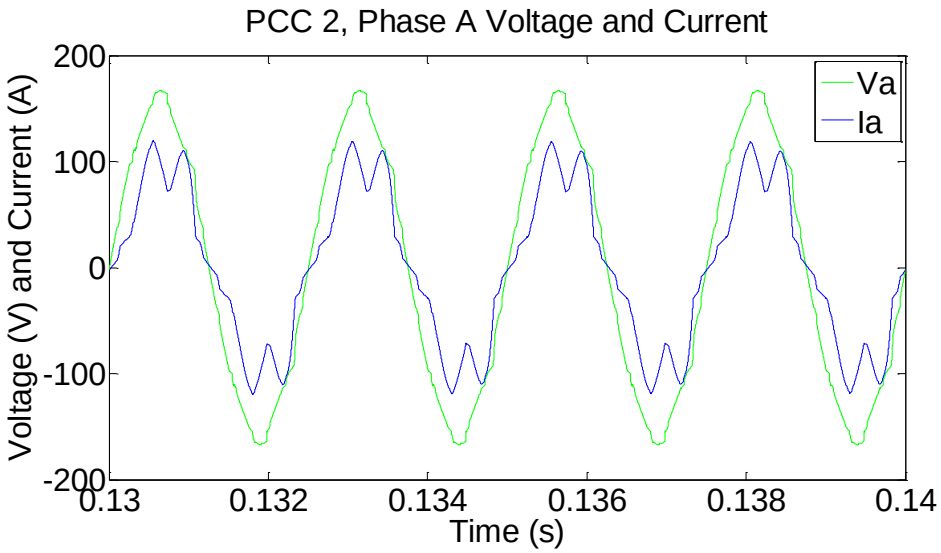

Figure 114- V, I Baseline extensive electrical network channel 2

7.2.2 Mimicking increase in power demand on the fast jet model

This section presents the hypothetical upgrade scenario used in this chapter to mimic through life demand increases onto the extended electrical system model presented in section 7.2.1. The power demand is increased incrementally to the final configuration with an approximate increase of 45kW overall over the two channels mimicking typical upgrades such as [2]-[12] discussed in chapter 1. These additions were specified as electronic type loads (non-linear in nature) to reflect the nature of power demand upgrades in real life fast jet aircraft. These are summarised in Table 17 which summarises the demand increase over five increments.

Table 17- 5 increment demand increase used in simulations

Upgrade	Type	Power (kW)	Aggregate power increase (kW)
Increment 1	Hardpoint load replacement Load A	3 (increase of 2.5)	2.5
Increment 2	Avionics/replace existing Load B	15 (increase of 7.5)	10
Increment 3	Avionics bay/replace existing Load C and D	2x 6 (increase in 2x 2.5)	15
Increment 4	Unidentified small load/addition	5 (increase 5)	20
Increment 5	Unidentified large load/addition	25 (increase of 25)	45

7.2.3 Concurrent power integration simulations

To cope with the simulated power demand increase on the generic fast jet electrical system presented in section 7.2.2, power integration methods of chapters 4, 5 and 6 are applied concurrently within the simulations.

The five incremental power integration applications corresponding to the power demand and conversion method used are summarised in Table 18. Through the application of these in the simulations, the proposed application of supplementary power to cope with through life increase in power demand on a generic fast jet electrical system can be illustrated.

In terms of application, one strategy adopted in this chapter is to apply the simplest and low risk, lower power options at the start of the lifecycle, leaving planning time for higher power applications as well opportunity for higher power density generation technologies to mature before their application. In terms of the simplest, low risk options; these are the application of the low voltage 28VDC integration outlined in chapter 4 which does not require three phase AC paralleling and as 28VDC power flow is already standardised for fast jet aircraft in general. This could then be supplemented later by more complex SAF (chapter 5) application, active TRU or active rectifiers (chapter 6) application further down in the lifecycle.

Table 18- 5 increment power integration coinciding with demand

Coinciding upgrade	Supplementary power application (kW)	Aggregate increase (kW)	**Method elaborated in**
Increment 1	2x3.5(Additional 28VDC power on DC busbars (maybe fuel cell of some sort, 2x3.5kw))	7	Chapter 4
Increment 2	2x3kW (Additional power on a 270VDC load at avionics bay)	13	Chapter 4
Increment 3	2x10kW (ATRU) in place of TRU DC DC power	26	Chapter 6
Increment 4	1X 7.5 (2x SAF and one with power)	33.5	Chapter 5
Increment 5	12 (Power onto the other SAF) +11(load D)	53.5	Chapter 5, chapter 4

7.3 Simulation results of power demand increase and power integration

This section presents the simulation results of the elaborated changes to the extended fast jet electrical model of section 7.2 and are summarised in Table 19 below.

To summarises: in increment 1, load A on one of the hardpoints on channel 2 is replaced by an avionics pod requiring 3kW instead of the previous 0.5kW. As such, an increase of 2.5kW in power demand on channel 2 is experienced by replacing the original 0.5kW load. To cope with this, and to add some provision for future loading, a 3.5kW supplementary power generation supply is connected to the 28VDC busbar of both channels through individual DC DC buck boost converters (this integration method was presented on its own in chapter 4). The *P, Q* and *S, V* and *I* profiles at the PCC of these are presented in Figure 115 to Figure 118. The shaping of voltage and current are similar to base system before these changes are applied (which the *VTHD* and *ITHD* are not drastically changed as a result).

In increment 2, load B on channel 1 is replaced by a more powerful equivalent load which consumes 15kW as oppose to the previous 7.5kW (increasing the demand by 7.5kW). Coinciding with this, the supplementary upgrade takes the form of adding supplementary power at a 270V DC link, (again using DC side integration presented in chapter 4), applying integration of power at the 270V DC links of the two avionics bay on each channel. This increases the supply on both channels by 3.5kW each. Again as a result, there is no significant increase in *ITHD* compared to increment 1 (though in real terms channel 1 increases slightly which is inferred by its 5^{th} and 11^{th} harmonic values of Table 19 due to the non-linear loading increase of load B as part of the upgrade). There is also a slight increase in the channel 1 *VTHD* due to the increase in absolute non-linear loading again. The real and apparent power for either channel is still within the 30kVA/kW limit of the unchanged baseline main generation capacity. This implies, even though with the power demand increases of increment 1 and 2, the main generation has not needed to be changed.

Similarly, for increment 3, there is an increase in power demand from loads C and D of the respective avionics bays in which the total demand is increased to 6kW from 2.5kW (or a 3.5kW net increase as a result of this for each channel). In terms of supplementary power generation, the passive TRU of both channels are changed to active TRUs to introduce more power into the system (using the integration method examined in chapter 6). With this, the supplementary power generation connected at the 28VDC busbars are increased to 7.5kW for each channel, meaning that 2.5kW can in theory flow through the Active TRU back into the AC system while providing

completely for its own loading on the DC side. In terms of effects, firstly, the power drawn from the main generators are still under the 30kVA mark and similar voltage and current waveform quality are exhibited when compared to previous increments and the baseline: with the *VTHD* still under the 8% limit of DO160 [56] and the *ITHD* of both channels raising to slightly over 30% with a slight increase in absolute terms (due to increase non-linear loading in general rather than the supplementary power integration).

For increment 4, an additional load is added onto channel 1 which adds an additional 5kW overall. In terms of supplementary generation to cope, SAFs (examined in chapter 5) are added in both channels at their respective PCC. Also, an additional 7.5kW is added at channel 1 through this SAF. From this, the power drawn from the main generation is still maintained below 30kVA mark again summarised in Table 19. The *VTHD* has increased in channel 1 but still below the 8% mark and in channel 2 this is decreased slightly to 4.87%. The main 5^{th} harmonic has reduced drastically in real terms with the application of shunt active filtering. The waveforms of these are presented through Figure 119 to Figure 122 which illustrates the *P, Q*, and *S*, *V* and *I* profiles for the two channels.

Finally, for increment 5, a large non-linear load is added onto channel 2 which increases the power demand by 25kW. To cope, supplementary power is inserted at the DC link of the SAF of the same channel (previously added for increment 4) which adds a theoretical power increase of 11kW. Also to cope, the rectifier of load D/avionics bay is changed into an active rectifier and the power integrated at this DC link is increased to 12kW. With this the power drawn from the main generation is still kept under the 30kVA. The *ITHD* levels are at 15.64% and 20.62% respectively even with the shunt SAF operating, however, the 5^{th} and 11^{th} harmonic remains low for both channels. The *VTHD* has also exceeded the 8% recommended limits slightly in this case. The illustrations of profiles for *P, Q* and *S* and *V* and *I* are given as Figure 123 to Figure 126.

The degradation of power quality with the application of a SAF is unexpected when compared to the initial examination of the SAF application in chapter 5. In this, after increment 4 and 5, even with the application of SAF, the voltage and current harmonics are still quite high (more profound after increment 5) although current quality is still better in the scenario with the SAF in the system than without it (as will be presented in section 7.3.1). Hence it is proposed that further work should be undertaken to further optimise the SAF performance under such high levels of non-linear loading.

Table 19 – summary of different increments of power integration

Increment	Case	Averaged PCC S (kVA)	Averaged PCC P (kW)	Averaged PCC Q (kVAR)	VTHD (%)	ITHD (%)	Fundamental Voltage RMS Phase A (V)	Fundamental Current RMS Phase A (A)	Current 5^{th} Harmonic (A)	Current 11^{th} Harmonic (A)
Baseline										
	Channel 1	28.75	28.3	3.79	5.71	24.18	113.05	85.13	18.48	2.17
	Channel 2	24.12	23.88	2.67	4.66	23.07	113.48	71.73	14.17	0.58
Increment 1										
	Channel 1	25.59	25.09	3.77	5.69	27.42	113.27	75.62	18.64	2.46
	Channel 2	23.29	22.94	3.05	5.06	26.79	113.51	68.99	16.27	1.71
Increment 2										
	Channel 1	29.46	28.79	4.57	6.44	27.03	112.92	86.94	21.46	3.28
	Channel 2	20.26	20.02	2.46	4.49	26.64	113.76	60.39	13.69	1.09
Incremental 3										

	Channel 1	26.99	25.27	8.59	6.93	31.19	112.56	79.8	22.82	3.72
	Channel 2	17.82	16.51	6.47	5.02	33.49	113.41	53.42	15.61	1.77
Incremental 4										
	Channel 1	28.52	28.24	-2.08	7.76	12.73	113.91	83.95	2.46	4.03
	Channel 2	19.82	19.67	-1.83	4.87	11.76	114.39	57.87	1.84	1.43
Incremental 5										
	Channel 1	28.79	28.55	-2.07	9.27 (exceeded DO 160 limit)	15.64	113.89	83.8	2.45	4.03
	Channel 2	26.55	26.01	-2.17	11.05 (exceeded DO 160 limit)	20.62	114.12	76.25	4.38	5.44

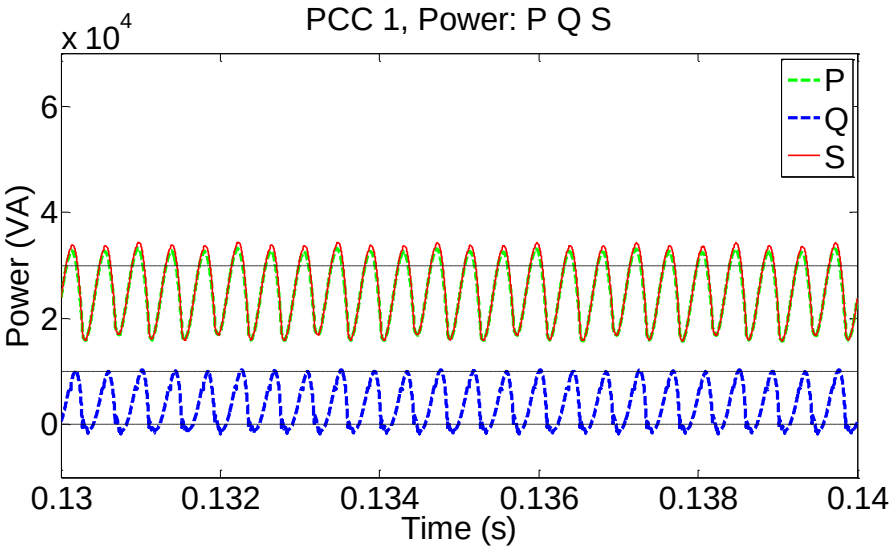

Figure 115- P, Q, S extensive electrical network channel 1 after increment 1

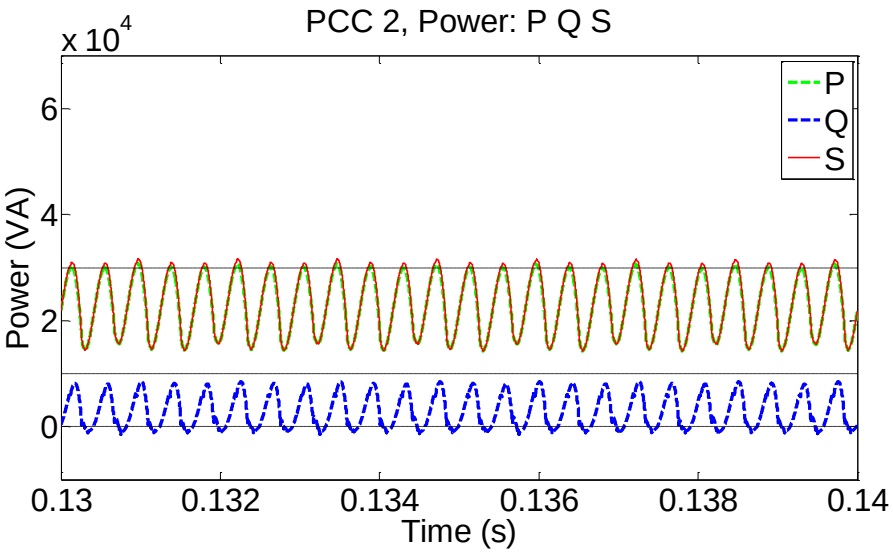

Figure 116- P, Q, S extensive electrical network channel 2 after increment 1

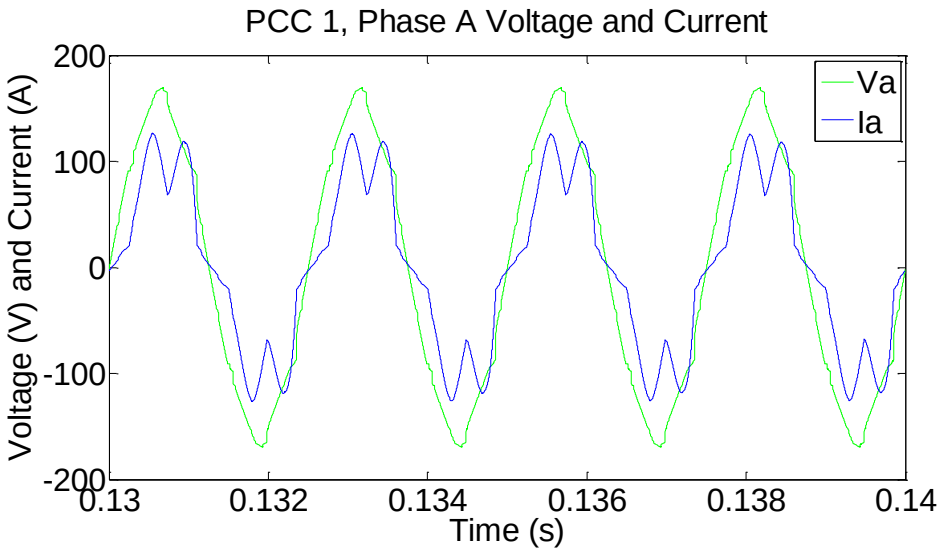

Figure 117- V, I extensive electrical network channel 1 after increment 1

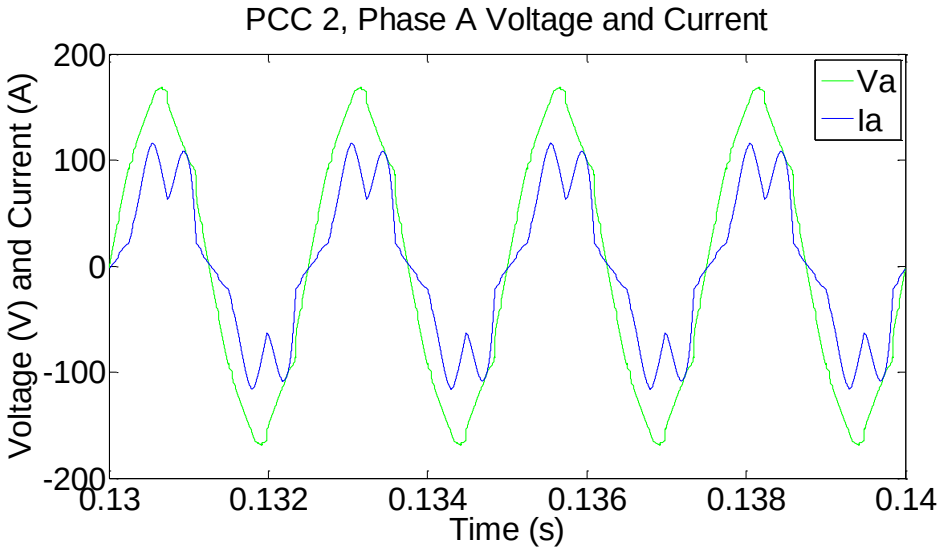

Figure 118- V, I extensive electrical network channel 2 after increment 1

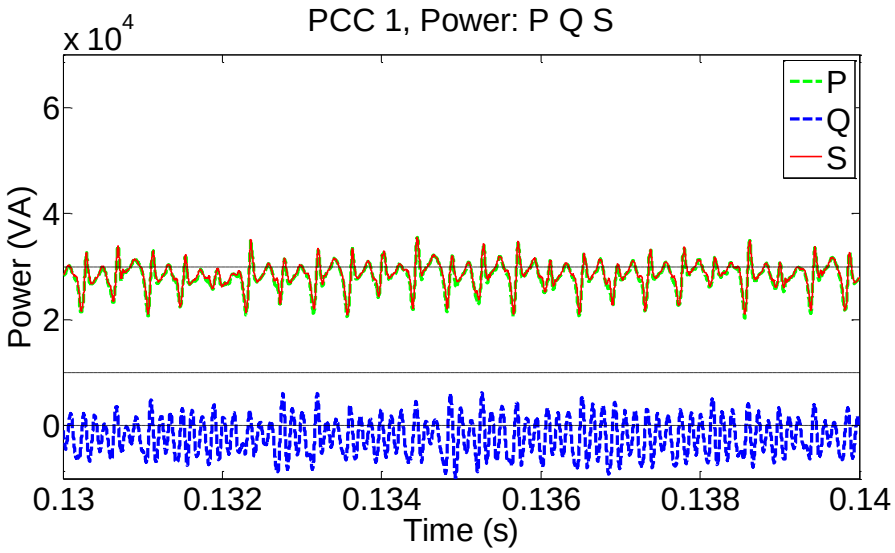

Figure 119- P, Q, S extensive electrical network channel 1 after increment 4

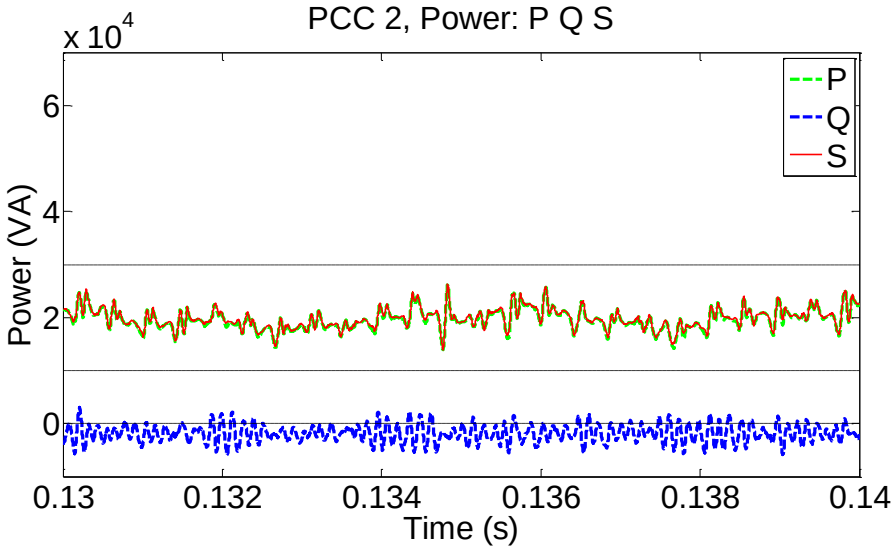

Figure 120- P, Q, S extensive electrical network channel 2 after increment 4

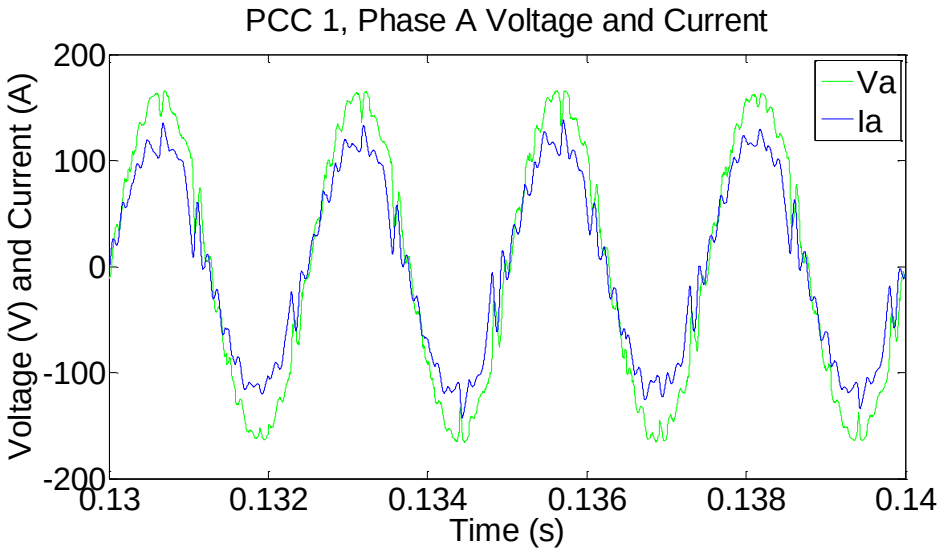

Figure 121- V, I extensive electrical network channel 1 after increment 4

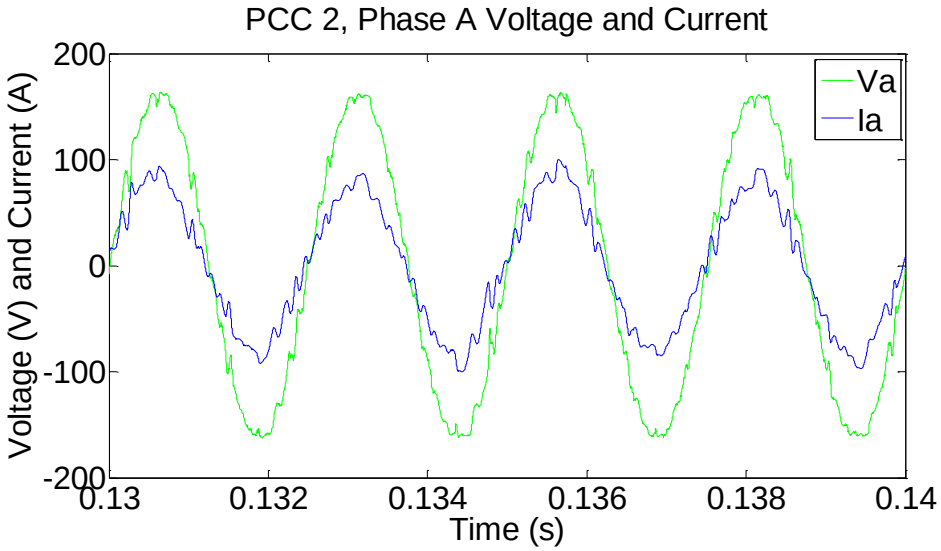

Figure 122- V, I extensive electrical network channel 2 after increment 4

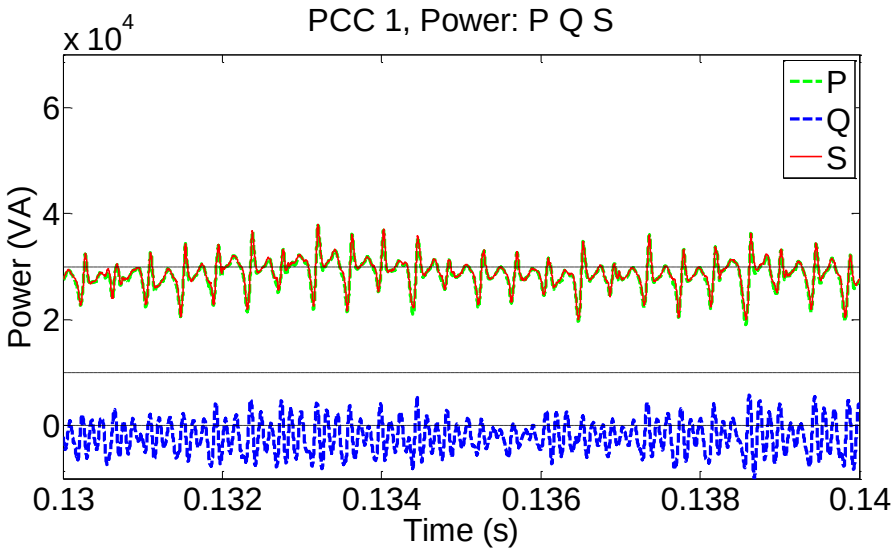

Figure 123- P, Q, S extensive electrical network channel 1 after increment 5

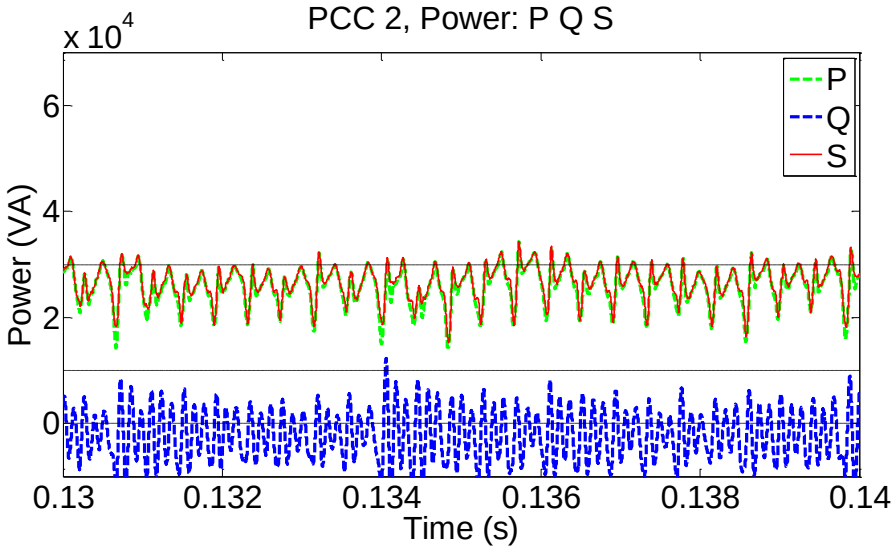

Figure 124- P, Q, S extensive electrical network channel 1 after increment 5

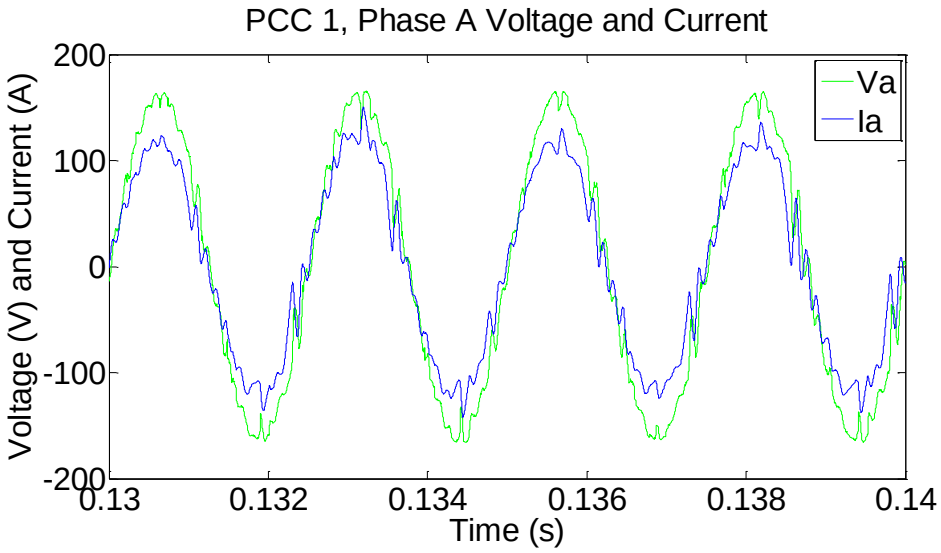

Figure 125- V, I extensive electrical network channel 1 after increment 5

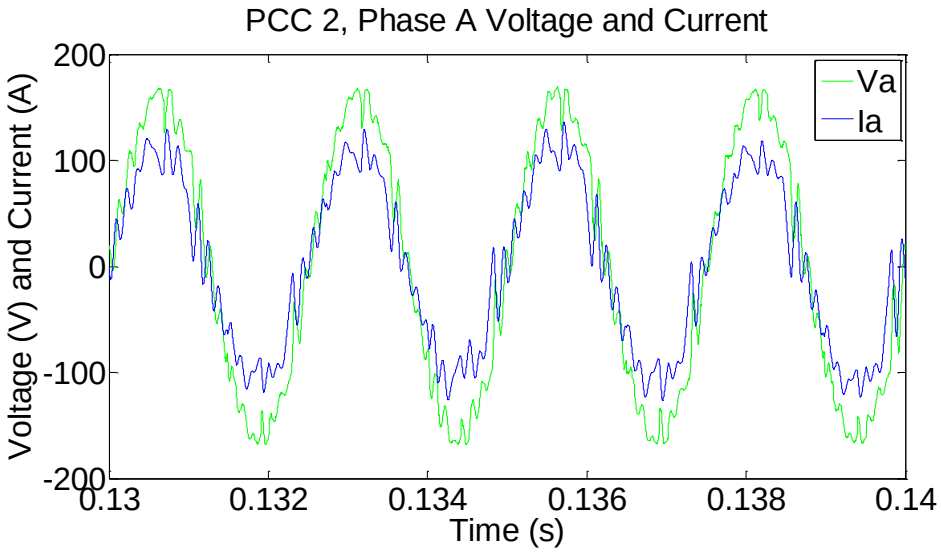

Figure 126- V, I extensive electrical network channel 2 after increment 5

7.3.1 Comparison to "if" main generation can be upgraded

To put the proposed supplementary generation for fast jet into context, this section presents the comparison of incrementally adding supplementary generation against the scenario of when increasing the main generation is possible.

Illustrative comparison of the two different scenarios are presented in Figure 127 to Figure 130 for *P, Q* and *S* and *V* and *I* plots in which the scenario of no supplementary generation but main generation increase are shown on the left of the figures and the supplementary generation scenario are shown on the right. The upper dashed trace of Figure 127 and Figure 130 represents the 30kVA line. Apart from needing to increase the main generation itself (which means that the mechanical off take, as well as associated feeders do not need to be changed) is the relatively more sinusoidal draw (work for proposed future work is to improve on this by further improving the SAF operation itself) from the PCC shown in Figure 127 and Figure 128. Also because of this the *P, Q* and *S* waveforms shown in Figure 129 and Figure 130 are flatter with less oscillating content that do not represent a net transfer of energy.

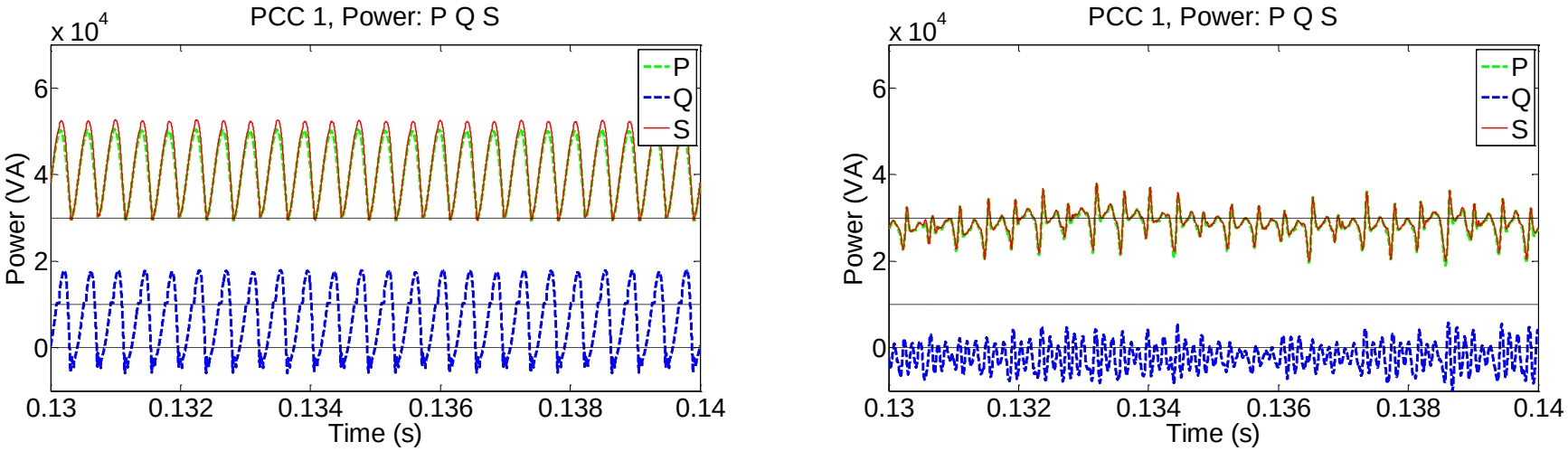

Figure 127- P, Q, S comparison of channel 1 increment 5 without (left) and with (right) supplementary generation

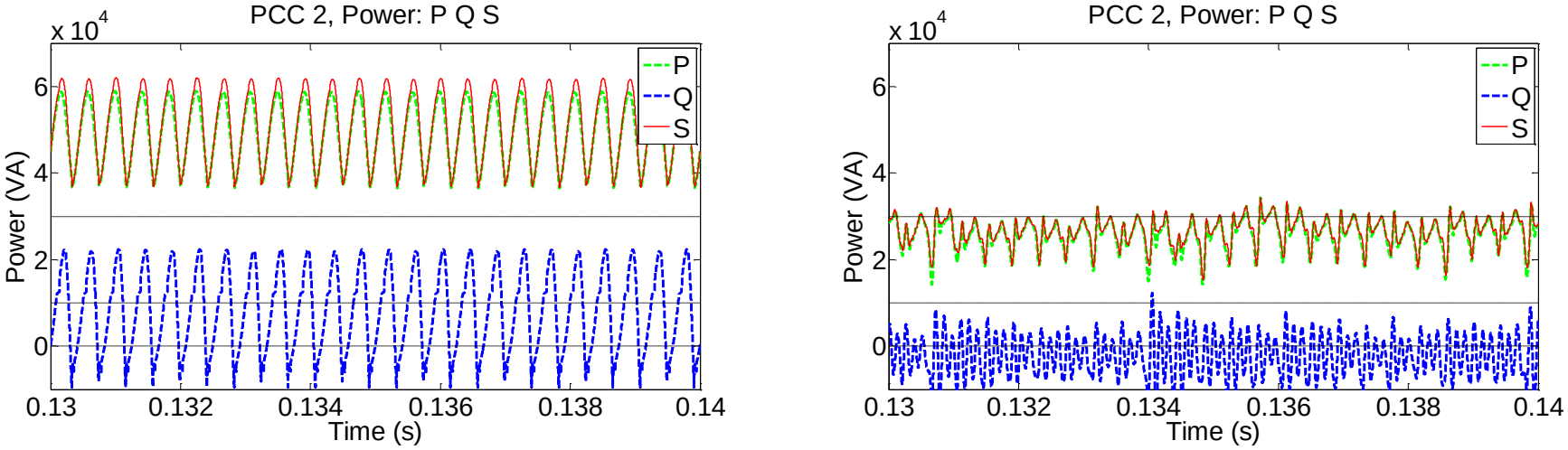

Figure 128- P, Q, S comparison of channel 2 increment 5 without (left) and with (right) supplementary generation

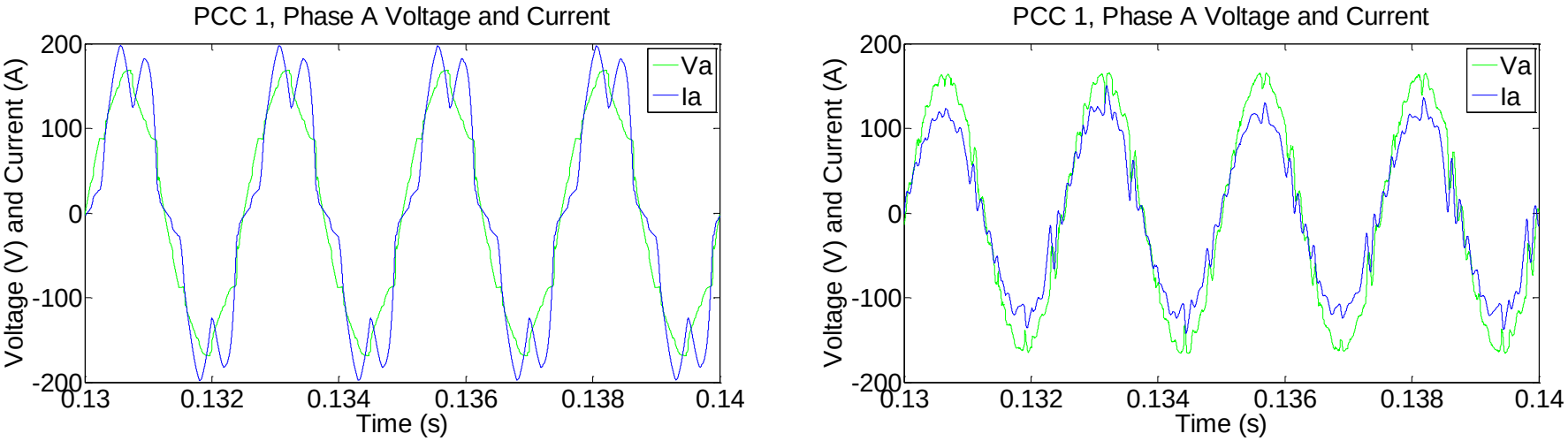

Figure 129- V, I comparison of channel 1 increment 5 without (left) and with (right) supplementary generation

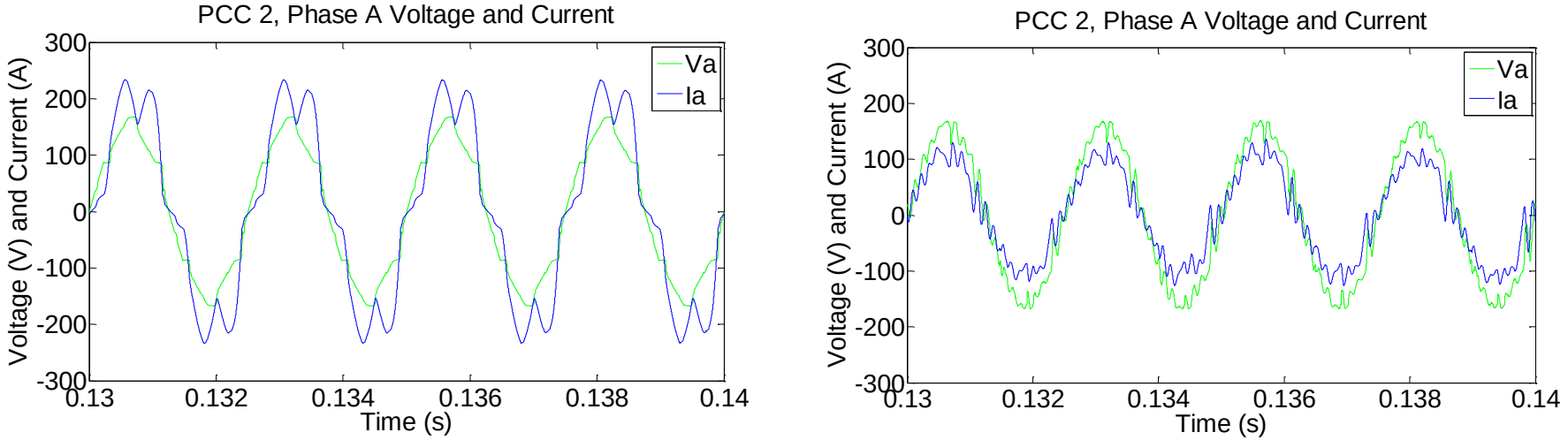

Figure 130- V, I comparison of channel 2 increment 5 without (left) and with (right) supplementary generation

7.3.2 Single engine operation scenario

The results in this section summarise the scenario in which one of the generators has also gone offline (after the 5th increment). To cope with this, the bus tie contactor has been connected to the two channels. During normal configuration without supplementary power integration, the remaining generator would be burdened with supplying power for both channels. However due to there being additional supplementary generation within the system, they stay online even after one of the main generators goes offline and as such have a higher degree of graceful degradation. Also the remaining generator does not become overburdened. The *P, Q,* and *S* and *V* and *I* plots are presented in Figure 131 to Figure 134. The scenario with no supplementary generation is shown on the left, with the scenario with supplementary generation shown in the right of the figures.

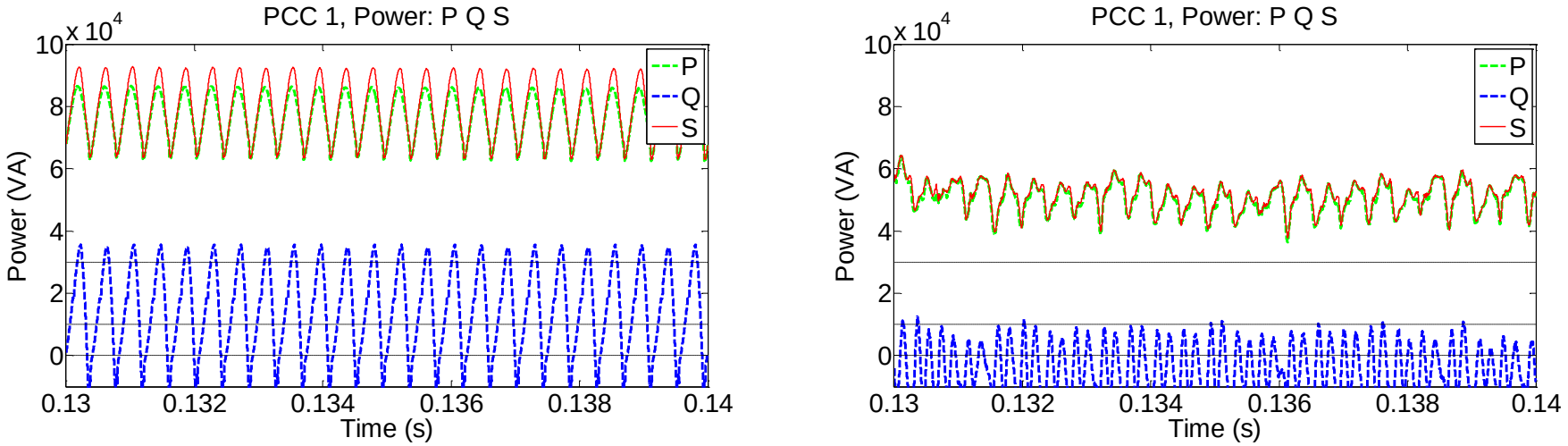

Figure 131- P, Q, S comparison of channel 1 increment 5 without (left) and with (right) supplementary generation

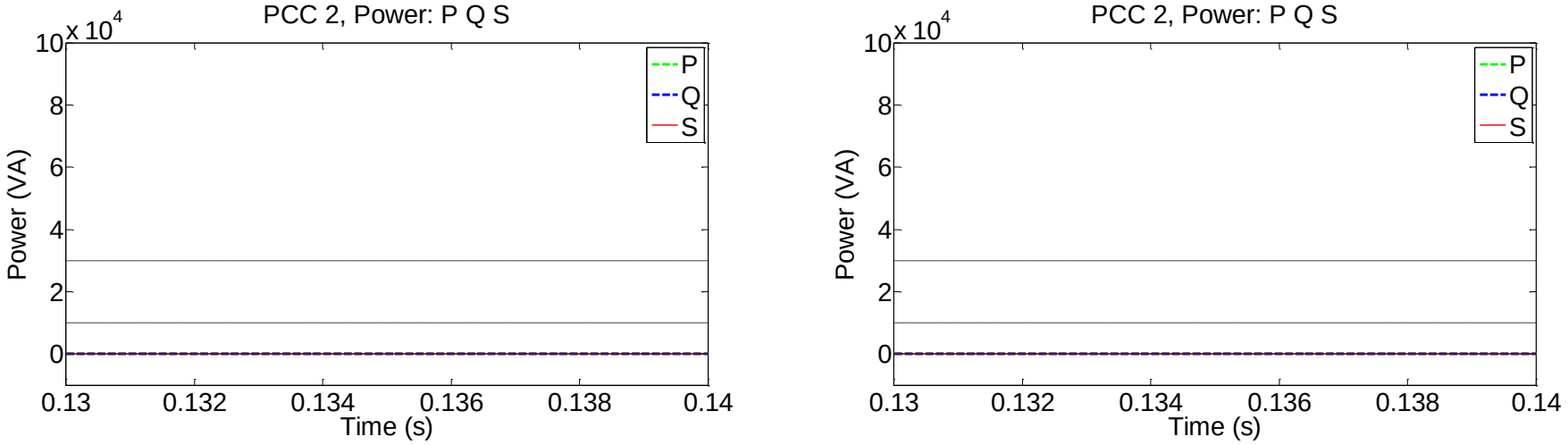

Figure 132- P, Q, S comparison of channel 2 increment 5 without (left) and with (right) supplementary generation

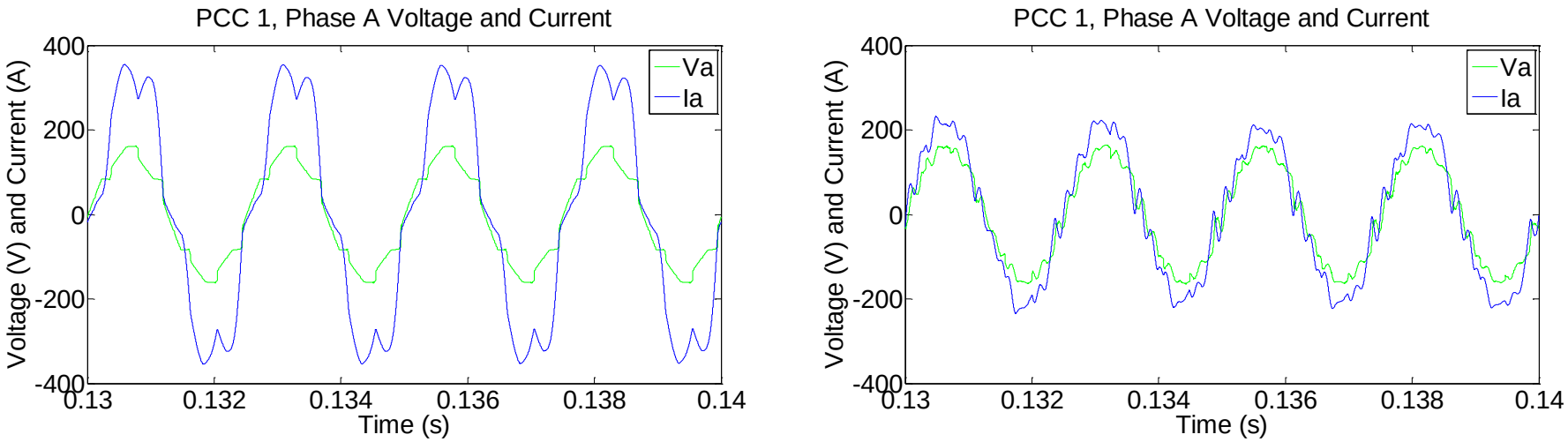

Figure 133- V, I comparison of channel 1 increment 5 without (left) and with (right) supplementary generation

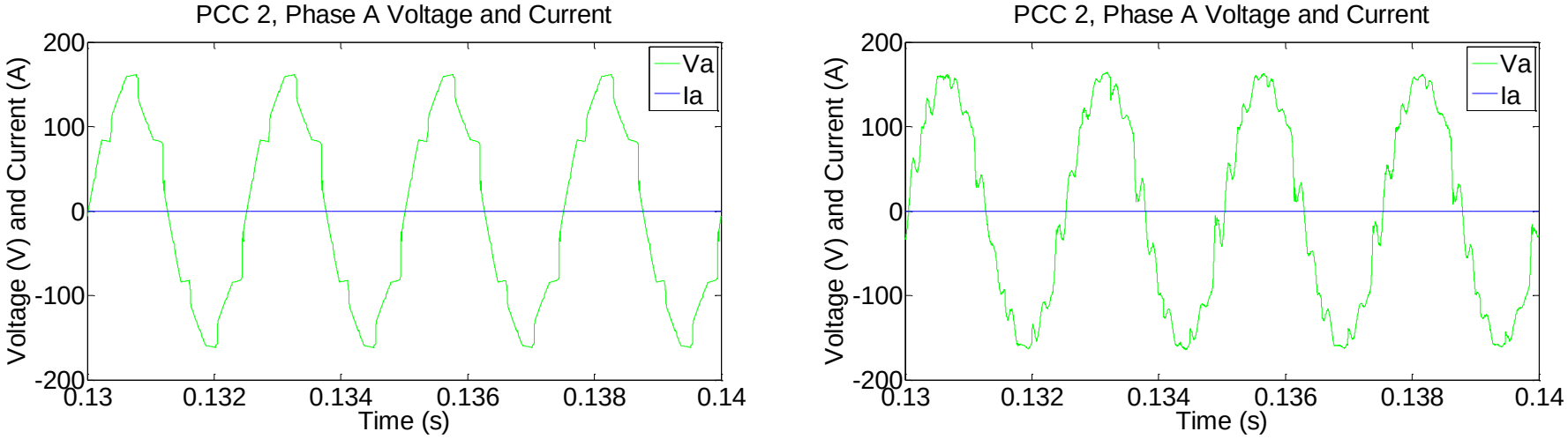

Figure 134- V, I comparison of channel 2 increment 5 without (left) and with (right) supplementary generation

7.4 Summary

In summary, this chapter has demonstrated concurrent operations of the three integration methods examined in chapter 4, 5 and 6 proposed in this thesis for fast jet application. A more extensive electrical system model is used to mimic a higher number of load additions more akin to a typical fast jet system. This includes a baseline loading level to represent the start of the fast jet service life. A theoretical demand increase scenario over five increments is applied to this model to gradually increase the power demand to represent through life upgrades similar to real life.

Combinations of the three integration methods proposed in this thesis were applied in conjunction to five incremental demand increases. This illustrates the modularity of the integration methods to operate with each other as well as to the main generation with minimal change. This also led to the maintaining of existing main generation power output to remain under the 30kVA existing limit mark (where the main generation itself does not need to be up rated). Although a reasonable first pass of the three integration methods concurrently operating with each other have been shown, it was realised with the higher number of loads, that the chosen SAF design started to struggle with maintaining power quality as intended and as examined in chapter 5. However, this still proved to be better for power quality within the system without a SAF at all as examined in section 7.3.1. Also, from this it is proposed that further optimisation of the SAF itself could potentially give better performance in power quality as the SAF design chosen in this chapter represents a workable design to demonstrate the first pass of using a SAF to integrating power onto the fast jet electrical system.

The single generator failure scenario was also demonstrated in which the graceful degradation offered by supplementary generation was illustrated.

Overall, the proposed application of power integration through the three proposed integration methods has been successfully illustrated.

8 Conclusions & further work

8.1 Chapter overview

In this concluding chapter, a summary of the work covered in this thesis is presented including conclusions and discussion of the proposed integration for fast jet application to cope with the through life power demand increase problem. The key contributions from this work are also highlighted as well as areas for further work are identified with suggestions for their progression.

8.2 Summary

The work of this thesis has focused on the specific power demand increase problem for fast jet aircraft. This is specifically for three phase, 400Hz, 115Vrms electrical systems that is most typical of in service legacy fast jets (e.g. F15, F16, F18, Typhoon, Gripen, Tornado, mirage 2000 [33]-[42]). In doing so the uniqueness of spatial and weight constraints that limit the ability to readily apply additional generation in this case, as well as constraints associated with replacing existing generation with more powerful equivalents are identified.

8.2.1 Proposed architecture changes

As an alternative to solely replacing the main generation and/or loading shedding which have their associated constraints: this thesis proposes a distributed application of supplementary generation to conform to the little remaining space around the fast jet aircraft whilst generally conforming to aerodynamic and mission specific constraints. Thus, this is an alternative strategy to the conventional power supply of the fast jet electrical system which is centralised with the main generation supplying all of the electrical power during normal operations.

To achieve this, the proposed solution of supplementary generation is to be applied in parallel to the main generation with the requirement of as little modifications as possible (keeping it intact and limiting retrofit changes). It is also desired that these generation sources themselves be engine independent to limit cumbersome rework. Examples of such possible sources used for distributed generation were identified in chapter 3 which included solid oxide fuel cell [61] or TEG based generation [68]-[71] as well as some more traditional auxiliary sources (used in fast jet) such as RATG [79],[80] or fuel powered engine independent gas turbine.

Another aligned strategy evaluated as part of the work of this thesis is to utilise existing auxiliary or emergency generation already on-board the fast jet during normal peak demand operations in parallel to the main generation (such as a RATG[79],[80] or engine independent turbine generators

[74] already installed on the fast jet aircraft). As such, sources that otherwise act as deadweight during flight can be utilised, making better use of the constrained space/weight.

The method of integration explored for both addition of power and paralleling existing auxiliary or emergency generation were treated as the same within this thesis (i.e. examined topologies and control to parallel such generation around the fast jet aircraft electrical system).

As such, this proposed strategy of adding and using supplementary generation would essentially turn the fast jet electrical system into a more decentralised equivalent (reflected by the title of this thesis) akin to those used in other high value applications (e.g. industrial micro-grids, finance). Respecting the timescales of the fast jet lifecycle [13], [14], [15] the aim is to apply these changes incrementally/gradually in conjunction with the equipment upgrades themselves (that increases the through life power demand), allowing the offline time of the fast jet to be minimised. Adopting this incremental approach also takes advantage of advances and maturation of generation technologies during the lifecycle and existing timeframes of the fast jet aircraft.

8.2.2 Proposed methods for supplementary power source integration

This approach although intuitive from an electrical perspective and with equivalents in other domains, has little precedence of standardised integration methods within the fast jet application. In particular the tackling of aggressive high power demand increases unique to the fast jet with its associated space and weight constrained environment. Hence the benefits and offerings in this thesis are in the exploration of possible integration and paralleling techniques of supplementary generation taken from other domains for application for the fast jet context. In particular the read through of topologies such as the utilisation of DC linkage of inverters connected to a main AC network/propulsion load was explored from EVs [82], [83], and M/DG/R [84]-[94]. From these, three complementary power integration methods were down selected and proposed for the fast jet application to meet the through life increase in power demand. The examinations of these are presented in the thesis with workable solutions in terms of control and topologies to illustrate their operations. These represented the “first pass” illustration of the proposed decentralisation solutions but could be further optimised (further improving efficiencies and power quality of power transfer etc).

8.2.2.1 Integration method 1

Firstly in terms of the first integration method proposed: slightly different to the applications of power at the DC link of inverters in EVs and M/DG/R, the proposal of the thesis is to use similar DC links on a fast jet aircraft electrical system not only with inverters connected into the system but as

well as the use of passive rectifier DC links (115Vrms to 270VDC rectifiers in non-linear loads as well as TRUs) that already exist in the system. By adding power at the passive rectifier DC links as well, the main generation can be alleviated with the added power supplying to the local loading of such rectifiers, ultimately increasing the overall power supply in the system. This in the context of fast jet electrical system: provides convenient distributed connection points around the fast jet for power integration which allow power generation to conform to the remaining space.

Associated read through of control such as voltage master current slave [44] were also explored as means to parallel the generation connected at the DC linkage of such passive rectifiers. This provides a means of controlling power injection into the DC link in the passive rectifier case allowing power integration/paralleling without the need to modify the main generation of the fast jet. In this, the DC link is held by the normal rectification of the main generation feed and essentially acting as the voltage master. Any sources connected to the DC link are operated as current slaves and control the amount of power injected back into the system.

This was primarily explored in chapter 4 of the thesis in that, to assess such integration against the generic fast jet electrical system. Simulation based benchmarking of typical fast jet electrical loading types under approximate power levels were used. Through such simulations, the function of indirect power alleviation was illustrated essentially representing paralleling of power with the main generation without the need to modify the main generation itself. The power quality benefits were also illustrated through the simulations from the reduced harmonic current draw from the main generation as the added source provides local power to the passive rectifier loads (non-linear load). This made up the first of three integration means proposed for the fast jet application in this thesis.

8.2.2.2 Integration method 2

SAF control was also proposed and explored as a means to inject power directly back to the AC grid and in parallel to the main generation of the fast jet electrical system while limiting the rework needed for the main generation itself. The primary functionality of harmonic current reduction of the generic SAF have been examined and proposed for aerospace [96]-[100]. Firstly, this primary functionality would be beneficial in meeting fast jet upgrades as the majority of through life upgrades would be non-linear loading (avionics requiring DC passive rectification) in general and ultimately reducing the harmonic current draw from the PCC. Another secondary functionality additional to harmonic current reduction which has been examined for terrestrial network application is to use the same SAF to inject additional power back into a main grid [101]. This provides a convenient means of adhering to the existing frequency, phase and magnitude of the voltage set of the main generation. This additional functionality of power injection has not been

explored for aerospace before and could potentially be a convenient means of power integration of supplementary generation for the unique fast jet problem facing aggressive through life upgrades. For commonality, in terms of the proposed SAF DC link control; the same voltage master and current slave control proposed for the DC link of passive rectifiers (integration method 1) is proposed again [44]. Here the voltage of the DC link is controlled actively by the SAF control itself and the proposal was elaborated and examined in chapter 5. Illustration of power injection as well as improvement of power quality was illustrated through simulations against the generic fast jet electrical system and representative loading.

8.2.2.3 Integration method 3

The third power integration method proposed in this thesis to tackle through life upgrades within a fast jet, is a follow up to the first integration method of applying power onto the DC links of passive rectifiers. This is additional to adding power solely at the DC link of passive rectifiers to provide for local loading (and alleviating the power drawn from the main generation). The follow up work is essentially to: change such passive rectifiers into active equivalents in order to allow excess power to be fed back into the main electrical system.

The advantages of this are: the local space around the distributed loads could be utilised (allowing for better conformance to the space constraints) and reusing of wiring of the existing loading is also possible (to allow excess power to flow back into the main fast jet electrical system). The size of the converter can also be smaller when compared to adding the same amount of power into the system with a standalone inverter as some of the power is locally consumed by the load. For commonality, the proposal is to make use of the voltage master and current slave scheme [44] to control the integration of the DC link and the proposed AC network interface made use of an adapted SAF control.

This method was presented in chapter 6 which looked at the application of such active rectifiers and active TRU working in parallel with normal loading. Their operations were illustrated through simulations against the generic fast jet electrical system with representative loading. In this, injection of power into the system in parallel to the main generation was demonstrated. Due to the control of the setup only injecting fundamental current back into the system, this approach works best when the remaining parallel loading in the system is largely linear.

8.2.2.4 Integration of all three methods

Together, these three proposed methods provided a high degree of loose electrical coupling. This is in accordance with the retrofit requirements of such integration limiting change to the main

generation and to allow an array of integration options to maximise the penetration of supplementary generation overall.

To illustrate such concurrency and loose coupling; simulation of all three integration methods operating within the same electrical system were presented in chapter 7. Degradation of power quality was displayed with the increase number of non-linear loads within the system even with the application of a SAF within the fast jet electrical system. However, it is proposed that further refinement of the SAF design could potentially improve such performance.

8.3 Further maturation of proposed integration solution for potential deployment

As the proposed integration of supplementary generation are provided in this thesis in their concept stages; there still requires refinement and work for further maturation before deployment can be pursued. Descriptions of these are provided in this section.

8.3.1 Transient, stability and load unbalancing analysis

Further work should include looking at loading transients effects (different loading profiles) as well as the ability for the main generation to hold up the DC link voltage (voltage master) under different power injection levels and loading.

Also, examination of transients from the main generation such as power up stages where there are large inrush currents flowing into the DC links of the system also requires further examination.

The scenarios covered in this thesis also consisted of balanced three phase loading scenarios and hence unbalanced loading should also be examined.

8.3.2 Weight and space calculations

A survey of state of the art and COTS examples of power electronics and generation sources could also be performed to further gauge the weight and space of such integration method would require. Projection of reduction in sizing of power electronics in general can also be examined to give an indication of what may be available in the future in keeping with the incremental retrofit nature of the proposed power integration.

8.3.3 Refinement of a SAF and active rectifier operations

The thesis proposes the decentralisation of power onto fast jet aircraft electrical system to cope with through life upgrades. With little precedence of such decentralised supplement any power on fast jets, the adaption of methods, read through from other domains were considered. This thesis can be thought of as the “first pass” of examining such application which included the application of a SAF and the modification for active rectifier functionality as well. Workable designs of these were used to illustrate the benefits of increasing power through distributed generation. However, further refinements can be made in the area of power quality (harmonics, reactive power) and efficiencies where alternative designs of a SAF and active rectifiers can be further examined.

8.3.4 Examining transferability to frequency wild systems

The integration methods presented in the thesis are aimed for three phase 115Vrms, 400Hz systems that are most typical in a legacy fast jet system. Further work can also be pursued to examine the

transfer of these to a frequency wild system (300-800Hz). In such cases, the ability of the SAF and active rectifiers to actively follow a variable frequency reference would also be beneficial

8.3.5 Survey access to 270VDC rectifiers

A key part of the DC link integration strategies comes with the access to the DC link itself within existing equipments. However as discussed in chapters 4 and 6, this is not always an option for existing rectifiers which may have the DC link hermitically sealed as part of the equipment. Therefore key to implementing the proposed strategies would be to define the extent of how accessible such DC links are through survey of real fast jet aircraft. This also provides requirements for future loads with rectifier DC links in that: change to the access terminal could potentially provide flexible options to powering of the load itself and would be highly beneficial (3 phase 115VAC or 270VDC).

8.4 Concluding remarks

In conclusion, the proposed application of supplementary generation in this thesis offers an alternative or supplementary solution to the conventional method of solely increasing the main generation or load shedding options. This is in the context to meet the unique aggressive through life power demand increases in fast jet aircraft. Solely increasing main generation can be cumbersome and requiring changes to the associated mechanical off take as well as still being limited by the same space constraints of the original generator. Load shedding is limited by the lack of hotel or non-critical loads within fast jet electrical systems. As an alternative, the proposed power integration allows the original main generation to remain intact and unchanged particular useful for retrofit applications where supplementary power generation added to the system can work in conjunction with it. With limited precedence of such power integration including standardised method of paralleling control and topologies, this thesis offers exploration of methods read across from other domains such as EV and M/DG/R [86], [44]. Three down selected proposals of integration were modelled.

Their individual and complementary operations have also been illustrated and allow potential maximised integration options within the limited remaining space of a fast jet aircraft airframe. Further works to mature these methods for fast jet have also been identified for potential deployment.

9 References

[1] Flightglobal.com, ‘Eurofighter Typhoon Cutaways’, 2015. [Online]. Available: http://www.flightglobal.com. [Accessed: 2014]

[2] Flightglobal.com, 'Northrop, Elbit to flight test terrain-following system for C-130 - 10/15/2012 - Flight Global', 2015. [Online]. Available: http://www.flightglobal.com/news/articles/northrop-elbit-to-flight-test-terrain-following-system-for-c-130-377572/. [Accessed: 27- Aug- 2015]

[3] Flightglobal.com, 'Israeli air force completes C-Music test - 10/17/2012 - Flight Global', 2015. [Online]. Available: http://www.flightglobal.com/news/articles/israeli-air-force-completes-c-music-test-377770/. [Accessed: 27- Aug- 2015] [2014]

[4] Flightglobal.com, 'US Air Force changes acquisitions strategy for F-16 radar modernization - 10/12/2012 - Flight Global', 2015. [Online]. Available: http://www.flightglobal.com/news/articles/us-air-force-changes-acquisitions-strategy-for-f-16-radar-modernization-377627/. [Accessed: 27- Aug- 2015]

[5] Flightglobal.com, 'Northrop begins production of B-2 satcom upgrade - 10/11/2012 - Flight Global', 2015. [Online]. Available: http://www.flightglobal.com/news/articles/northrop-begins-production-of-b-2-satcom-upgrade-377584/. [Accessed: 27- Aug- 2015]

[6] Flightglobal.com, 'PICTURE: France accepts first AESA-equipped Rafale - 10/2/2012 - Flight Global', 2015. [Online]. Available: http://www.flightglobal.com/news/articles/picture-france-accepts-first-aesa-equipped-rafale-377216/. [Accessed: 27- Aug- 2015]

[7] Flightglobal.com, 'US Navy to add sensor fusion to Super Hornet fleet - 9/26/2012 - Flight Global', 2015. [Online]. Available: http://www.flightglobal.com/news/articles/us-navy-to-add-sensor-fusion-to-super-hornet-fleet-376973/. [Accessed: 27- Aug- 2015]

[8] Flightglobal.com, 'USN developing new Super Hornet upgrades - 5/28/2012 - Flight Global', 2015. [Online]. Available: http://www.flightglobal.com/news/articles/usn-developing-new-super-hornet-upgrades-372392/. [Accessed: 27- Aug- 2015]

[9] Flightglobal.com, 'Boeing integrates Joint Helmet Mounted Cueing System into F-15SE - 7/31/2012 - Flight Global', 2015. [Online]. Available: http://www.flightglobal.com/news/articles/boeing-integrates-joint-helmet-mounted-cueing-system-into-f-15se-374904. [Accessed: 27- Aug- 2015]

[10] Flightglobal.com, 'Seoul names BAE Systems for F-16 avionics upgrade - 8/1/2012 - Flight Global', 2015. [Online]. Available: http://www.flightglobal.com/news/articles/seoul-names-bae-systems-for-f-16-avionics-upgrade-374962/. [Accessed: 27- Aug- 2015]

[11] Flightglobal.com, 'USAF plans F-15 modernization, but pilots want better displays - 8/17/2012 - Flight Global', 2015. [Online]. Available: http://www.flightglobal.com/news/articles/usaf-plans-f-15-modernization-but-pilots-want-better-displays-375612/. [Accessed: 27- Aug- 2015]

[12] Flightglobal.com, 'FARNBOROUGH: CMC launches NexGen cockpit technology demonstrator - 7/9/2012 - Flight Global', 2015. [Online]. Available: http://www.flightglobal.com/news/articles/farnborough-cmc-launches-nexgen-cockpit-technology-demonstrator-373906/. [Accessed: 27- Aug- 2015]

[13] Flightglobal.com, 'USAF details F-16 life extension programme - 8/30/2012 - Flight Global', 2015. [Online]. Available: http://www.flightglobal.com/news/articles/usaf-details-f-16-life-extension-programme-375914/. [Accessed: 27- Aug- 2015]

[14] Flightglobal.com, 'RAAF F/A-18A/B use could extend beyond 2020: audit - 9/27/2012 - Flight Global', 2015. [Online]. Available: http://www.flightglobal.com/news/articles/raaf-fa-18ab-use-could-extend-beyond-2020-audit-376992/. [Accessed: 27- Aug- 2015]

[15] Flightglobal.com, 'US Air Force looks to dramatically extend F-15 service life - 11/23/2011 - Flight Global', 2015. [Online]. Available: http://www.flightglobal.com/news/articles/us-air-force-looks-to-dramatically-extend-f-15-service-life-365200/. [Accessed: 27- Aug- 2015]

[16] Rafael.com [Online]. Available: http://www.rafael.com.il/marketing/334-914-en/marketing.aspx. [Accessed: 27- Aug- 2015]

[17] Lockheedmartin.co.uk, 'F-16 Fighting Falcon · Lockheed Martin', 2015. [Online]. Available: http://www.lockheedmartin.co.uk/us/products/f16/html. [Accessed: 27- Aug- 2015]

[18] Wikipedia, 'Byelka (radar)', 2015. [Online]. Available: http://www.wikipedia.org/wiki/Byelka_(radar). [Accessed: 27- Aug- 2015]

[19] Mbda-systems.com, 'Missile systems, defence systems - MBDA missiles', 2015. [Online]. Available: http://www.mbda-systems.com/products/air-dominance/spear/29/. [Accessed: 27- Aug- 2015]

[20] Utcaerospacesystems.com, 'DB-110 Tactical Dual-Band Reconnaissance System | UTC Aerospace Systems', 2015. [Online]. Available: http://www.utcaerospacesystems.com/cap/products/Pages/db-110-reconnaissance-system.aspx. [Accessed: 27- Aug- 2015]

[21] Lockheedmartin.co.uk, ' Lockheed Martin', 2015. [Online]. Available: http://www.lockheedmartin.co.uk/products/Sniper/html. [Accessed: 27- Aug- 2015]

[22] Thalesgroup.com, 'SPECTRA | Combat Systems | Thales Group', 2015. [Online]. Available: http://www.thalesgroup.com/en/worldwide/defence/spectra. [Accessed: 27- Aug- 2015]

[23] Baesystems.com, 2015. [Online]. Available: http://www.baesystems.com/product/BAES_162774/electronic-warfare. [Accessed: 27- Aug- 2015]

[24] NAVAIR US Navy, 'ALQ-99 Tactical Jamming System', 2015. [Online]. Available: http://www.navair.navy.mil.cfm?fuseaction=home.displayPlatform&key=24b1b2e4-3410-4808-adbb-287fcd83c984. [Accessed: 27- Aug- 2015]

[25] Aviamarket, 'All the World's Aircraft', 2015. [Online]. Available: http://www.aviamarket.org/reviews/military-aircraft/1046-dassault-rafale. [Accessed: 27- Aug- 2015]

[26] J. Hunter, Jane's All the world's aircraft 2014-2015.

[27]Forbes. 'What planes cost—and why $550 million is cheap for a new bomber', 2015. [Online]. Available: http://www.forbes.com/sites/lrenthompson/2013/11/22/what-planes-cost-and-why-550-million-is-cheap-for -a-new-bomber/. [Accessed: 27- Aug- 2015]

[28] Raytheon. 'Raytheon's Next Generation Jammer: Power You Can Count On', 2015. [Online]. Available: http://www.raytheon.com/capabilities/productss/ngj. [Accessed: 27- Aug- 2015]

[29]Karimi, K.J.; Mong, A.C., "Modeling nonlinear loads for aerospace power systems," *Energy Conversion Engineering Conference, 2002. IECEC '02. 2002 37th Intersociety* , vol., no., pp.33,38, 29-31 July 2004
doi: 10.1109/IECEC.2002.1391970

[30] K. Furmanczyk, "Powering DC Brushless Motors on Airplanes with Variable Frequency Systems," in *Motor, Drive & Automation System Conference* Orlando, Florida, 2009.

[31] Thales. 'Passive Infra-Red Airborne Tracking Equipment', 2015. [Online]. Available: http://www.thalesgroup.comen/united-kingdom/defence/air-group/infra-red-search-track/pirate. [Accessed: 27- Aug- 2015]

[32] US Navy. "Navy Training System Plan For The F/A-18 Aircraft N88-NTSP-A-50-7703H/A," Nov, 2000

[33] Fighter-aircraft.com, 'Eurofighter Typhoon » Fighter Aircraft', 2015. [Online]. Available: http://www.fighter-aircraft.com/eurofighter-typhoon.html. [Accessed: 27- Aug- 2015]

[34] Fighter-aircraft.com, 'Panavia Tornado ADV » Fighter Aircraft', 2015. [Online]. Available: http://www.fighter-aircraft.com/panavia-tornado-adv.html. [Accessed: 27- Aug- 2015]

[35]Fighter-aircraft.com, 'Dassault Rafale » Fighter Aircraft', 2015. [Online]. Available: http://www.fighter-aircraft.com/rafale.html. [Accessed: 27- Aug- 2015]

[36]Fighter-aircraft.com, 'Dassault Mirage 2000 » Fighter Aircraft', 2015. [Online]. Available: http://www.fighter-aircraft.com/mirage-2000.html. [Accessed: 27- Aug- 2015]

[37]Fighter-aircraft.com, 'Saab JAS 39 Gripen » Fighter Aircraft', 2015. [Online]. Available: http://www.fighter-aircraft.com/jas-39-gripen.html. [Accessed: 27- Aug- 2015]

[38]Fighter-aircraft.com, 'McDonnell Douglas F-15 Eagle » Fighter Aircraft', 2015. [Online]. Available: http://www.fighter-aircraft.com/mcdonnell-douglas-f-15-eagle.html. [Accessed: 27- Aug- 2015]

[39]Fighter-aircraft.com, 'The McDonnell Douglas (now Boeing) F-15E Strike Eagle is an all-weather multirole fighter, derived from the McDonnell Douglas F-15 Eagle. » Fighter Aircraft', 2015. [Online]. Available: http://www.fighter-aircraft.com/mcdonnell-douglas-f-15e-strike-eagle.html. [Accessed: 27- Aug- 2015]

[40]Fighter-aircraft.com, 'General Dynamics F-16 Fighting Falcon » Fighter Aircraft', 2015. [Online]. Available: http://www.fighter-aircraft.com/f-16-fighting-falcon.html. [Accessed: 27- Aug- 2015]

[41]Fighter-aircraft.com, 'McDonnell Douglas F/A-18 Hornet » Fighter Aircraft', 2015. [Online]. Available: http://www.fighter-aircraft.com/fa-18-hornet.html. [Accessed: 27- Aug- 2015]

[42]Fighter-aircraft.com, 'The Boeing F/A-18E/F Super Hornet – A twin-engine carrier-based multirole fighter aircraft andmore advanced derivatives of the F/A-18C and D Hornet. » Fighter Aircraft', 2015. [Online]. Available: http://www.fighter-aircraft.com/boeing-fa-18ef-super-hornet.html. [Accessed: 27- Aug- 2015]

[43]Baesystems.com, 2015. [Online]. Available: http://www.baesystems.com/enhancedarticle/BAES_156125/typhoon. [Accessed: 27- Aug- 2015]

[44] Ferreira, A.A.; Pomilio, J.A.; Spiazzi, G.; de Araujo Silva, L., "Energy Management Fuzzy Logic Supervisory for Electric Vehicle Power Supplies System," in Power Electronics, IEEE Transactions on , vol.23, no.1, pp.107-115, Jan. 2008 doi: 10.1109/TPEL.2007.911799

[45]Fong, K.; Galloway, S.; Harrington, I.; Burt, G., "Aircraft electrical systems - coping with harmonics for changing power demands," in Universities Power Engineering Conference (UPEC), 2009 Proceedings of the 44th International , vol., no., pp.1-5, 1-4 Sept. 2009

[46]Fletcher, S.D.A.; Norman, P.J.; Fong, K.; Galloway, S.J.; Burt, G.M., "High-Speed Differential Protection for Smart DC Distribution Systems," in Smart Grid, IEEE Transactions on , vol.5, no.5, pp.2610-2617, Sept. 2014 doi: 10.1109/TSG.2014.2306064

[47]Aviamarket, 'All the World's Aircraft', 2015. [Online]. Available: http://www.aviamarket.org/reviews/military-aircraft/1046-dassault-rafale. [Accessed: 27- Aug- 2015]

[48]I. Moir and A. Seabridge, *Aircraft systems*. Chichester, West Sussex, England: Wiley, 2008.

[49]Koerner, M., "Recent developments in aircraft emergency power," in Energy Conversion Engineering Conference and Exhibit, 2000. (IECEC) 35th Intersociety , vol.1, no., pp.12-19 vol.1, 2000
doi: 10.1109/IECEC.2000.870618

[50]DOD. “Aircraft/Store Electrical Interconnection System,” Military Standard (Mil Std) 1760. Revision C

[51]NAVAIR US Navy, ‘ALQ-99 Tactical Jamming System’, 2015. [Online]. Available: http://www.navair.navy.mil.cfm?fuseaction=home.displayPlatform&key=24b1b2e4-3410-4808-adbb-287fcd83c984. [Accessed: 27- Aug- 2015]

[52]K. Furmanczyk, "Powering DC Brushless Motors on Airplanes with Variable Frequency Systems," in *Motor, Drive & Automation System Conference* Orlando, Florida, 2009.

[53]D. Chapman, Copper Development Association, "Harmonics: Cause and Effects," *Power Quality Application Guide,* March 2001.

[54] Akagi, H., "Active Harmonic Filters," in Proceedings of the IEEE , vol.93, no.12, pp.2128-2141, Dec. 2005
doi: 10.1109/JPROC.2005.859603

[55]Khadkikar, V., "Enhancing Electric Power Quality Using UPQC: A Comprehensive Overview," *Power Electronics, IEEE Transactions on* , vol.27, no.5, pp.2284,2297, May 2012 doi: 10.1109/TPEL.2011.2172001

[56]RTCA, "Environmental Conditions and Test Procedures for Airborne Equipment," DO- 160F.

[57] H. Akagi, *Instantaneous active and reactive power theory and applications*. Piscataway, NJ: IEEE Press, 2007.

[58]Uk.mathworks.com, 'Electrical Power Systems Simulation - SimPowerSystems - Simulink', 2015. [Online]. Available: http://uk.mathworks.com/products/simpower/. [Accessed: 01- Sep- 2015]

[59]Bataller-Planes, E.; Lapea-Rey, N.; Mosquera, J.; Orti, F.; Oliver, J.A.; Garcia, O.; Moreno, F.; Portilla, J.; Torroja, Y.; Vasic, M.; Huerta, S.C.; Trocki, M.; Zumel, P.; Cobos, J.A., "Power Balance of a Hybrid Power Source in a Power Plant for a Small Propulsion Aircraft," *Power Electronics, IEEE Transactions on* , vol.24, no.12, pp.2856,2866, Dec. 2009 doi: 10.1109/TPEL.2009.2022943

[60]Diamond-air.at, 'HK36 Super Dimona – Born to shine :: Diamond Aircraft Industries', 2015. [Online]. Available: http://www.diamond-air.at/single-engine-aircraft/hk36-super-dimona.html. [Accessed: 27- Aug- 2015]

[61]Rajashekara, K.; Grieve, J.; Daggett, D., "Solid Oxide Fuel Cell/Gas Turbine Hybrid APU System for Aerospace Applications," *Industry Applications Conference, 2006. 41st IAS Annual Meeting.*

Conference Record of the 2006 IEEE , vol.5, no., pp.2185,2192, 8-12 Oct. 2006 doi: 10.1109/IAS.2006.256845

[62]Nasa.gov, 'NASA - Helios', 2015. [Online]. Available: http://www.nasa.gov/centers/dryden/news/ResearchUpdate/Helios/, http://www.nasa.gov/pdf/64317main_helios.pdf. [Accessed: 27- Aug- 2015]

[63]Airforce-technology.com, 'Zephyr Solar-Powered HALE UAV - Airforce Technology', 2015. [Online]. Available: http://www.airforce-technology.com/projects/zephyr/. [Accessed: 30- Aug- 2015]

[64]Defense Industry Daily, 'DARPAs Vulture: What Goes Up, Neednt Come Down', 2015. [Online]. Available: http://www.defenseindustrydaily.com/DARPAs-Vulture-What-Goes-Up-Neednt-Come-Down-04852/. [Accessed: 27- Aug- 2015]

[65]Flightglobal.com, 'Lockheed wins ISIS airship contract from DARPA', 2009. [Online]. Available: https://www.flightglobal.com/news/articles/lockheed-wins-isis-airship-contract-from-darpa-325714/. [Accessed: 03- Sep- 2015]

[66]Wikipedia, 'Integrated Sensor is Structure', 2015. [Online]. Available: https://en.wikipedia.org/wiki/Integrated_Sensor_is_Structure#/media/File:Integrated_Sensor_is_Structure_1.jpg. [Accessed: 03- Sep- 2015]

[67] Horizon Energy Systems, 'Aeropak -1: Long Endurance Battery Alternatives for Electric UAS', 2015. [Online]. Available: http://resources.arcolaenergy.com/docs/Brochures/AEROPAKBrochure.pdf. [Accessed: 30- Aug- 2015]

[68]J. LaGrandeur, 'Thermoelectric waste heat recovery program for passenger vehicles', 2015.

[69] A. Eder and M. Linde, 'BMW EfficientDynamics: Less emission. More driving pleasure.', 2015.

[70]The Boeing Company, 'Thermal integration of thermoelectronic device', US 20120118345 A12015.

[71]J. Huang, 'Aerospace and aircraft thermoelectric applications', 2015.

[72]The Boeing company, 'Thermoelectric power generation using aircraft fuselage temperature differential', US 20130298956 A12015.

[73] Flightglobal.com, 'Aircraft Cutaways | Flightglobal.com', 2015. [Online]. Available: http://www.flightglobal.com/cutaways/. [Accessed: 30- Aug- 2015]

[74] Koerner, M., "Recent developments in aircraft emergency power," *Energy Conversion Engineering Conference and Exhibit, 2000. (IECEC) 35th Intersociety* , vol.1, no., pp.12,19 vol.1, 2000
doi: 10.1109/IECEC.2000.870618

[75]Yu, S. and Ganev, E., "Next Generation Power and Thermal Management System," *SAE Int. J. Aerosp.* 1(1):1107-1121, 2009, doi:10.4271/2008-01-2934.

[76] Janes.com, 'Defence & Security Intelligence & Analysis - IHS Jane's 360', 2015. [Online]. Available: http://www.janes.com/. [Accessed: 30- Aug- 2015]

[77] Wikipedia, 'Northrop Grumman EA-6B Prowler', 2015. [Online]. Available: https://en.wikipedia.org/wiki/Northrop_Grumman_EA-6B_Prowler#/media/File:EA-6B_Prowler_takes_off_from_Eielson_AFB.jpg. [Accessed: 30- Aug- 2015]

[78]Wikipedia, 'Boeing EA-18G Growler', 2015. [Online]. Available: https://en.wikipedia.org/wiki/Boeing_EA-18G_Growler#/media/File:EA-18G_Growler_VX-9_from_below_2008.jpg. [Accessed: 30- Aug- 2015]

[79]ATGI – Advanced Technologies Group, 'Ram Air Turbines - ATGI – Advanced Technologies Group', 2015. [Online]. Available: http://atgi.us/products-and-services/ram-air-turbines/. [Accessed: 27- Aug- 2015]

[80]Mfgpages.com, 'GHETZLER AERO-POWER CORPORATION: Turbines, Heat exchangers- MFGpages', 2015. [Online]. Available: http://www.mfgpages.com/company/GHETZLER-AERO-POWER-in-ILLINOIS-USA-7990841/. [Accessed: 30- Aug- 2015]

[81]Roboam, X.; Langlois, O.; Piquet, H.; Morin, B.; Turpin, C., "Hybrid power generation system for aircraft electrical emergency network," *Electrical Systems in Transportation, IET* , vol.1, no.4, pp.148,155, December 2011
doi: 10.1049/iet-est.2010.0045

[82]Jih-Sheng Lai; Nelson, D.J., "Energy Management Power Converters in Hybrid Electric and Fuel Cell Vehicles," in Proceedings of the IEEE , vol.95, no.4, pp.766-777, April 2007
doi: 10.1109/JPROC.2006.890122

[83]Attaianese, C.; Di Monaco, M.; Tomasso, G., "Power Control for Fuel-Cell–Supercapacitor Traction Drive," *Vehicular Technology, IEEE Transactions on* , vol.61, no.5, pp.1961,1971, Jun 2012
doi: 10.1109/TVT.2012.2191987

[84] Dasgupta, S.; Mohan, S.N.; Sahoo, S.K.; Panda, S.K., "Lyapunov Function-Based Current Controller to Control Active and Reactive Power Flow From a Renewable Energy Source to a Generalized Three-Phase Microgrid System," *Industrial Electronics, IEEE Transactions on* , vol.60, no.2, pp.799,813, Feb. 2013
doi: 10.1109/TIE.2012.2206356

[85]Ghazanfari, A.; Hamzeh, M.; Mokhtari, H.; Karimi, H., "Active Power Management of Multihybrid Fuel Cell/Supercapacitor Power Conversion System in a Medium Voltage Microgrid," *Smart Grid,*

IEEE Transactions on , vol.3, no.4, pp.1903,1910, Dec. 2012
doi: 10.1109/TSG.2012.2194169

[86]Rui Li; Dianguo Xu, "Parallel Operation of Full Power Converters in Permanent-Magnet Direct-Drive Wind Power Generation System," in Industrial Electronics, IEEE Transactions on , vol.60, no.4, pp.1619-1629, April 2013
doi: 10.1109/TIE.2011.2148684

[87]Karlsson, P.; Svensson, J., "DC bus voltage control for a distributed power system," *Power Electronics, IEEE Transactions on* , vol.18, no.6, pp.1405,1412, Nov. 2003
doi: 10.1109/TPEL.2003.818872

[88] Marwali, M.N.; Jin-Woo Jung; Keyhani, A., "Control of distributed generation systems - Part II: Load sharing control," *Power Electronics, IEEE Transactions on* , vol.19, no.6, pp.1551,1561, Nov. 2004
doi: 10.1109/TPEL.2004.836634

[89] Kurohane, K.; Senjyu, T.; Yona, A.; Urasaki, N.; Goya, T.; Funabashi, T., "A Hybrid Smart AC/DC Power System," in Smart Grid, IEEE Transactions on , vol.1, no.2, pp.199-204, Sept. 2010
doi: 10.1109/TSG.2010.2053392

[90]Prieto-Araujo, E.; Bianchi, F.D.; Junyent-Ferré, A.; Gomis-Bellmunt, O., "Methodology for Droop Control Dynamic Analysis of Multiterminal VSC-HVDC Grids for Offshore Wind Farms," in Power Delivery, IEEE Transactions on , vol.26, no.4, pp.2476-2485, Oct. 2011
doi: 10.1109/TPWRD.2011.2144625

[91]Marwali, M.N.; Jin-Woo Jung; Keyhani, A., "Control of distributed generation systems - Part II: Load sharing control," in Power Electronics, IEEE Transactions on , vol.19, no.6, pp.1551-1561, Nov. 2004
doi: 10.1109/TPEL.2004.836634

[92]Guerrero, J.M.; Vasquez, J.C.; Matas, J.; de Vicuña, L.G.; Castilla, M., "Hierarchical Control of Droop-Controlled AC and DC Microgrids—A General Approach Toward Standardization," *Industrial Electronics, IEEE Transactions on* , vol.58, no.1, pp.158,172, Jan. 2011
doi: 10.1109/TIE.2010.2066534

[93]Rokrok, E.; Golshan, M.E.H., "Adaptive voltage droop scheme for voltage source converters in an islanded multibus microgrid," in Generation, Transmission & Distribution, IET , vol.4, no.5, pp.562-578, May 2010
doi: 10.1049/iet-gtd.2009.0146

[94] Li Zhang; Kai Sun; Yan Xing; Lanlan Feng; Hongjuan Ge, "A Modular Grid-Connected Photovoltaic Generation System Based on DC Bus," in Power Electronics, IEEE Transactions on ,

vol.26, no.2, pp.523-531, Feb. 2011
doi: 10.1109/TPEL.2010.2064337

[95]Akagi, H., "Active Harmonic Filters," *Proceedings of the IEEE* , vol.93, no.12, pp.2128,2141, Dec. 2005
doi: 10.1109/JPROC.2005.859603

[96]Yingpeng Luo; Zhong Chen; Miao Chen; Jianxia Li, "A cascaded shunt active power filter with high performance for aircraft electric power system," *Energy Conversion Congress and Exposition (ECCE), 2011 IEEE* , vol., no., pp.1143,1149, 17-22 Sept. 2011
doi: 10.1109/ECCE.2011.6063904

[97]Junyi Liu; Zanchetta, P.; Degano, M.; Lavopa, E., "Control Design and Implementation for High Performance Shunt Active Filters in Aircraft Power Grids,"*Industrial Electronics, IEEE Transactions on* , vol.59, no.9, pp.3604,3613, Sept. 2012
doi: 10.1109/TIE.2011.2165454

[98]Haibing Hu; Wei Shi; Ying Lu; Yan Xing, "Design Considerations for DSP-Controlled 400 Hz Shunt Active Power Filter in an Aircraft Power System,"*Industrial Electronics, IEEE Transactions on* , vol.59, no.9, pp.3624,3634, Sept. 2012
doi: 10.1109/TIE.2011.2165452

[99]Venturini, R.P.; Mattavelli, P.; Zanchetta, P.; Sumner, M., "Adaptive Selective Compensation for Variable Frequency Active Power Filters in More Electrical Aircraft," *Aerospace and Electronic Systems, IEEE Transactions on* , vol.48, no.2, pp.1319,1328, APRIL 2012
doi: 10.1109/TAES.2012.6178064

[100] A. Eid, M. Abdel-Salam, H. El-Kishky and T. El-Mohandes, “Active power filters for harmonic cancellation in conventional and advanced aircraft electric power systems”, Electric Power Systems Research, vol. 79, Issue 1, pp. 80-88, January 2009

[101] Singh, M.; Khadkikar, V.; Chandra, A.; Varma, R.K., "Grid Interconnection of Renewable Energy Sources at the Distribution Level With Power-Quality Improvement Features," *Power Delivery, IEEE Transactions on* , vol.26, no.1, pp.307,315, Jan. 2011
doi: 10.1109/TPWRD.2010.2081384

[102] Upload.wikimedia.org, 2015. [Online]. Available: https://upload.wikimedia.org/wikipedia/commons/b/bf/F-16C_Fighting_Falcon.JPEG. [Accessed: 30- Aug- 2015]

[103] Fuelcells.org, 'Fuel Cells 2000 - Benefits', 2015. [Online]. Available: http://www.fuelcells.org/base.cgim?template=benefits. [Accessed: 30- Aug- 2015]

[104] Uk.mathworks.com, 'Perform transformation from three-phase (abc) signal todq0 rotating reference frame or the inverse - Simulink', 2015. [Online]. Available: http://uk.mathworks.com/help/physmod/sps/powersys/ref/abctodq0dq0toabc.html. [Accessed: 01- Sep- 2015]

[105] R. Clarke, 'Power losses in wound components', *Info.ee.surrey.ac.uk*, 2015. [Online]. Available: http://info.ee.surrey.ac.uk/Workshop/advice/coils/power_loss.html. [Accessed: 01- Sep- 2015]